THE DEGRADATION OF COPOLYMERS OF METHYL METHACRYLATE

A thesis submitted to the University of Glasgow for the degree of Doctor of Philosophy in the Faculty of Science.

by

Alastair J. Davidson. B.Sc.

Supervisor

Professor N. Grassie

Date: January 1977

ACKNOWLEDGEMENTS

The work described in this thesis was carried out during the period October 1971 to September 1974 at the University of Glasgow in the Department of Physical Chemistry which is under the direction of Professor G. A. Sim. During this period of research I was in receipt of a grant from the Science Research Council.

I wish to express my thanks to my colleagues in the Polymer Group and in particular to my supervisor Prof. N. Grassie for the opportunity of studying in such an enjoyable and stimulating environment.

January 1977

Alastair J. Davidson

CONTENTS

SUMMARY

The degradatative reactions of Poly(methyl methacrylate) are well known. So by introducing another monomer such as maleic anhydride, methyl vinyl ketone or methyl isopropenyl ketone, alterations in the mode of degradation of PMMA can be readily identified.

In particular, in thermal, photothermal and photodegradation of copolymers of methyl methacrylate and maleic anhydride, the effect of maleic anhydride appears to be one of inhibiting the normal unzipping mechanism of PMMA while accelerating the degradation by chain scission. Because of the much increased rate of degradation due to small amounts of maleic anhydride, care in the interpretation of the results had to be excercised particularly during photothermal degradation, since in some cases the products of degradation are not detected.

In studying the copolymers of methyl methacrylate with methyl vinyl ketone and methyl isopropenyl ketone, it was found that, again, unzipping of methyl methacrylate is suppressed but that the normal ring formation found in the degradation of poly(methyl vinyl ketone) and poly(methyl isopropenyl ketone) is inhibited. A degradation rate maximum is found at 20-30% ketone content in photodegradation in solution.

Although the effect of solvents on the degradation of the maleic anhydride copolymers is not thought to seriously affect the basic mode and rate of degradation, chloroform assists the photo-

degradation in solution of the methyl isopropenyl copolymers.

The reactivity ratios for each polymer system are determined by a variety of methods including several novel uses of spectroscopic techniques. The results for the maleic anhydride system compare well with published data but the reactivity ratios for the methyl isopropenyl ketone and methyl vinyl ketone systems are determined for the first time.

CHAPTER ONE

INTRODUCTION

1. The useful life of a polymeric material will ultimately depend upon the environment in which it is utilized and, in particular, upon the degradation reactions which that environment can induce in the polymer. For this reason, it has been important to obtain a fundamental understanding of the chemical effects of a wide variety of degradation agencies, including high energy radiation, moisture, ozone, atmospheric pollutants such as the oxides of nitrogen and sulphur and even intermittent mechanical stress. The three basic agencies, to which all polymers are subjected either during fabrication or during their subsequent useful life, are heat, light and oxygen. At the present time, a great deal is known about the thermal, photolytic and oxidative reactions in homopolymers, but in recent years copolymers have found increasing commercial application so that it has become important to extend degradation studies to this class of material.

In this thesis are described some studies of the thermal degradation and photolysis of copolymers of methyl methacrylate in the absence of oxygen.

Thermal degradation simply involves the heating of a polymer sample, normally as a film, powder or pressed disc until the thermal energy induces physical and chemical changes in the sample. In poly(methyl methacrylate) and the copolymers examined, the physical

changes are relatively unimportant. The polymer merely becomes less viscous as the increasing temperature takes the sample through its glass transition temperature and melting point. Although the polymer chains are mobile above the melting point and cooling can cause a change in crystallinity and therefore an alteration in physical properties, the more drastic chemical changes at elevated temperatures have provided fuel for investigations of polymer degradation for many years. For example, at 250° poly(methyl methacrylate) undergoes "reverse polymerisation" and monomer is evolved, while with poly(methyl vinyl ketone), no monomer is evolved, the main chemical process being simultaneous elimination of water and ring formation.

Photodegradation, on the other hand, is very much more complicated and many of its basic features are still not well understood. The energy is received in the form of photons which raises the molecule from a singlet ground state to an excited singlet state. The molecule may revert to the ground state by emission of a photon (fluorescence) or by radiationless transitions and the generation of heat. In some instances, intersystem crossing can take place and the molecule will find itself in an excited triplet level of lower energy. Again the reversion to the ground state may be accompanied by photon emission (phosphorescence) or heat. If the molecule has sufficient energy in the excited state, either singlet or triplet, dissociation or rearrangement may take place. Reversion to the ground state may be accomplished by transfer of energy between the excited molecule and a second molecule. These processes are illustrated in FIGURE I. I.

FIGURE I.1

EXCITED STATES AND PHOTOPHYSICAL TRANSITIONS

BETWEEN THESE STATES

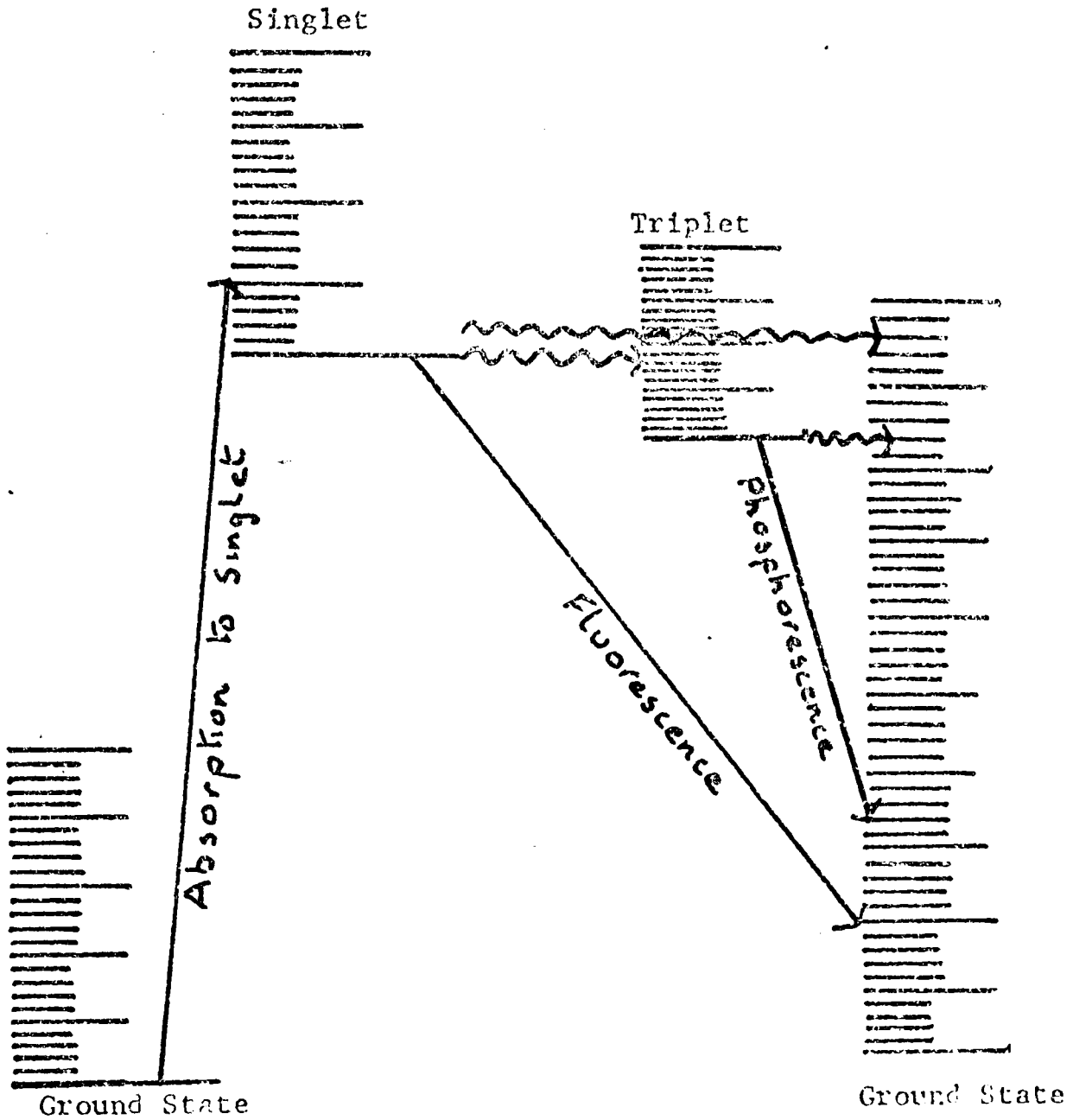

Solid lines = radiative transitions

Wavy lines = radiationless processes

Photolytic processes can be separated into two groups - primary and secondary. A primary process involves the immediate effect of the light on the absorbing molecule: deactivation through fluorescence, heat emission, energy transfer etc., or destruction by transformation of the starting material into new compounds. Secondary processes are the reactions of the molecules, atoms or radicals produced by the primary process. One of several things may happen in a secondary process: a) energy transfer, which initiates a chemical reaction may occur through collisions between excited molecules and other molecules, b) atoms or radicals produced in the primary process may react to give stable products, or c) the excited molecules may react directly with other molecules in the system to form products.

If the energy of the excitation is greater than, or equal to, the bond dissociation energy of the weakest link in a molecule, then cleavage reactions may occur. It is important to remember that, because the absorbed energy may be transferred, the site at which ultra-violet light is absorbed is not necessarily the same as that at which bond rupture may take place. Bond dissociation in polymers may lead to a main chain break, ie. scission. This is one of the two principal reactions involving the polymer backbone which may take place when polymers are exposed, to ultra-violet radiation, the other being cross-linking.

The reactions occuring in a polymeric system undergoing photolysis may be classified as direct or indirect. Direct reactions come about from the absorption of a photon by the polymer followed by bond homolysis and the formation of degradation products. For example,

if a C-C bond is broken:-

$$P_{n+m} + h\upsilon \longrightarrow P^{*}_{n+m}$$

$$P^{*}_{n+m} \longrightarrow P_{n}^{\cdot} + P_{m}^{\cdot} \longrightarrow \text{products.}$$

In the indirect reactions, "foreign" molecules, polymeric or small molecule impurities, or even other functional groups in the same polymer become involved. They similarly can be excited and undergo reactions to form free radicals. These excited molecules or fragments may eventually interact with the polymer to give products similar to those arising from the direct reaction. The reverse reactions may also occur:- excited polymer or polymer radicals may interact with the "foreign" molecules. These "indirect" processes can lead to degradation and they may involve energy transfer or free radical processes:-

$$P_{n+m} + S^{*} \rightleftharpoons S + P^{*}_{n+m}$$

$$P_{n+m} + S^{\cdot} \rightleftharpoons S + P^{\cdot}_{n+m}$$

These considerations lead to a discussion of the more important kinds of degradation processes.

1) Chain Scission

a) Initiation. There are two possible mechanisms. The first is random initiation in which chain scission occurs at random points along the chain leaving radicals which tend to be large compared to a monomer unit. The photodegradation of poly(methyl methacrylate) at 25°C is an

example of this. In the second mechanism, end-initiation, the bonds joining the end units to the rest of the chain are particularly vulnerable and are thus exclusively broken. The result is the formation of a long chain polymer radical and an end-group radical. The thermal degradation of poly(methyl methacrylate) (PMMA) at 200°C is a classic example.

b) Depropagation. This is the reverse of the propagation step in radical polymerisation. Polymer radicals peel off monomer molecules and again, the thermal degradation of PMMA illustrates this.

2) Crosslinking. Under some circumstances ultra-violet radiation can cause crosslinking, the formation of intermolecular covalent links which leads to a three-dimensional network. The polymer ultimately becomes insoluble. Crosslinking is usually associated with the reactions of polymer radicals formed by cleavage of side groups from the main chain. The crosslinking may be by radical combination or by addition to an unsaturated site in another chain. Whether or not crosslinking takes place is dependent to a large extent upon the structure of the polymer. For example the labile tertiary hydrogen on poly(methyl vinyl ketone) (PMVK) is readily abstracted and crosslinking may subsequently occur. In poly(methyl isopropenyl ketone) (PMIK) and PMMA there is no tertiary hydrogen and so crosslinking does not readily take place.

When crosslinking does occur, it has a considerable effect on photodegradation studies. It makes molecular weight determinations impossible although sedimentation pattern and gel studies can be made. Crosslinking also interferes with the determination of the rate of evolution of volatiles. Thus the rigid structure has a much higher

bulk viscosity which slows down the rate of diffusion of volatile products from the degrading polymer and since these products remain longer in the degrading polymer, complicating side reactions become more probable.

3) Decomposition of side groups. This type of reaction involves a chemical change in a side group which results in the formation of volatile products and a non volatile residue. In PMMA, the ester side group can break up to form methane, methanol, carbon monoxide etc.

4) Rearrangement. A typical rearrangement is the cyclisation of PMIK, in which the polymer is seen to change colour as double bond conjugation develops.

Before examining the degradation of PMMA and its copolymers, it is necessary to review, briefly, the work already in the literature. More extensive reviews of degradation and photochemistry are available[1,2,3,4,5].

2. The Polymerisation of Maleic Anhydride.

Maleic anhydride is capable of copolymerising quite readily with many other monomers including methyl methacrylate but it does not easily polymerise. The principal reason for this reluctance to polymerise was supposed to be the steric hindrance imposed by the 1,2 disubstitution of the double bond of the monomeric species. The resonance and polar characteristics of maleic anhydride were also mentioned as contributing to the sterically inherent non-homo-polymerisable character.

However, several workers[6,7] obtained evidence that, on occasions, adjacent units of maleic anhydride are found in copolymers. Investigation of the styrene - itaconic anhydride system demonstrated that the itaconic anhydride was capable of homopolymerisation[8,9] and this lead Lang and coworkers[10] to attempt polymerisation using several initiating systems. Although free radical initiation using azobisisobutyronitrile at 1% concentration in molten monomer produced very small amounts of polymer, greater than 30% conversion was achieved using benzoyl peroxide. High conversion was claimed when using Co^{60} initiated polymerisation in several different solvents and such a polymer had a molecular weight of 23,000 determined by light scattering techniques.

Braun[11], after polymerising itaconic acid, also polymerised maleic anhydride using azobisisobutyronitrile and other radical initiators but noted simultaneous loss of carbon dioxide.

From e.s.r. studies of copolymers of methyl methacrylate and maleic anhydride[12,13] the existence of adjacent anhydride groups in the polymer chain for copolymers containing as little as 7% maleic anhydride was deduced.

Polymerisation of maleic anhydride has also been achieved by reaction with pyridine to form oligomeric and polymeric products[14,15]. Photoinduced homopolymerisation[16] in dioxane at 35°C without initiator gave an oligomer of four maleic anhydride units and one dioxane molecule per molecule and a small quantity of cyclic dimer.

3. The Thermal Degradation of Poly(methyl methacrylate)

PMMA has possibly received more attention than any other polymer in an effort to elucidate the mechanism of its degradation[17-27]. Grassie and Melville[28,29] showed that almost pure monomer is evolved on heating PMMA under vacuum and postulated an "unzipping" mechanism of radical depolymerisation in which monomer units peel off from unsaturated chain ends[30-32] at temperatures up to 270°C. For systems in which the molecular chain length is less than the kinetic chain length, low molecular weight molecules are entirely lost to the system as monomer. If the molecular chain length exceeds the kinetic chain length, molecules of reduced molecular weight are left in the system. These two cases are illustrated by lines A and B in FIGURE 1.2. Because it is impossible for more than half the chains to be terminated by unsaturated units, due to disproportionation termination in polymerisation, monomer weight loss cannot exceed 50% at temperatures up to 270°C.

However, quantitative yields of methyl methacrylate have been obtained at 300°C[23,33] and this has been explained as due to random scission followed by depolymerisation. Line C shows a typical degradation profile at this temperature.

In the present study, the molecular chain length generally exceeds the kinetic chain length and therefore we should observe two distinct modes of degradation - the first, in which monomer is peeled off from unsaturated chain ends and the second in which monomer is evolved after random main chain scission. These reactions are well illustrated by the technique of Thermal Volatilisation Analysis which

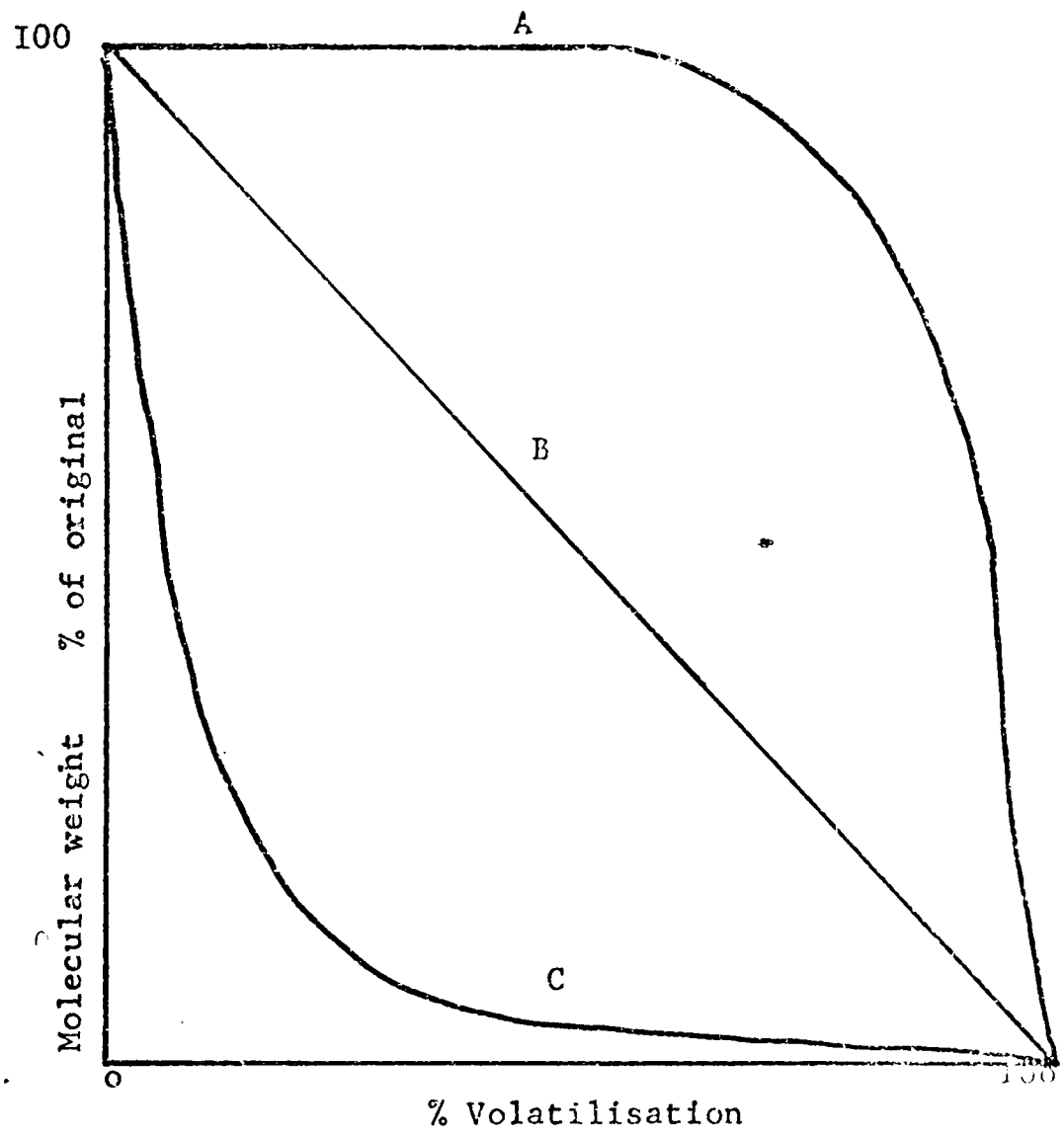

FIGURE I.2

Theoretical molecular weight versus volatilisation diagram for degradation reactions

is discussed in subsequent chapters.

4. The Thermal Degradation of Methyl Methacrylate/Maleic anhydride Copolymers

Using the dynamic molecular still method,[29,34] Grassie and McLaren[35] degraded a 19/1 copolymer of methyl methacrylate and maleic anhydride between 200°C and 240°C. The amount of methyl methacrylate evolved even at 240°C for four hours did not exceed 6% of the starting weight, as determined by vapour phase chromatography, indicating an inhibition of the depolymerisation mechanism of PMMA.

The molecular weight of the degraded polymer was measured by viscometry and by osmometry. In any particular degradation, the number of bonds broken was defined as

$$\text{Bonds broken} = \frac{\text{Molecular weight of undergraded polymer}}{\text{Molecular weight of degraded polymer}} - 1$$

Plots of bonds broken versus time for any temperature are a measure of the rate of degradation, which was found to increase with temperature and yield an energy of activation of 45.6 k cal./mole from viscosity measurements and 48.8 k cal./mole from osmometry data.

The infra-red spectra of the degraded and non-degraded polymer indicated that the anhydride group is unchanged but the bond next to it is broken in main chain scission.

With this copolymer, Grassie[36] commented that volatilisation

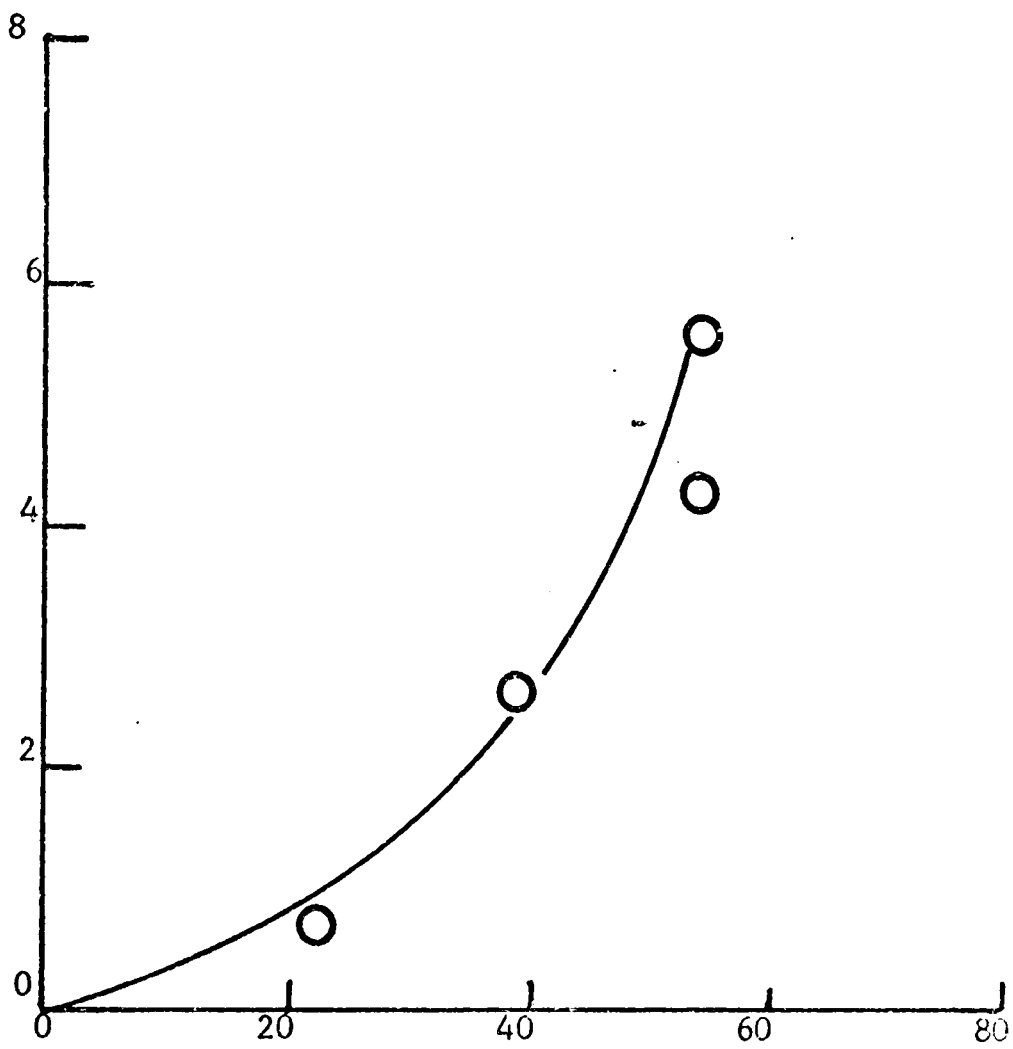

FIGURE I.3

Relationship between bonds broken and volatilisation in a copolymer of methyl methacrylate (95 mole %) and maleic anhydride (5 mole %) heated to 220°.

is not linear with the number of bonds broken, but exhibits auto-catalytic behaviour (FIGURE 1.3). However, this is due to the increased number of new chain ends being formed as a result of increased chain scission.

MacCallum[37] has proposed that PMMA suffers from "weak links" in the main chain. Thus the initial rate of chain scission of PMMA at 320°C is apparently greater than the rate of subsequent degradation.

5. The Photodegradation of Poly(Methyl Methacrylate)

a) Thin film degradation. Small amounts of gases are evolved[38-41] which arise from the splitting out of the ester side groups. These are methyl formate, methanol, methyl formate, methane, hydrogen, carbon monoxide and carbon dioxide. However, chain scission is the main manifestation of degradation with no crosslinking[42]. Quantum yields for chain scission lie within the range $2.3-3.9 \times 10^{-2}$ scissions per absorbed photon[43,44] in vacuum and $1.2-1.7 \times 10^{-2}$ scissions per absorbed photon in air or nitrogen[45,39].

The energy of ultra-violet radiation is of the same order of magnitude as the energy of chemical bonds. This means that the effects can vary with wavelength. 253.7nm has been the most common wavelength used though 301nm has also been used. In addition, the intensity of irradiation decreases with penetration of the film[43]. Surface effects have also been investigated[46].

A new chromophore is observed near 285nm in the absorption

spectrum after irradiation,[39,40,43,45,47] which has been ascribed to the formation of C = C double bonds.

Fox[39] observed that quantum yields were essentially independent of the incident intensity of the radiation and appeared to be a function only of the total energy absorbed. In the photolysis of gases, this is generally interpreted to mean that the termination step is first order with respect to the radicals involved. In a polymer sample, small reactive radicals might interact rapidly, but the somewhat immobile polymer radicals resulting from homolysis of a chain are unlikely to combine readily. Therefore, it was concluded that some sort of disproportionation reaction is involved. The authors suggested the following mechanism involving main chain carbon-carbon bonds:-

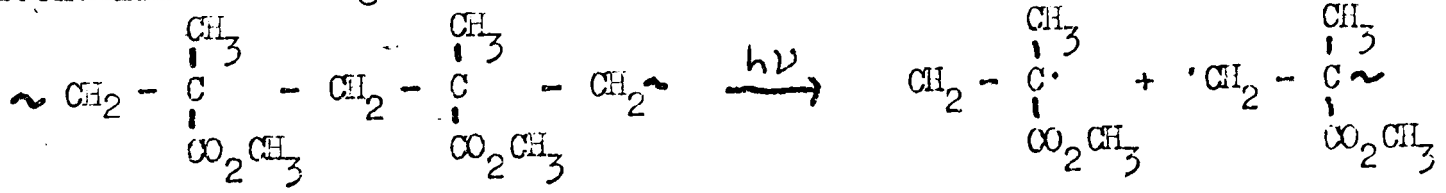

This would be followed by disproportionation:-

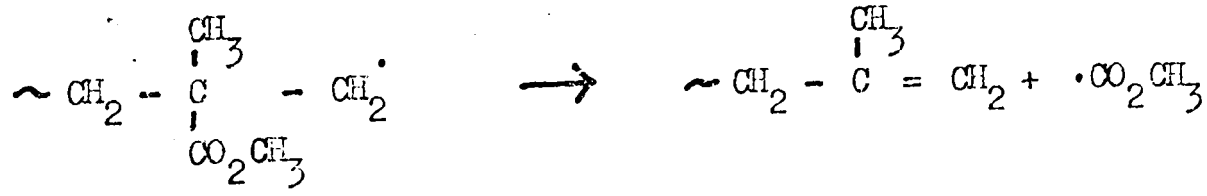

The ester radical can now react to form a number of products:-

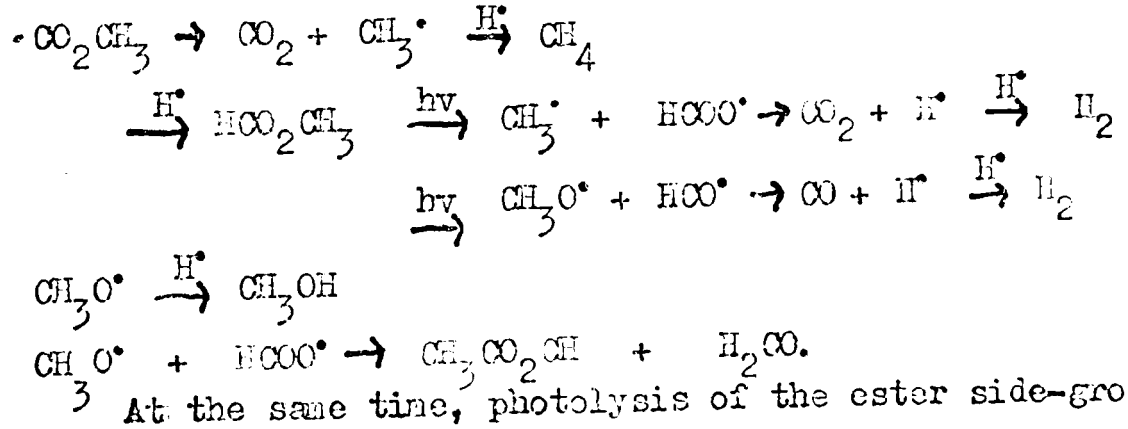

At the same time, photolysis of the ester side-groups could occur in either or both of two ways:-

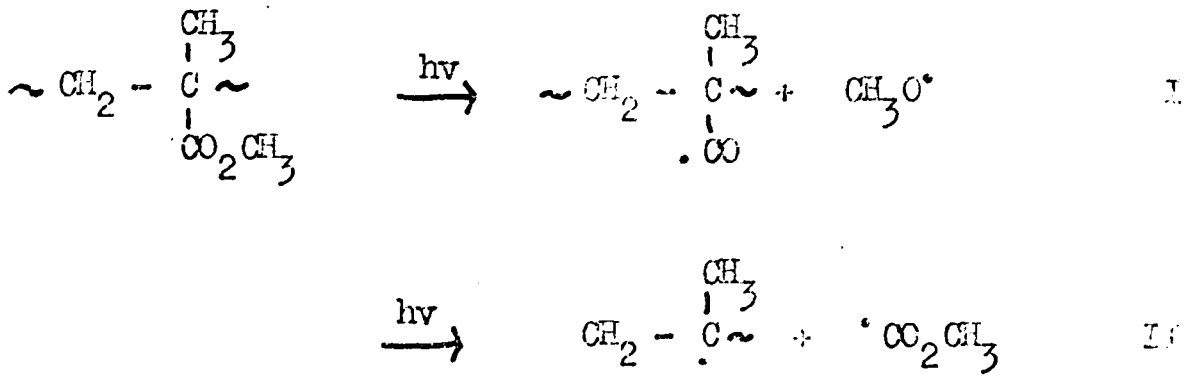

Allison[40] considered I a necessary precursor to main chain scission:-

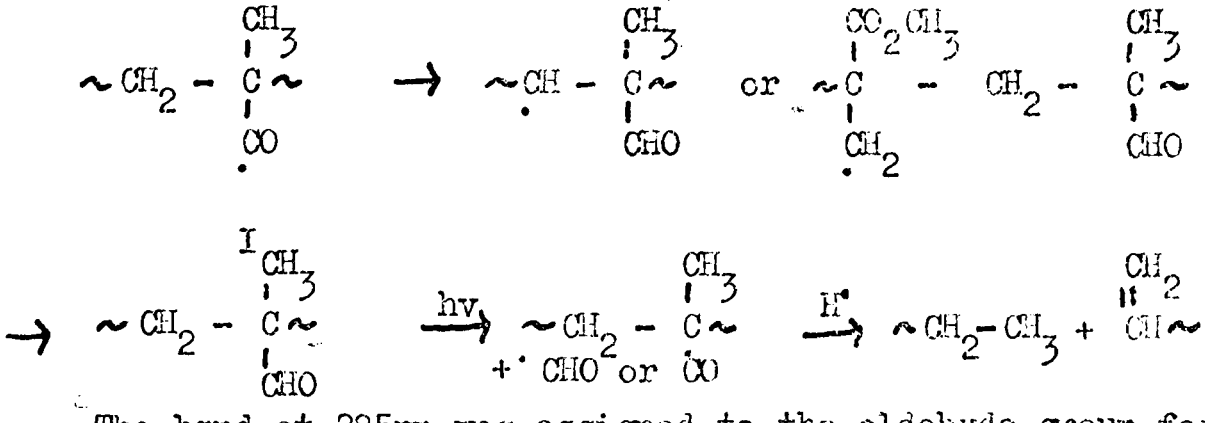

The band at 285nm was assigned to the aldehyde group formed on the polymer. The evolution of one carbon monoxide molecule per main chain break suggests that photoinduced aldehyde groups are precursors to main chain scission.

b) Solution Photodegradation. Several workers[42,48,49] have observed the effects of different solvents on the photolysis of PMMA. Although the main mode of degradation is that of chain scission, the extent depends on the solvent but not on the concentration of polymer.[42,45,49] After allowing for the effect of optical filtering by the solvent, Fox[49] obtained a quantum yield of 0.14 scissions per quantum.

In contrast, Jellinek and Wang[50] showed that the concentration of polymer in 2-chloroethanol under nitrogen affects the rate of

photolysis. It has also been suggested[51] that, in benzene solution, solvent radicals are formed which react with the polymer.

Photodegradation in solution has the advantage of eliminating many of the problems associated with bulk irradiation such as solid phase transitions, gaseous diffusion and crosslinking.

Previous work[52] has shown that even small amounts of maleic anhydride in PMMA accelerate the rate of photodegradation in solution. This is discussed more fully in Chapter 5.

c) Photodegradation at Elevated Temperatures. Cowley and Melville[53] studied the evolution of monomer during the irradiation of thin films between 130°C - 200°C, temperatures at which the thermal degradation of PMMA is negligible. In common with others,[45,54] they concluded that the primary process was photo-initiation at the chain ends. However, it is now believed that random initiation is followed by monomer evolution.[50,55] Quantum yields vary with temperature[56] but are very much higher than at room temperature.

6. The Thermal Degradation of Poly(methyl isopropenyl ketone) and Poly(methyl vinyl ketone).

The thermal degradation of PMIK and PMVK has been studied recently by McNeill and Neil[26,57]. The authors corroborated earlier reports[58-65] that, on heating the polymers, water is eliminated by aldol condensation, to give the cyclohexenone ring system:-

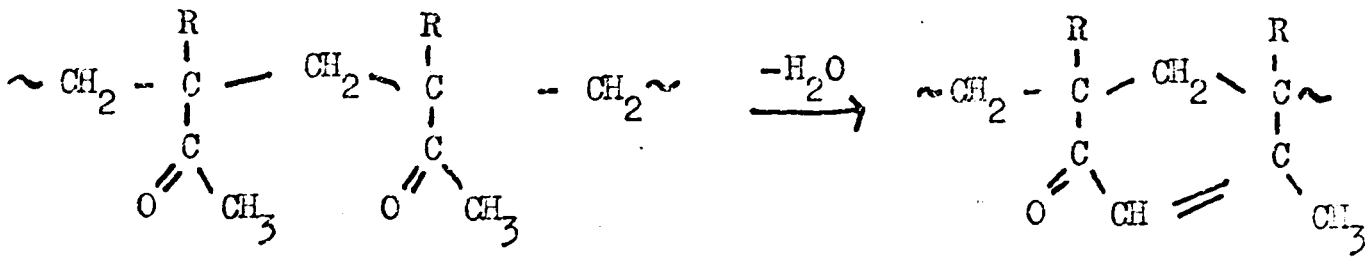

R = CH_3 for PMIK and R = H for PMVK

The cyclisations follow a random sequence limiting the loss of oxygen as water to a maximum of 85% in PMVK and 63% in PMIK.

The thermal degradation is described in detail in Chapter 6 in comparison with the copolymers with methyl methacrylate.

7. The Photodegradation of Poly(methyl isopropenyl ketone) and Poly(methyl vinyl ketone).

Studies of degradation in solution were carried out by Guillet and Norrish[66] on PMVK in dioxane using light of wavelength 313.0nm. In common with aliphatic ketones, two reactions are possible:-

Norrish Type I,

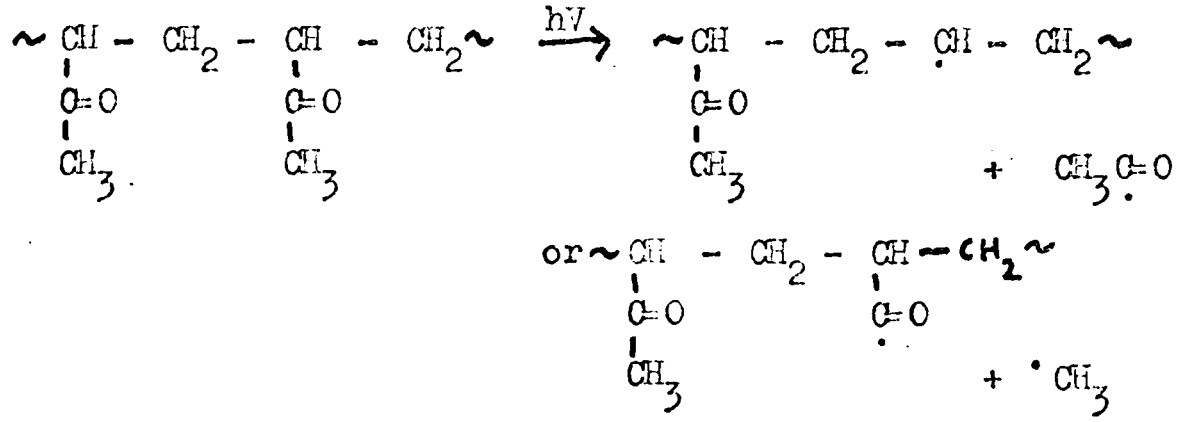

Norrish Type II, leading to chain scission,

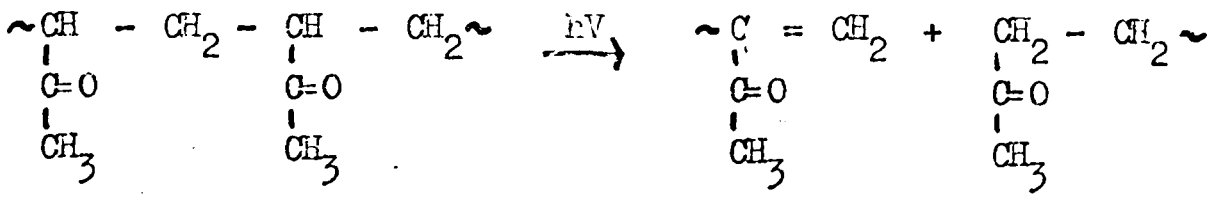

During the initial stages of the reaction, chain scission was found to vary linearly with time. However, the reaction slows down in later stages indicating an opposing reaction which may be due to a repolymerisation process:-

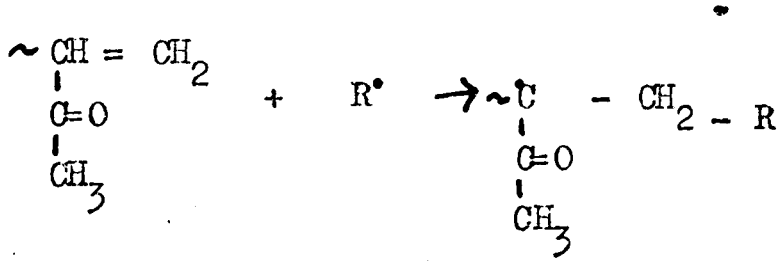

where R· is any other radical. The quantum yield for chain scission was estimated as 2.5×10^{-2}. Carbon monoxide, methane and acetaldehyde are formed as a result of the Type I reaction. Similar behaviour with PMVK was detected by Wissbrun[67] in thin films, with a similar quantum yield. The Type II reaction again appears to be independent of temperature.

At elevated temperatures, PMIK tends to release pure monomer in a similar manner to PMMA. While indicating that the mechanism of photodegradation of PMIK is very complex, the rapid drop in molecular weight is accounted for by a random initiation step:-

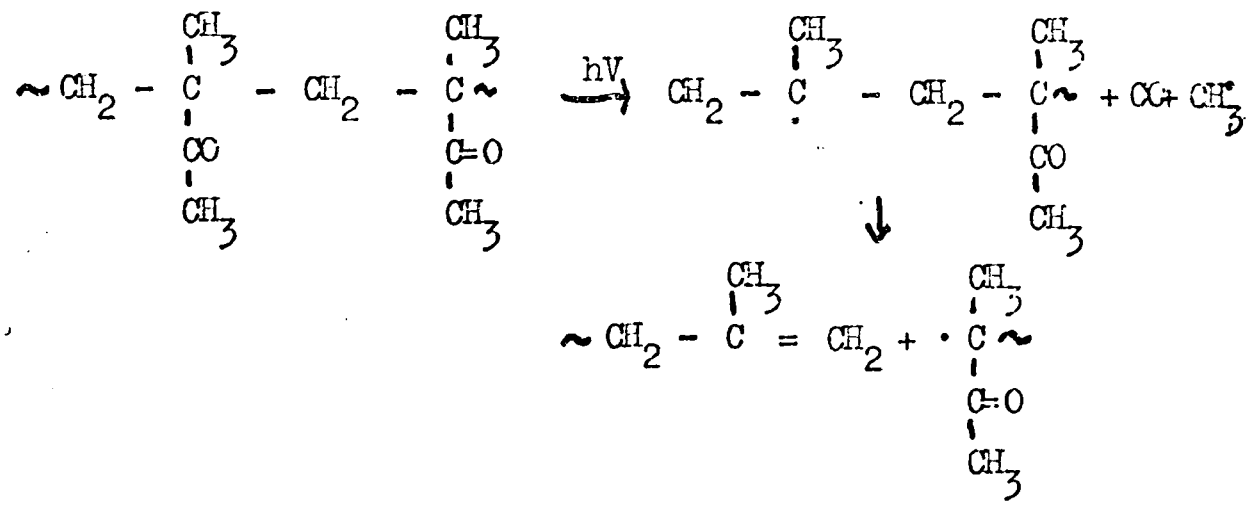

Small amounts of CO and CH_4 were detected.

Schultz[68] observed a quantum yield of 0.22 for random scission of PMIK films at 23°C in air which is an order of magnitude greater than that reported for PMVK[66,67] and is explained as being due to the higher energy radiation (253.7nm) and weaker main chain bonds of PMIK.

In a series of papers on the photochemistry of ketone polymers[69-77] Guillet has examined many of the properties of PMVK and PMIK. In particular,[71] a copolymer of methyl methacrylate with 3% methyl vinyl ketone was irradiated in benzene solution, thus each MVK unit had adjacent MMA units. 313.0nm radiation was used which was only absorbed by the ketone group. The quantum yield for chain scission was found to be approximately 0.2 which was unexpectedly high, almost ten times the value for PMVK.[66,67,71] Earlier work[69] with ethylene - carbon monoxide copolymers indicated that a six membered ring transition state with a γ H is a necessary precursor for the Norrish Type II process to occur. The MMA/MVK copolymer does not have a γH and the authors, therefore, suggest a seven - membered transition state:-

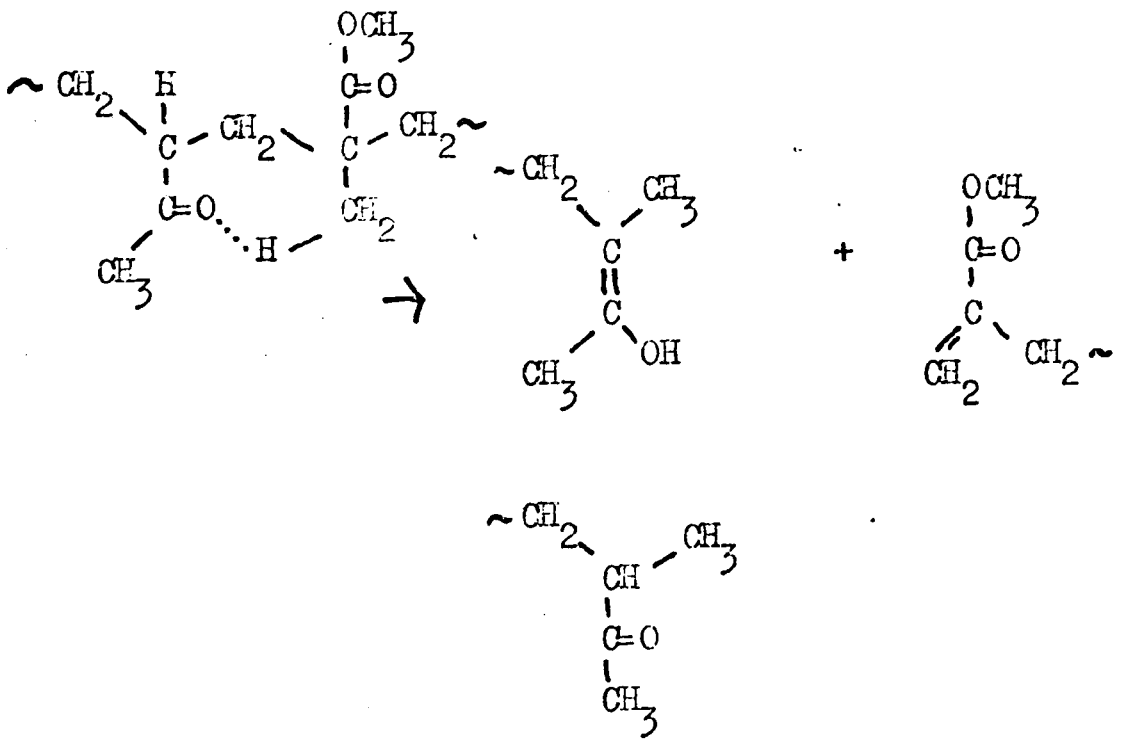

The quantum yield for chain breaking at 86°C which is above the glass transition temperature (75°C) was 0.12. At 25°C, the quantum yield is 0.0065. With the quantum yield equal to 0.21 in solution, it appears that molecular mobility is required in order to form the transition state.

The high value for the quantum yield is compared with that in PMVK in which the absorption of light by a ketone chromophore will result in the formation of an excited carbonyl group. This carbonyl will be in close proximity to a series of other ketone groups having similar energy levels and located at regular intervals along the backbone of the chain. On the other hand, an excited carbonyl in the MMA/MVK copolymer will be surrounded by MMA groups which have much higher energy levels, and so energy transfer will not be so efficient as in PMVK. This "trapping" of the energy at the ketone group will lead to chain scission whereas in PMVK, the energy is "diluted" among adjacent groups.

This mechanism has been criticised by Kato and Yoneshige[78] who irradiated a phenyl vinyl ketone/ methyl styrene alternating copolymer in benzene solution. This copolymer which lacks a γ H, degrades at a much slower rate than styrene/phenyl vinyl ketone and so does not seem to adopt the seven - membered ring transition state postulated by Guillet[71]. Norrish Type II degradation is inhibited and the polymer is said to degrade by Type I followed by photooxidation.

Instead, the authors suggest that the MMA/MVK copolymer shows higher hydrogen abstracting reactiviy toward the photoexcited ketone carbonyl than the styrene copolymer. Subsequent photooxidation accounts for the increased rate of degradation. Quantum yields were not quoted.

David et al[79] have described the photolysis of MVK and other polyketones and examined energy transfer in them.

8. Aim of this Work

Copolymers of methyl methacrylate and maleic anhydride are subjected to various degradation agencies in an attempt to determine the mechanisims of degradation and also to quantify the degradation. Similarly, copolymers of methyl methacrylate with methyl vinyl ketone and methyl isopropenyl ketone are examined and reactivity ratios determined.

CHAPTER TWO

EXPERIMENTAL

1. Preparation of Polymers

a) Monomers. Before polymerisation, methyl methacrylate (Hopkins and Williams), was distilled under reduced pressure to remove the hydroquinone inhibitor. The infra-red spectrum of a sample of the purified gaseous monomer was identical with that of published spectra.[80]

The inhibitor in methyl vinyl ketone (Fluka - supplied by Fluorochem Ltd) was removed by washing the monomer three times with dilute alkali solution followed by four washings with distilled water. It was dried over anhydrous magnesium sulphate.

Similarly, methyl isopropenyl ketone (Texaco Ltd.) was washed with alkali but drying over anhydrous magnesium sulphate apparently failed to remove all water, since, after freezing and thawing in liquid nitrogen, another phase appeared. This phase persisted even after distilling the monomer three times under reduced pressure. Neither did drying over calcium hydride completely dry the monomer which discoloured after several days. Although, it was not confirmed that this impurity was water, (it may have been stabilizer, inhibitor or dimer etc), its presence may have contributed to the unexpectedly low molecular weight obtained in polymerisations with methyl isopropenyl ketone (MIK). Castellano and Waugh[81] found that the water content in methyl vinyl ketone (MVK) was reduced to below 2% only after distilling the monomer

at 756mmHg. pressure, drying over anhydrous magnesium sulphate and another distillation. This could be reduced to below 1% by further drying over anhydrous magnesium sulphate and distillation under reduced pressure. In the purification of MIK in the present study, it was estimated that the second phase constituted less than 1% of the reaction volume in polymerisation.

Published reference spectra of MVK[80] and MIK[82] were identical to those obtained for gaseous MIK and MVK. MVK is also named as 3-buten-2-one and MIK as 3-methyl-3-buten-2-one in the literature.

Maleic anhydride (B.D.H. Ltd) was used as supplied since it was greater than 99.5% pure and the infra-red spectrum of the powder in a KBr disc was identical to published spectra[80]. Acid groups were not present.

The initiator used was 2,2' azobisisobutyronitrile (Eastman-Kodak) (also named 2,2' azobis(2 methyl propionitrile)). It was purified by twice recrystallising from ethanol, filtered and dried under vacuum. The initiator and monomers were stored in the dark at $-15^{\circ}C$.

b) Polymerisation. A weighed amount of initiator crystals was poured into a pyrex graduated dilatometer which was evacuated to a pressure of 10^{-6}torr. The dilatometer had a volume of 165mls. and a 5ml stem (see FIGURE 2.1) although smaller vessels were used on occasions. In maleic anhydride polymerisations a known weight of powdered monomer was added with the initiator.

TABLE 2.I

%Volume expansion on heating from 20°C to 60°C

MMA	MVK	MIK	MalA
4.5%	5.6%	5.4%	----

TABLE 2.2

%Volume contraction on I00% conversion

MMA[II6]	MVK[II5]	MIK[II4]	MalA
2I%	25%	24%	----

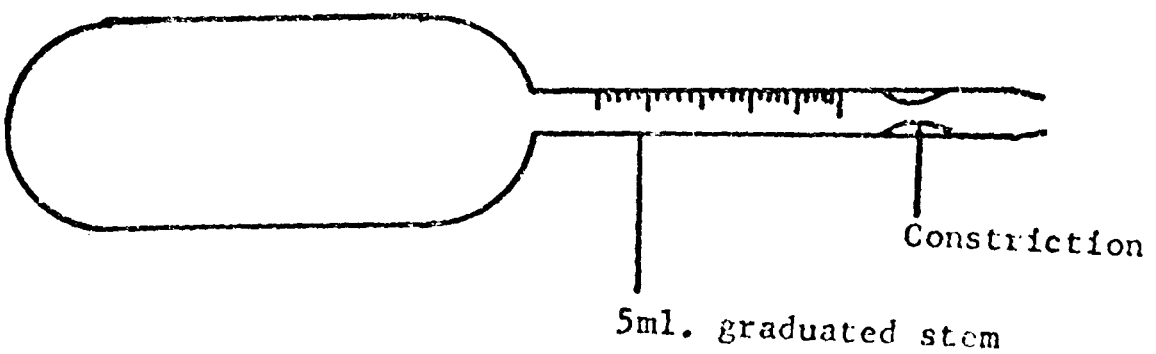

FIGURE 2.I

Polymerisation dilatometer

The liquid monomers MMA, MVK and MIK were degassed by three or four freezing and thawing cycles under vacuum using graduated reservoirs and distilled three times before the final distillation into the dilatometer. The first and last 5% in each distillation were discarded. MIK proved difficult to thaw because of its tendancy to crack the reservoirs and produce bright blue electrical discharges as it did so. This was overcome by thawing slowly over a period of one hour or more.

The dilatometer was sealed off and placed in a thermostat at $60^{\circ}C \pm 0.5^{\circ}C$ after ensuring that the initiator had dissolved in the liquid phase. Allowance had to be made for the expansion of the monomers from room temperature to $60^{\circ}C$ and so bringing the level of the reaction mixture to the 5ml graduated stem on the dilatometer. Therefore, the volume expansion was measured using a graduated measuring cylinder and the percentage expansion for each monomer is shown in TABLE 2.1. The solubility of maleic anhydride in MMA limited the range of copolymers that could be made by bulk polymerisation. The more stringent solubility requirements of the copolymers in toluene for molecular weight determination by osmometry restricted the range even further.

Polymerisation was terminated by immersing the dilatometer in liquid nitrogen. The conversion of monomer to polymer was followed by measuring the volume contraction that takes place during polymerisation. The percentage contraction for 100% conversion to polymer for each monomer is shown in TABLE 2.2. Conversion was never allowed to exceed 10%.

c) Recovery of Polymer. After breaking open the dilatometer, the contents were added dropwise to 3l. of methanol. The precipitate was dried and, in the case of PMMA and copolymers with maleic anhydride, redissolved in chloroform and reprecipitated in methanol. The copolymers with MVK and MIK were redissolved in acetone. The purification was repeated three times with the polymer solution being passed through a sintered filter of porosity 1 before final precipitation. The polymers were easily ground to a fine powder with the exception of those containing MVK, which became progressively more rubbery with increasing MVK content. The polymers were dried at 60°C under vacuum overnight. Analar reagents were used throughout. The composition of these polymers is discussed in the following chapter.

2. Degradation Apparatus

a) The Ultra Violet Source. Low pressure mercury Hanovia Chromatolite Lamps were used as the source of 253.7nm radiation in this work. They were connected to a L.T.H. Transistorised 1KVA Voltage Regulator to ensure that the lamps received a consistent voltage and were not affected by variations in mains output.

The mercury arc produces a typical mercury spectrum of which the 253.7nm wavelength has the strongest intensity. The output of this lamp is shown in FIGURE 2.2.

Under the experimental conditions employed, the U.V. light had to pass through air, fused silica, and, in the case of thin film degradation, a vacuum, before reaching the sample. These media, except vacuum since it should have no effect on radiation, will modify the

radiation from the lamp. In air, only oxygen will absorb any of the wavelengths emerging from the lamp, other common gases being transparent. The oxygen absorption spectrum consists of two sets of bands. One converges at 240.0nm but the more important Schumann - Range system has a threshold wavelength at 200nm converging towards 176.1nm[83,84]. These two absorptions correspond to two photo-disscciations of oxygen molecules:

$$O_2 + h\nu \longrightarrow O\,(^3P) + O\,(^1D)$$

and

$$O_2 + h\nu \longrightarrow 2\,O\,(^3P) \quad \text{respectively}$$

Ozone gas, which was noticeable by its smell whenever the lamps were in use, is produced concurrently as follows:

$$O(^1D) + O_2 + M \longrightarrow O_3 + M$$

$$O(^3P) + O_2 + M \longrightarrow O_3 + M$$

where M is the necessary third body.

The wavelength 253.7nm is not of sufficient energy to exceed the threshold of dissociation of oxygen. But the 184.9nm wavelength, the second strongest emitted line from the lamp, can and does dissociate oxygen. However, in doing so, it is completely absorbed in 1cm of air[85] and does not reach the polymer sample. Water vapour also absorbs this wavelength but is transparent to the main wavelength, 253.7nm. Fused silica transmits 96% of 253.7nm wavelength as can be seen from FIGURE 2.3.

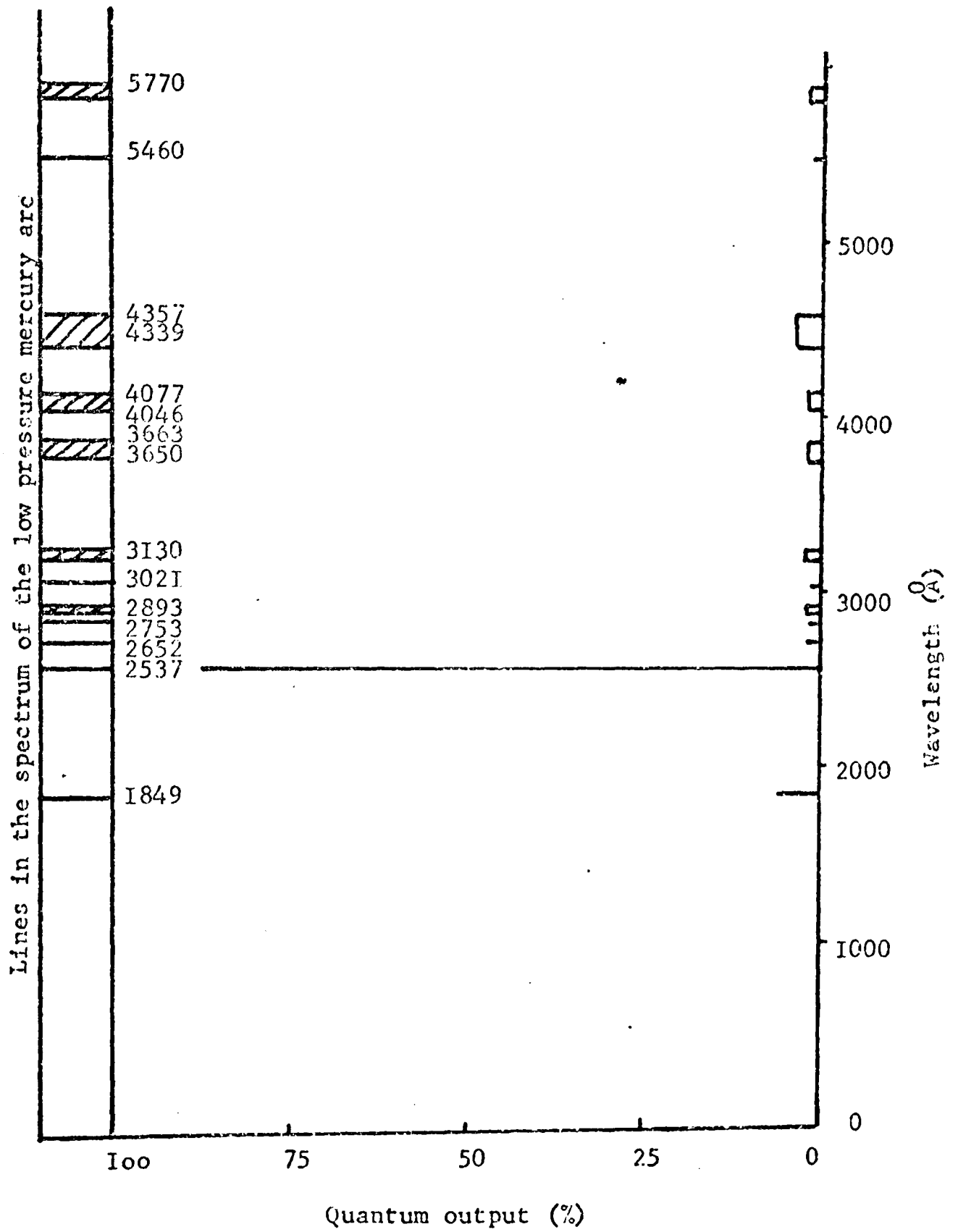

FIGURE 2.2

Output of Hanovia lamp

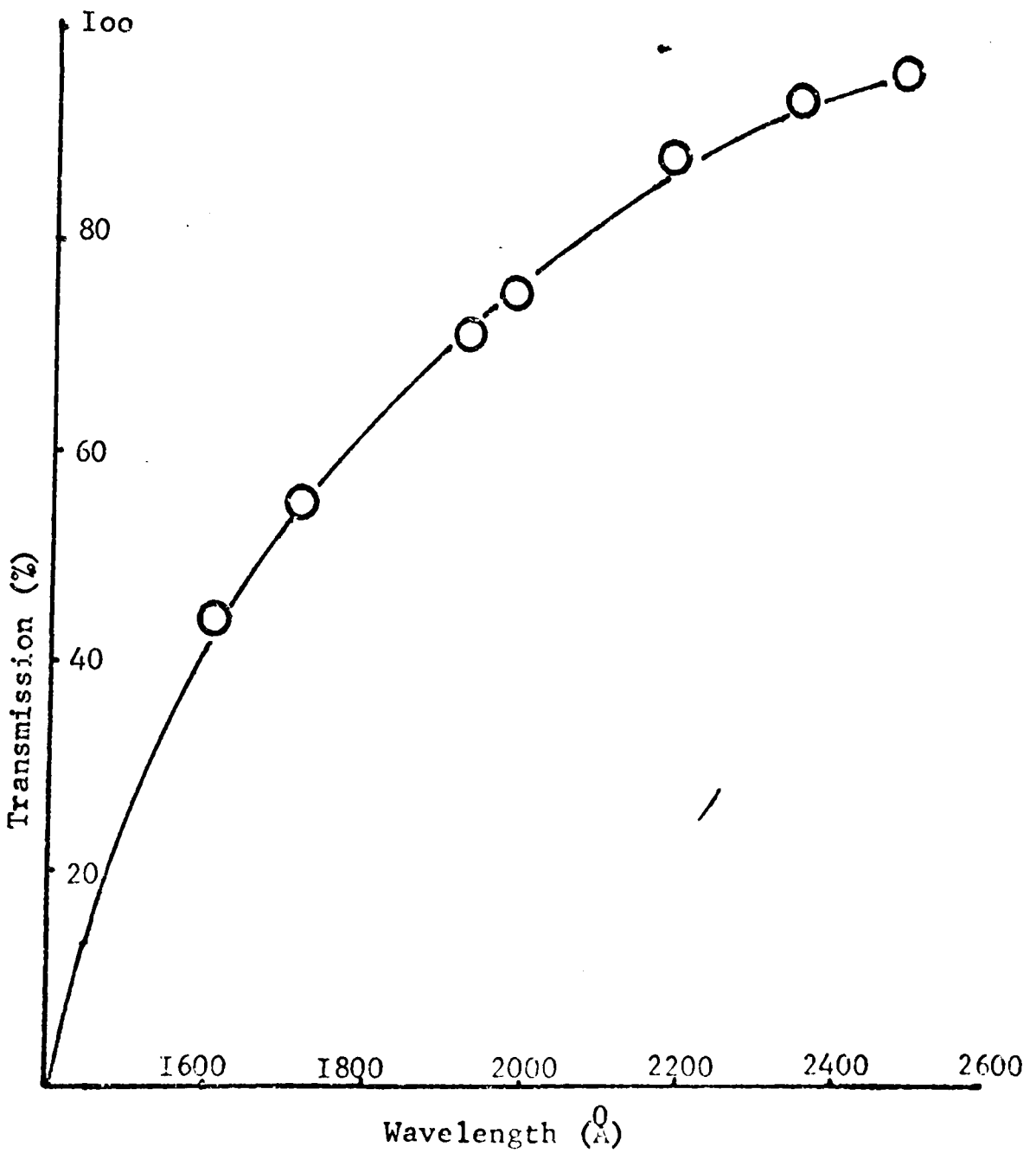

FIGURE 2.3
Absorbtion spectrum of fused silica (2mm.)

In view of the complete absorption of the 184.9nm line and the slight attenuation of the 253.7nm line, and, according to Hanovia literature[86], 90% of the lamp's output is 253.7nm, it was concluded that the source was virtually monochromatic. The lamps were allowed 15 minutes to warm up before sample irradiation commenced.

b) Actinometry. To check that the intensity of radiation emitted by the lamps did not vary with time, the number of quanta emitted by each source was determined by actinometry periodically. The method employed in this investigation involved the use of the potassium ferrioxalate solution phase chemical actinometer developed by Hatchard and Parker[87] which is simple to use but very sensitive over a wide range of wavelengths. It is based on the fact that when solutions of $K_3Fe(C_2O_4)_3$ in sulphuric acid are irradiated with light of wavelength 250-577nm, the iron is reduced to the ferrous state and the oxalate is oxidised. After irradiation, the ferrous ion can be converted into the red coloured 1, 10 phenanthroline - Fe^{2+} complex, which is highly absorbing and easily analysed spectrophotometrically. The experimental procedure was as follows:-

Solid green crystals of $K_3Fe(C_2O_4)_3$ were prepared as described by Hatchard and Parker[87] and Calvert and Pitts,[88] the latter giving a fully detailed summary of the procedure. The preparation and handling of the ferrioxalate solutions were carried out in a dark room. A standard calibration graph for the analysis of the Fe^{2+} complex was prepared, as shown in FIGURE 2.4, using a Hitachi Perkin Elmer 139UV-Visible Spectrophotometer.

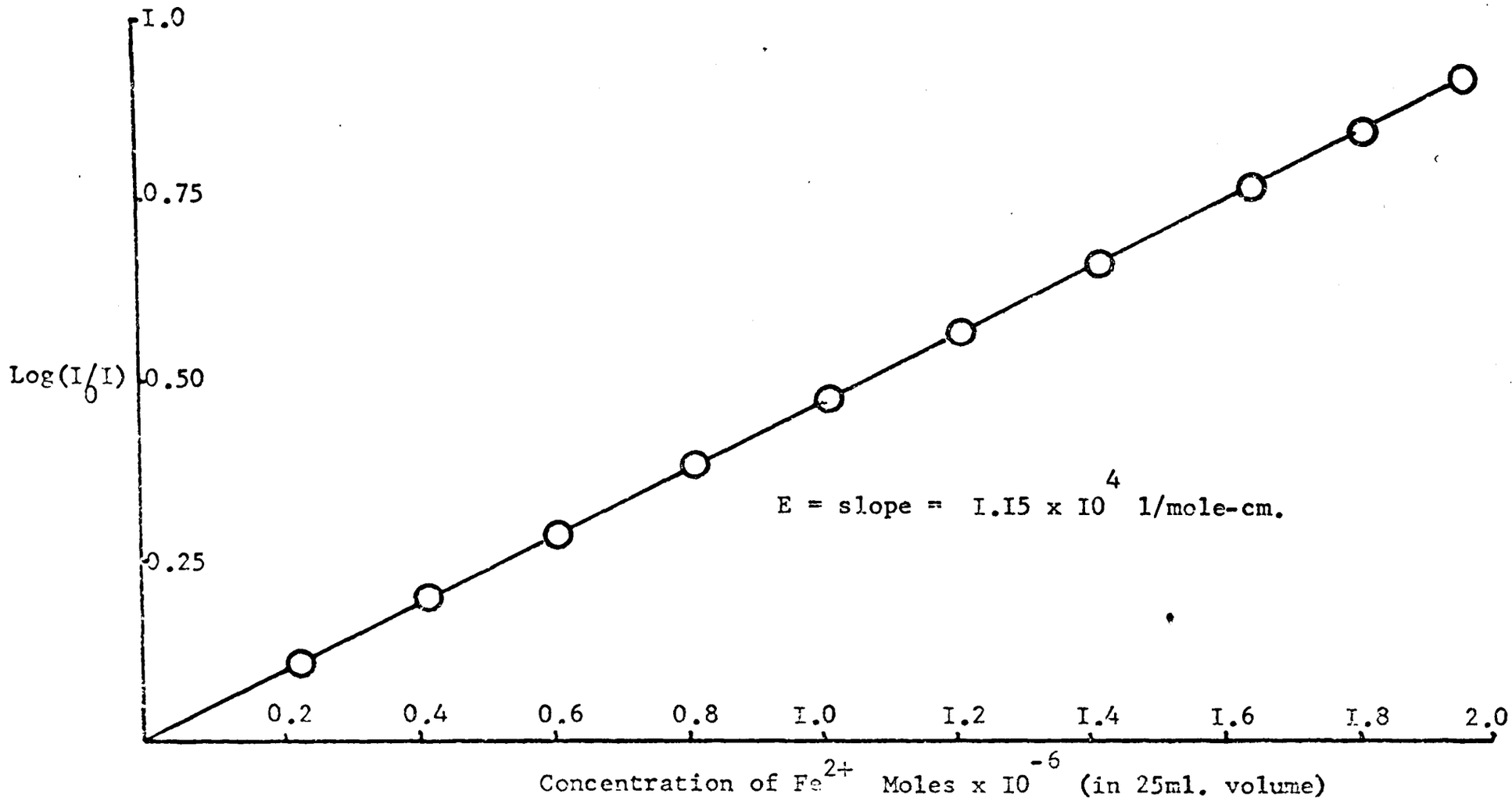

FIGURE 2.4

Calibration graph for ferrous ions (OD at 5I00 Å in a I cm. cell)

The intensity of light in any photolysis cell was determined by irradiating 15ml of ferrioxalate solution (V_1) for a period of 30 or 60 seconds. After mixing the solution, 10mls(V_2) was pipetted into a 25mls volumetric flask (V_3), 2mls of the phenanthroline solution and 5mls of buffer solution added, and the volume made up to 25mls with water. An identical blank solution was similarly prepared using unirradiated ferrioxalate solution. The transmission of the complex solution was measured at 510nm in a 1cm cell using the blank solution as a reference.

The number of Fe^{2+} ions formed during the photolysis (nFe^{2+}) was calculated using the formula

$$nFe^{2+} = \frac{6.023 \times 10^{20} V_1 V_3 \log (Io/I)}{V_2 LE}$$

where V_1 = volume of actinometer solution irradiated (mls)

V_2 = volume of aliquot taken for analysis (mls)

V_3 = Final volume to which the aliquot V_2 is diluted (mls)

$\log (Io/I)$ = Measured optical density of the solution at 510nm

L = Path length of the spectrophotometer cell used (cm)

E = Experimental value of the molar extinction Coefficient of the Fe^{2+} complex as determined from the slope of the calibration plot (FIGURE 2.4)

The light intensity at the sample, I_o^i, was calculated from the equation[88].

$$I_o^i = \frac{nFe^{2+}}{\Phi_{Fe^{2+}} t(1-10^{-E(A)L})} \quad \text{quanta/sec}$$

where $\bar{\Phi}_{Fe^{2+}}$ = quantum yield of the product Fe^{2+} (equal to 1.25 for the radiation of wavelength 253.7nm)

t = time of exposure

$(1 - I/I_o)$ = $(1 - 10^{-E(A)L})$ = fraction of incident light absorbed.

It was found that there was no reduction in the lamps efficiency during the photodegradative experiments.

c) Photodegradation in Solution. Photochemical reactions must be carried out in a vessel transparent to the wavelength of light used. Accordingly, photolysis cells were made of silica. A Hanovia Chromatolite lamp which has been described was inverted to irradiate the samples from below as shown in FIGURE 2.5. A typical irradiation cell is shown in FIGURE 2.6. Each cell was separated by a cardboard screen which effectively enables four distinct degradations to be carried out at the same time, ie. by removing a cell every half hour, irradiations of $\frac{1}{2}$, 1, $1\frac{1}{2}$ and 2 hours could be performed in 2 hours. There was no evidence of either the position of any one cell or the character of any one cell being different from any other position or cell.

About 500mg of polymer were dissolved in 20mls of dry solvent which was in general methyl acetate although other solvents were used on occasions. A graduated syringe was used to transfer 4mls of the solution to each cell. The solution was degassed four times on the vacuum line by freezing and thawing cycles in liquid nitrogen. This technique removed all the dissolved gases in particular oxygen, which might inhibit or accelerate the photodegradation. The cells were

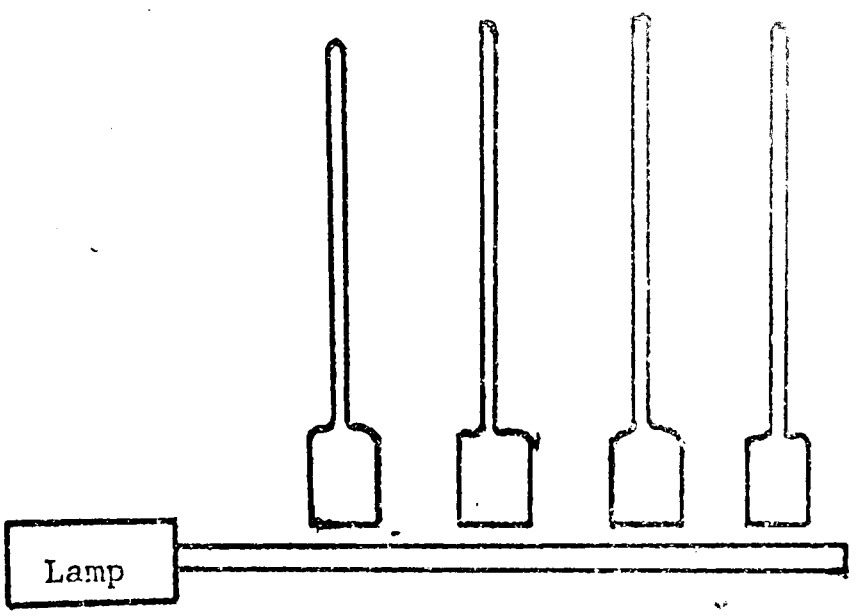

FIGURE 2.5
Ultraviolet irradiation of silica cells

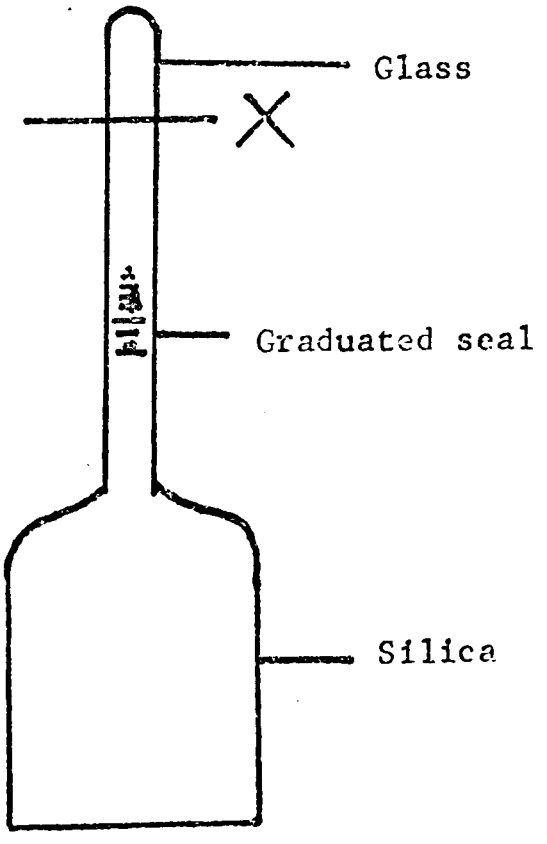

FIGURE 2.6
Silica irradiation cell

sealed off at a pressure of 10^{-6}torr.

On completion of degradation, each cell was broken open at the position marked x in FIGURE 2.6 and the contents transferred to a 10ml sample bottle, washing out the cell with solvent to transfer as much of the polymer solution as possible. A boiling stone was added and the bottle placed in an oven at 80°C to boil off most of the solvent. The bottle was then transferred to the vacuum line as shown in FIGURE 2.7 and the remainder of the solvent removed. This technique prevents the formation of a glass or film as the solvent is removed, and leaves the polymer in a flakey, powdery form. Finally, the bottle was left at 60°C overnight in a vacuum oven.

The samples were prepared for osmometry, by adding approximately, the correct volume of solvent (toluene or methyl ethyl ketone) to give a 1% w/v solution. The exact concentrations were determined by evaporating, at 80°C overnight, 1ml portions taken from the solution by pipette to a constant weight in a pre-weighed bottle.

d) Thermal and Photothermal Degradation. The apparatus is shown in FIGURE 2.8. The furnace was a Precision Oven capable of reaching temperatures over 400°C. Although the oven had a temperature control dial, the actual temperature in the cell was measured using a chromel-alumel thermocouple inserted through the top of the cell with the tip touching the silica disc. The cell was evacuated and TABLE 2.3 and FIGURE 2.9 show the oven setting versus cell temperature relationship. The heating rate of the oven is shown in FIGURE 2.10.

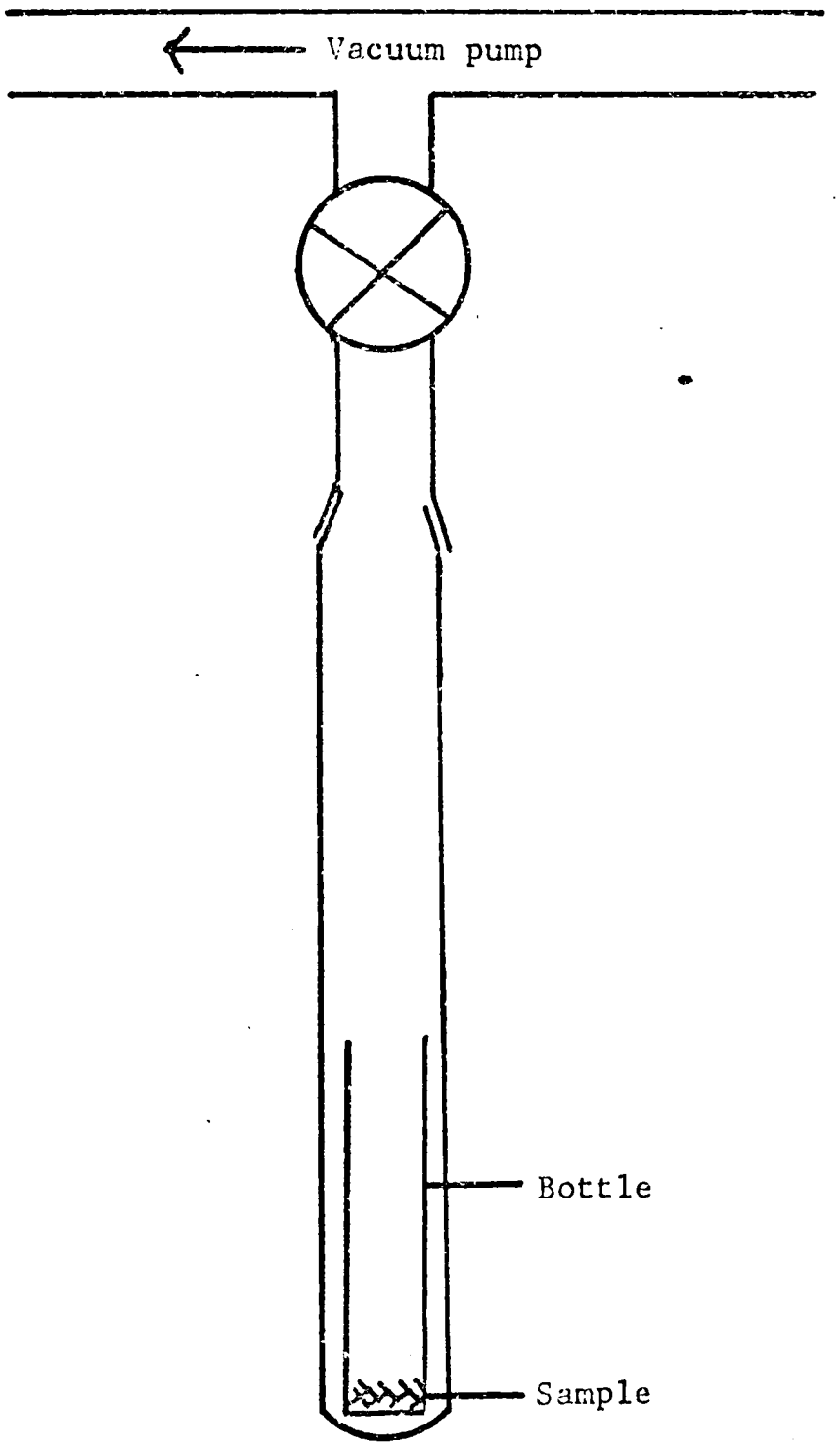

FIGURE 2.7
Removal of solvent on vacuum line

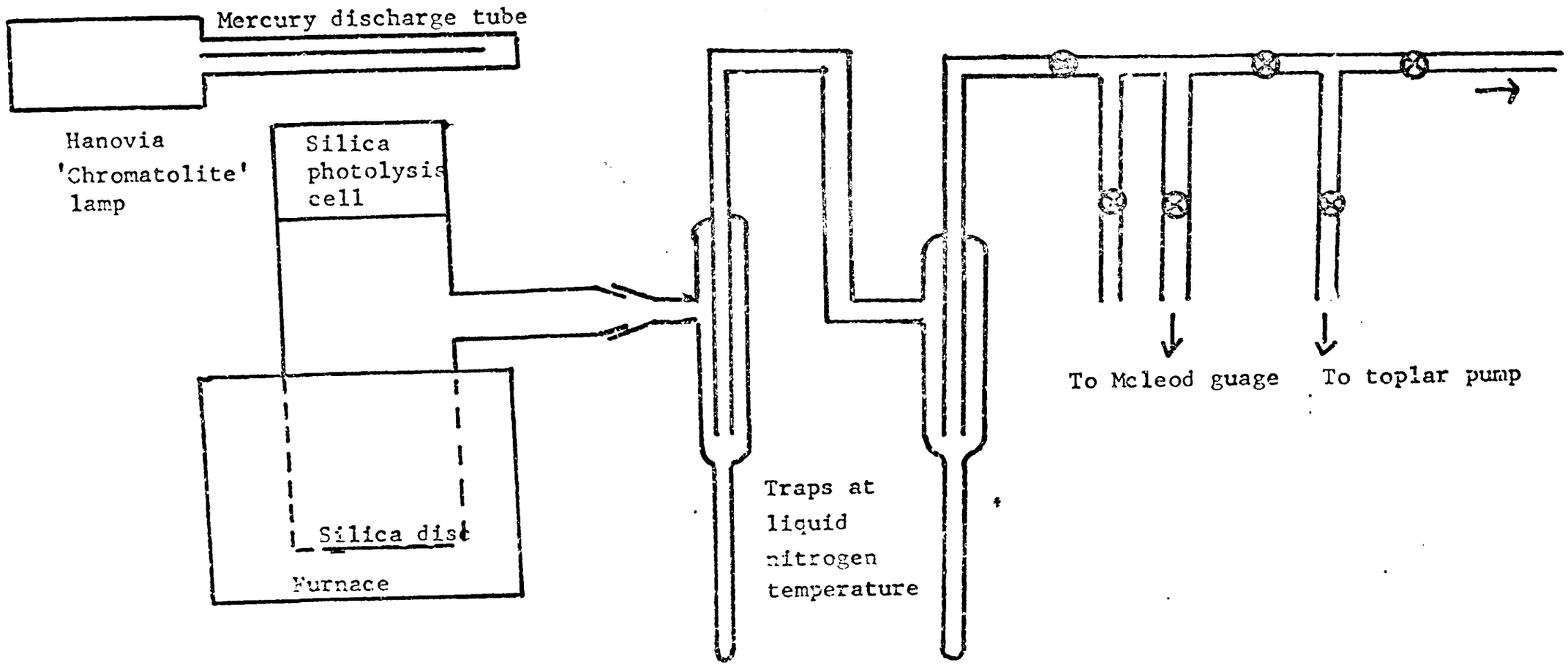

FIGURE 2.8
Photothermal degradation apparatus

TABLE 2.3

Oven setting versus cell temperature relationship

Oven setting °C	Cell temperature °C
50	47
I00	94
I20	II3
I40	I34
I60	I53
I80	I73
200	I93
220	2I3
240	234
260	255
280	276
300	297

FIGURE 2.9

Oven setting versus cell temperature relationship

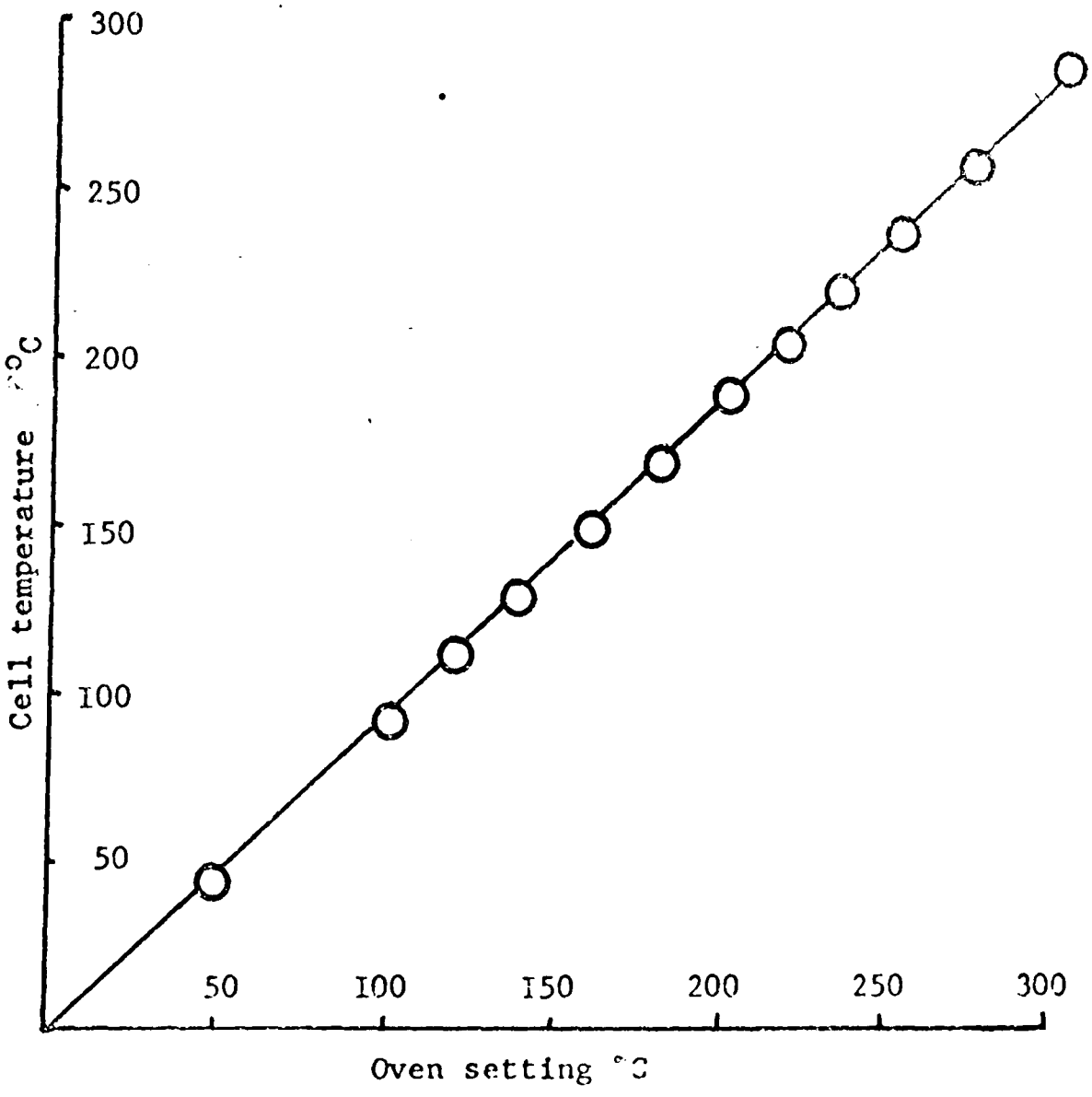

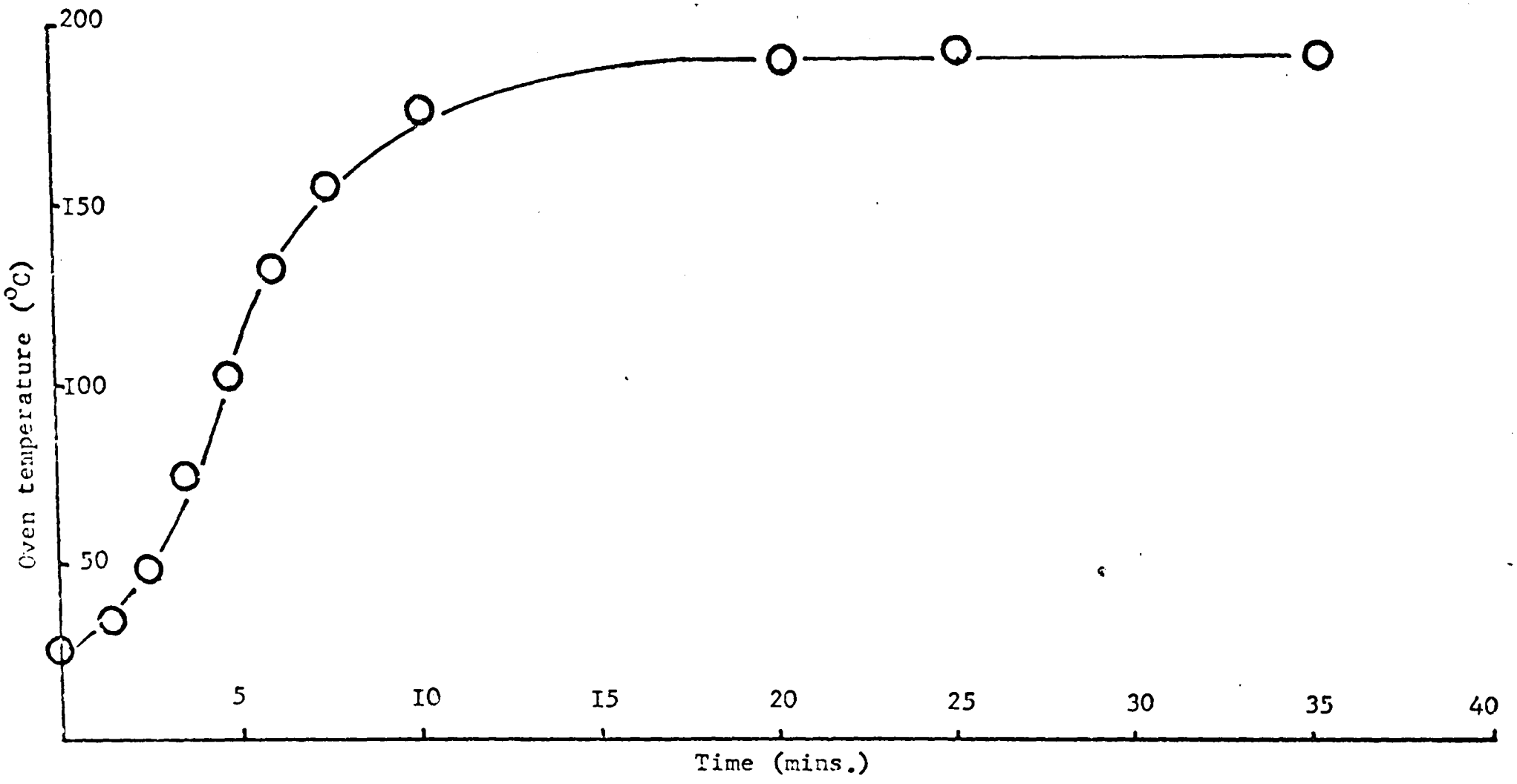

FIGURE 2.10 Oven heating rate

In thermal degradations, the sample, either in film or disc form, was weighed on a silica disc of known weight and placed at the bottom of the cell. The cell was evacuated to a pressure of 10^{-6} torr, tap T_1 closed and liquid nitrogen placed around the traps. The starting time was taken as the time at which the oven was switched on.

In photothermal degradations, the sample was exposed to ultra-violet radiation after it had reached the required temperature. Since this temperature was always lower than the threshold of thermal degradation, it was assumed that no degradation had taken place prior to exposure to U.V. light.

After completion of degradation, the gases in the traps were transferred under vacuum to an infra-red cell either by distillation or by töpler pump and the spectrum recorded. On occasions, the volatiles were distilled into a "cold finger" and weighed. The residue was reweighed and then dissolved in the appropriate solvent for molecular weight analysis.

c) Sample Preparation. Pressed discs of polymer were made by compressing typically 80-100mg of sample under vacuum at a pressure of 20tons/square inch. The diameter of each disc was 20mm and its thickness about 250μ. Because these discs were opaque, they were not used in photodegradation.

Films were prepared by adding, in two stages, 2mls of polymer solution of concentration about 50mg/ml. The solvent was evaporated in air overnight and then under vacuum at 120°C for 17 hours. The

problems of solvent removal are discussed in Chapter 5. The film thickness calculated from a knowledge of the diameter of the film, its mass and its density, and by measurement with a micrometer screw gauge, was about 80μ.

f) Photodegradation of Thin Films at Room Temperature. Films were cast placed in the irradiation cell and the system evacuated as in the previous section and as illustrated in Figure 2.8. After warming up the lamp, the sample was exposed to U.V. radiation without the oven being switched on, gases being trapped in liquid nitrogen. The products of degradation were treated as previously described.

g) Thermogravimetry. Thermogravimetry (TG) was carried out using a Du Pont 950 Thermogravimetric Analyser which employs a null type balance in which any weight change in the sample is opposed by an equal restoring force applied to the beam. This restoring force is then a measure of the change in the weight of the sample. The balance can be operated up to 1200°C, either isothermally or by programming at a heating rate of 0.5°C to 30°C per minute. The main disadvantage of this particular instrument is that it cannot be used under high vacuum conditions. Thus, exact comparison of result from TVA cannot be made.

In this study, a heating rate of 10°C per minute was used to degrade 5 or 10mg samples in an atmosphere of nitrogen.

h) Thermal Volatilisation Analysis. The technique of Thermal Volatilisation Analysis (TVA) was first described by McNeill[89] and measures the thermal conductivity of the volatile material evolved

from a heated polymer sample which is continuously being pumped.

In the basic TVA system, a Pirani gauge is attached to a vacuum system at a convenient point between the heated sample and the cold trap (-196°C). The products which leave the hot zone pass through the system and produce a response on the Pirani gauge. If an additional trap, at some temperature between ambient and that of the main trap, is placed before the Pirani gauge, as shown in FIGURE 2.11, then the gauge will now respond only to substances sufficiently volatile to pass through the trap. By varying the first trap temperature in a series of experiments a considerable amount of information about the nature of the products may be obtained.

The differential condensation TVA apparatus (DCTVA), shown in FIGURE 2.12 was later developed by McNeill[90] and allows the above information to be obtained in a single experiment. This system employs a series of five traps maintained at different temperatures, each followed by a Pirani gauge. The responses from the Pirani gauges are fed into a multi-point recorder so that they are recorded simultaneously. These traces of the responses are a measure of the rate of volatilisation against time. The traces give an indication of the amounts of the various products which are volatile at the various trap temperatures. A separate temperature versus time trace is also recorded so that when a linear temperature programme is used, as in normal practice, any deviations of the heating rate from linearity may be checked.

McNeill has extended TVA even further by incorporating a thermobalance similar to that in TG to give an additional trace

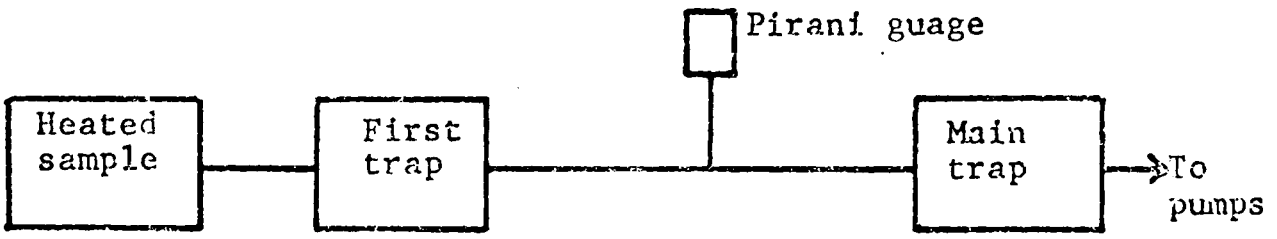

FIGURE 2.II

Basic TVA system

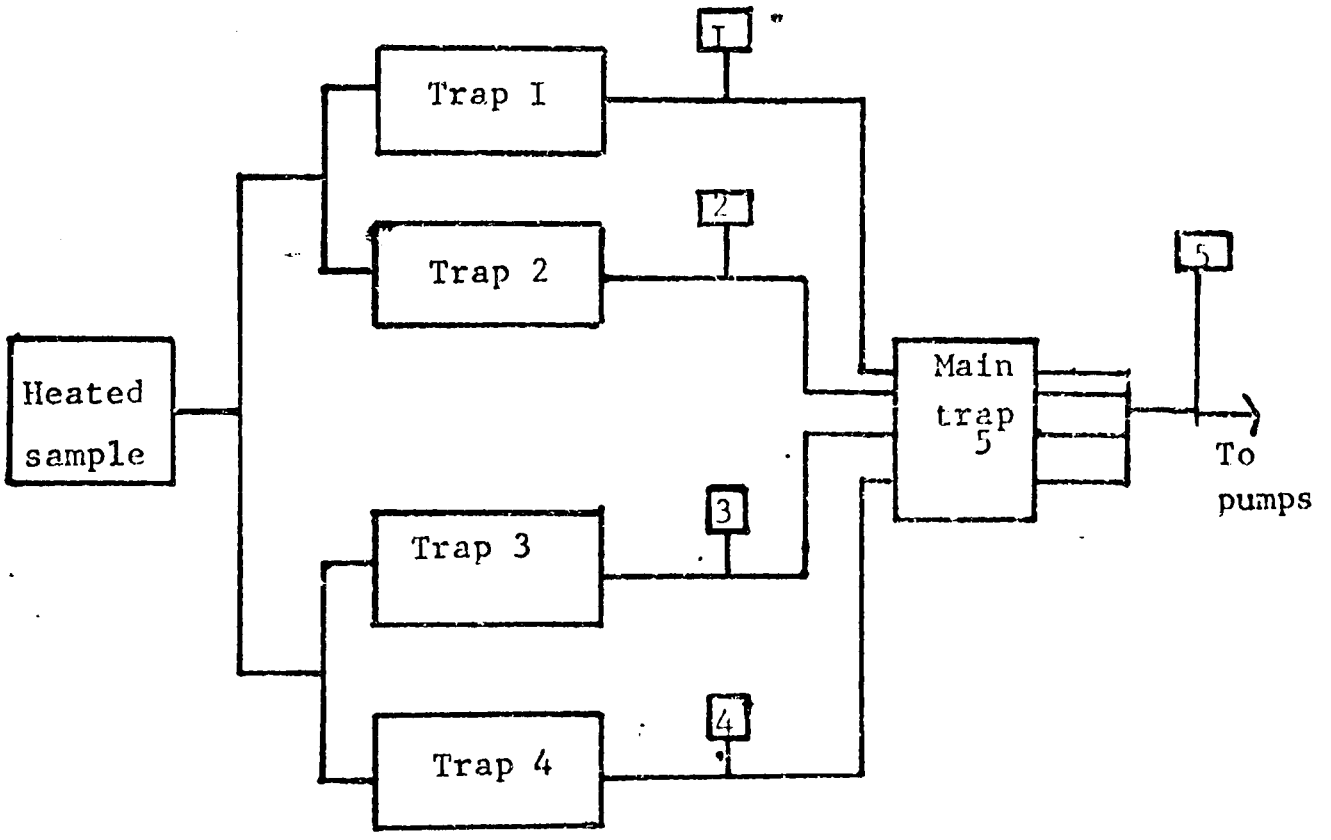

Normal working temperatures :

Trap I -100°C

Trap 2 - 75°C

Trap 3 - 45°C

Trap 4 0°C

Trap 5 -196°C

FIGURE 2.I2

Schematic representation of the four line differential condensation TVA system

recording the weight loss of the sample as it degrades.

It has been found that polymers give very characteristic thermograms and much information about stability, reaction mechanisms and the nature of the volatile products can be deduced. Further information can be obtained by analysis of the volatile materials which have condensed in the various traps, the short chain fragments which condense on the walls of the reaction tube outside the furnace and the residue.

3. Techniques of Analysis

a) Molecular Weight Measurement. The number average molecular weight was determined by a Mechrolab 501 High Speed Osmometer using Cellophane 300 membranes. Both toluene and methyl ethyl ketone were used as solvents.

The basic equation relating osmotic pressure to number average molecular weight $\bar{M}_n$, is the expression of Van't Hoff= $\pi = \frac{RTc}{\bar{M}_n}$

where R is the gas constant, T is the temperature, π is the osmotic pressure and c is the concentration of polymer in g/100g of solvent.

The molecular weight is obtained by measuring the osmotic pressure of the solution at different concentrations and by plotting π/c versus c. This should give a straight line plot from which $\pi/_{co}$ may be obtained by extrapolation to infinite dilation. A conversion factor depending on the solvent used, gives the number average molecular weight from $\pi/_{co}$. A typical plot is shown in FIGURE 2.13.

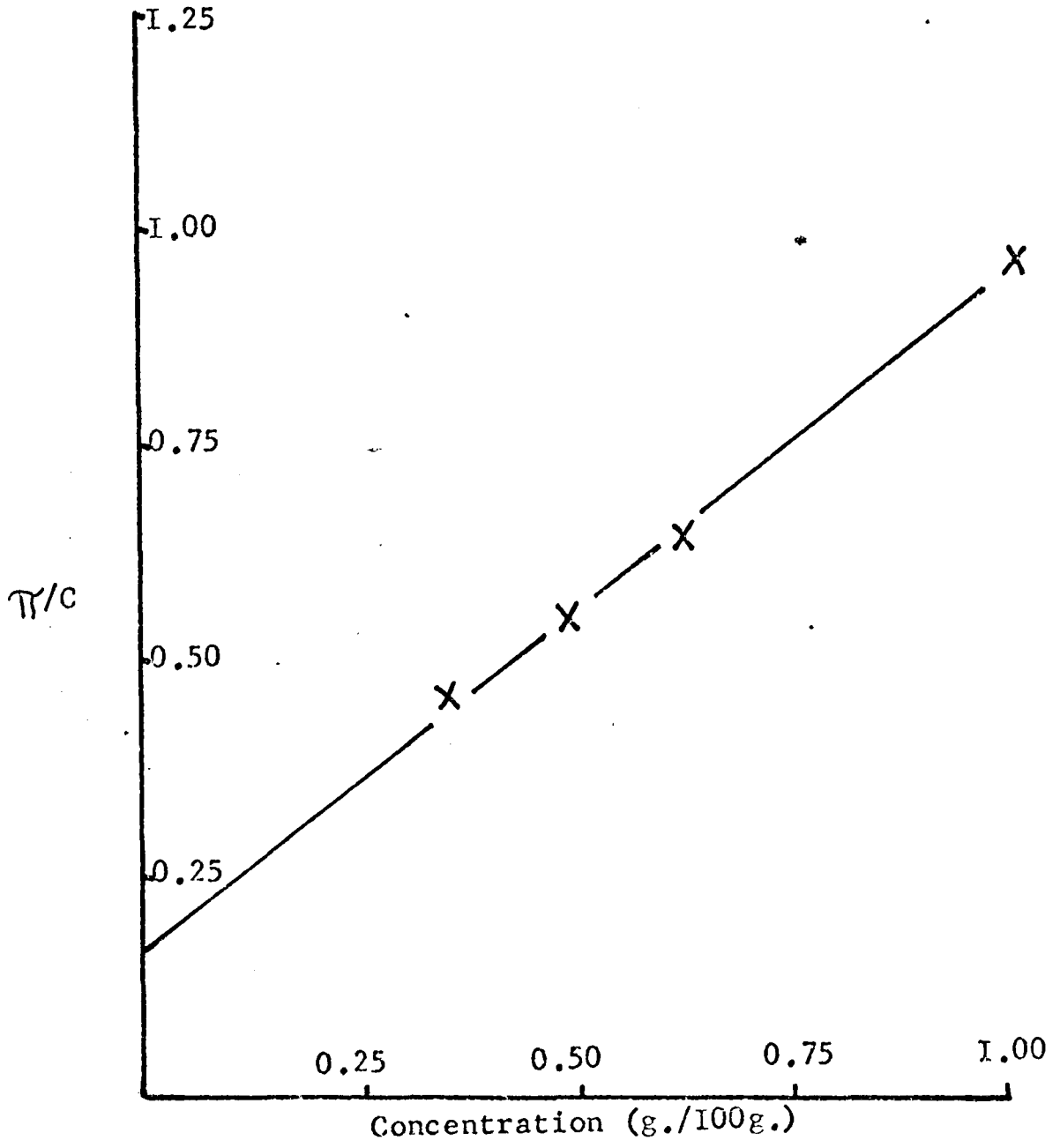

FIGURE 2.I3

A typical molecular weight plot

b) Spectroscopic Techniques. Infra-red spectra were recorded on a Perkin Elmer 257 Grating Spectrophotometer using, for gases, a cell of path length 10cm and for solids, KBr discs of mass 300mg containing 3mg of sample.

Ultra-violet spectra were recorded on a Unicam SP800 spectrophotometer using 10mm quartz cells.

Nuclear Magnetic Resonance spectra were recorded on a Varian 100 MH spectrometer using standard solutions in $CDCl_3$.

CHAPTER THREE

COPOLYMERISATION AND REACTIVITY RATIOS

1. Introduction

In the copolymerisation of two monomers, there are four possible propagation steps[91]

Reaction	Rate
$M_1^{\cdot} + M_1 \rightarrow M_1$	$K_{11}(M_1^{\cdot})\ (M_1)$
$M_1^{\cdot} + M_2 \rightarrow M_2$	$K_{12}(M_1^{\cdot})\ (M_2)$
$M_2^{\cdot} + M_1 \rightarrow M_1$	$K_{21}(M_2^{\cdot})\ (M_1)$
$M_2^{\cdot} + M_2 \rightarrow M_2$	$K_{22}(M_2^{\cdot})\ (M_2)$

Development of this scheme[92-95] leads to the copolymer composition equation:-

$$\frac{dM_1}{dM_2} = \frac{M_1}{M_2} \frac{r_1(M_1) + M_2}{M_1 + r_2(M_2)} \qquad - (1)$$

in which $r_1 = \frac{K_{11}}{K_{12}}$ and $r_2 = \frac{K_{22}}{K_{21}}$ and are known as the reactivity ratios. M_1 and M_2 are the molar amounts of monomer which lead to a copolymer containing the monomers in the ratio $\frac{dM_1}{dM_2}$

If F and (1-F) are the mole fractions of monomers 1 and 2 in the copolymer and f and (1-f) are the mole fractions of monomers 1 and 2 in the monomer feed, then the copolymer composition equation can be written:-

$$\frac{f(1-2F)}{(1-f)F} = r_2 + \frac{f^2(F-1)}{(1-f)2F} r_1 \quad - \quad (2)$$

By preventing the polymerisation reaction from exceeding 10% conversion to polymer, the monomer feed composition is assumed to be constant. If the composition of the monomer mixture and the resulting copolymer can be determined, then the reactivity ratios may be calculated.

Using C^{14} labelled MMA, Blackley and Melville[96] obtained the values $r_{MMA} = 3.5$ and $r_{Ma1A} = 0.03$ for the reactivity ratios of methyl methacrylate (MMA) and maleic anhydride (Ma1A) system polymerised at 60°C. Since, under the polymerisation conditions employed, maleic anhydride does not homopolymerise r_{Ma1A} should be zero. However, it was found that a copolymer containing more than 50% Ma1A could be prepared. This was ascribed to the effect of the penultimate group in the methyl metharylate radical affecting the reactivity of maleic anhydride. De Wilde and Smets[97] obtained the values $r_{MMA} = 6.7 \pm 0.2$ and $r_{Ma1A} = 0.02$ at 75°C. Copolymer composition analysis was done electrotitrimetrically, a method also used by Loucheux and Banderet[98,99] in addition to analysis for nitrogen after reaction with p-toluidine.

Reactivity ratios for MIK/MMA and MVK/MMA have not yet been evaluated.

2. Preparation of the polymers

The polymers were prepared employing the techniques described in Chapter 2 and the conditions in TABLE 5.1. The density of methyl

TABLE 3.1

Polymer	Codename	Volume of methyl methacrylate (mls.)	Amount of comoner	Mole fraction of comoner	% of initiator w/v
PMMA	PMMA	I65	———	———	0.0509
PMMA	new PMMA	I64	———	———	0.0396
PMMA	Aug PMMA	I65	———	———	0.0295
PMMA	73 PMMA	I65	———	———	0.0247
PMMA/MalA	I00/I	I60	5.I4I0g	0.0339	0.0077
PMMA/MalA	50/I	I56	I2.0363g	0.0776	0.0I39
PMMA/MalA	20/I	I45	24.3572g	0.I382	0.05I4
PMMA/MalA	I9/I	I45	24.6909g	o.I399	0.030I
PMMA/MalA	I8/I	I44	26.2754g	0.I485	0.03I8
PMMA/MalA	I2.5/I	I35	37.5570g	0.2I00	0.0495
PMMA/MIK	I/2	II0	54mls	0.344	0.0308
PMMA/MIK	I/I	82	82mls	0.5I7	0.0297
PMMA/MIK	2/I	50	II4mls	0.7I0	0.0322
PMIK	PMIK	0	I62mls	I.000	0.0350
PMMA/MVK	2%MVK	47	0.8mls	0.020	0.I00
PMMA/MVK	7%MVK	45	3mls	0.086	0.I00
PMMA/MVK	90/I0	I03	I0mls	0.II5	0.0278
PMMA/MVK	I5%MVK	4I	7mls	0.I84	0.I00
PMMA/MVK	70/30	48	I6mls	0.308	0.040
PMMA/MVK	70/30 (AD)	60	40mls	0.400	0.0297
PMMA/MVK	50/50	35	28mls	0.500	0.04
PMMA/MVK	50/50 (AD)	57	I02mls	0.705	0.0306
PMMA/MVK	30/70	I8	34mls	0.7I6	0.07
PMMA/MVK	I0/90	7	52mls	0.908	0.08
PMVK	PMVK	0	54mls	I.000	0.07

methacrylate was taken as 0.936g/c.c.[100], for methyl vinyl ketone as 0.864g/c.c[101], methyl isopropenyl ketone as 0.841g/c.c[101] and maleic anhydride as 1.48g/c.c[101], recorded at 20°C with a water reference at 4°C. The respective molecular weights were 101.11, 70.09, 84.12 and 98.06.

3. Methods of Analysis

The following techniques were used to determine the composition of the copolymers:-

a) Microanalysis
b) Infra-red spectroscopy
c) Ultra-violet spectroscopy
d) Nuclear magnetic resonance spectroscopy

a) Microanalysis. Powdered samples of polymer were submitted for elemental analysis for carbon and hydrogen. The results are shown in TABLE 3.2.

For the methyl methacrylate/maleic anhydride copolymers, the theoretical carbon content will range from 60% for PMMA to 59.2% for a 12.5/1 copolymer. This difference is obviously too small to make quantitative analysis worthwhile. While it can be seen from TABLE 3.2 that the expected trend of carbon content is maintained, the data is clearly of insufficient accuracy to warrant the determination of copolymer composition by this method. Even using a maleic anhydride mole fraction of 0.229 to 0.897 in the monomer feed, Blackley and

TABLE 3.2

Microanalysis results

Polymer	%C	%H	Polymer	%C	%H
PMMA	60.48	8.19	2%MVK	59.94	7.86
Aug PMMA	59.71	8.05	7%MVK	60.13	8.44
73 PMMA	59.80	7.86	90/10	61.38	8.39
100/1	61.58	8.30	15%MVK	58.77	8.52
50/1	60.40	8.14	70/30	61.60	8.33
20/1	59.46	7.91	70/30 (AD)	61.60	7.98
19/1	58.37	7.58	50/50	62.70	8.32
18/1	58.50	7.51	50/50 (AD)	64.64	8.27
12.5/1	58.81	7.62	30/70	64.21	8.32
1/2	63.70	8.74	10/90	65.88	8.43
1/1	65.00	8.90	PMVK	68.32	8.84
2/1	67.41	9.08	PMIK	71.18	9.59

Melville[96] found that microanalysis gave a considerable spread of results and noted that an error of 17% in carbon content would give rise to an error of 10% in the methyl methacrylate content of a copolymer.

The position is not so bad for the MIK/MMA and the MMA/MVK copolymers. The carbon content for PMIK and PMVK is theoretically, 71.43% and 68.57% respectively. Thus, by constructing standard curves (FIGURE 3.1) it is possible to determine the amount of MIK or MVK in any copolymer with MMA. Rather than take the theoretical values for the carbon content of PMMA, PMVK and PMIK, the experimentally determined values for these polymers were used in order to keep any constant inherent error in the microanalytical determination to a minimum. The results were in good agreement with theory.

The hydrogen content of these polymers is treated in a similar way (FIGURE 3.2). The mole fraction of the ketone groups in the copolymers as determined by this method is shown in TABLE 3.3.

Using equation (2) in which F is the mole fraction of the ketone in the copolymer and f is the mole fraction of the ketone in the monomer feed, and plotting $f\left(\frac{1-2F}{(1-f)F}\right)$ against $\frac{f^2(F-1)}{(1-f)^2F}$, then the intercept, r_2, will be the reactivity ratio of MMA and gradient, r_1, will be the reactivity ratio of the ketone. This is known as a Fineman - Ross plot[102]. The results for the copolymers of MVK as determined by hydrogen analysis were not plotted since it is obvious from TABLE 3.3 that the scatter of points would be wide. It

Figure 3.I

Standard curve of %C from microanalysis versus mole fraction of ketone

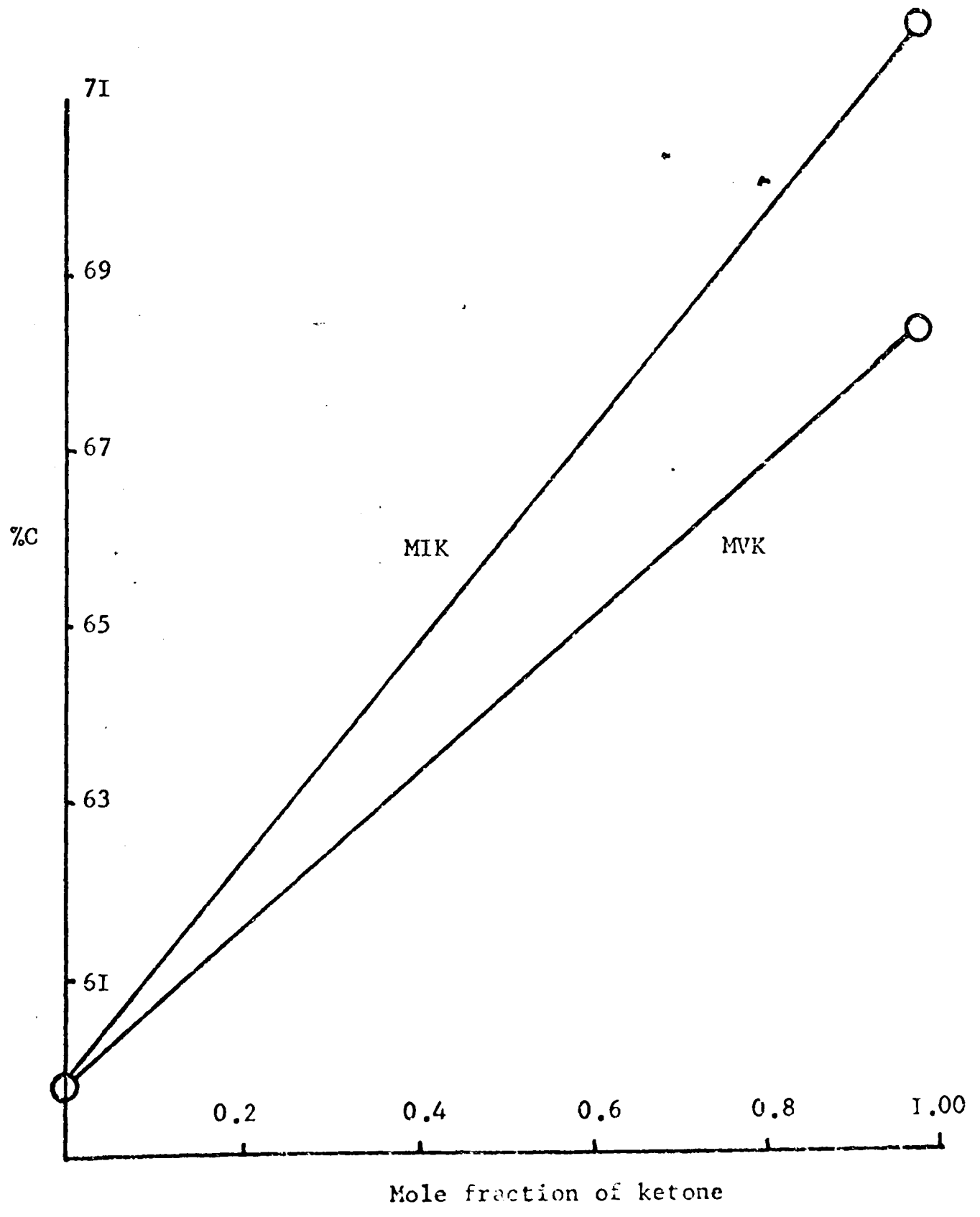

Figure 3.2

Standard curve of %H from microanalysis versus mole fraction of ketone

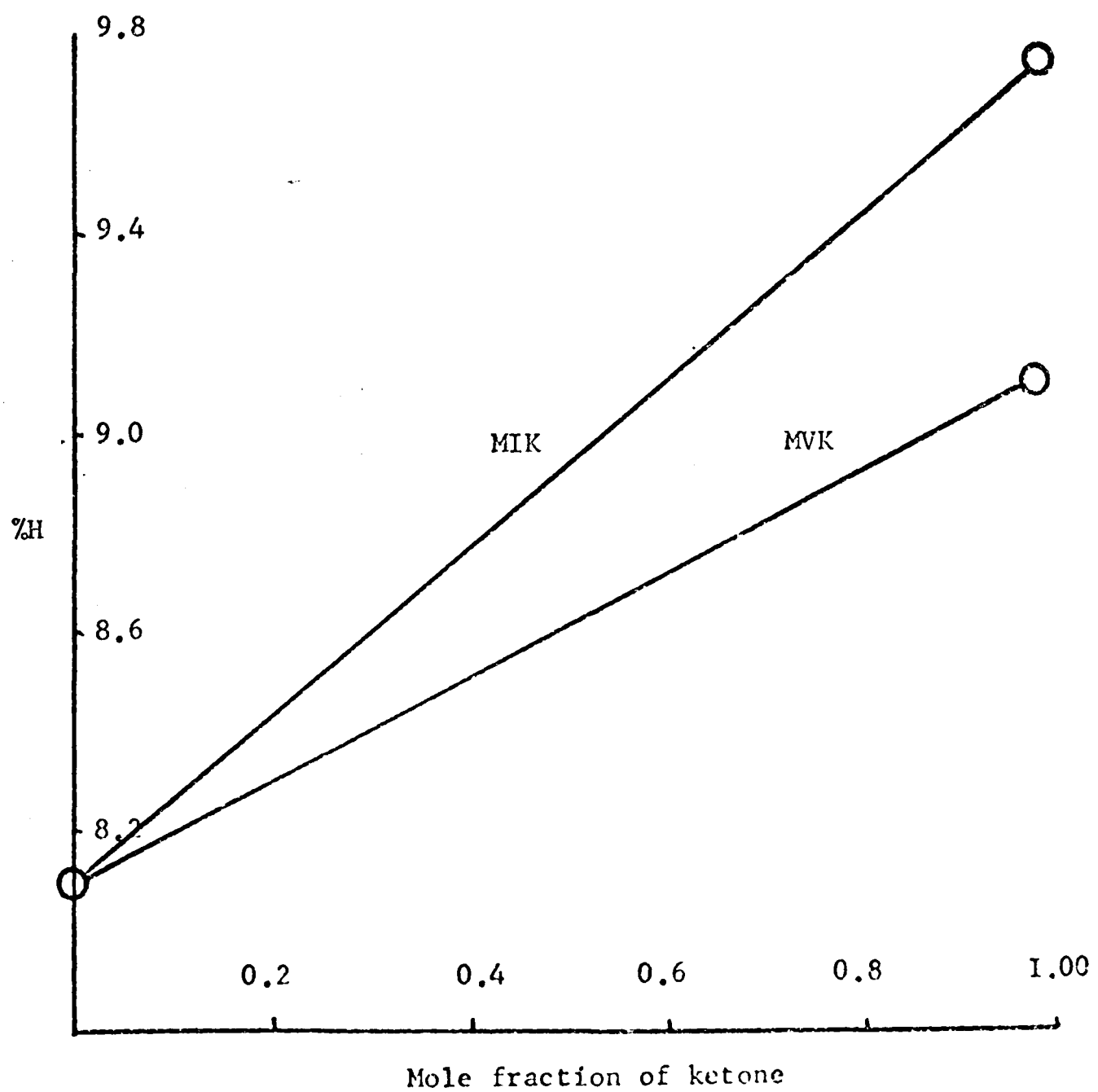

Table 3.3

Polymer	Mole fraction of ketone group from carbon analysis	Mole fraction of ketone group from hydrogen analysis
73 PMMA	0	0
1/2	0.342	0.508
1/1	0.457	0.601
2/1	0.669	0.705
PMIK	1.000	1.000
2%MVK	0.017	0.000
7%MVK	0.039	0.592
90/10	0.185	0.541
15%MVK	0	0.674
70/30	0.211	0.480
70/30 (AD)	0.211	0.122
50/50	0.340	0.469
50/50 (AD)	0.568	0.418
30/70	0.517	0.469
10/90	0.714	0.581
PMVK	1.000	1.000

can be seen from FIGURE 3.2 that an error 0.3% in hydrogen content, the best which can be expected from microanalysis, will lead to an error of 30% in the content of ketone in any MMA/MVK copolymer.

The Fineman - Ross plot for the MIK/MMA copolymers is shown in FIGURE 3.3 using the carbon and hydrogen microanalysis figures. The reason for the difference in the two lines is due to the relatively inaccurate determination of the hydrogen content in the copolymers. FIGURE 3.2 indicates that an error of 0.3% in hydrogen content can lead to an error of 20% in the ketone content of any MIK/MMA copolymer. However, using the carbon analysis data the error will be about 3% and therefore it is this line which will lead to the more accurate values for the reactivity ratios of the MIK/MMA copolymers. They are shown in Table 3.12.

Similarly, the Fineman-Ross plot for the MMA/MVK copolymers is shown in FIGURE 3.4. The reactivity ratios are presented in Table 3.12. From FIGURE 3.1 the error of 0.3% in carbon content will lead to an error of 4% in ketone content. A further source of error in microanalysis results from the rubbery texture of copolymers with high MVK content which makes microanalytical measurements more difficult and explains the relatively wider scatter of points in FIGURE 3.4 as compared with FIGURE 3.3. It is obvious from these results that the method of carbon and hydrogenanalysis is not sufficiently sensitive for the accurate determination of reactivity ratios in these systems.

b) Infra-red Spectroscopy. Previous work[103] on the determination of the reactivity ratios of MMA/MalA copolymers by quantitative infra-red

FIGURE 3.3

Fineman Ross plot for the MIK/MMA copolymers

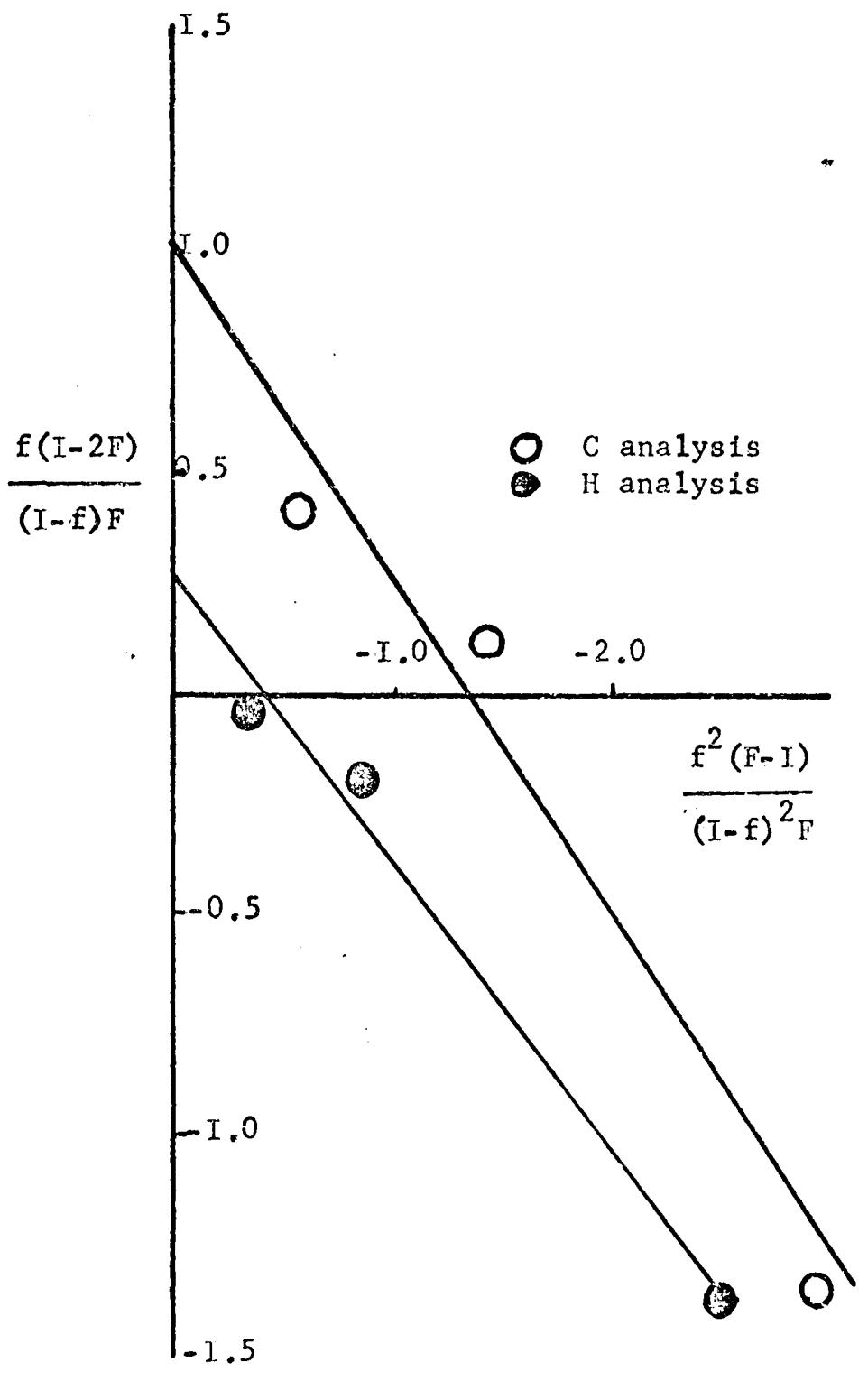

FIGURE 3.4
Fineman Ross plot for MMA/MVK from C analysis

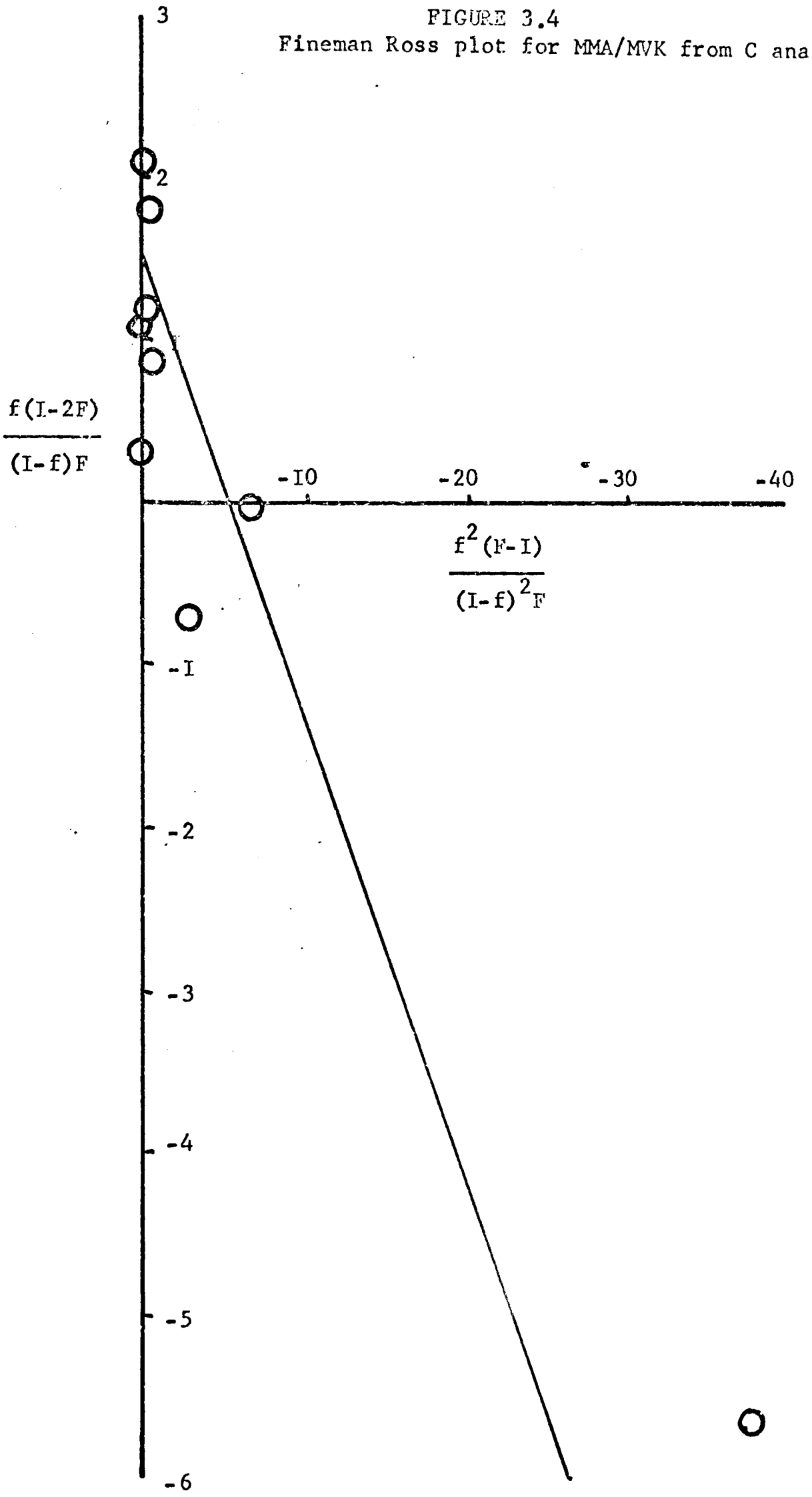

spectroscopy gave values in good agreement with those of Blackley and Melville.[96] The technique depends on the abnormally high extinction coefficient of the anhydride carbonyl stretching mode at 1790cm^{-1} (5.6μ) which is readily observed even in a copolymer containing as little as 1% of maleic anhydride. The ratio of methyl methacrylate to maleic anhydride in any copolymer is found by comparing the intensity of the anhydride absorption to an absorption due to the methyl methacrylate groups. The peak at 750cm^{-1} (13.5μ) is unique to PMMA. However, the extinction coefficients of these absorptions are not equal. In order to make quantitative comparisons with these peaks, mixtures of PMMA and succinic anhydride were prepared in known compositions. Succinic anhydride was chosen since it possesses a similar structure to the anhydride group in the copolymer. It was assumed that the extinction coefficient of the succinic anhydride and the copolymer anhydride were the same.

The spectra of the mixtures, as KBr discs, were recorded on a Perkin - Elmer 257 Grating Infra-red Spectrophotometer. The anhydride carbonyl absorption appears at 1785cm^{-1} (5.6μ). The absorbance or optical density of the anhydride carbonyl peak was measured by drawing a base line for each peak and reading off the transmittance at the peak height and base. These two values are converted to absorbance and thus the absorbance due to the carbonyl peak is calculated. The absorbance of the PMMA peak was similarly obtained.

Defining X by:-

$$X = \frac{\text{absorbance of succinic anhydride}}{\text{absorbance of PMMA}}$$

and plotting against the known PMMA composition of the mixtures, FIGURE 3.5 can be drawn. By measuring X for the copolymers, the composition of the copolymers can be read directly from FIGURE 3.5. From the results, a Fineman - Ross curve was drawn giving values of $r_2 = 3.36$ and $r_1 = 0.04$ (FIGURE 3.6, line b)) which were in close agreement with those of Blackley and Melville, $r_2 = 3.5$ and $r_1 = 0.03$ (see FIGURE 3.6 line a)). Since the resolution of the anhydride peak from the ester peak can be poor on occasions when the sample is not sufficiently well ground to avoid broadening of these peaks, the infra-red spectra were recorded in chloroform solution on a Perkin - Elmer 225 Grating Infra-red Spectrophotometer. Once again, mixtures of succinic anhydride and PMMA were prepared and the solution spectra recorded. However, this time, the anhydride peak was compared with the ester absorbance. TABLE 3.4 shows the results obtained by comparing the absorbances of the anhydride and ester peaks, and FIGURE 3.7 the standard curve from plotting Y, where $Y = \frac{\text{absorbance of anhydride}}{\text{absorbance of ester}}$, against the mole fraction of anhydride. Because of the relative insolubility of succinic anhydride in chloroform, mixtures containing higher percentages of anhydride could not be prepared and so the line was extrapolated to cover the range necessary for comparison with all the copolymers.

Although PMMA does not contain anhydride groups, there is a small absorption at $1780cm^{-1}$ due to the shoulder of the ester peak at $1730cm^{-1}$. By including this absorption in FIGURE 3.7, this contribution is removed from the calculation of the anhydride absorbance. A typical spectrum, that of the 20/1 copolymer, is shown in FIGURE 3.8. The

FIGURE 3.5

Calibration curve of X versus % methyl methacrylate

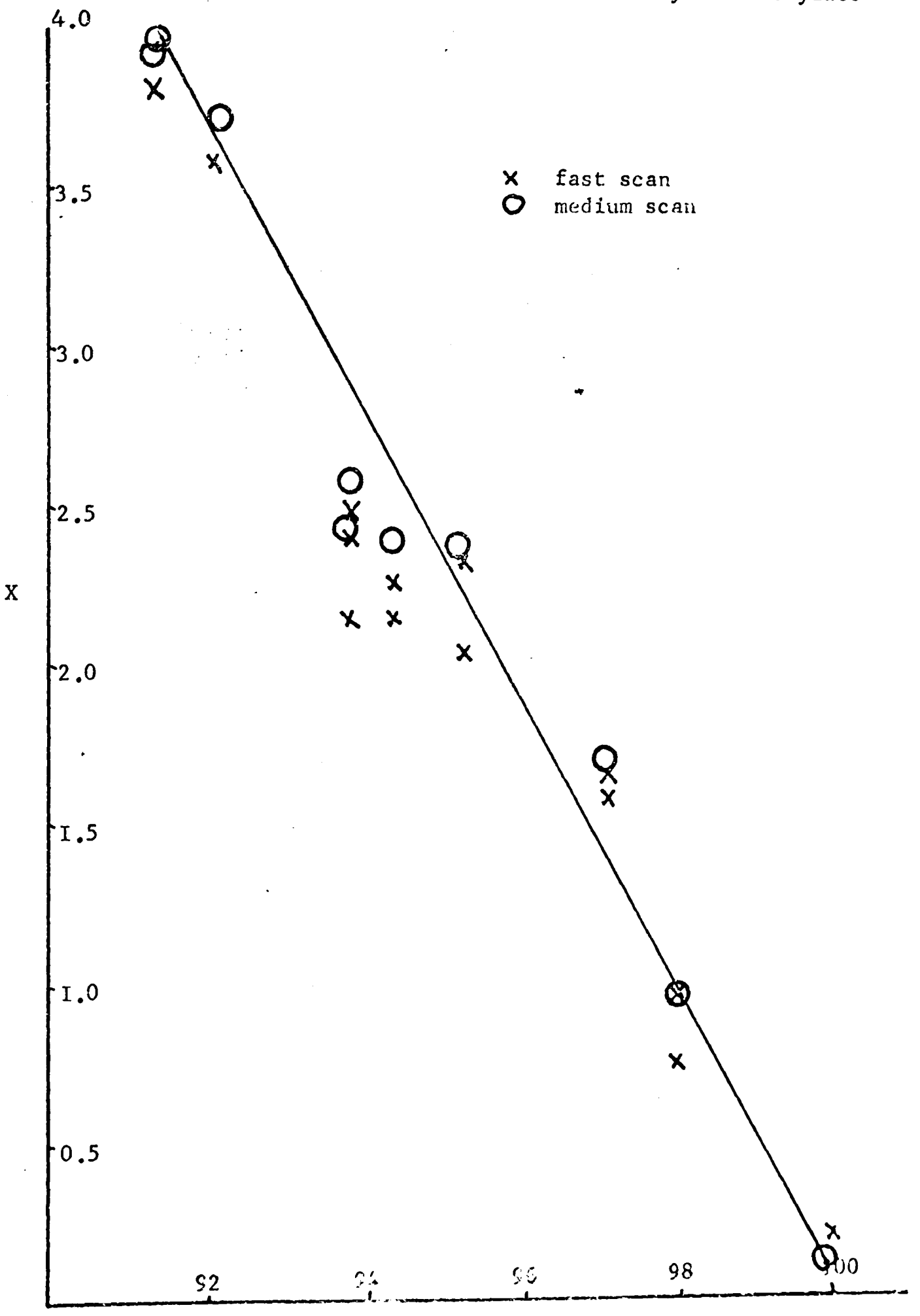

FIGURE 3.6
Fineman Ross plot for MMA/MalA copolymers

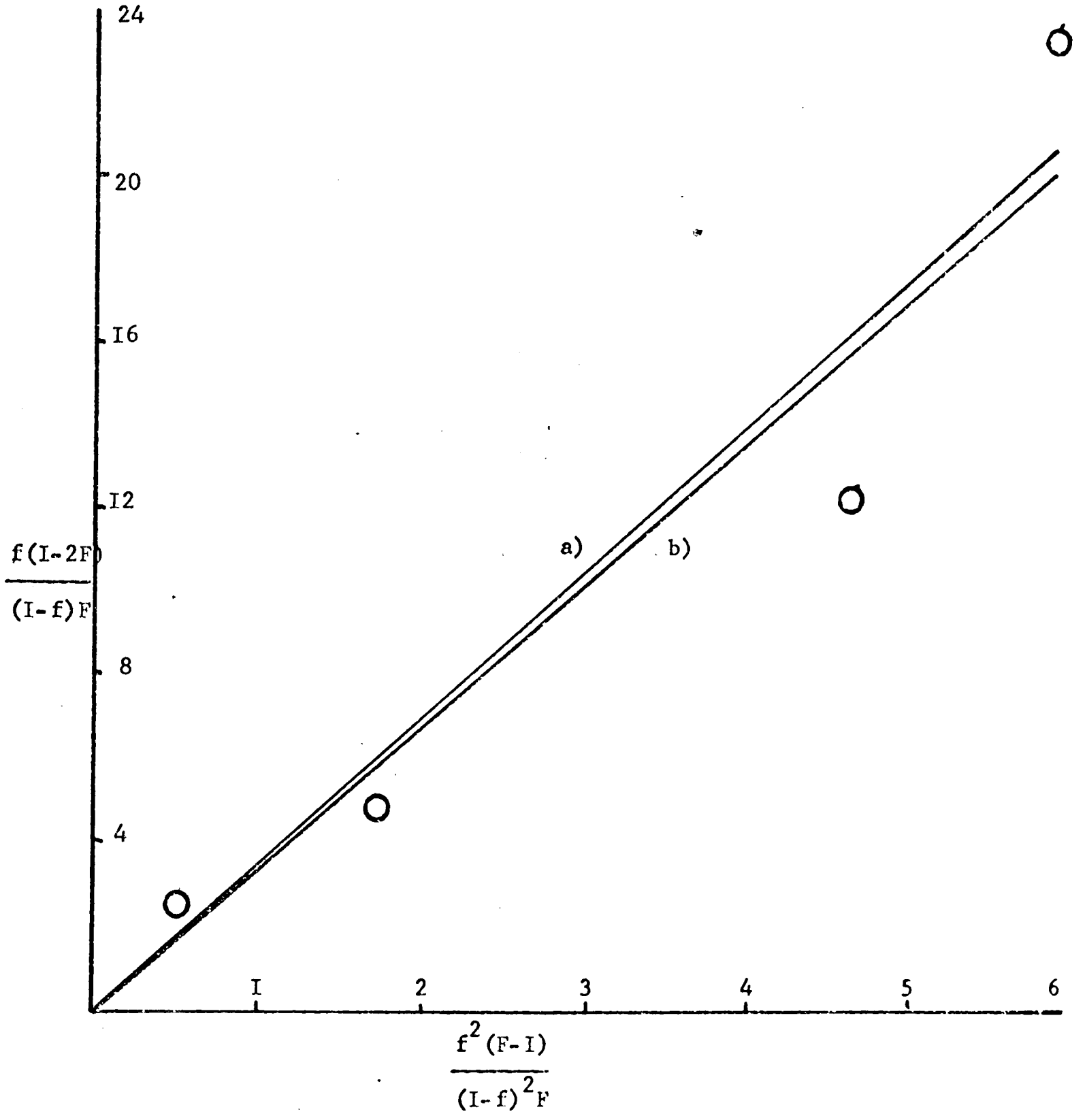

FIGURE 3.7
Calibration plot of Y versus mole fraction
of succinic anhydride

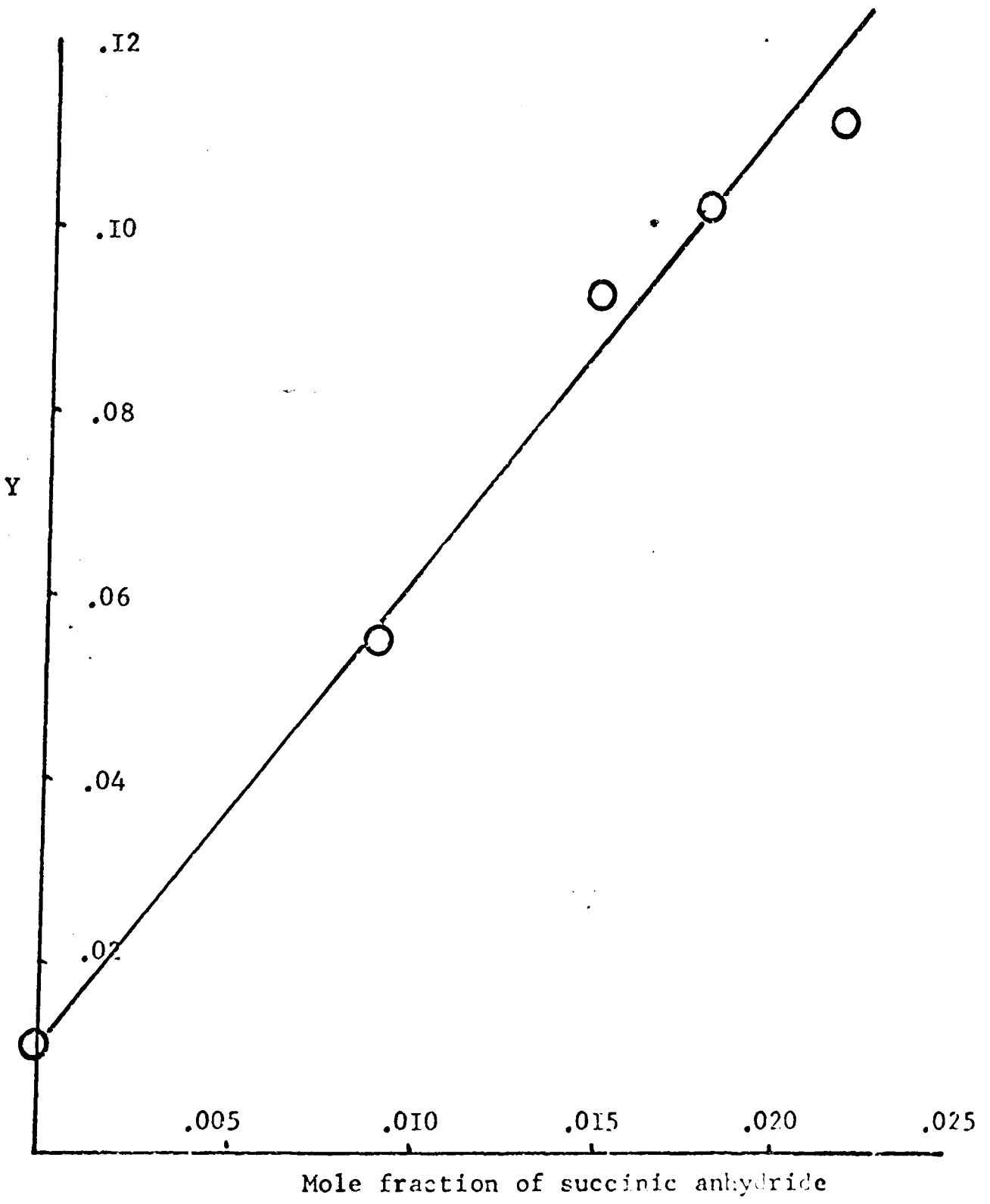

Table 3.4

Mixture	Mole fraction of anhydride	Absorbance		Y
		Anhydride	Ester	
A	0.02060	0.045	0.400	.1124
B	0.01745	0.038	0.368	.1031
C	0.01437	0.034	0.354	.0960
D	0.00905	0.019	0.354	.0537
PMMA	0.00000	0.005	0.370	.0135

Table 3.5

Polymer	Absorbance		Y	Mole fraction of MalA
	Anhydride	Ester		
12.5/1	.258	1.028	0.251	.0490
18/1	.212	1.066	0.199	.0386
19/1	.179	1.035	0.173	.0332
20/1	.211	1.094	0.193	.0374
50/1	.088	1.025	0.0858	.0151
100/1	.046	0.905	0.0508	.0078

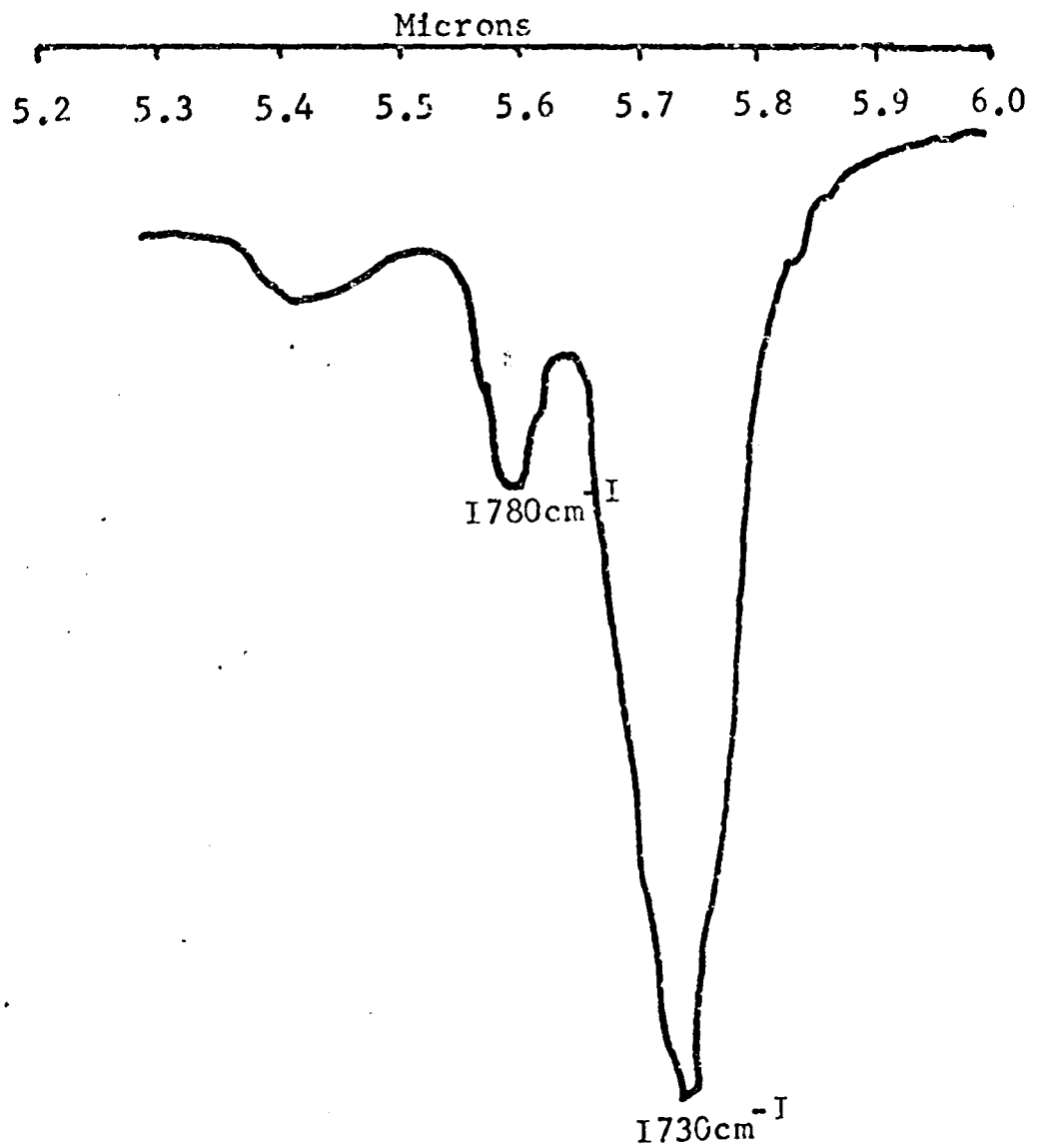

FIGURE 3.8

Carbonyl region of infra-red spectrum of 20/I copolymer in chloroform solution

results of the comparison with the standard curve are shown in TABLE 3.5. The reactivity ratios in TABLE 3.12 were obtained from the Fineman - Ross plot in FIGURE 3.9.

A modification of this technique can be used for the MIK/MMA copolymers. The molar absorbance for the carbonyl stretching frequency for each homopolymer is measured. It is assumed that the amount of, say, the ketone in a copolymer will be directly proportional to the molar absorbance of the ketone peak in the infra-red spectrum. For example, in the 1/1 copolymer, the molar absorbance of the ester and of the ketone absorptions at 1735cm^{-1} and 1700cm^{-1} will be half that for the corresponding homopolymers. The appropriate region in the infra-red spectrum of the 1/1 copolymer is shown in FIGURE 3.10.

The mole fraction of ketone in any copolymer is found as follows:-

Let x = mole fraction of ketone in copolymer

Let y = absorbance of ketone at 1700cm^{-1} as recorded

Let M = molar absorbance of ketone

Let Z = concentration of ketone in mg/ml.

Let M. W. = molecular weight of an average unit

$$\therefore M = \frac{\text{absorbance}}{\text{no. of moles}} \times \text{mole fraction}$$

$$= \frac{y.M.W.x}{Z} \quad - \quad (1)$$ assuming the linear relationship between M and x previously described.

Obviously when $x = 1$, we will get, the molar absorbance of

FIGURE 3.9

Fineman Ross plot of MMA/MalA copolymers

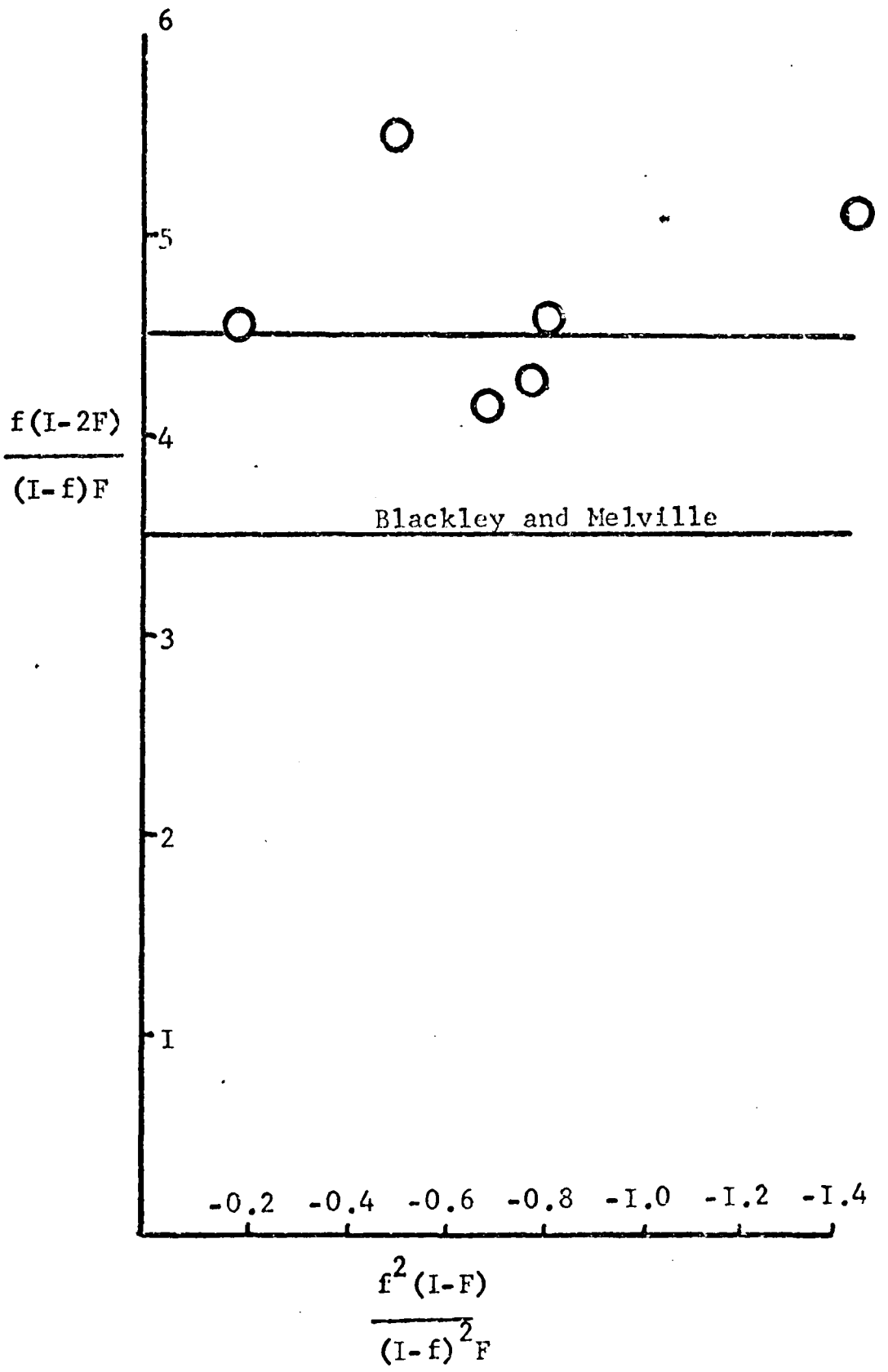

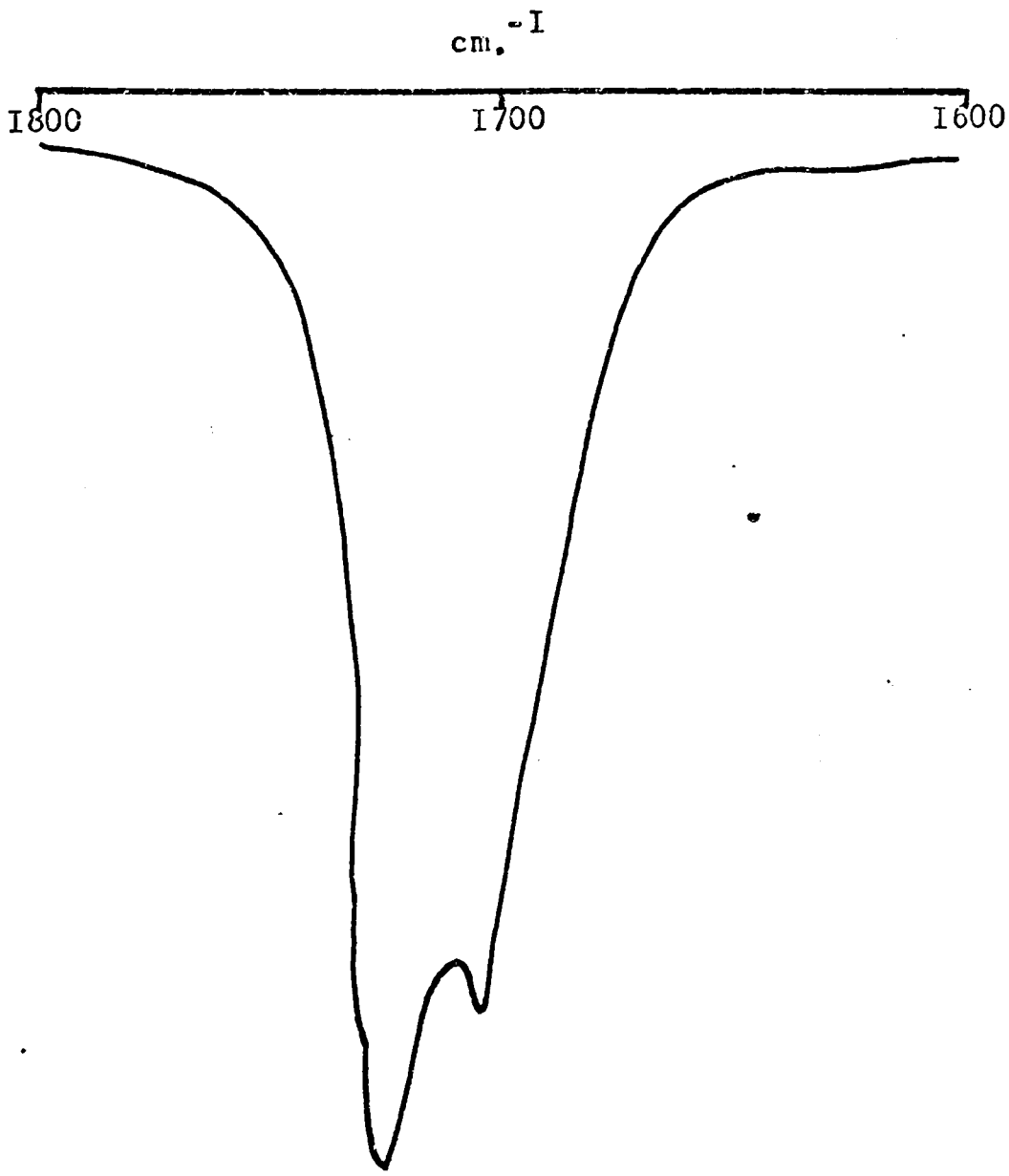

FIGURE 3.10 Carbonyl region of the infra-red spectrum of the I/I copolymer in chloroform solution

the homopolyketone which can be calculated, and when x = 0 there will be no absorbance since there is no chromophore present.

$$\text{Now, } M.W. = M.W._{MMA}\,(1-x) + M.W._{ketone}\,x$$

ie. when x=1, for PMIK, M.W. = 100 (1-1) + 84 x 1 = 84

and when x=0, M.W. = 100 (1-0) + 84 x 0 = 100

substituting in (1),

$$M = \frac{xy}{Z}\left[M.W._{MMA}\,(1-x) + M.W._{ketone}\,x\right] \quad - (2)$$

For PMIK, $M = \frac{84y}{Z}$, thus M can be calculated. This value is substituted in equation (2) and x can be determined. A similar calculation with PMMA will give x based in the ester absorption. The results are shown in TABLE 3.6. In theory, the mole fraction for the ketone should be the same for both methods of measurement. However, because the peaks are close together and are to some extent overlapping, the precise absorbance of each peak cannot be measured absolutely. But the average value of x for the two methods described above will give the most accurate value for this technique since, for any contribution to say, the ketone absorbance from the ester, the same contribution will be lost from the ester absorbance and therefore by taking the average, any contribution from one absorption to the otherwill be eliminated.

The corresponding Fineman - Ross plot is shown in FIGURE 3.11 and the reactivity ratios in TABLE 3.12.

Unfortunately, the carbonyl absorptions of the ester and the ketone were not resolved in the MMA/MVK copolymers. However, it is possible to make semi-quantitative measurements of the ketone content

TABLE 3.6

Polymer	Concentration (mg/ml)	Absorbance of ketone	Absorbance of ester
73 PMMA	2.II	0.000	0.370
I/2	2.3I	0.I37	0.263
I/I	2.I0	0.I94	0.2I8
2/I	2.27	0.239	0.I50
PMIK	2.I7	0.350	0.000

Polymer	mole fraction of ketone from ketone absorbance X	Mole fraction of ketone from ester absorbance X	Average X
73 PMMA	0.000	0.000	0.000
I/2	0.407	0.390	0.399
I/I	0.6I2	0.450	0.53I
2/I	0.690	0.658	0.674
PMIK	I.000	I.000	I.000

FIGURE 3.II

Fineman Ross plot for MIK/MMA copolymers analysed by infra-red spectroscopy

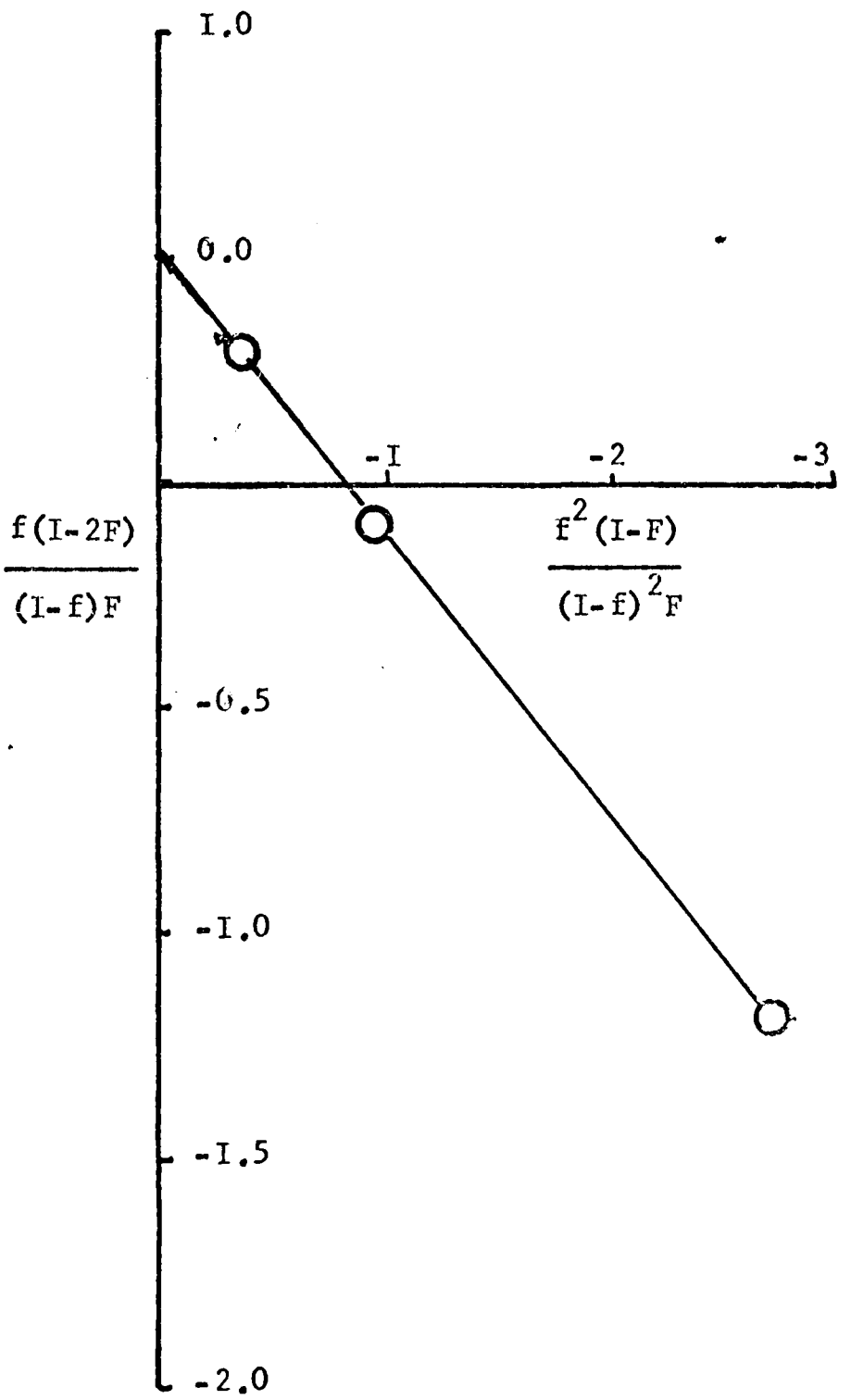

from examination of the infra-red spectrum in the region 1300-1400cm.$^{-1}$ Infra-red spectra of the copolymers were recorded by casting a film from chloroform solution on to a KBr disc. The rubbery texture of the MMA/MVK copolymers make grinding very difficult. The spectra of two polymers showing the appropriate frequency range are illustrated in FIGURES 3.12 and 3.12a. The peaks at 1385cm^{-1} and 1355cm^{-1} are due to C - H deformations in PMMA and PMVK. The relative extinction coefficient of the 1355cm^{-1} peak compared to the 1385cm^{-1} peak is found by measuring the absorbance of each peak in the spectra of the homopolymers and comparing it with the absorbance of the carbonyl stretching mode at 1735cm^{-1} in PMMA and 1705cm^{-1} in PMVK. Since the extinction coefficients of the carbonyl absorptions are similar (see TABLE 3.6) the ratio of the 1355cm^{-1} peak to the 1385cm^{-1} peak is found to be 2.77. The absorbances of the 1355cm^{-1} and 1385cm^{-1} are measured in the copolymers and, after allowing for the difference in extinction coefficients, the amount of ketone in the copolymers can be found. The results are shown in TABLE 3.7 but the reactivity ratios have not been calculated because of the relative inaccuracy of these measurements. Polymers with large amounts of ketone produce spectra in which the 1355cm^{-1} peak obscures the 1385cm^{-1} peak. The 1355cm^{-1} peak in the 2% MVK copolymer was too small to be measured.

c) Ultra-Violet Spectroscopy. The same methods which were applied to infra-red spectroscopy can be applied to ultra-violet spectroscopy to determine the ketone content in copolymers with MMA. The $n \rightarrow \pi^*$ transition of the ketone group appears at a wavelength of 280-290mμ (FIGURE 3.13). PMMA is transparent at this wavelength and so the same considerations apply here as in the previous section. The absorbances of the homopolymers are shown in TABLE 3.8.

FIGURE 3.I2 Infra-red of 70/30 copolymer

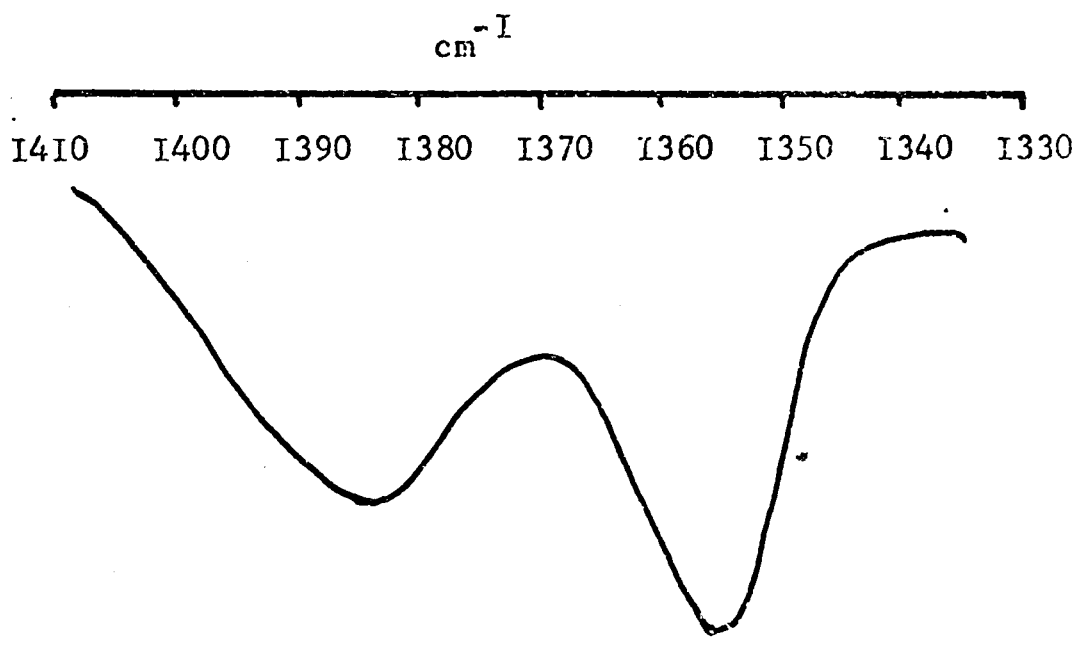

FIGURE 3.I2a Infra-red of 50/50 copolymer

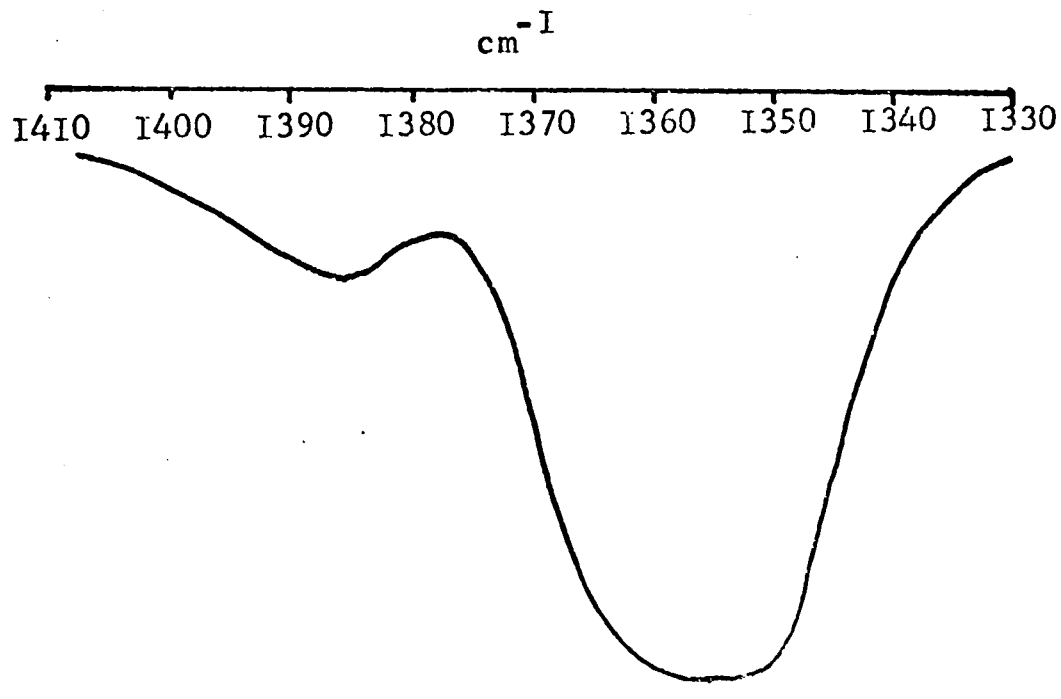

TABLE 3.7

Polymer	Mole fraction of ketone
7%MVK	0.154
15%MVK	0.214
70/30	0.312
50/50	0.431
30/70	0.530

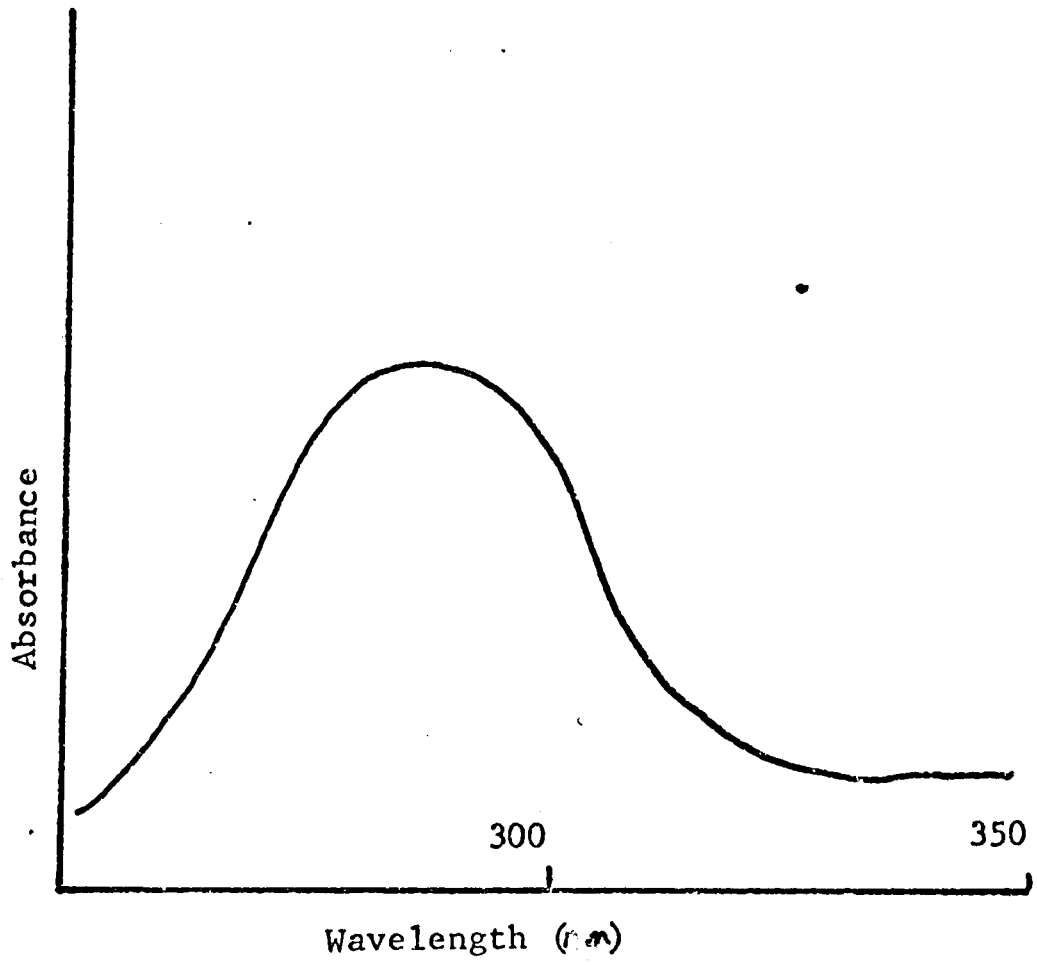

FIGURE 3.I3

Ultra-violet spectrum of PMIK

TABLE 3.8

Polymer	Concentration Z (mg/ml)	Absorbance Y	Mole fraction X
PMMA	I.75	0.000	0.000
2%MVK	I.9I	0.000	0.000
7%MVK	2.06	0.040	0.046
90/I0	2.23	0.073	0.077
I5%MVK	2.25	0.I37	0.I4I
70/30 (AD)	2.II	0.328	0.337
50/50	2.I0	0.468	0.463
50/50 (AD)	I.97	0.637	0.633
30/70	2.27	0.75I	0.645
I0/90	I.98	I.040	0.9I7
PMVK	I.39	0.822	I.000
I/2	2.03	0.3I8	0.352
I/I	2.08	0.525	0.545
2/I	I.88	0.680	0.756
PMIK	0.96	0.482	I.000

For PMIK, $M = \frac{0.482 \times 84}{0.96}$

$= 42.2$

$\therefore$ equation (2) now reads,

$$42.2\,x = (100-16x)\frac{y}{Z}$$

$$\therefore x = \frac{100\frac{y}{Z}}{42.2 + \frac{16y}{Z}}$$

The results are shown in TABLE 3.8

For PMVK $M = 41.4$

$$= x = \frac{100\frac{y}{Z}}{41.4 + \frac{30y}{Z}}$$

Again, the results are shown in TABLE 3.8 FIGURES 3.14 and 3.15 show the Fineman - Ross plots for the MIK/MMA and MMA/MVK copolymers respectively. The reactivity ratios obtained from these plots were calculated and are shown in TABLE 3.12.

Once again it has been assumed that the extinction coefficient of the ketone absorption is not affected by the neighbouring units. However, two points arise from the U.V. spectra:-

i) λ_{max} for PMIK is 289mμ and for PMVK λ_{max} is 286nm, thus illustrating the effect of substitution in the α position to the carbonyl group in the ketone unit.

ii) for the MIK/MMA series λ_{max} varies from 287nm for the 1/2 copolymer to 289nm for PMIK and in the MMA/MVK series from 280nm for the 7% MVK copolymer to 286nm for PMVK. Thus λ_{max} is shifted to

FIGURE 3.14

Fineman Ross plot for MIK/MMA copolymers

by ultra-violet spectroscopy

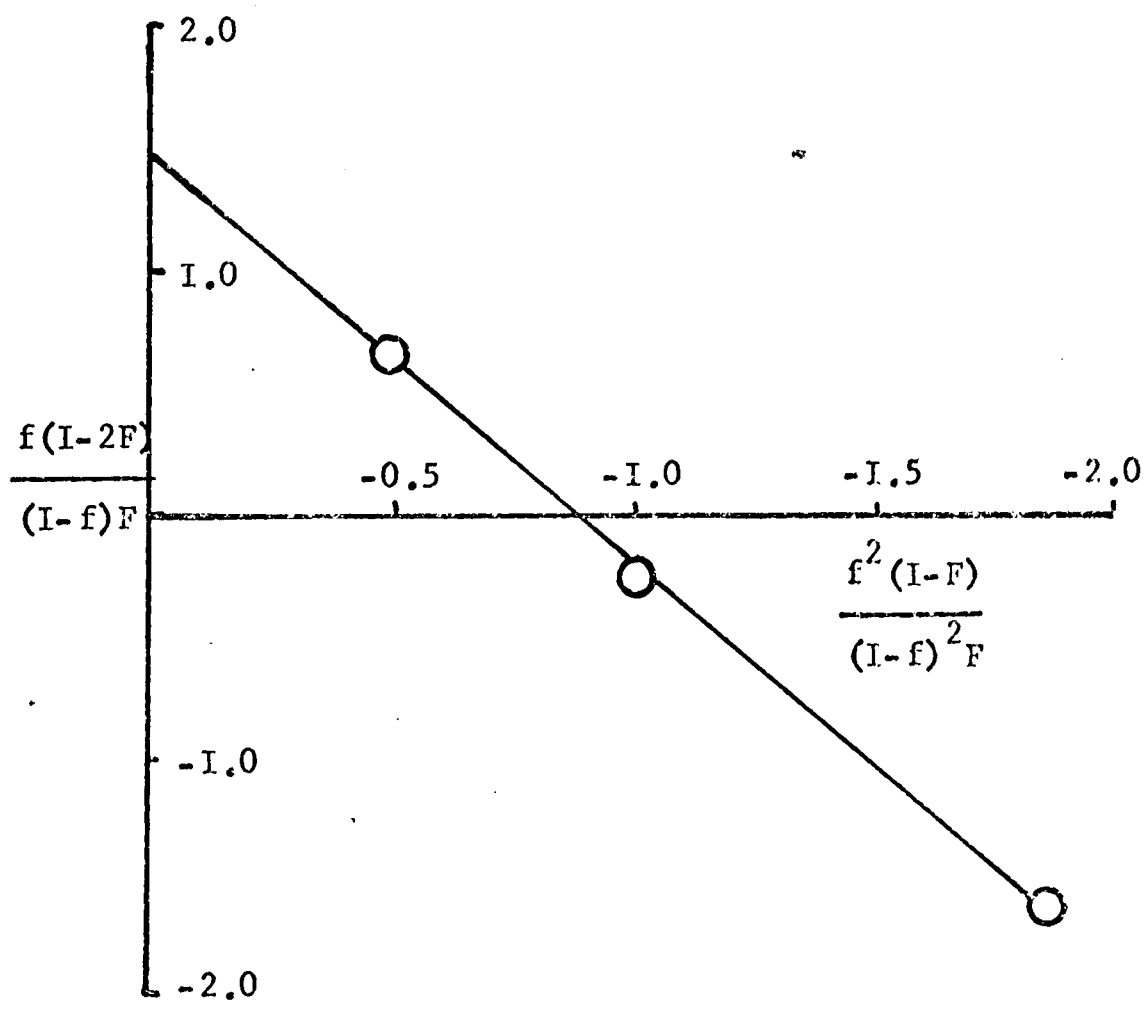

FIGURE 3.I5

Fineman Ross plot for MMA/MVK copolymers by ultra-violet spectroscopy

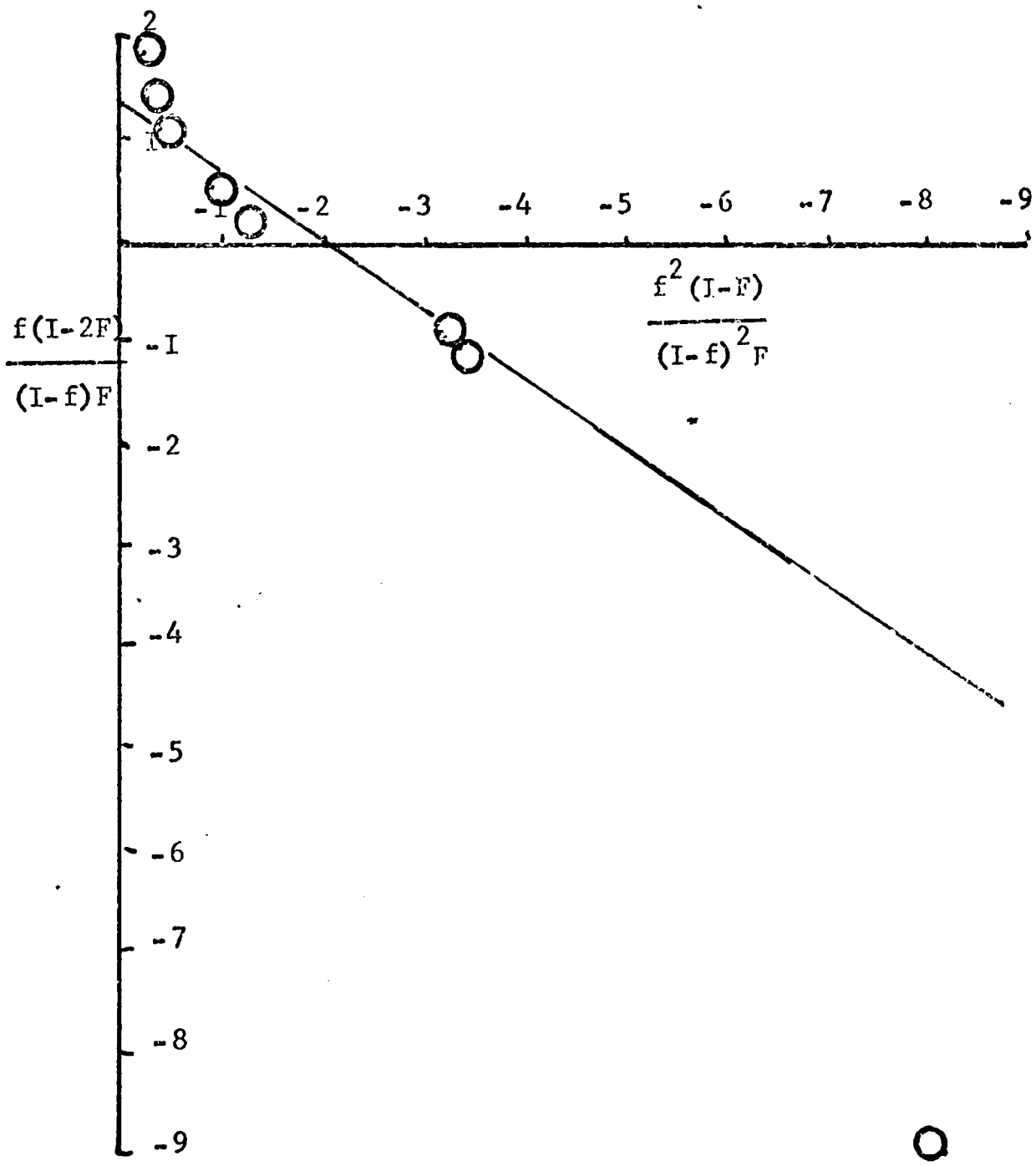

lower wavelengths with the increasing incidence of adjacent MMA units.

The molar absorbances of PMIK and PMVK were very close in spite of the effect of the substitution in PMIK, therefore the extinction coefficient has not been significantly altered. It is assumed that the same holds for the effect of even more remote groups.

d) Nuclear Magnetic Resonance Spectroscopy. N.m.r. has already been shown[104-107] to be a valuable method for determining the reactivity ratios of pairs of monomers in which the elemental compositions are similar.

i) MIK/MMA copolymers. FIGURE 3.16 shows a typical spectrum. Two separate regions of the trace were used to determine the amount of each monomer in the polymer.

a) Using 250Hz expansions from τ 6 - 8.5 and from τ 7.5 - 10.0, the peak at τ 9, which is due to α-Me protons, is taken to be equivalent to three protons. The methylene peak at 8.2 τ is always due to 2 protons. Therefore, by subtraction, the area due to the ketone protons can be calculated. Comparison of this area with the area under the MMA ester peak at 6.5 τ will give the proportion of MIK in the copolymer. The areas under the peaks were measured by averaging the five integrals on the spectra, by measuring directly the areas by planimeter and by tracing the spectra and weighing the traces. The results are shown in TABLE 3.9, and Fineman Ross plots in FIGURE 3.17. The reactivity ratio calculated are shown in TABLE 3.12.

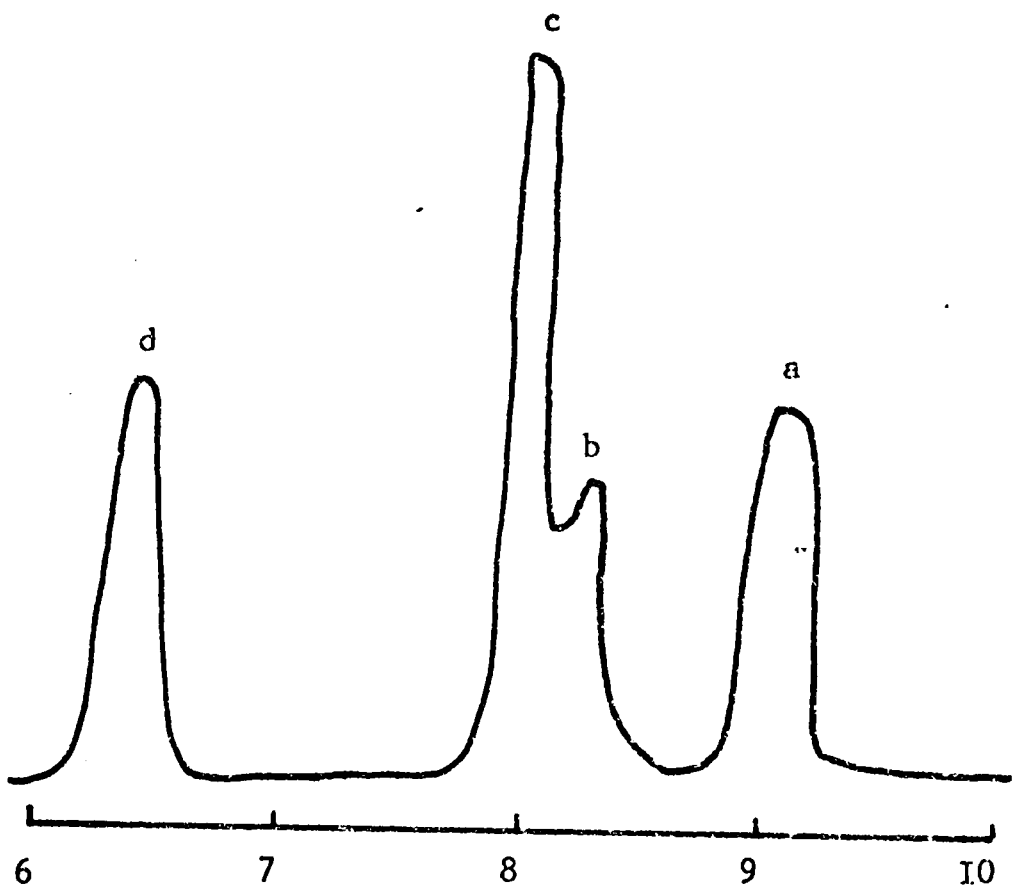

FIGURE 3.I6

N.M.R. spectrum of I/I copolymer

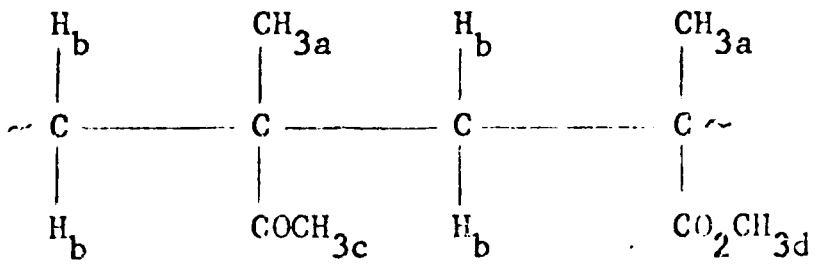

TABLE 9

POLYMER	Mole fraction of ketone from integrals planimeter trace		
I/2	0.265	0.320	0.245
I/I	0.475	0.422	0.445
2/I	0.690	0.649	0.638

TABLE I0

POLYMER	Mole fraction of ketone from	
	integrals	weight
I/2	0.33I	0.22I
I/I	0.5I6	0.429
2/I	0.7I0	0.660

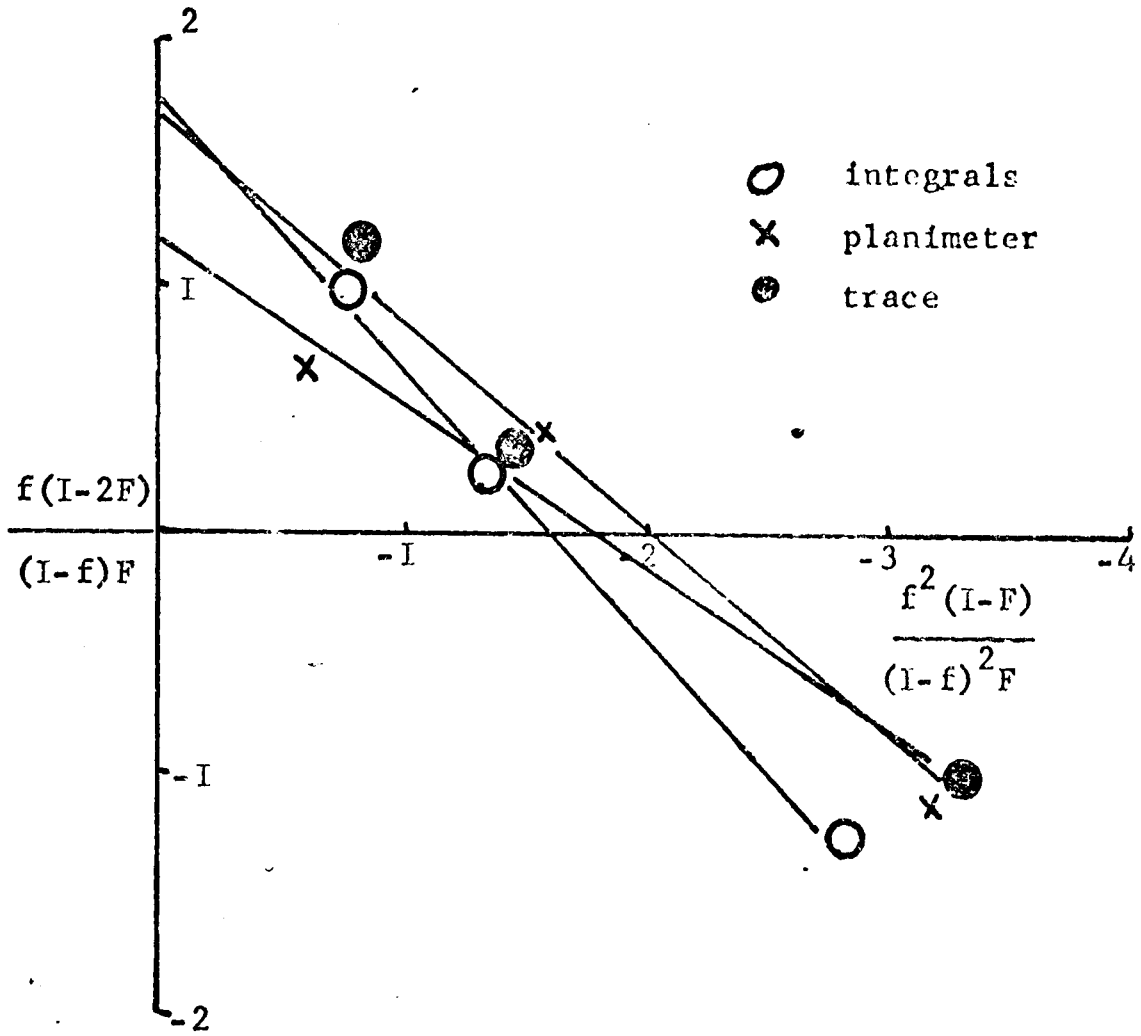

FIGURE 3.17

Fineman Ross plot for MIK/MMA copolymers from N.M.R. data

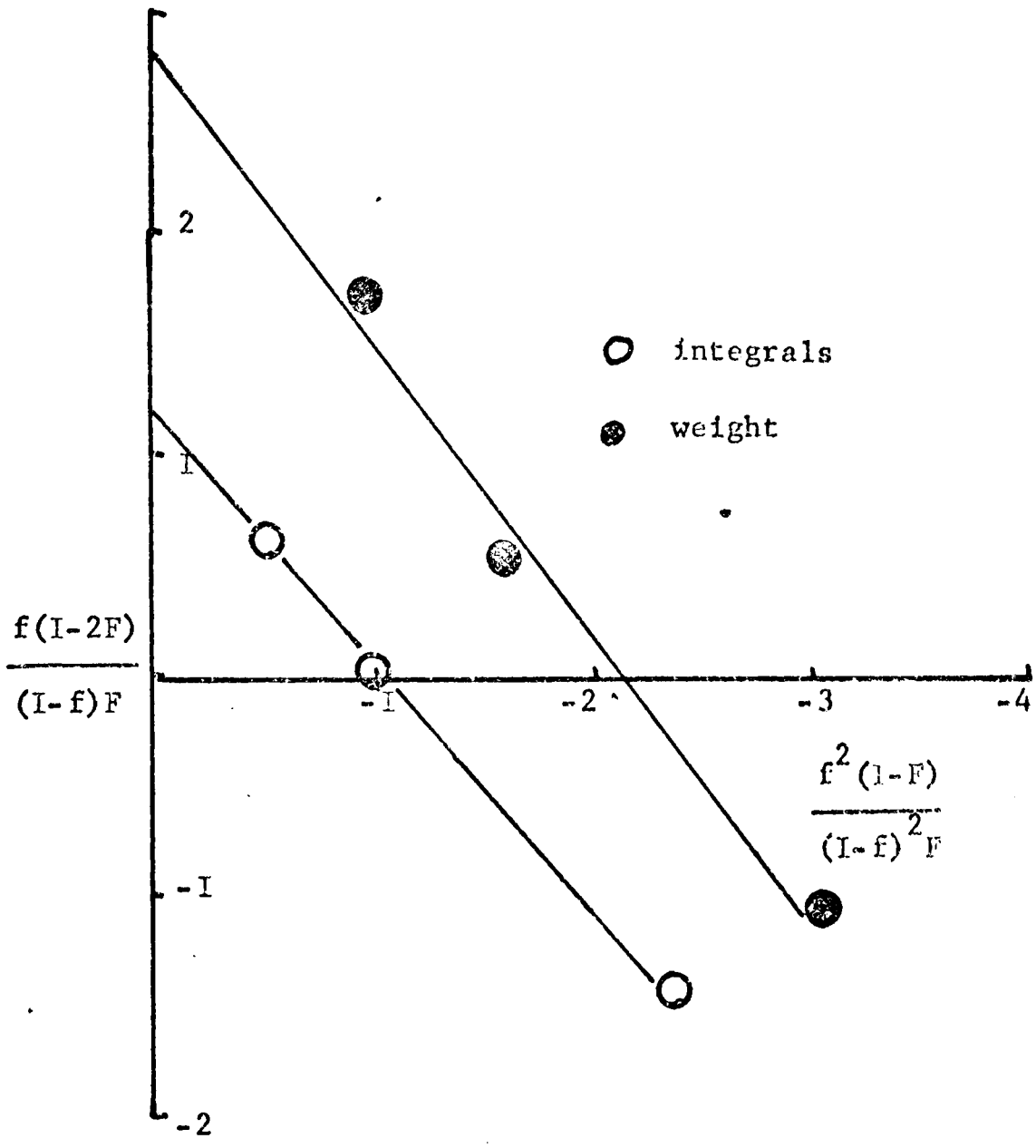

FIGURE 3.18

Fineman Ross plot for MIK/MMA copolymers from N.M.R. data

b) By using the 250Hz expansion from 6.0τ - 8.5τ only, the error involved in comparing two spectra is removed. The sum of the areas under the peak at 6.5τ and the peaks at 8.0τ and 8.2τ must be due to five protons - the two methylene protons and contributions from the pendant ester and ketone methyl groups which will represent three protons in the average unit. By subtracting the area due to the two methylene protons from the total area of the peaks at 8.0τ and 8.2τ, the area due to the ketone protons remains and this is compared with the area due to the ester methyl protons at 6.5τ. The relative proportions of ketone to ester were found from the integrals as before and by photocopying the spectra and weighing the areas under the peaks. The results are shown in TABLE 3.10, FIGURE 3.18 and TABLE 3.12.

ii) MVK/MMA. FIGURE 3.19 shows the n.m.r. spectrum of the 50/50 copolymer. Unfortunately, the methine proton H_b on the ketone unit lies close to the protons of MMA(H_a) and separation is poor. The ketone methyl protons are again super imposed on the methylene protons and the general quality of the spectra deteriorates with increasing ketone content. The ketone content of the copolymers is found indirectly by measuring the area under the peak at 6.5 τ which is due to the ester methyl protons and comparing this with the total area of all the other peaks. If x and y are the mole fractions of MMA and MVK respectively, then the ester protons will have area 3x and the other protons will have area 5x and 6y. The areas under the peaks were measured by taking the average of five integrals. The results are shown in TABLE 3.11 and the Fineman - Ross plot in FIGURE 3.20.

iii) MMA/Ma1A. The spectrum of the 12.5/1 copolymer is shown in FIGURE 3.21. The broad peak at 7.2 τ due to the anhydride protons is typical of protons attached to the main polymer chain and accurate measurement of the area under this peak is impossible.

4. The Tacticity of PMMA

The three distinct peaks at 8.8 τ, 8.95 τ and 9.1 τ in the n.m.r. spectrum of PMMA, as illustrated in FIGURE 3.22, have been ascribed to the isotactic, heterotactic and syndiotactic configurations of PMMA. Isotactic PMMA arises when the neighbouring groups to any MMA unit adopt the same steric configuration, ie. ddd or lll. Less strained will be that configuration where an MMA unit has neighbouring units adopting a different configuration ie. dll, ddl, lld or ldd. The

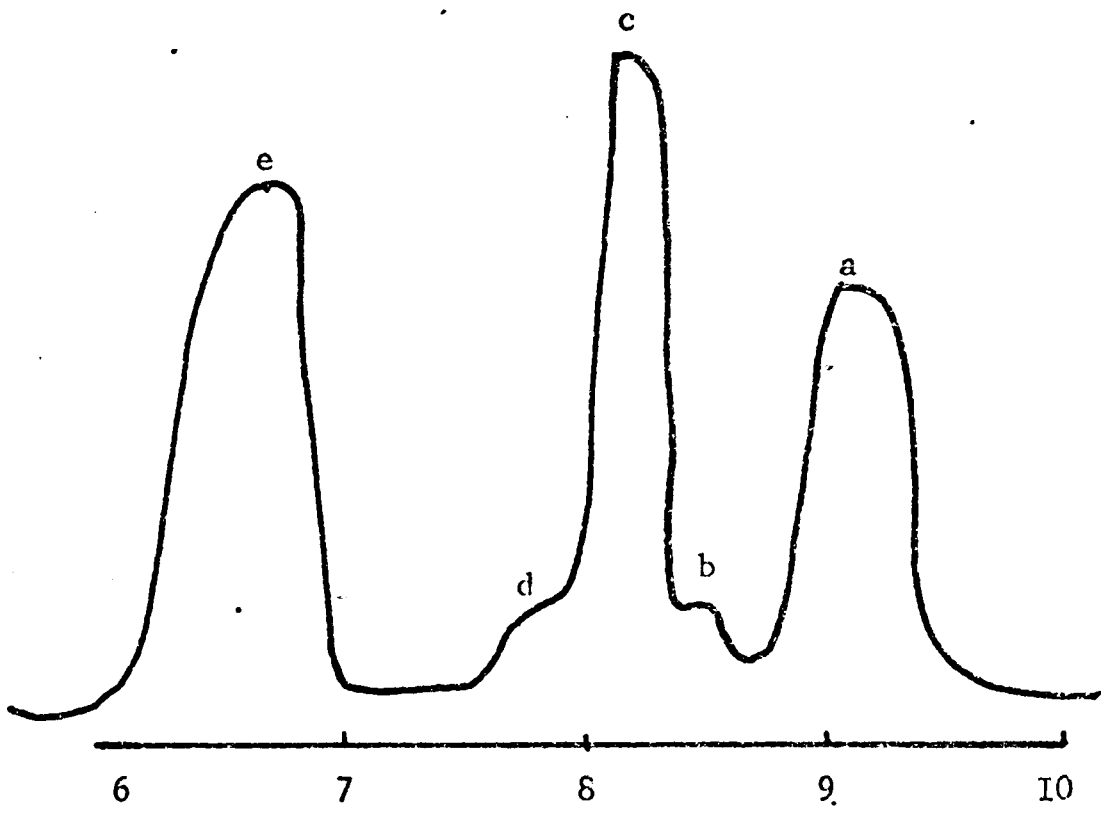

FIGURE 3.19

N.M.R. spectrum of 50/50 MMA/MVK copolymer

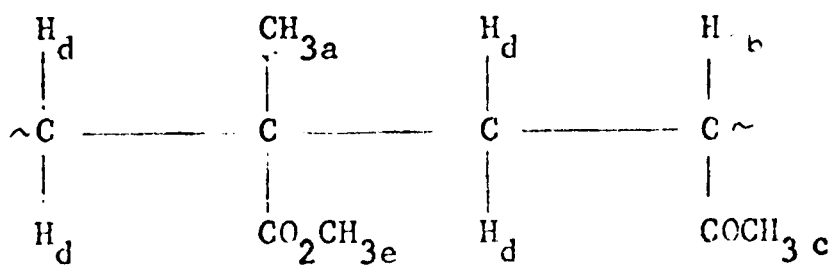

TABLE 3.II

Polymer	Area due to ester protons	Area due to other protons	Mole fraction of MVK
73 PMMA	78	I3I	0.000
2%MVK	64	I77	0.049
7%MVK	63	I78	0.074
90/I0	58	I75	0.I50
I5%MVK	62	I88	0.I80
70/30	53	I96	0.329
70/30 (AD)	53	203	0.365
50/50	46	I90	0.458
50/50 (AD)	23	I54	0.665
30/70	33	I99	0.627
I0/90	I6	I96	0.830
PMIK	0	—	1.000

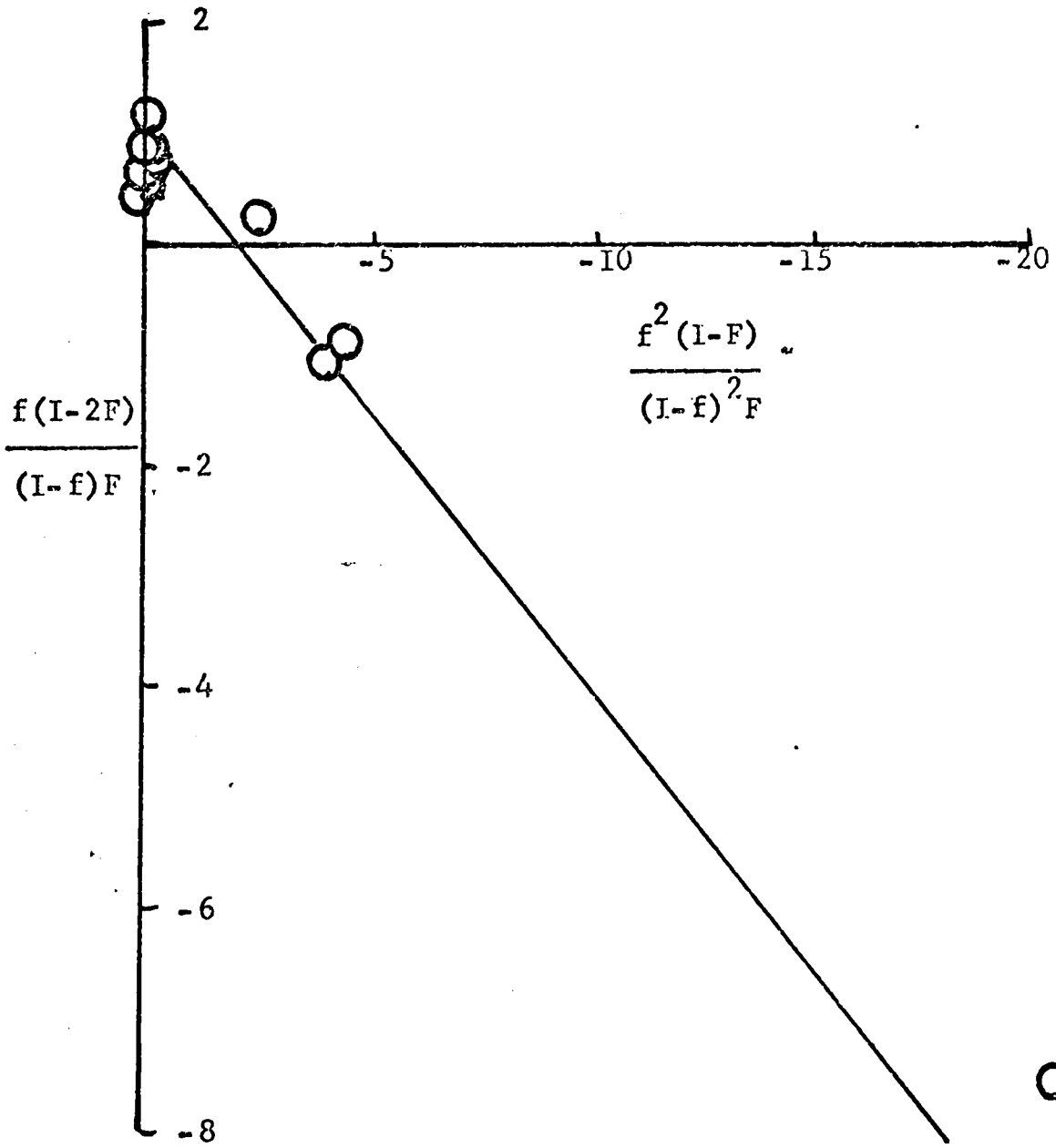

FIGURE 3.20

Fineman Ross plot for MMA/MVK copolymers from N.M.R. data

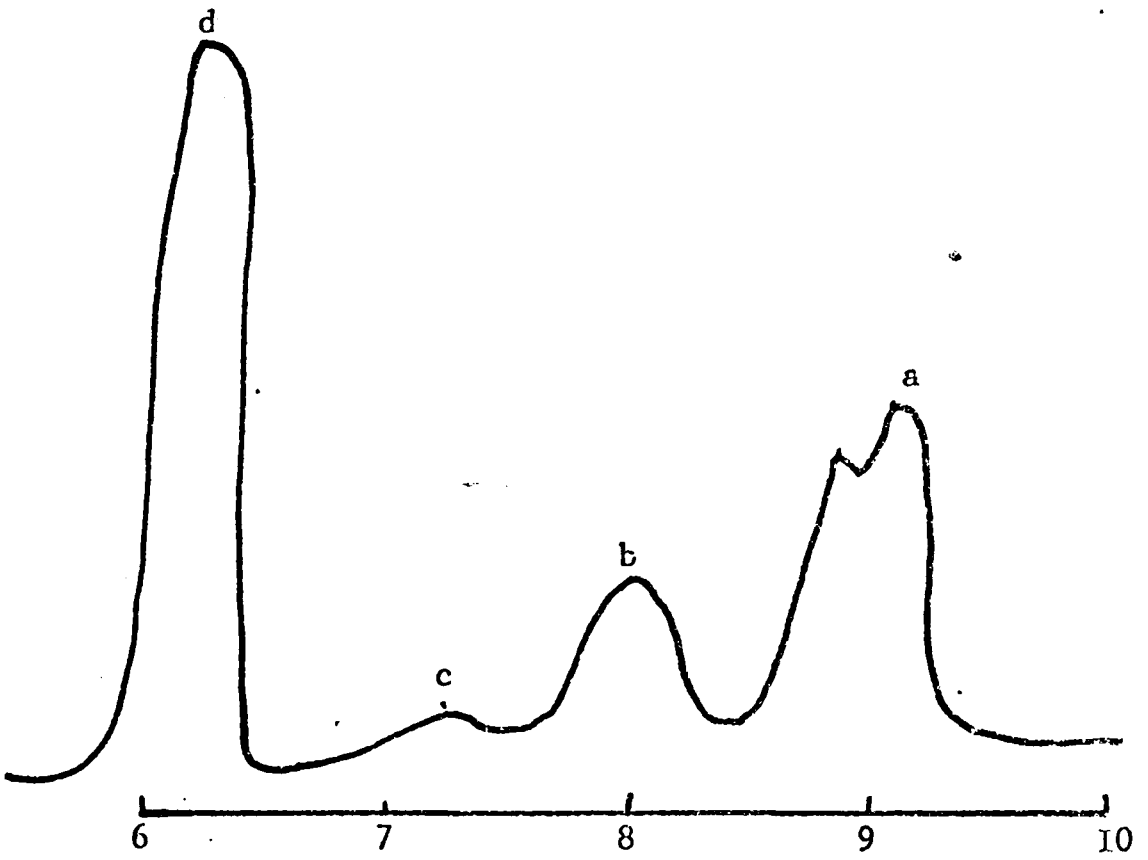

FIGURE 3.2I

N.M.R. spectrum of I2.5/I MMA/MalA copolymer

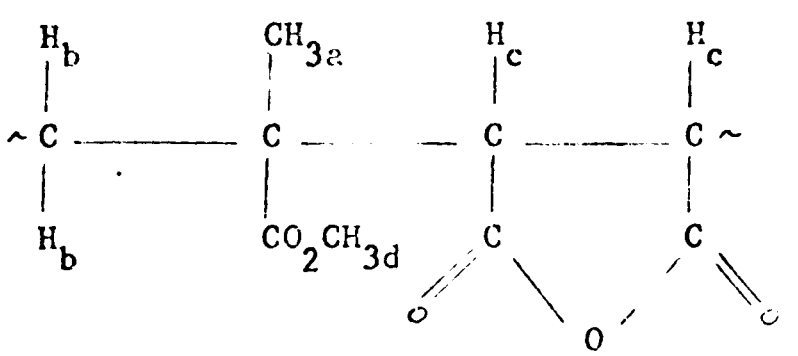

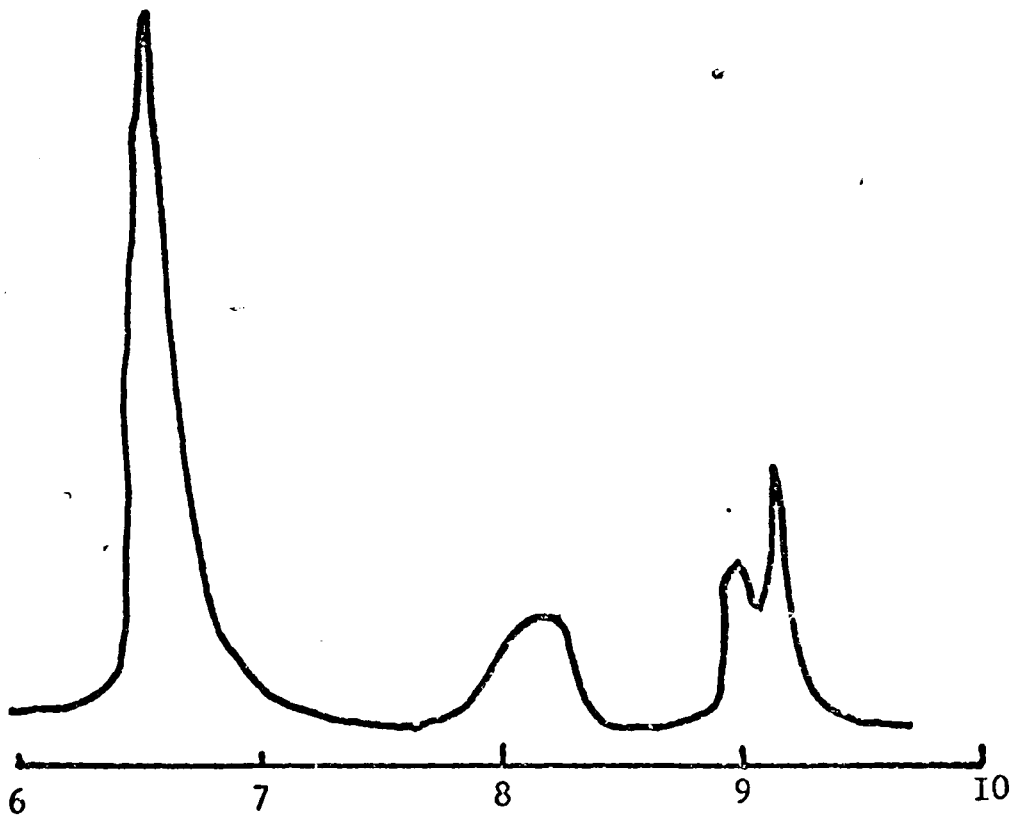

FIGURE 3.22 N.M.R. of PMMA

least strained configuration and hence the most abundant will occur when both neighbouring groups adopt the opposite configuration to the central group ie. LdL or dld. By measuring the areas under these peaks by intergration in the 250Hz expansion, the relative amounts of each configuration are found to be 6.3% isotactic, 34.2% heterotactic and 59.5% syndiotactic. This is in agreement with previous determinations of the tacticity of free radically initiated PMMA at similar temperatures.[108] These configurations are identifiable in copolymers of MMA/MVK up to 15% MVK content.

The equivalent configurations in PMIK are not observed presumably because the temperature of polymerisation (60^{o}) is high enough above the melting point of PMIK ($40-60^{o}$) to enable the MIK units to assume their most stable configuration, probably syndiotactic.

5. Chemical Methods

It is possible to react the anhydride groups in the MMA/MaIA copolymers with p - toluidine and then determine the amount of nitrogen by microanalysis.[98] However, even complete reaction with p - toluidine and the 12.5/1 copolymer will give elemental nitrogen microanalysis of less than one per cent and so this method will not be sufficiently accurate.

High molecular weight polymer molecules tend to coil up thus rendering penetration of chemical reagents difficults if not impossible even in dilute solution. Large molecules such as p - toluidine mentioned above may not react completely because of the protection of

the inner reaction sites by the twisted polymer surrounding. Quantitative reaction of iodoform with the ketone polymers may prove to be a good method to determine the ketone content of the copolymers if 100% reaction can be guaranteed.

6. Discussion

It can be seen from TABLE 3.12 that the values obtained for the reactivity ratios can vary substantially. The reactivity ratios are particularly sensitive to small errors in the accuracy of determination of the composition of the copolymers. For example, the mole fraction of MIK in the copolymers as determined by UV spectroscopy (TABLE 3.8) and by n.m.r. integration (TABLE 3.10) varies by less than 6% yet the values of r_1, determined by these methods varies by approximately 40%.

The errors involved in microanalysis have already been discussed. U.V. and infra-red spectroscopic methods suffer in their indirectness, standard calibration, assumptions concerning extinction coefficients and insensitivity to small amounts of a constituent in a copolymer. N.m.r. is one of the most direct methods but requires that the peaks are well separated, a criterion not well satisfied in MVK polymers particularly at high MVK content. Measuring peak areas by planimeter, trace or weighing photocopied spectra generally give low values for MIK content because of the problem of overlapping peaks. For this reason, areas measured by integration give simply and more directly the polymer composition and is therefore, the most accurate method although the peak overlap and broad band problems cannot be

TABLE I2

Method	MMA/MalA		MIK/MMA		MMA/MVK	
	r_1	r_2	r_1	r_2	r_1	r_2
Carbon analysis	–	–	0.725	0.990	0.330	I.530
Hydrogen analysis	–	–	0.620	0.075	–	–
Infra-red analysis	0.0	4.57	0.640	0.550	–	–
Ultra-violet analysis	–	–	I.44	I.I7	0.677	I.37
N.M.R. a) integrals	–	–	0.700	I.70	0.63I	0.89I
N.M.R, planimeter	–	–	0.675	I.I7	–	–
N.M.R. trace	–	–	0.587	I.64	–	–
N.M.R. b) integrals	–	–	I.07	I.I2	–	–
N.M.R. weight	–	–	I.I6	2.34	–	–

wholly overcome.

Because each method has a certain degree of error associated with it, Fineman - Ross plots containing all experimentally determined points were constructed and are shown in FIGURE 3.23 for the MIK/MMA system and FIGURE 3.24 for the MMA/MVK system. A straight line determined by the method of least squares was drawn through all the points in FIGURE 3.23 with the exception of those determined by H analysis, the point due to the n.m.r. expansion by weight of the 1/2 copolymer and the U.V. determination of the 2/1 copolymer. The reactivity ratios were found to be $r_{MMA} = 0.977$ and $r_{MIK} = 0.692$.

Similarly, in FIGURE 3.24, the microanalytical figures of the U.V. determination of the 2% and 7% copolymers were eliminated and the reactivity ratios calculated to be $r_{MMA} = 0.628$ and $r_{MVK} = 0.526$.

On the basis of these figures, the copolymer compositions were recalculated and are shown in TABLE 13. In subsequent discussions it will be these compositions which will be quoted. The reactivity ratios determined by Blackley and Melville[96] are used for the maleic anhydride copolymers and the compositions are shown in TABLE 14.

In the determination of the reactivity ratios, no account has been made for the effect of units other than the terminal unit in a growing polymer radical. Statistical treatment of the sequence distribution of units in polymers has led to expansion of the copolymerisation equation.[109-111] It has been observed[112] that an anhydride unit in copolymers of maleic anhydride and styrene as far removed as four units

FIGURE 3.23

Composite Fineman Ross plot

for the MMA/MIK copolymers

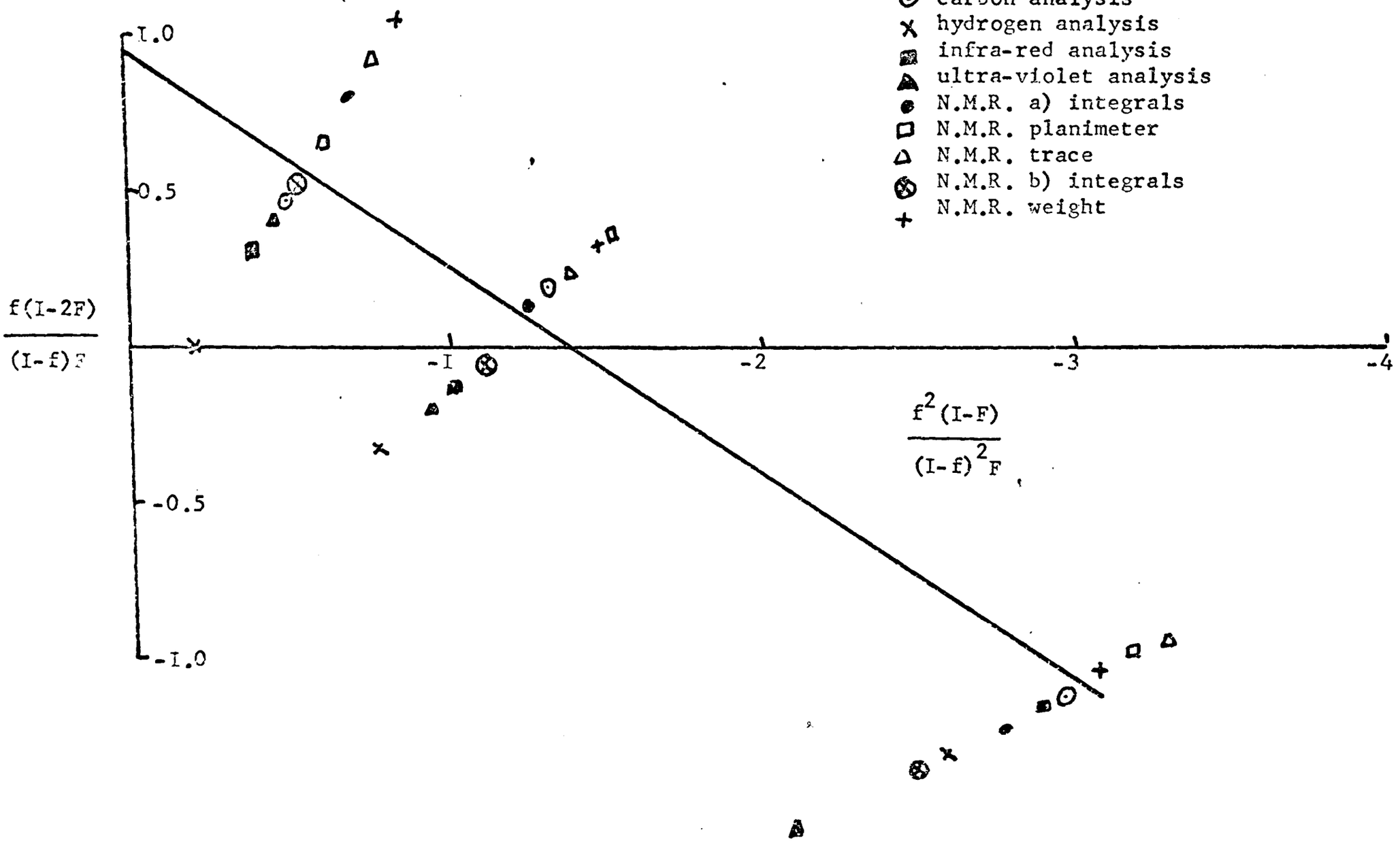

FIGURE 3.24

Composite Fineman Ross plot for the MMA/MVK copolymers

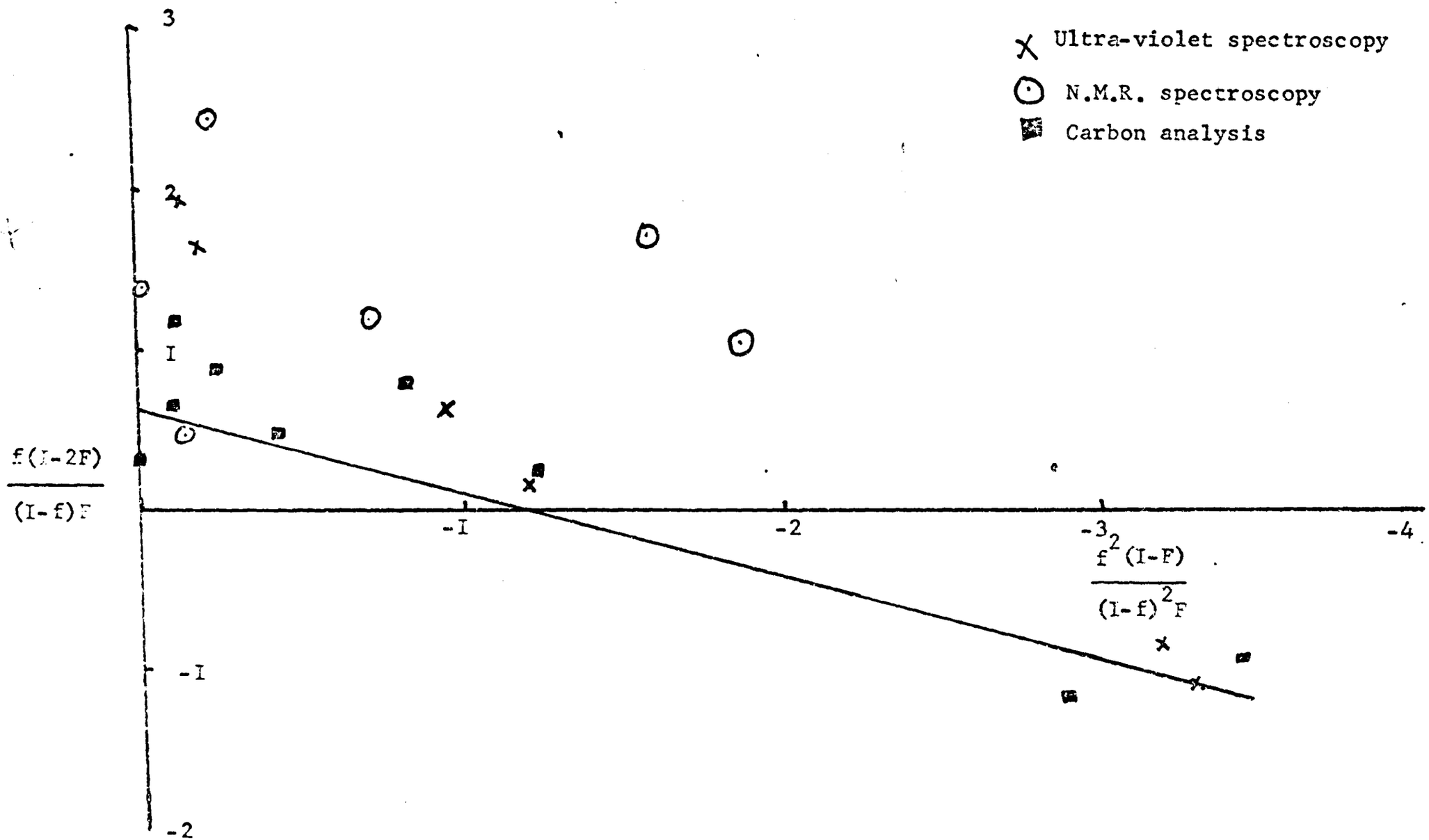

TABLE I3

Polymer	Mole fraction of ketone	Polymer	Mole fraction of ketone
I/2	0.323	I5%MVK	0.228
I/I	0.477	70/30	0.339
2/I	0.658	70/30 (AD)	0.4I0
2%MVK	0.03I	50/50	0.484
7%MVK	0.I20	50/50 (AD)	0.64I
90/I0	0.I55	30/70	0.649
		I0/90	0.853

TABLE I4

Polymer	Mole fraction of anhydride	Polymer	Mole fraction of anhydride
I00/I	0.0099	I9/I	0.0427
50/I	0.0230	I8/I	0.0455
20/I	0.0422	I2.5/I	0.0664

from the end of a growing polymer radical has an effect on the reactivity of the radical. This effect may be in operation in the copolymers presently under study and may explain the unexpected result of greater than 50% incorporation of maleic anhydride into MMA/MaIA copolymers by Blackley and Melville.[96]

CHAPTER FOUR

THE DEGRADATION OF POLY(METHYL METHACRYLATE) AND ITS COPOLYMERS WITH MALEIC ANHYDRIDE

In this chapter, the thermal degradation, photodegradation and photothermal degradation of methyl methacrylate/maleic anhydride copolymers are compared with that of poly(methyl methacrylate). Thus, it is possible to examine the effects of the anhydride groups and to propose mechanisms through which these effects operate.

1. Pressed Disc Thermal Degradation

Pressed discs of polymer, prepared as described in Chapter 2, were placed on weighed silica discs of diameter 30mm and thickness 1mm. The silica and sample discs were weighed together and both placed in the degradation apparatus. The system was evacuated to 10^{-6} torr and oven temperature settings of 200°C, 220°C and 240°C were chosen since it is over this range that monomer evolution from PMMA is most conveniently measured. The actual oven temperatures as measured in Chapter 2 are not significantly different from the oven temperature settings and only the latter are therefore quoted in this chapter.

The degradations were carried out in a closed evacuated system with two nitrogen traps to collect volatile products. After degradations, the silica and sample discs were reweighed and the

polymer residue submitted for molecular weight determination. The results are shown in TABLE 4.1.

The graphs of percentage weight loss versus time in FIGURES 4.1, 4.2 and 4.3, illustrate the blocking of the normal unzipping mode of degradation of PMMA by the presence of anhydride groups. The greater the anhydride content in the polymer, then the greater the inhibition of the depolymerisation.

In the PMMA plots, the rate of monomer production falls off quickly and tends to reach a plateau at about 17% degradation. This effect could be caused by the following factors or a combination of them:-

a) The most labile sites for initiation of depolymerisation are unsaturated chain ends, caused by disproportionation termination in polymerisation. In high molecular weight material, there are relatively few of these end groups and, as they are used up, the more stable saturated end groups remain and so the rate of monomer evolution decreases.

b) It has been suggested that weak links exist in PMMA[25] and it may be their rupture and subsequent unzipping of monomer which leads to the initially high rate of monomer production.

c) Since the molten polymer is still highly viscous even above 200°C, the initial evolution of monomer may come only from which it can escape most freely. Once the reaction from molecules near the surface is

TABLE 4.I

Polymer	Degradation time (hr.)	Degradation temperature (°C)	%weight loss	Molecular weight	Number of scissions per monomer unit xI0 ^{5}
PMMA	0	0	0	8I5,000	0
PMMA	I	200	2.4	6I7,000	3.54
PMMA	2.5	200	4.8	550,000	5.04
PMMA	4	200	5.6	538,000	5.26
PMMA	I2	200	I2.9	409,000	9.03
PMMA	I7	200	I6.I	443,000	6.68
50/I	0	0	0	I,I50,000	0
50/I	I	200	0.8	973,000	I.49
50/I	3	200	I.I	287,000	25.8
50/I	6	200	I.3	239,000	32.6
50/I	I2	200	I.7	308,000	23.2
50/I	I7	200	I.3	228,000	34.6
20/I	0	0	0	I,I50,000	0
20/I	I	200	0.2	575,000	8.66
20/I	2	200	0.8	548,000	9.40
20/I	6	200	0.9	429,000	I4.4
20/I	I2	200	0.8	389,000	I6.8
20/I	I7	200	I.0	288,000	25.7

TABLE 4.I(continued)

Polymer	Degradation time(hr.)	Degradation temperature(^{o}C)	%weight loss	Molecular weight	Number of scissions per monomer unit x10^{5}
PMMA	I	220	6.8	562,000	4.30
PMMA	2	220	I0.5	575,000	3.2I
PMMA	4	220	I3.3	526,000	4.I8
PMMA	6	220	I5.6	436,000	7.09
PMMA	I2	220	I6.6	452,000	6.I8
PMMA	I7	220	I7.0	477,000	5.I5
50/I	I	220	I.2	30I,000	24.2
50/I	2	220	I.4	I69,000	49.6
50/I	3	220	3.0	I4I,000	60.0
50/I	6	220	2.9	84,000	I07
50/I	I2	220	2.9	68,500	I33
50/I	I7	220	3.5	48,600	I90
20/I	2	220	I.3	389,000	I6.7
20/I	6	220	I.5	I69,000	49.5
20/I	I2	220	I.5	II3,000	78.3
20/I	I7	220	I.6	70,000	I3I

TABLE 4.I(continued)

Polymer	Degradation time(hr.)	Degradation temperature (^{o}C)	%weight loss	Molecular weight	Number of scissions per monomer unit xI0^{5}
PMMA	2	240	I4.2	396,000	9.42
PMMA	3	240	I5.7	422,000	7.70
PMMA	6	240	I6.8	367,000	9.46
PMMA	II.5	240	I8.I	272,000	I8.3
PMMA	I7	240	20.2	275,000	I7.5
50/I	I.25	240	2.6	———	———
50/I	2	240	3.I	4I,000	227
50/I	4	240	5.0	36,300	253
50/I	6	240	6.5	24,200	378
50/I	I2	240	8.0	2I,400	425
50/I	I7	240	I6.4	I5,I00	544
20/I	2	240	I.4	98,500	9I.5
20/I	4	240	2.5	39,600	237
20/I	5	240	2.8	———	———
20/I	6	240	5.I	2I,I00	44I
20/I	I2	240	5.9	I5,I00	6I2
20/I	I7	240	8.4	I2.700	7II

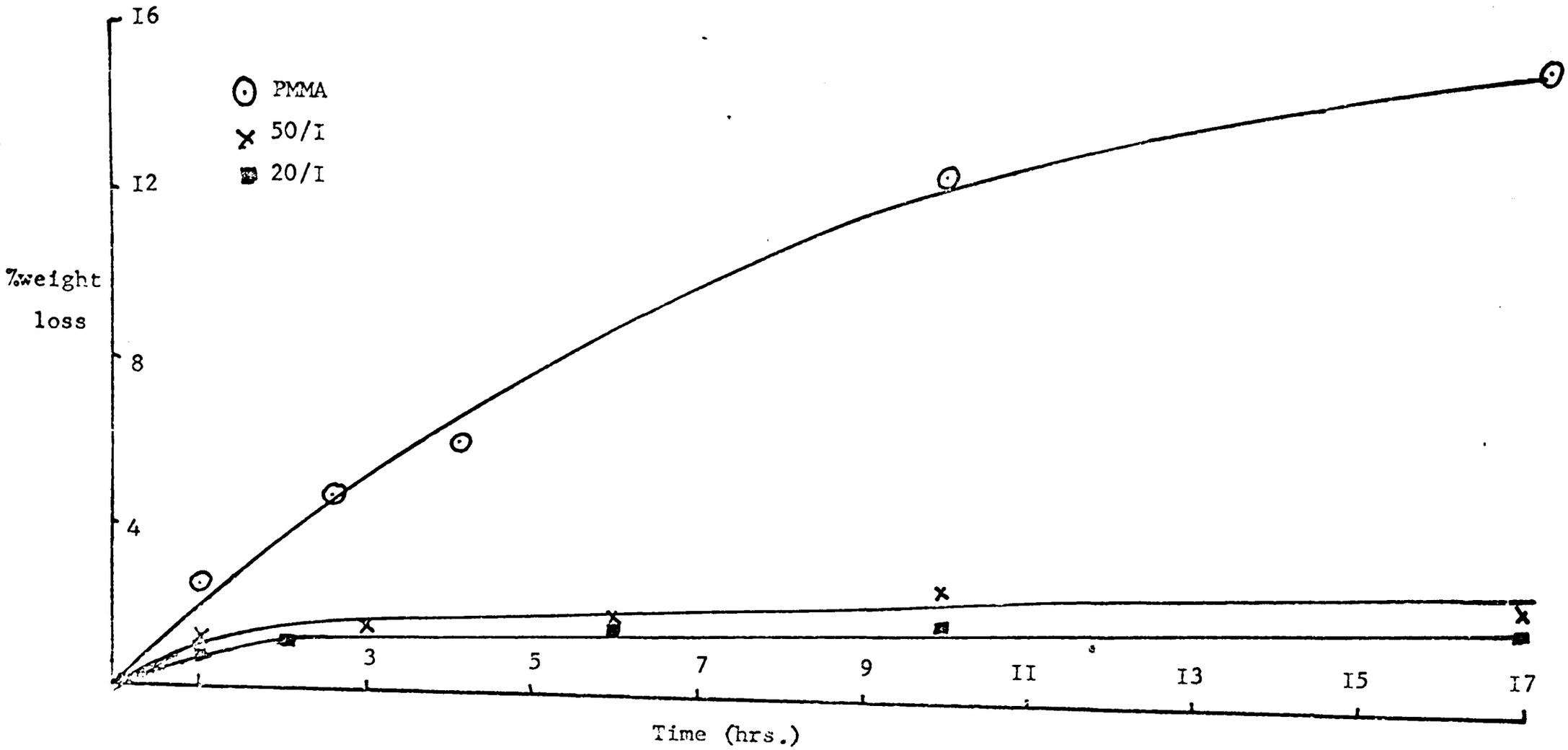

FIGURE 4.I

%weight loss versus time for thermal degradation at 200°C

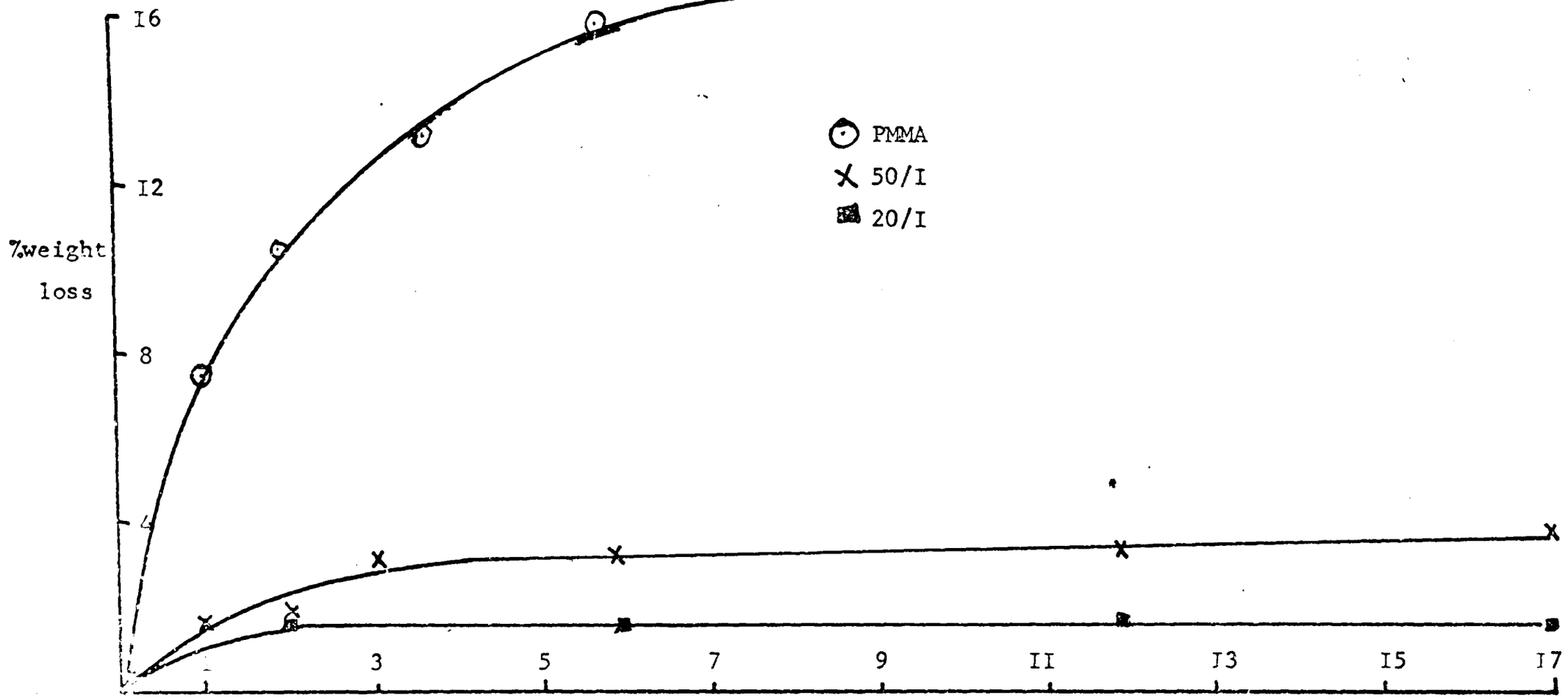

FIGURE 4.4

%weight loss versus time for thermal degradation at 220°C

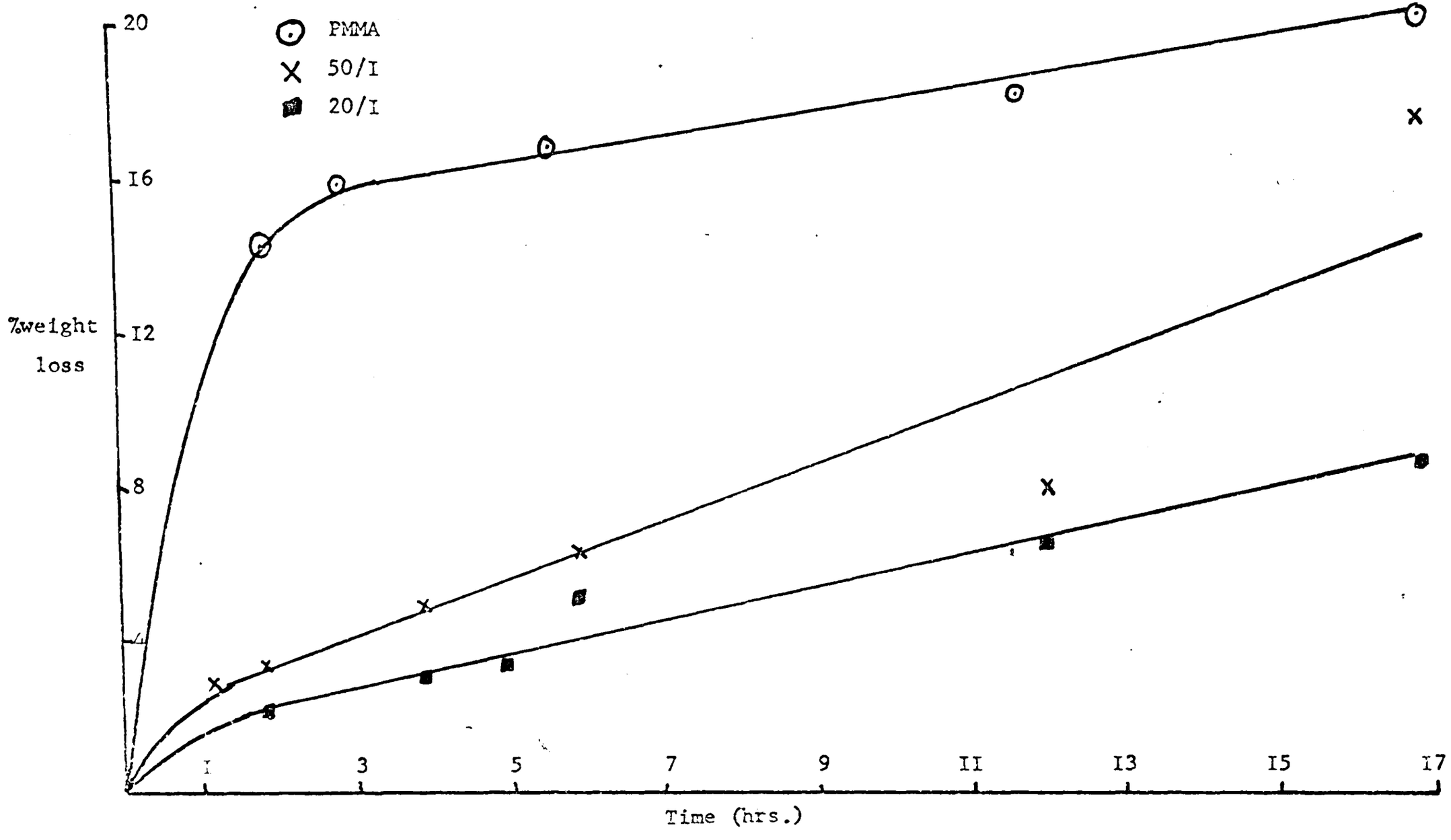

FIGURE 4.3

%weight loss versus time for thermal degradation at 240°C

complete, the rate of evolution of monomer from the sample may be controlled by the rate of diffusion of monomer from the body of the sample.

These possibilities will be discussed later in more detail.

The copolymers also show an initially fast rate of weight loss but this is relatively short lived and is probably due to the early evolution of solvent trapped during precipitation of the polymer after polymerisation. Chloroform, the solvent used to redissolve the precipitate in the purification of the polymer, can be detected by infra-red analysis of the volatile products of degradation. It is present in trace amounts in the degradation products of PMMA and rather greater concentrations in the products from copolymer degradation, although in both cases, methyl methacrylate is by far the major component.

A plot of molecular weight versus percentage weight loss was discussed in Chapter 1 and should be a straight line in which the percentage decrease in molecular weight is equal to the percentage volatilisation when a polymer undergoes only depolymerisation. In FIGURE 4.4, line A represents this theoretical plot and line B the observed plot for PMMA. It is apparent that some chain scission is occurring at 200 - 240°C but that it is independent of temperature in this range. By contrast, the molecular weight changes which occur in the copolymers and which are illustrated in FIGURE 4.5, demonstrate that considerable chain scission is occurring. A rapid decrease in molecular weight is observed with little volatilisation. The effect of temperature does not appear to be significant.

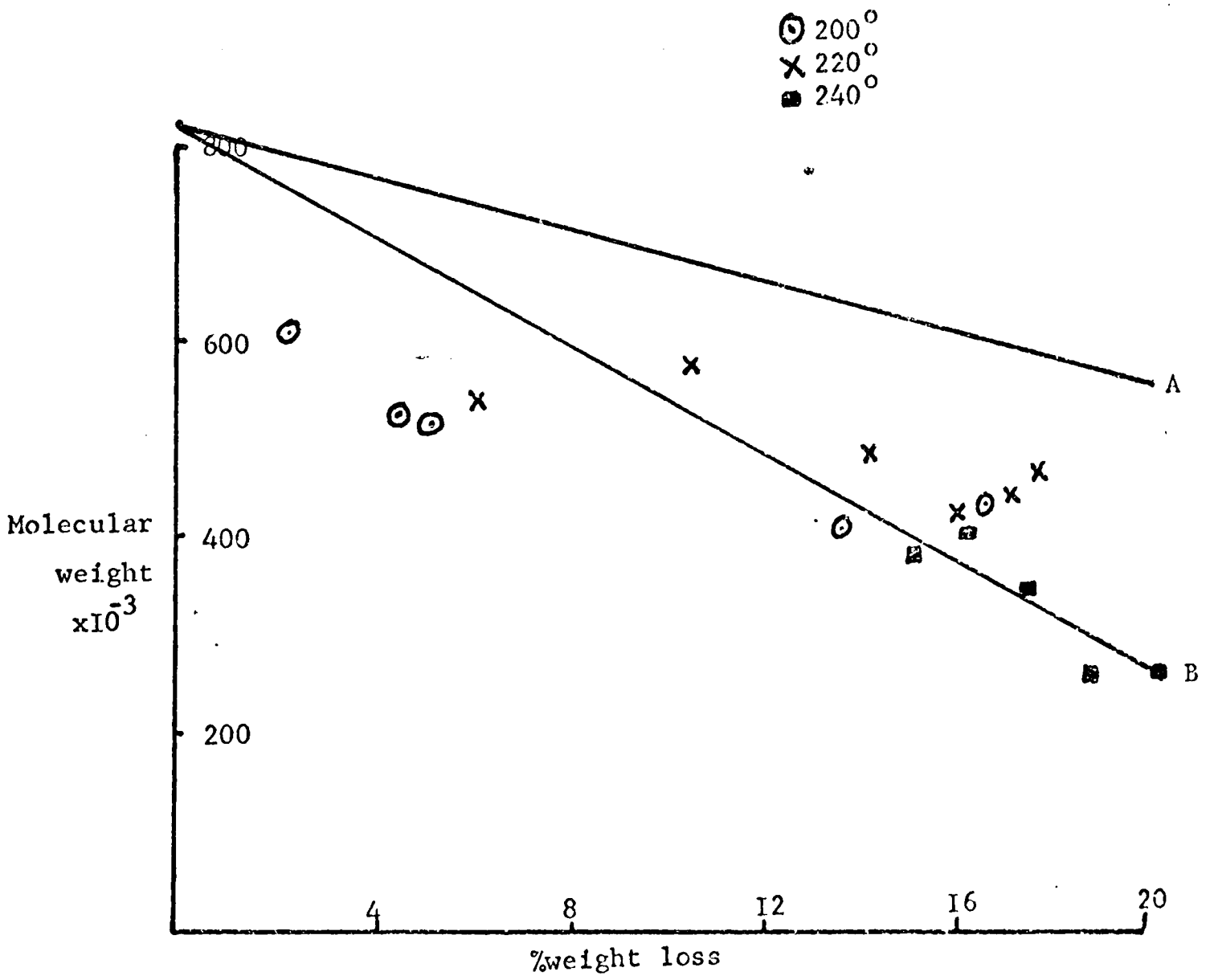

FIGURE 4.4

Molecular weight versus %weight loss for the thermal degradation of PMMA at 200°C, 220°C and 240°C

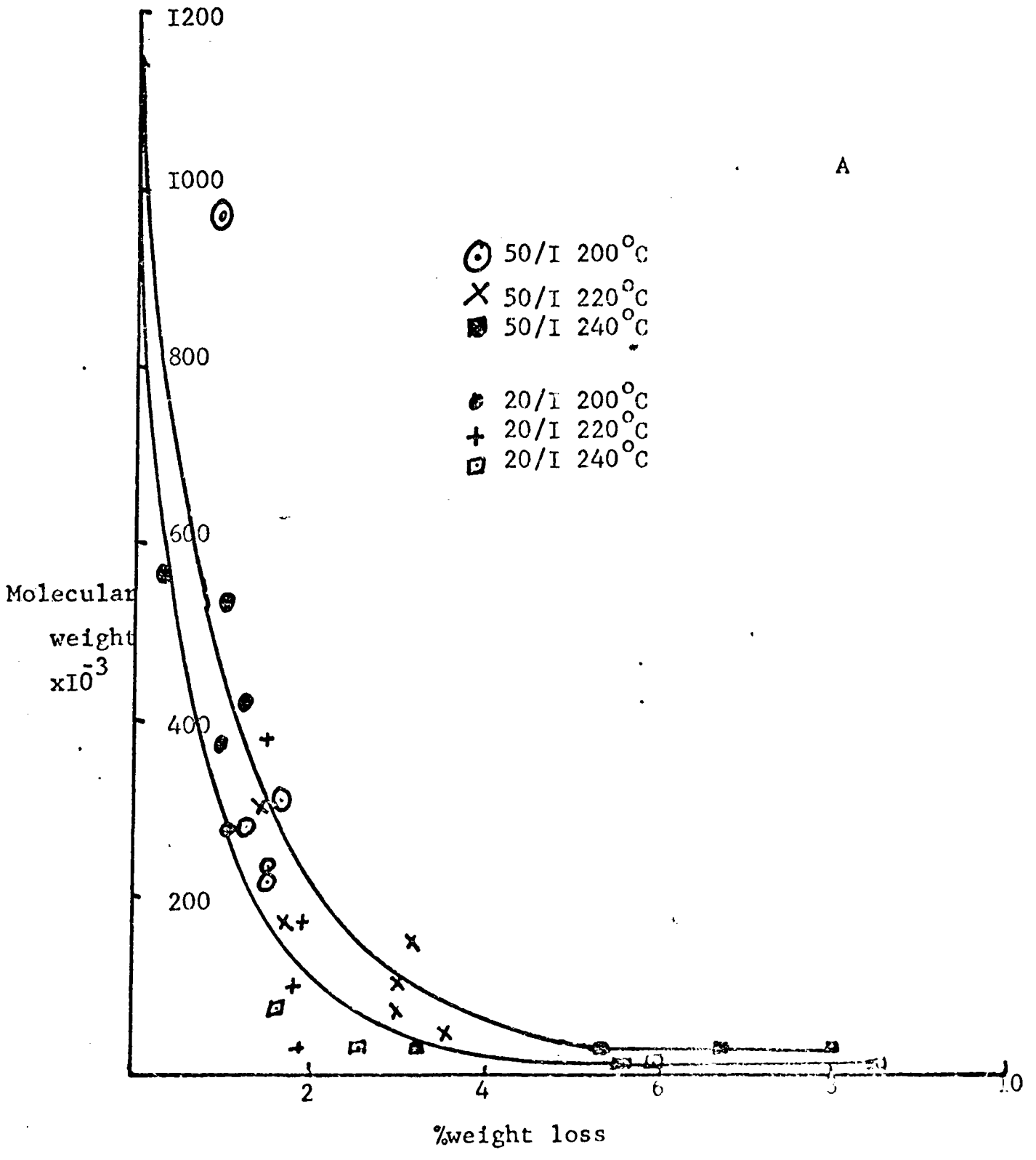

A

FIGURE 4.5

Molecular weight versus %weight loss for the thermal degradation of the 50/I and 20/I copolymers at 200°C 220°C and 240°C

The rate of chain scission can be found by considering the effect of n chain scissions on a polymer of chain length P_o monomer units. Since n+1 molecules are formed, the resulting average chain length P_t is given by $\frac{P_o}{n+1}$

Rearranging, $n = \frac{P_o}{P_t} - 1$

Since each polymer may have a different initial molecular weight, the number of breaks per monomer unit s, is a more useful and meaningful quantity. Thus:-

$$S = \frac{n}{P_o}$$

$$\therefore \quad S = \frac{1}{P_t} - \frac{1}{P_o} \qquad - (1)$$

When volatilisation occurs in addition to chain scission,

$$P_t = \frac{P_o(1-x)}{n+1}$$ where x = weight fraction lost in volatilisation

$$\therefore \quad S = \frac{1-x}{P_t} - \frac{1}{P_o} \qquad - (2)$$

FIGURES 4.6, 4.7 and 4.8 show how chain scission varies with time at 200°C, 220°C and 240°C. It is immediately obvious that the copolymers undergo chain scission at a substantially higher rate than PMMA. However, approximate values for initial rates have been estimated from the initial slopes of the curves in FIGURES 4.6, 4.7 and 4.8 and are shown in TABLE 2.

Additional information about the thermal behaviour of PMMA

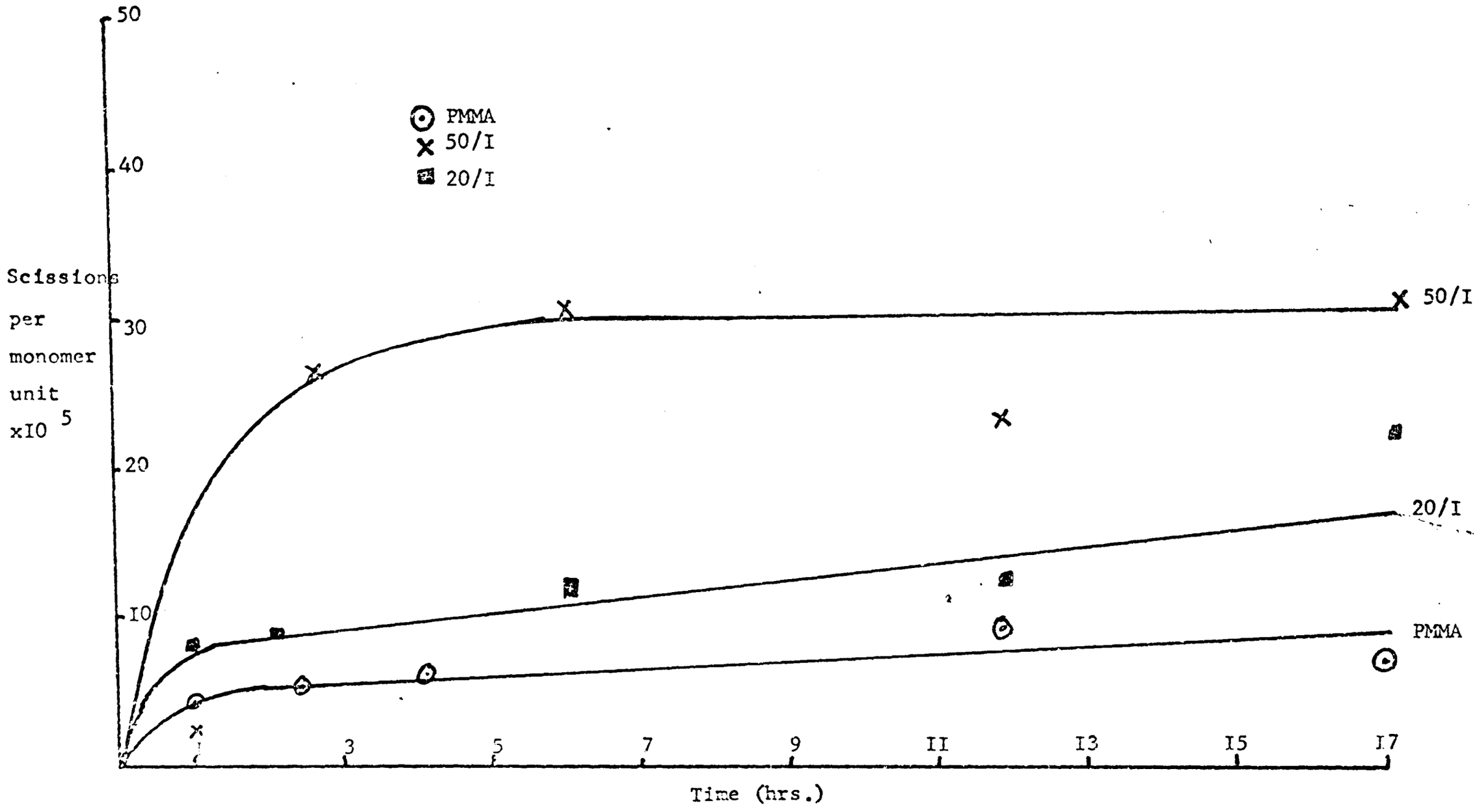

FIGURE 4.6

Scissions per monomer unit versus time for the thermal degradation of the polymers at 200°C

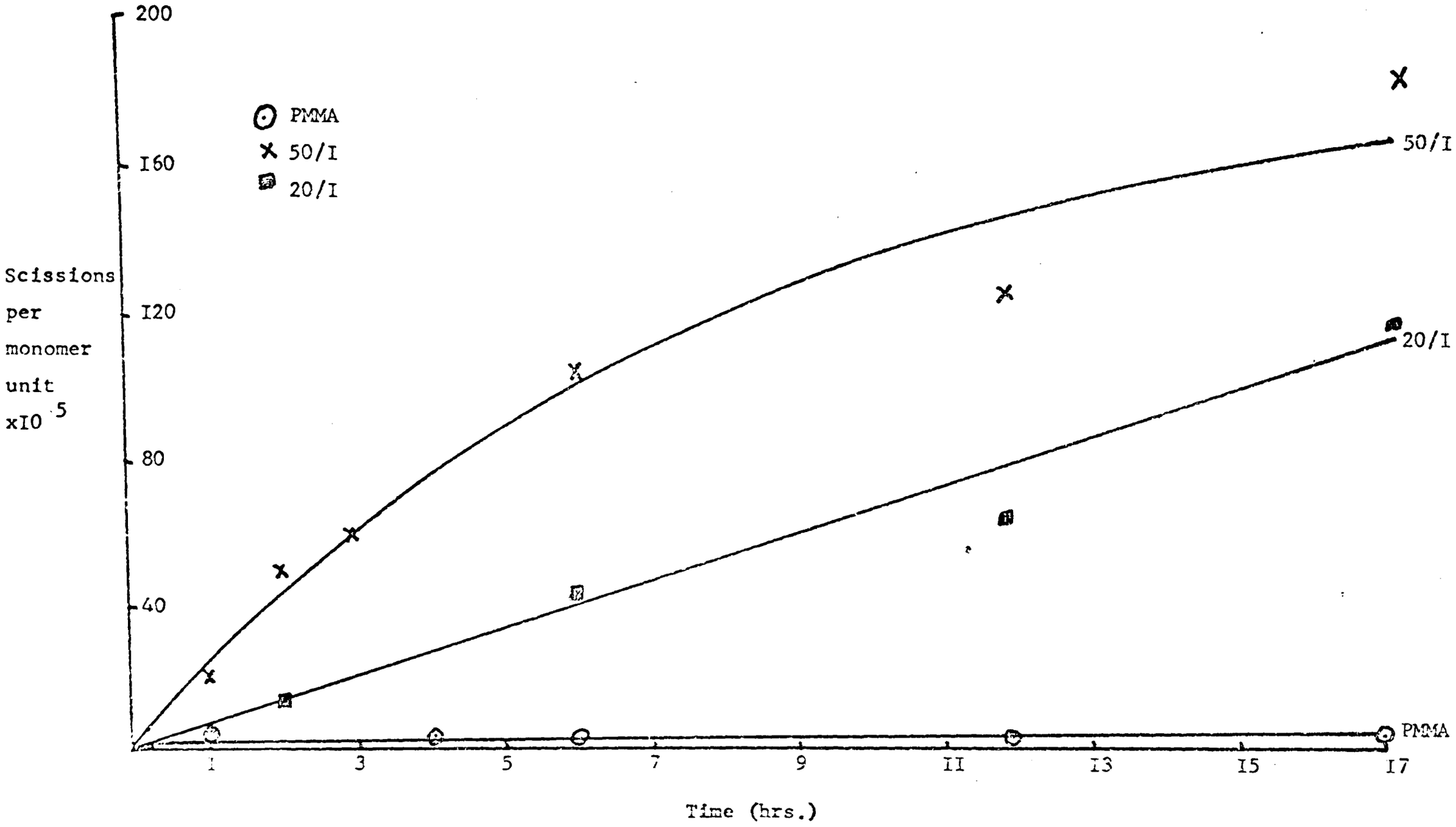

FIGURE 4.7

Scissions per monomer unit versus time for the thermal degradation of the polymers at 220°C

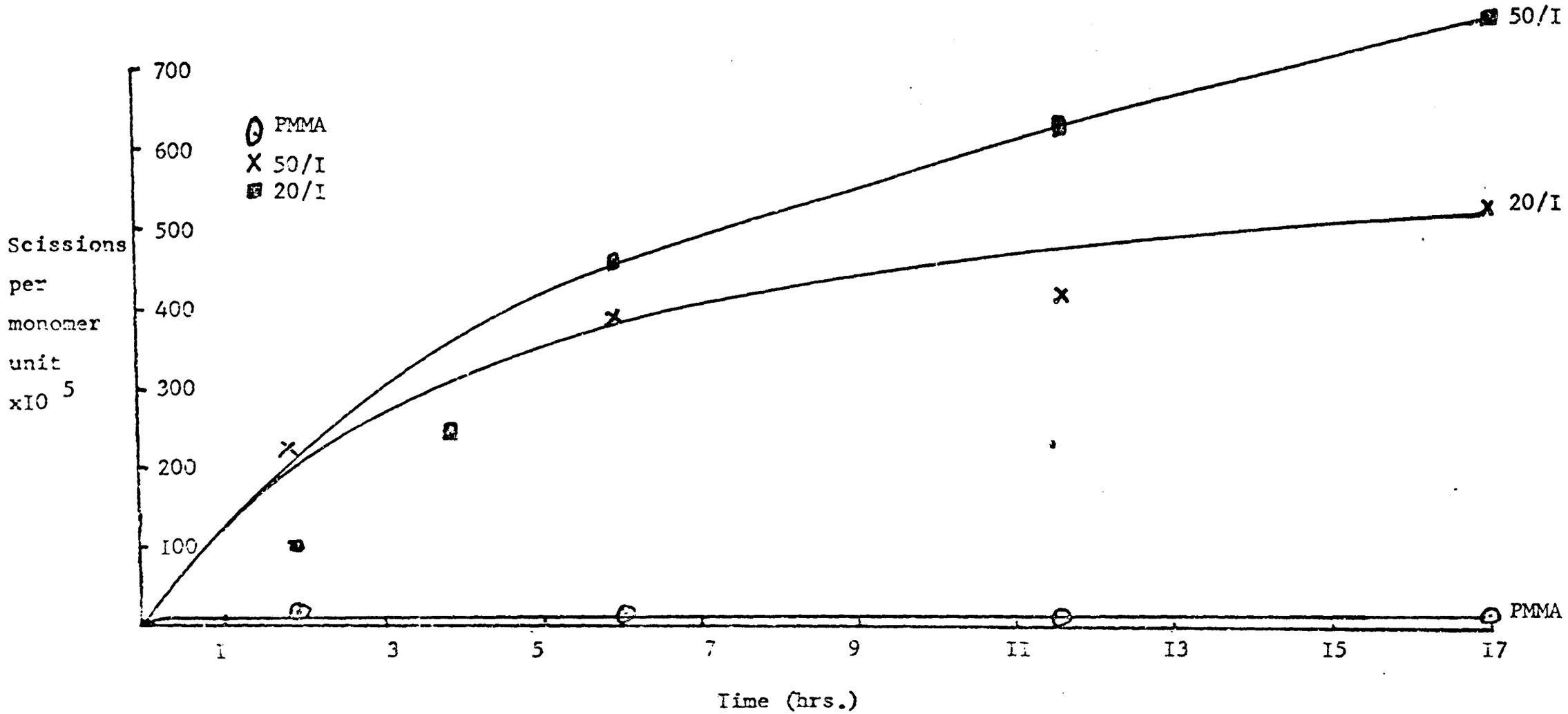

FIGURE 4.8 Scissions per monomer unit versus time for the thermal degradation of the polymers at 240°C

TABLE 4.2

Polymer	Temperature of degradation (^{o}C)	Initial rate of chain scission (sc./m.u./hr.xI0 ^{5})
PMMA	200	3.5
50/I	200	8.5
20/I	200	8.5
PMMA	220	4.3
50/I	220	26
20/I	220	I7
PMMA	240	I0
50/I	240	230
20/I	240	90

TABLE 4.3

Polymer	T_{max} (^{o}C)		
	Peak I	Peak 2	Peak 3
PMMA	289	374	___
I00/I	___	334	409
50/I	___	338	409
20/I	___	345	4I4
I9/I	___	338	425
I2.5/I	___	345	409

and the copolymers can be obtained from thermogravimetry and thermal volatilisation analysis (TVA).

2. Thermogravimetry

FIGURE 4.9 shows the thermogravimetric traces of 73 PMMA, 100/1 and 12.5/1 polymers. Ten mg powdered samples were heated at a rate of 10°/min in an atmosphere of nitrogen. The copolymers appear more stable than the homopolymer, at least as far as weight loss is concerned. In addition, two distinct stages of degradation can be identified.

3. Thermal Volatilisation Analysis

TVA thermograms are shown in FIGURES 4.10, 4.11 and 4.12 and indicate - the rate of evolution of volatiles with increasing temperature

The thermogram in FIGURE 4.10 is typical of high molecular weight ($\bar{M}_n$ = 815,000) PMMA. The 0°C and -45°C lines are coincident and record the amount of volatiles passing through the traps which in this case is methyl methacrylate. The -75°C trace shows a limiting rate effect due to the fact that although methyl methacrylate condenses in the -75°C trap, it is sufficiently volatile to distil slowly into the main trap (-196°C). The monomer is virtually totally condensed in both the -100°C and -196°C traps.

There are two rate maxima in the PMMA thermogram. The first, at 280°C, is due to degradation by initiation and subsequent unzipping

FIGURE 4.9

Thermogravimetric traces

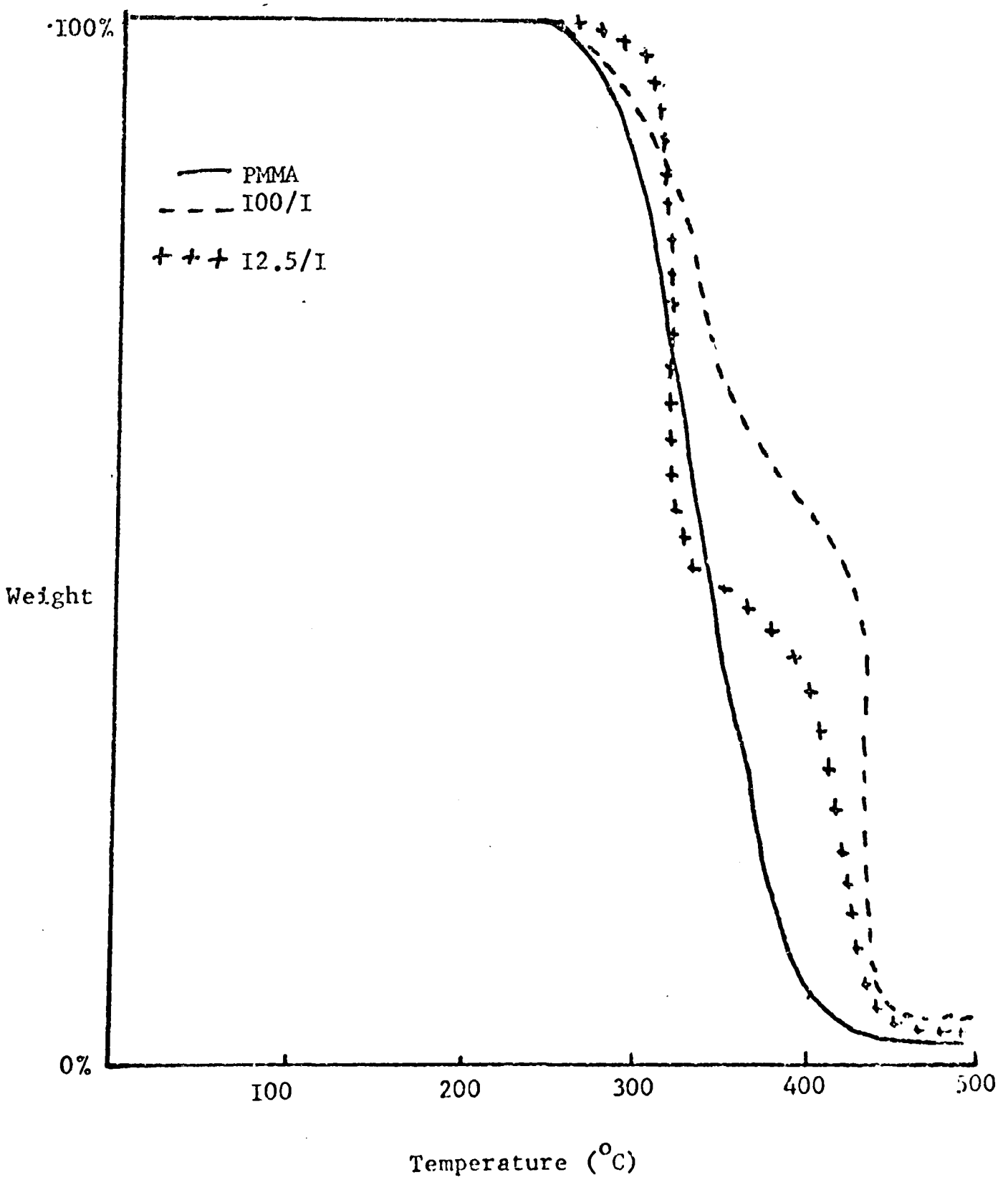

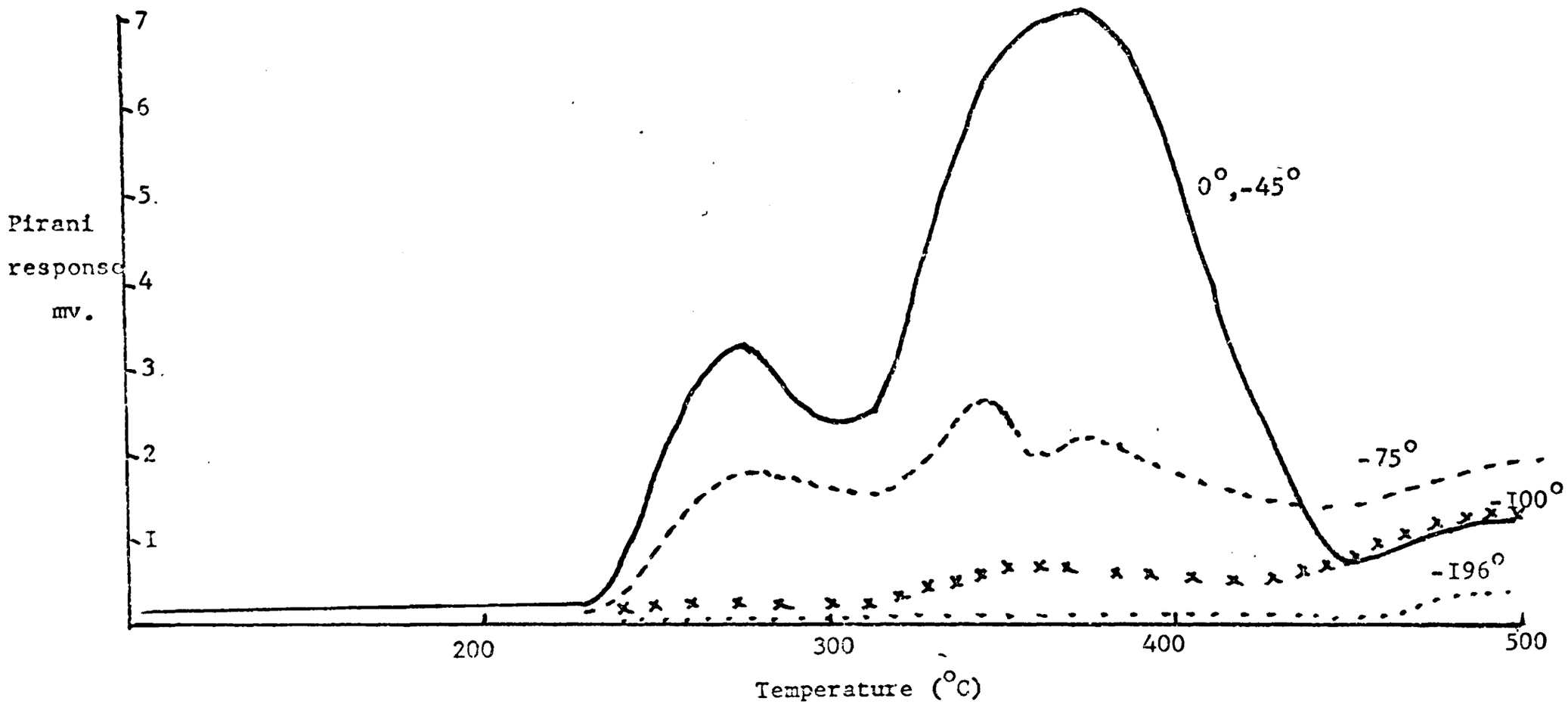

FIGURE 4.I0 T.V.A. thermogram for PMMA

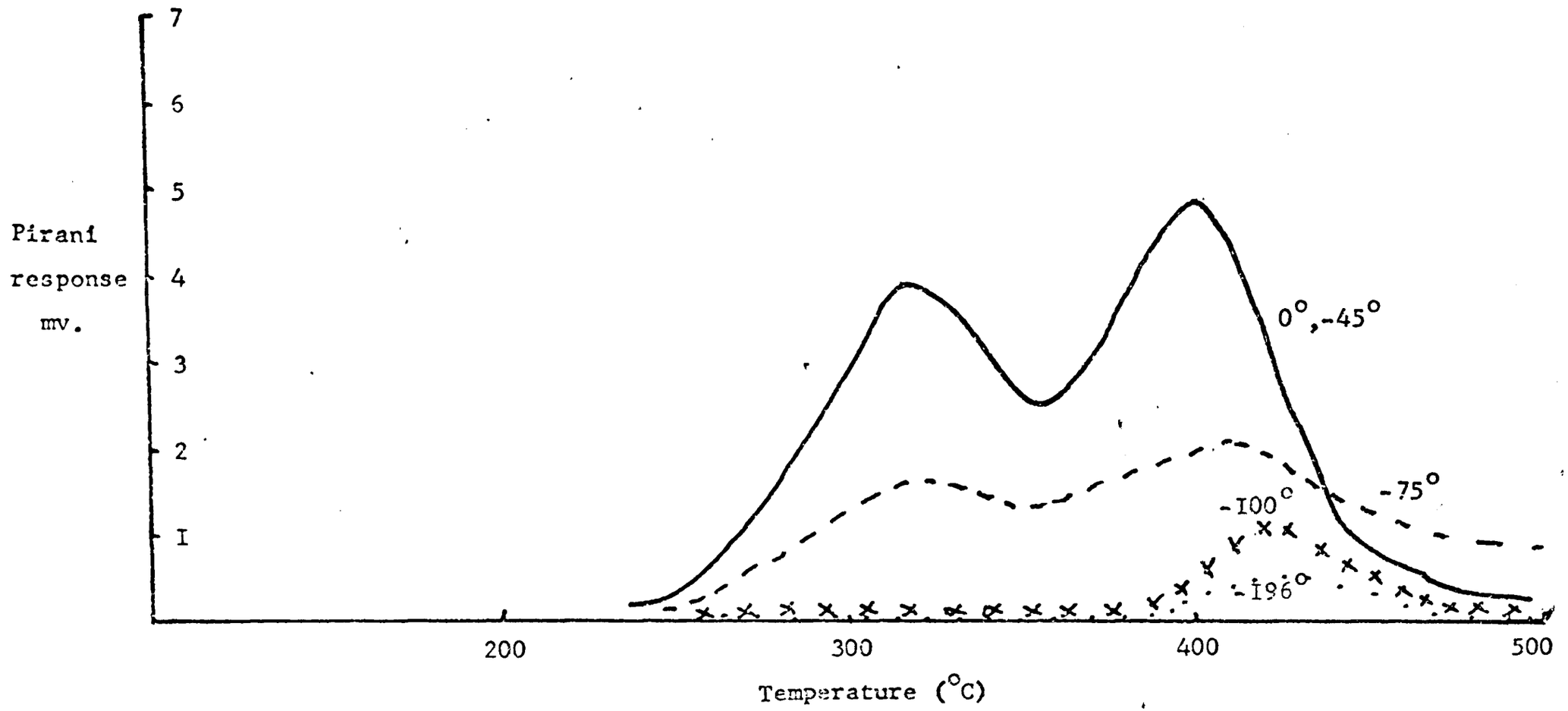

FIGURE 4.II

T.V.A. thermogram for I00/I copolymer

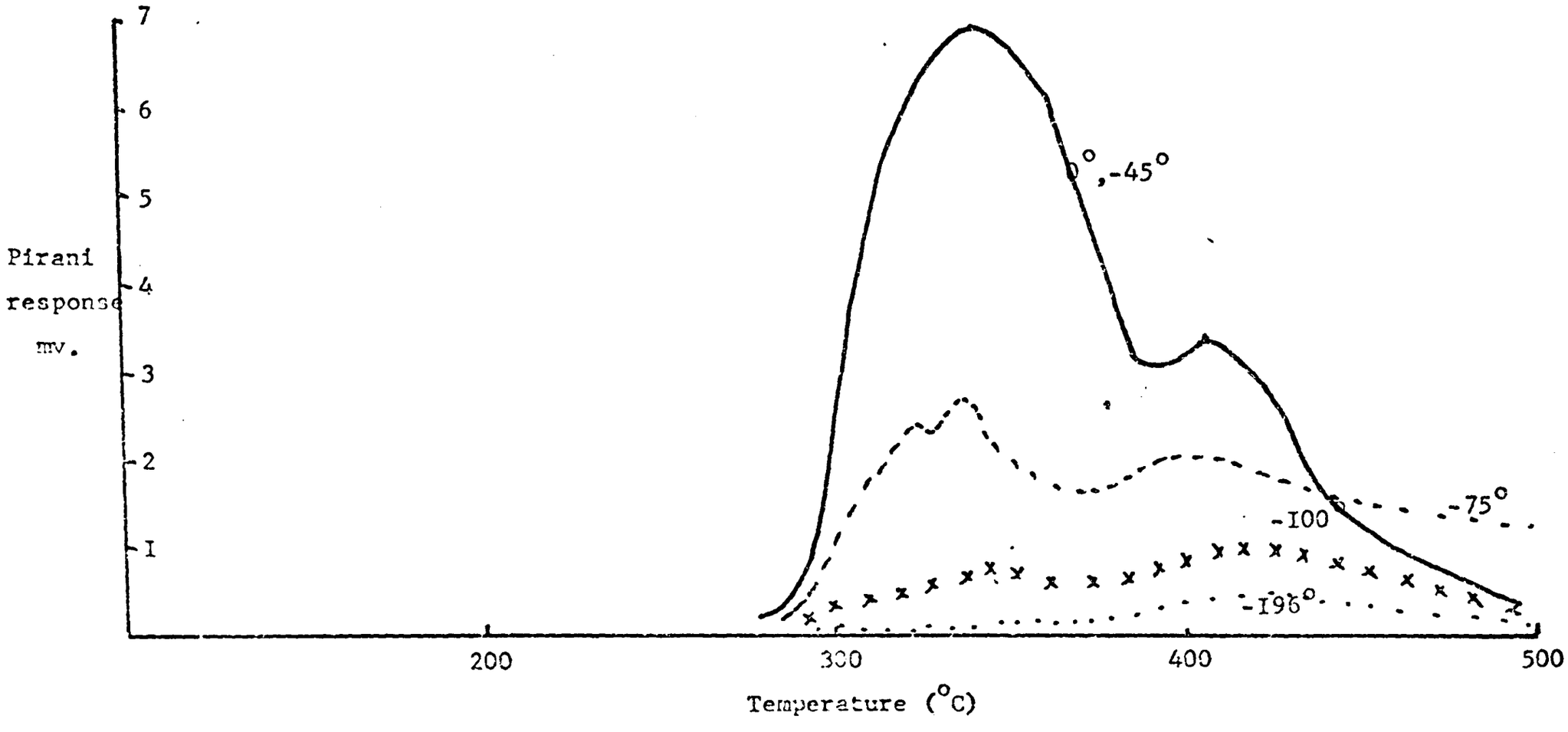

FIGURE 4.12 T.V.A. thermogram for I2.5/I copolymer

of monomer units from unsaturated chain ends. In high molecular weight PMMA this first peak is small compared to the second, partly because there are relatively fewer unsaturated chain terminal structures and partly because the kinetic chain length of unzipping is considerably less than the molecular chain length. PMMA of low molecular weight (eg. $\bar{M}_n$ = 20,000) has two peaks of almost equal size since there are more unsaturated chain ends from which unzipping may begin and the chain length for unzipping is greater than the molecular chain length.

The effect of introducing one per cent of maleic anhydride into the PMMA chain is illustrated in FIGURE 4.11. Here, the peak due to end - initiated depolymerisation has disappeared and the first peak observed corresponds to the second peak in the PMMA thermogram. That is, it is due to the evolution of monomer after chain fragmentation. If T_{max} represents the temperature at which the rate of volatilisation reaches a maximum, then TABLE 4.3 show T_{max} for the various peaks on the recorded thermograms of several maleic anhydride /MMA copolymers. It appears that T_{max} for peak 2 is reduced by 30-40°C when anhydride groups are built into the chain. Peak 3 which is associated only with the copolymers, appears at a temperature above that of the second peak in PMMA.

T_{max} is influenced by several factors including molecular weight. While this is sufficient to account for the relatively small variations of T_{max} within the copolymer range, separate mechanisms must be involved to explain the large drop of T_{max} in peak 2, the disappearance of peak 1 and the appearance of peak 3.

It has already been explained that, in PMMA, peak 1 is due to unzipping initiated at unsaturated chain ends and that peak 2 is due to chain fragmentation and subsequent unzipping. If it is accepted that the anhydride group blocks the unzipping mechanism in MMA, yet acts as a weak link in the PMMA chain, that is, it becomes a more active site for chain scission than a methyl methacrylate unit then the absence of peak 1 in the thermograms of the copolymer is explained. However, should chain scission occur between a MMA and an anhydride unit, then two chains would be formed, one with a terminal anhydride group and the other with a MMA group which could immediately unzip as far as the next anhydride unit in the chain. Because this chain scission reaction occurs 30-40°C below the corresponding reaction in PMMA, it would appear that the anhydride tends to encourage chain scission. The unzipping of MMA from this chain break gives rise to peak 2. The anhydride terminated chain, however, carries on its blocking function and it is not until above 400°C that the thermal energy is sufficient to overcome this with corresponding loss of MMA resulting in peak 3.

A higher rate of chain scission and therefore a larger peak 2 is to be expected as the anhydride content is increased on progressing from 100/1 to 12.5/1 copolymers. This is seen to be the case.

4. Solution Photodegradation

In solution at room temperature, it is possible to investigate pure chain scission without the complications of crosslinking, diffusion etc, which can occur in bulk.

Using methyl acetate as solvent, MMA and the anhydride copolymers were degraded photolytically as described in Chapter 2. The concentration of sample was normally about 25mg/ml. Concentration effects have been shown to be small over a large range of concentrations. Molecular weight data are shown in TABLE 4.4, and the number of scissions per monomer unit calculated using equation (1) are shown in TABLE 4.5. By plotting the number of chain scissions against time (FIGURE 4.13), the initial rate of chain scission can be obtained. These rates are shown in TABLE 4.6. The linear relationship between the rates and the mole fraction of anhydride in each polymer is illustrated in FIGURE 4.14. It can be seen that the effect of the anhydride group in enhancing chain scission in photodegradation is less than its effect on chain scission at elevated temperatures in the absence of ultra-violet light.

Infra-red analysis of the polymer after degradation suggests that chain scission occurs at the bond linking an anhydride group with an MMA group, the essential anhydride structure being preserved, since the intensity of the anhydride absorption band in the carbonyl region is unaltered.

5. Thin Film Photodegradation

It is not appropriate to degrade photolytically pressed disc samples of PMMA because of the high degree of reflection of the light by the opaque disc. For this reason, the polymer samples were prepared in the form of thin films, generally cast from chloroform solutions and degraded as described in Chapter 2.

TABLE 4.4

Molecular weights after ultra-violet irradiation in solution

Polymer	Degradation time (hrs.)				
	0	0.5	I.0	I.5	2.0
Aug PMMA	I,I00,000	72,000	———	25,800	20,400
new PMMA	649,000	———	32,500	23,900	I8,800
I00/I	I,690,000	65,700	49,500	22,300	I6,800
50/I	I,I50,000	60,500	28,200	2I,800	I7,900
20/I	I,I50,000	45,400	26,I00	I9,300	I7,300

TABLE 4.5

Number of chain scissions per monomer unit

Polymer	Degradation time (hrs.)				
	0	0.5	I.0	I.5	2.0
Aug PMMA	0	I30	———	378	480
new PMMA	0	———	292	403	5I6
I00/I	0	I46	I96	443	590
50/I	0	I57	346	450	550
20/I	0	2I2	375	5I0	572

TABLE 4.6

Polymer	Rate of chain scission ($sc./m.u./hr. \times I0^{5}$)
Aug PMMA	247
new PMMA	265
I00/I	290
50/I	340
20/I	4I3

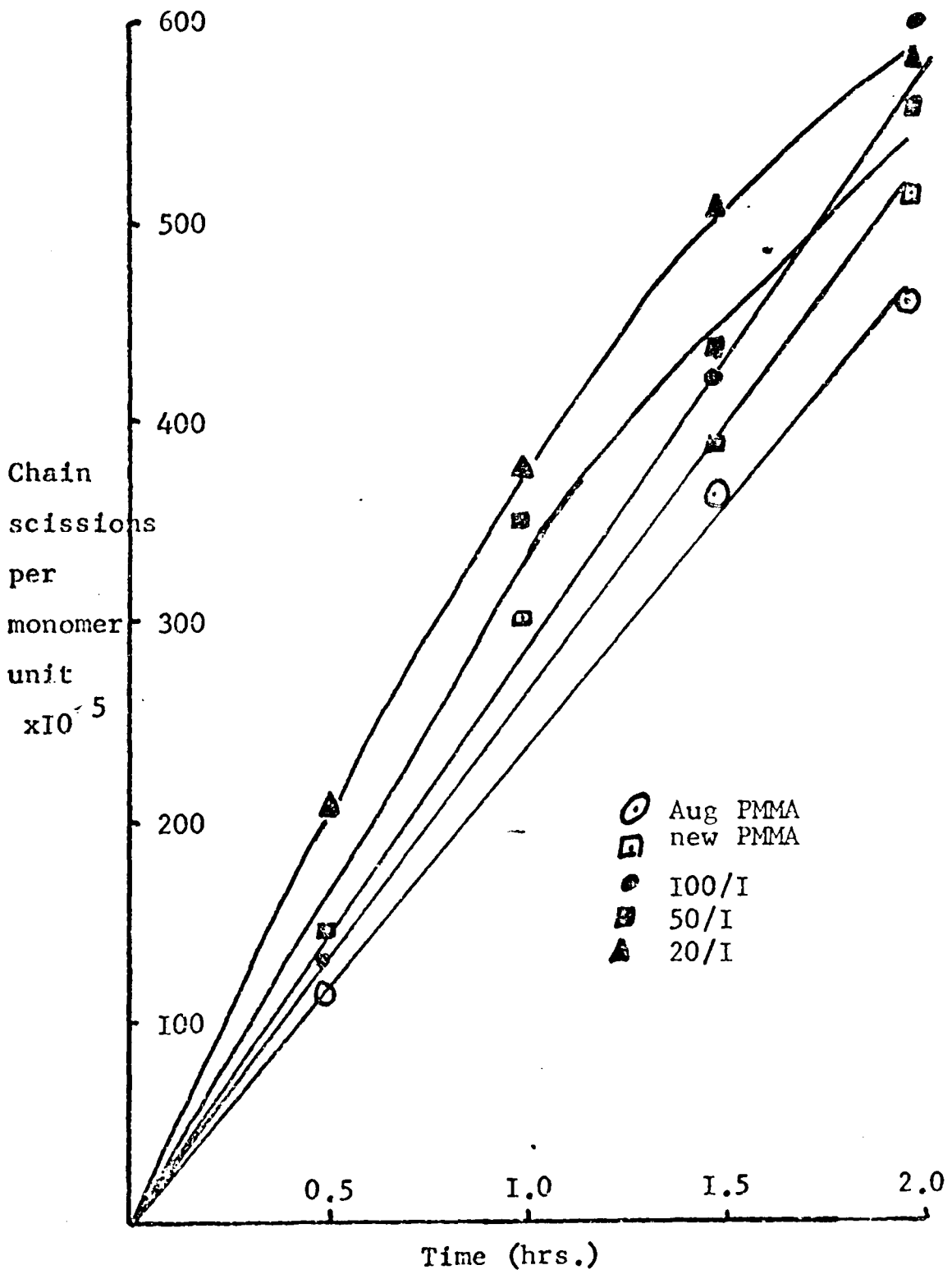

FIGURE 4.I3 Rates of photodegradation in solution

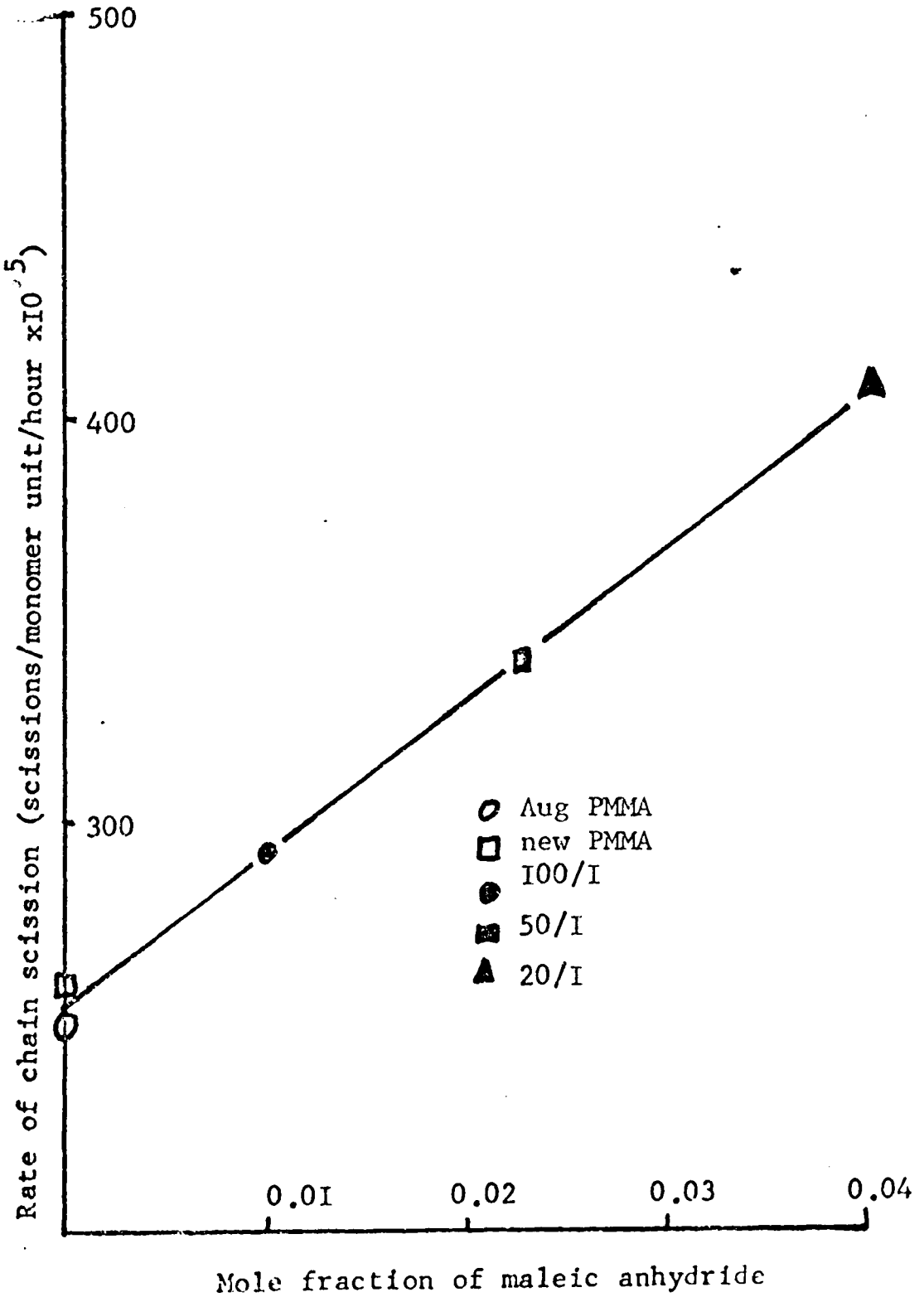

FIGURE 4.I4

Rate of chain scission versus mole fraction of maleic anhydride

As in solution degradation, because volatile products are not formed, molecular weight changes should be described by equation (1). TABLE 4.7 details the results of photodegradation on three polymers and FIGURE 4.15 shows the rate at which each polymer degrades. Again, the relationship between the rate of chain scission and anhydride content is shown in FIGURE 4.16 from the rates calculated from FIGURE 4.15 and shown in TABLE 4.8.

The data appear to indicate that the polymers degrade less readily in the solid state than in solution. However, this may be partly due to the fact that a less powerful U.V. lamp was employed which was placed further from the sample than in the solution photo-degradations although radicals formed in the thin films also tend to recombine more readily than in solution. The effect of solvent on the reaction will be discussed in the following chapter.

Although weight losses were negligible, traces of MMA were observed amoung the volatile products together with the solvent chloro-form. As in the case with photodegradation in solution the anhydride function appears unaltered in infra-red after degradation.

These results on thin film photodegradation do not show particularly clearly the effect of the anhydride groups on the photo-stability of PMMA. The photodegradation in solution achieves this rather more accurately although the trend of increasing instability to ultra-violet light with increasing anhydride content is evident in the thin film degradations. However, they are useful for comparison with the effects of light at room temperature and at elevated temperatures

TABLE 4.7

Polymer	Degradation time (hrs.)	Molecular weight $xI0^3$	Chain scissions per monomer unit $xI0^5$
Aug PMMA	0	I,100	0
Aug PMMA	6	I93	42.7
Aug PMMA	8	I88	44.I
Aug PMMA	I0	I4I	6I.9
I00/I	0	I,690	0
I00/I	I.75	6I7	I0.3
I00/I	4	244	35.0
I00/I	6.05	202	43.5
I00/I	8	I43	64.0
I00/I	9.55	I32	69.8
I9/I	0	685	0
I9/I	2	396	I0.7
I9/I	4	234	28.2
I9/I	6	I77	4I.7
I9/I	8	I35	59.5
I9/I	I0.25	90	96.5

TABLE 4.8

Polymer	Rate of chain scission (sc./m.u./hr. $xI0^5$)
Aug PMMA	6.2
I00/I	7.5
I9/I	7.9

FIGURE 4.I5

Thin film photodegradation

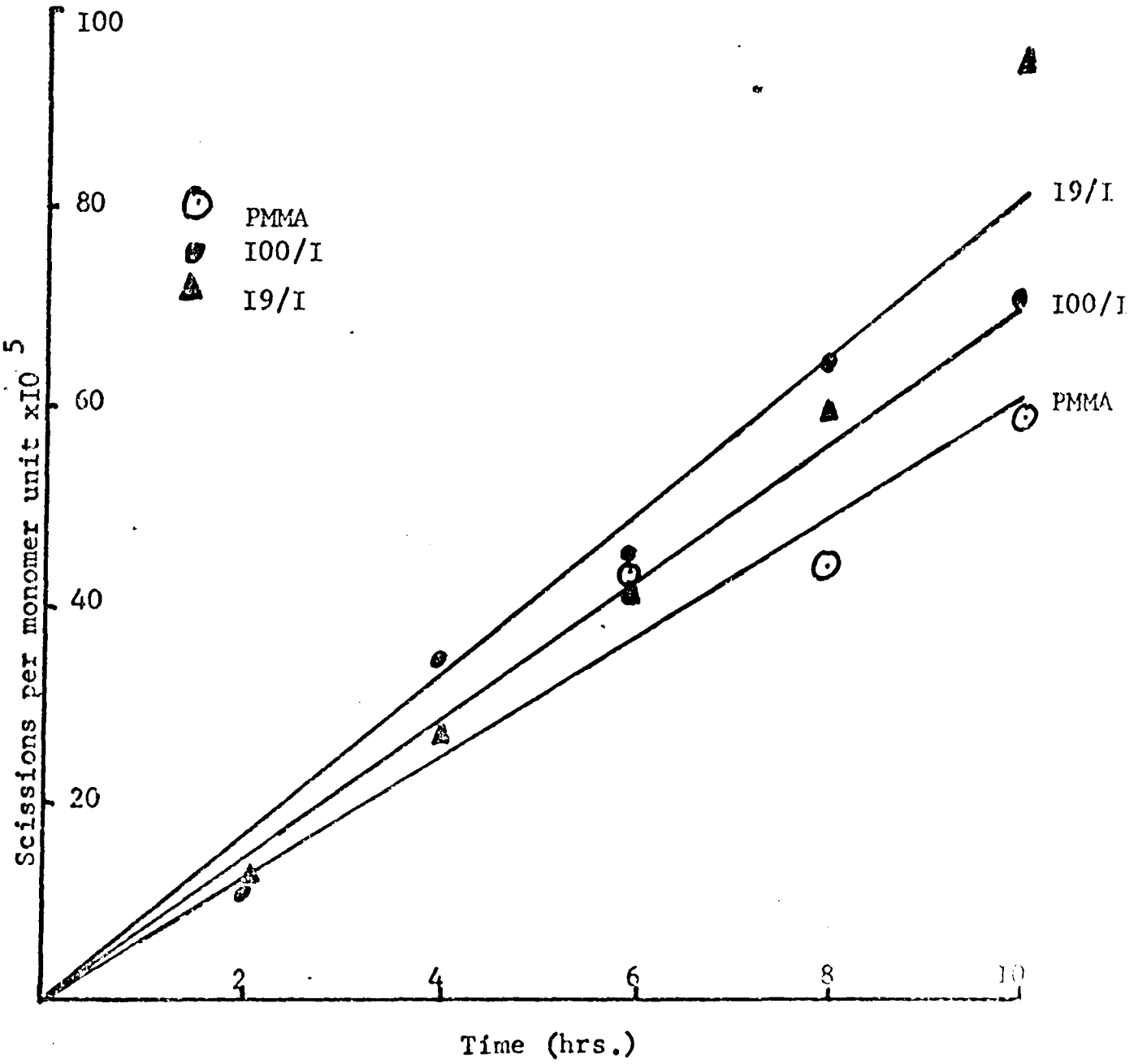

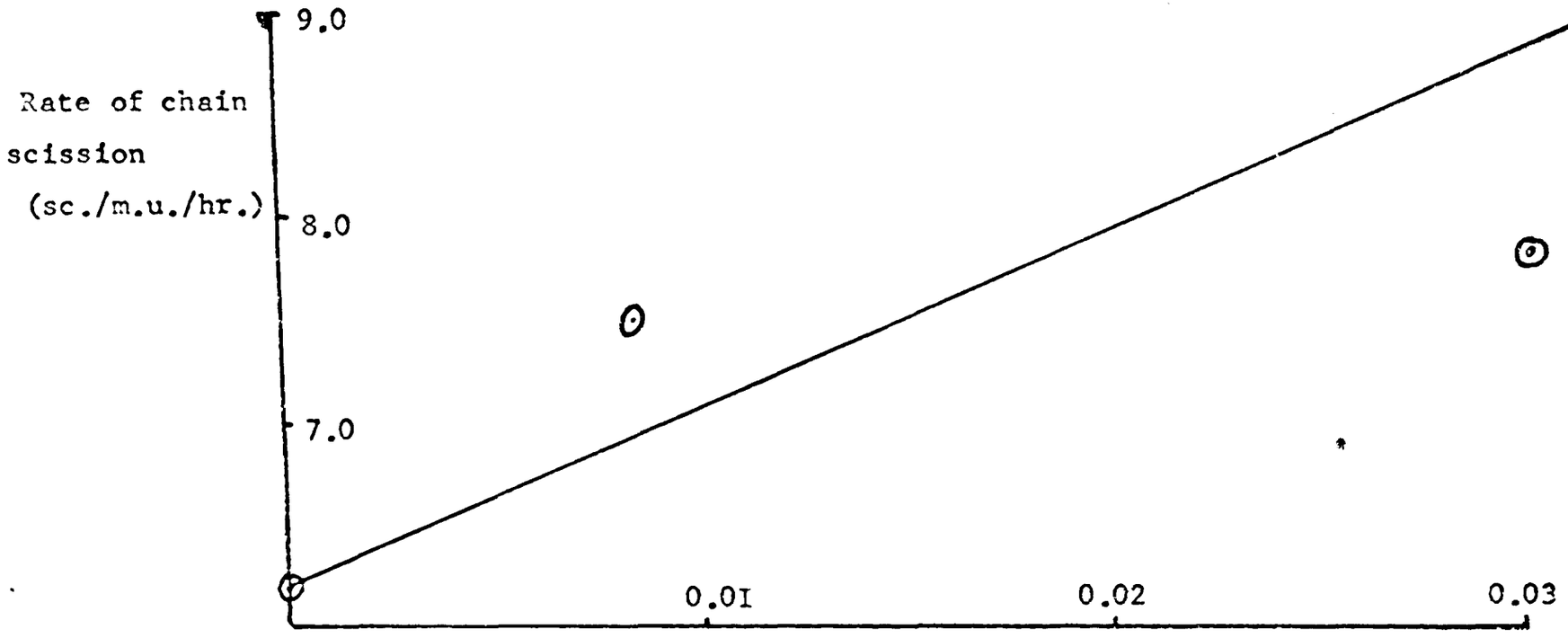

FIGURE 4.16

Rate of chain scission versus mole fraction of anhydride

which is described in the following section.

6. Photothermal Degradation

Experiments described above have shown that the mechanism of thermal and photodegradation of PMMA and copolymers of MMA with maleic anhydride are markedly different. It is, therefore, of interest to examine the photothermal degradation in which the effects of heat and light are combined.

Two temperatures were chosen: Initially, 150°C was used since thermal degradation is negligible at this temperature although the polymer is near its melting point and the molecules should thus be relatively mobile. Results are shown in TABLE 4.9. The graph of % weight loss versus time (FIGURE 4.17) confirms what might be expected, namely that the rate of weight loss of MMA from PMMA is greater than from the copolymers. The rate of degradation of PMMA is also much faster under ultra-violet light at 150°C than it is even at 240°C without light as has previously been shown by other workers.[53] However, the weight loss shown by the copolymers is now appreciable. What is even more significant is that the rate of chain scission (FIGURE 4.18) of PMMA is even greater than that of the copolymers. In considering the possible reasons why the rate of chain scission under photothermal conditions is greater in PMMA than in the copolymers while under pure thermal and pure photo conditions the reverse is true, the following factors may play a part:-

a) The effect of temperature and the physical condition of the polymers.

TABLE 4.9

Polymer	Degradation time (hrs.)	Degradation temperature (^{o}C)	%weight loss	Molecular weight	Scissions/ monomer unit xIO^{-5}
Aug PMMA	0	0	0	I,I00,000	0
Aug PMMA	I	I50	6.6	42,200	212
Aug PMMA	2.5	I50	I4.0	20,900	402
Aug PMMA	5	I50	30.6	I0,500	65I
I00/I	0	0	0	I,690,000	0
I00/I	I	I50	5.9	60,800	I49
I00/I	2	I50	II.5	34,400	252
I00/I	4	I50	I7.5	20,600	395
I00/I	6	I50	23.2	I9,300	39I
I9/I	0	0	0	685,000	0
I9/I	0.5	I50	I.6	252,000	24.4
I9/I	I	I50	4.3	99,I00	82.0
I9/I	2	I50	7.9	53,800	I56
I9/I	4	I50	I3.7	34,200	238
	(Minutes)				
73 PMMA	0	0	0	2,810,000	0
73 PMMA	I5	I70	8.3	3I6,000	25.5
73 PMMA	30	I70	I5.4	I60,000	49.4
73 PMMA	35	I70	I6.I	II0,000	72.8
73 PMMA	60	I70	27.2	72,900	96.5
73 PMMA	60	I70	32.7	50,000	I3I.0
73 PMMA	65	I70	26.9	62,000	II4.0
73 PMMA	90	I70	26.2	49,000	I46.0
73 PMMA	I20	I70	54.I	———	———

TABLE 4.9(continued)

Polymer	Degradation time (mins.)	Degradation temperature (^{o}C)	%weight loss	Molecular weight	Scissions/ monomer unit $\times 10^{5}$
I00/I	0	0	0	I,690,000	0
I00/I	I5	I70	5.8	436,000	I5.7
I00/I	30	I70	7.9	209,000	38.2
I00/I	60	I70	I7.4	II0,000	69.4
I00/I	90	I70	27.0	79,000	86.5
I00/I	I27	I70	30.2	8I,000	80.3
50/I	0	0	0	I,I50,000	0
50/I	I5	I70	3.3	408,000	I5.0
50/I	30	I70	7.0	226,000	32.4
50/I	60	I70	II.I	I2I,000	64.6
50/I	90	I70	I7.5	90,000	83.0
50/I	I20	I70	I8.8	95.I00	76.7
I8/I	0	0	0	2,530,000	0
I8/I	I5	I70	2.7	347,000	24.0
I8/I	35	I70	5.3	I98,000	43.9
I8/I	60	I70	8.7	I3I,000	65.6
I8/I	90	I70	II.2	I0I,000	84.0
I8/I	I20	I70	I3.5	89,000	93.3

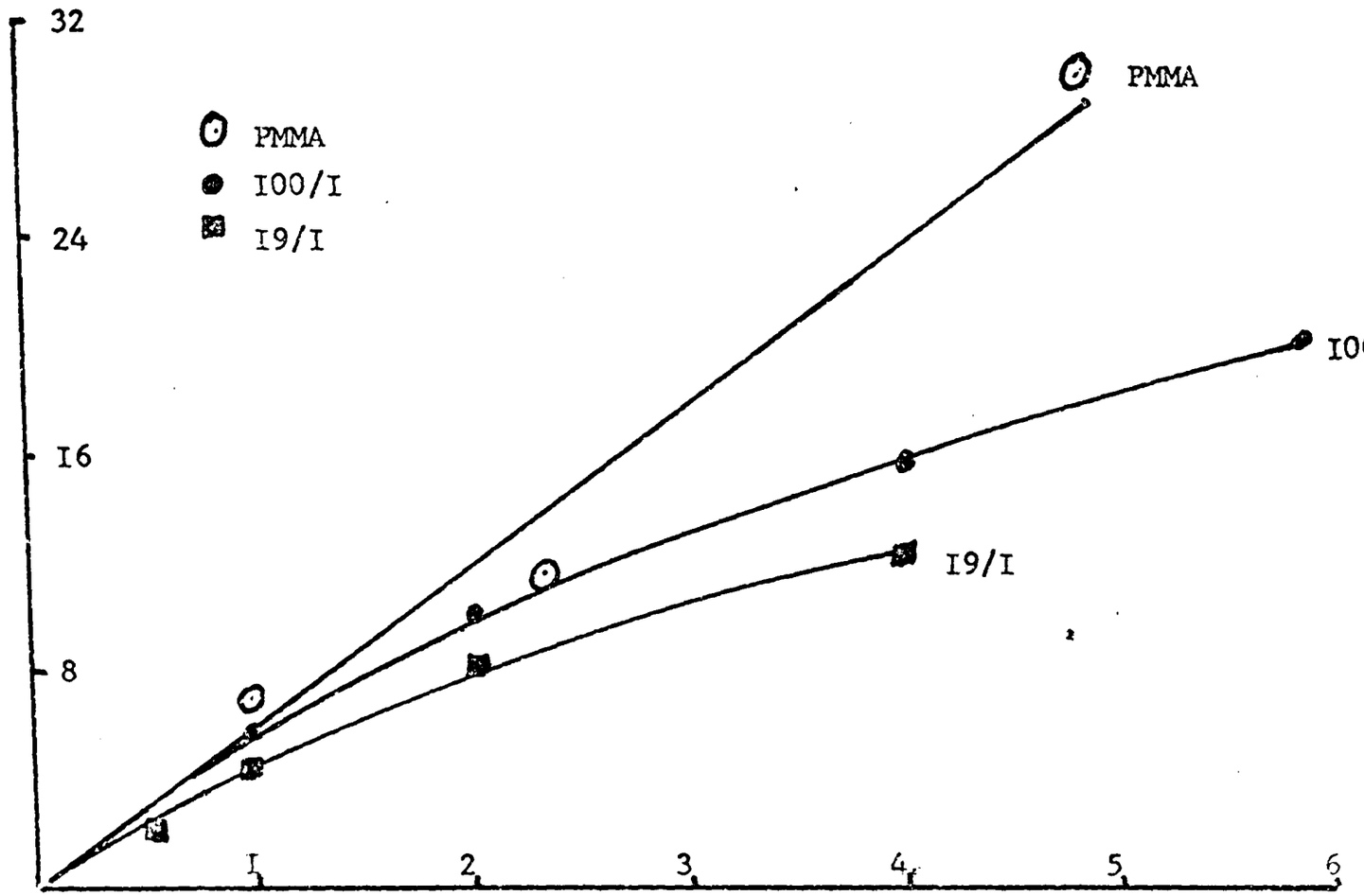

FIGURE 4.17 Photothermal degradation at 150°C

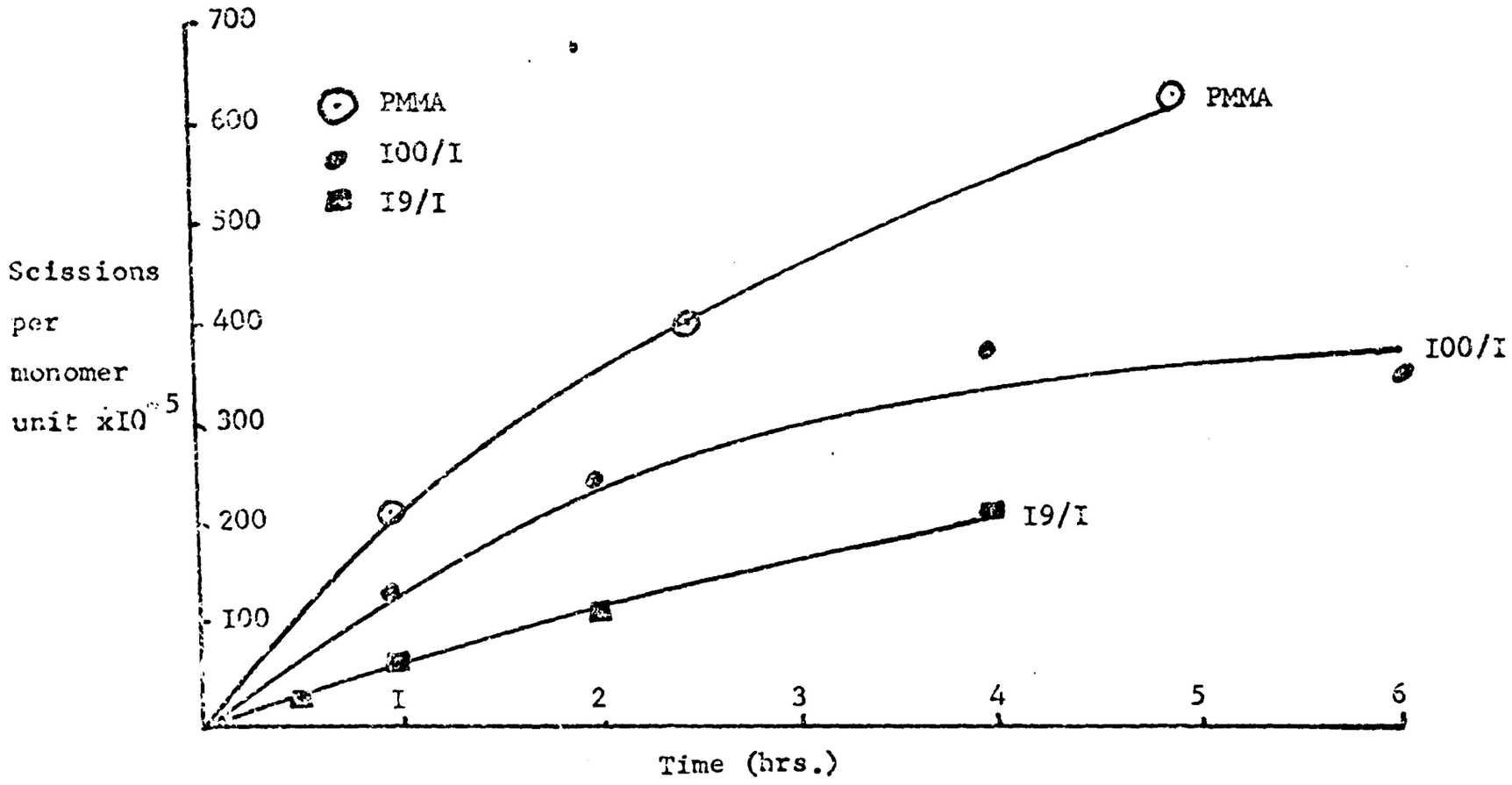

FIGURE 4.I8 Photothermal degradation at I50°C

b) The effect of solvent trapped in the polymer films.

c) Cross-linking in the anhydride polymers which could lead to apparently lower rates of chain scission.

d) Some other explanation.

a) The melting point of PMMA is approximately 165°C. The introduction of anhydride units may lower this melting point until it is below the temperature of degradation and so may affect the mode and rate of degradation. Accordingly, the experiments were repeated at 170°C. The results are shown in TABLE 4.9 and in FIGURE 4.19. The effect appears to be one of greater degradation and rate of weight loss. However, FIGURE 4.20 confuses the picture by indicating that the rate of chain scission is less at 170°C than at 150°C for all polymers. This is contrary to most theories of the kinetics of degradation. The answer is obviously not simply one of degradation temperature.

b) Residual solvent in the polymer films may affect the degradation. The solvent, an impurity, may lower the melting point of the sample and, at the temperatures used in this analysis, alter the rate of degradation. It is known that chloroform may enhance the rate of photodegradation since it can form radicals fairly easily. Should the homopolymer retain chloroform more readily than the copolymers, then this may explain why PMMA undergoes chain scission faster than the copolymers. It may also explain why the rate of chain scission at 170°C is less than at 150°C since less solvent will be trapped in the film at 170°C which is above the melting point.

The question of solvent effects and the removal of solvent

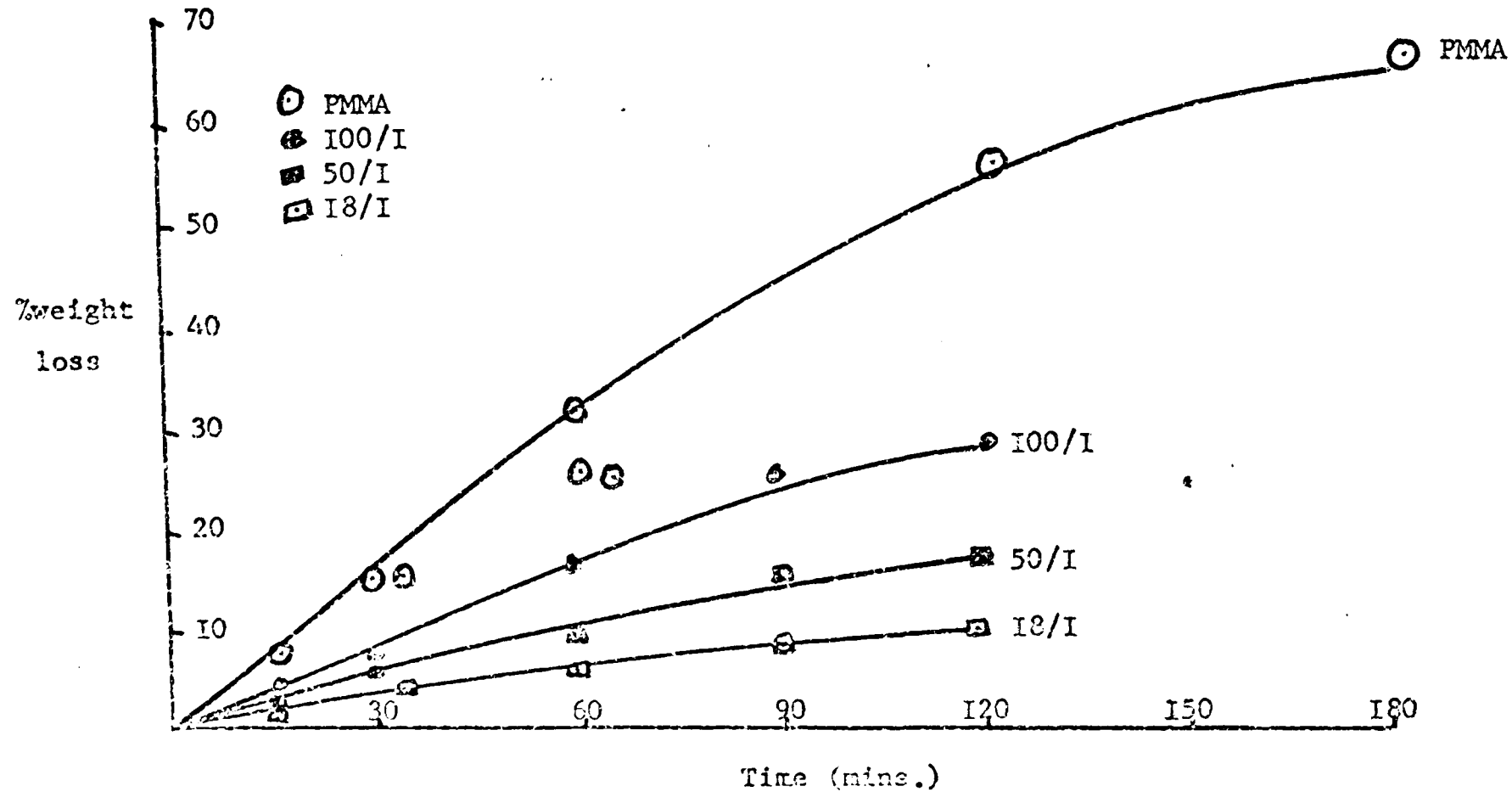

FIGURE 4.I9 Photothermal degradation at I70°C

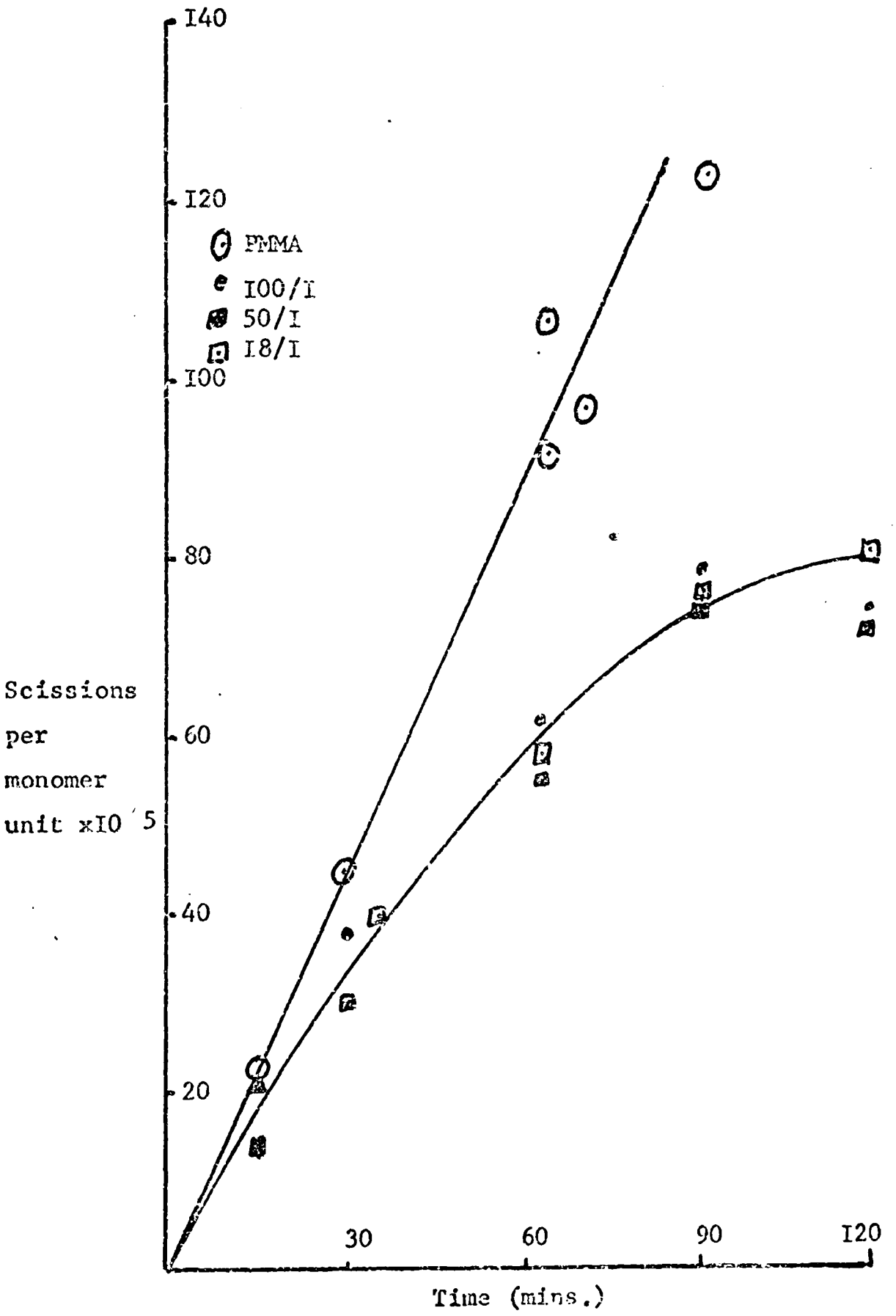

FIGURE 4.20 Photothermal degradation at I70°C

are discussed more fully in the following chapter.

c) Each anhydride unit in the polymer chain contained two tertiary hydrogen atoms. These are susceptible to removal by ultra-violet radiation with radical formation. At room temperature, since all the molecules are immobile, recombination or double bond formation can take place. However, above the melting, the molecules may possess sufficient mobility to combine with other polymer radicals and so grow in size. Should the melting point for the copolymers be depressed by the existence of the anhydride groups such that at 150°C the polymer chains are sufficiently mobile, cross linking could explain why the copolymers appear to undergo chain scission slower than PMMA. This will also apply at 170°C but this theory cannot explain why PMMA undergoes chain scission to a lesser degree at 170°C than at 150°C.

d) The major contributing reason for this anomalous behaviour forms the discussion section of this chapter which follows.

7. Discussion

The introduction of maleic anhydride as a comonomer into PMMA appears to have two effects on the thermal degradation:-

a) The mechanism by which PMMA degrades by unsaturated chain end initiation followed by unzipping, is inhibited by anhydride groups. This is seen in the reduction of monomer produced from anhydride containing polymers at 200 - 240°C, the increased weight stability in thermogravimetry and the loss of the first peak in TVA thermograms.

b) The presence of anhydride groups enhances the rate of

chain scission. Molecular weight determinations reveal a sharp drop in the molecular weight of the copolymers compared to PMMA. The position of the second peak in the PMMA TVA thermograms, due to main chain scission followed by unzipping, is reduced by 30-40°C in the copolymer thermograms.

The mechanism of degradation will now be discussed.

a) PMMA. It is generally agreed that PMMA undergoes reverse polymerisation initiated at unsaturated chain ends at temperatures below 270°C. Two types of unsaturated terminal structures may exist:-

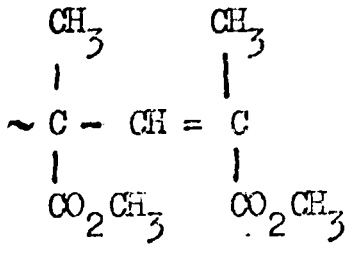

I

and

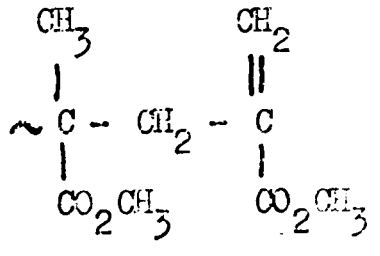

II

If the polymerising radical has the same structure as the polymerising radical,

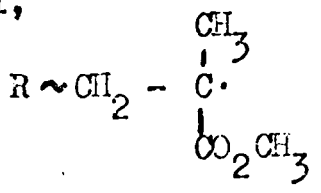

then, to obtain this radical by scission of a bond β to a c = c group, the structure of the polymer molecule end must be II. However, according to McCallum, some

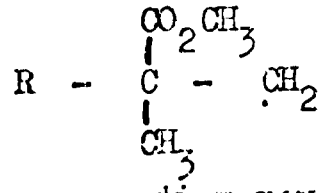

could be formed which could depropagate. The depropagation may be terminated by mutual destruction of pairs of radicals, and the probability that termination will occur before

complete unzipping of a polymer chain must increase with the molecular weight of the polymer.

The unsaturated ends arise from disproportionation reactions terminating the growing chains in the polymerisation of PMMA. In this way one unsaturated chain end and one saturated chain end are formed. Unsaturated terminal structures are not formed if termination occurs by combination of radicals during polymerisation. Therefore it is impossible to achieve more than 50% conversion to monomer with a mechanism involving unsaturated chain end initiation in the absence of chain scission, and for high molecular weight polymer this figure should be even less. In the polymers under discussion, it has been noted that the rate of monomer evolution falls away sharply at about 17% conversion.

However, FIGURE 4.6 had demonstrated that some chain scission is occurring even at 200°C. If the number of chain scissions is calculated from equation (2) and plotted against time (FIGURE 4.6), it can be seen that there appears to be initial chain scission which is quickly stabilised with very little subsequent scission particularly at 200°C and 220°C (FIGURES 4.6 and 4.7). These "weak links" have been observed previously.[37]

In spite of this random cleavage of the main chain, it should be possible to account for the amount of monomer evolved and estimate the mean kinetic chain length.

If it is assumed that the evolution of monomer is not inhibited

by its diffusion through the sample disc, and this would appear to be the case since the evolution of MMA from PMMA at 200°C is at a linear rate (FIGURE 4.1), then the weight loss of the sample is due to loss of monomer from unsaturated chain ends and from unzipping after main chain scission.

If y represents the number of monomer units lost and x represents the zip length of PMMA, then $y = \frac{x}{2}$ where 50% of the chain ends are unsaturated. In cases where the mean molecular chain length is less than the mean kinetic chain length, y will equal 50% of the available units and therefore x will equal the chain length of the polymer.

In cases where the kinetic chain length is less than the molecular chain length, a fraction less than 50% of the available units will be evolved. Termination of unzipping is assumed to be a disproportionation reaction leaving a saturated end group on the polymer which will not unzip.

If chain scission occurs and both the radicals unzip to the mean zip length, then this will increase the number of MMA units evolved. This will be equal to $2xz$ where z is the number of scissions.

Therefore the total number of units evolved will be:-

$$y = 2zx + \frac{x}{2}$$

rearranging $$x = \frac{y}{2z + 0.5} \qquad \text{---} \qquad (3)$$

FIGURE 4.21, in which zip length, x, is plotted against % weight loss, shows how after reaching 14–15% weight loss, the zip length remains constant at about 700 units. This figure is a minimum value and will increase as the fraction of unsaturated end groups tends to zero and when the radical . $CH_2-\overset{CH_3}{\overset{|}{C}}\sim$ formed after chain scission $\underset{CO_2CH_3}{|}$ does not unzip fully, which may occur since it is relatively unstable.

FIGURES 4.6 and 4.7 suggest that the weak links in PMMA result in about 5×10^{-5} scissions per monomer unit occurring at 200 - 220°C. If the radicals formed from each chain scission unzip to the mean zip lengths of 700 units, 1400 units will be evolved which represents only about 8% of the observed losses in FIGURES 4.1 and 4.2. Therefore it would appear that the reason for the levelling out of these plots is because the number of unsaturated chain ends available for unzipping have been used up. Further increases in weight loss are due to monomer evolved from chain scission which starts to become important at 240°C (FIGURE 4.8).

b) Anhydride containing polymers. Several differences are apparent in the mode of degradation of these polymers compared to PMMA.

i) In thermal degradation unzipping is blocked. Therefore either or both of the following mechanisms is assumed to operate.

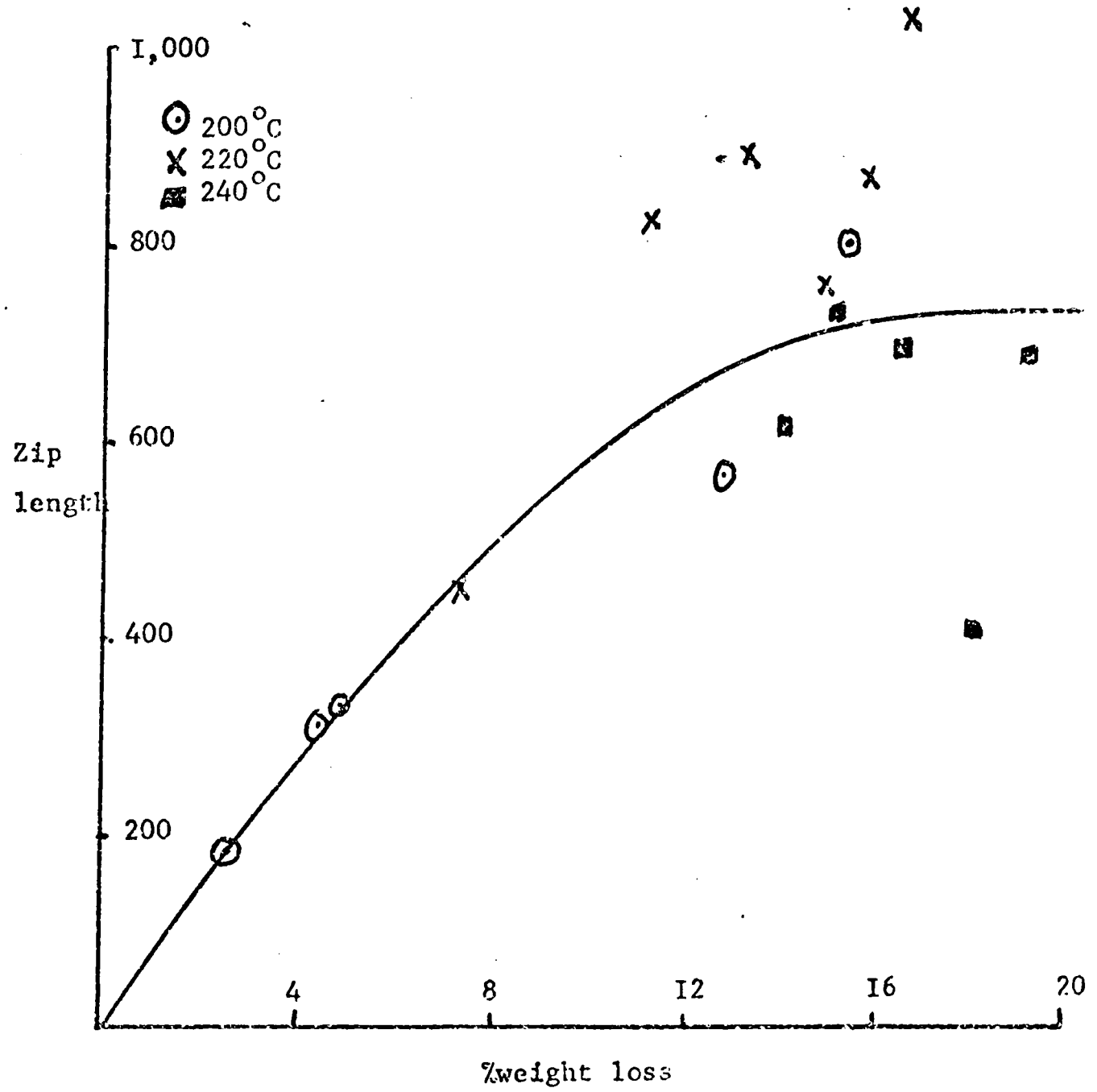

FIGURE 4.21 Zip length versus %weight loss for PMMA

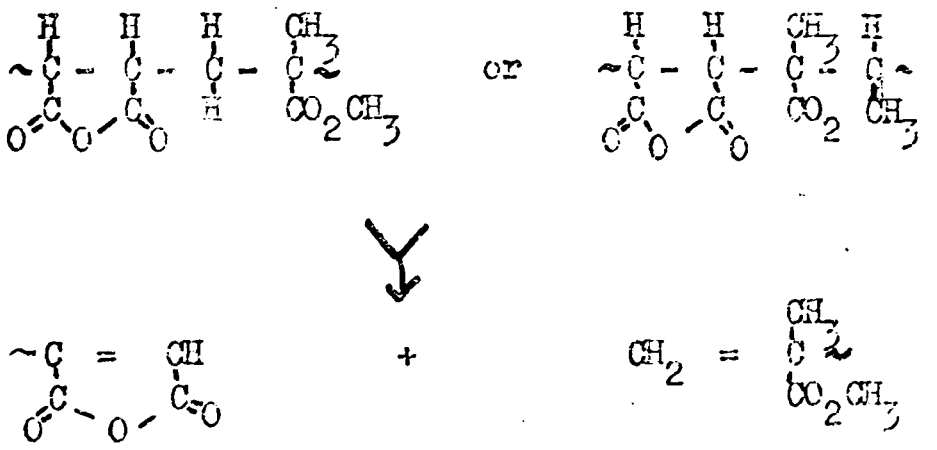

Support for this mechanism comes from the observation that anhydride frequencies in the infra-red region are not diminished in intensity. However, because of the relatively few terminal anhydride groups formed by chain scission and because of the generally broad peaks associated with anhydride absorbances it was not possible to identify any infra-red absorbances associated with unsaturated cyclic anhydrides which would appear at slightly longer wavelengths in the infra-red.

ii.) In photodegradation a slight increase in chain scission is observed with increasing anhydride content. This is more apparent in thermal degradation where the increase in chain scission is several times greater than that in PMMA at 200-240°C.

This would suggest that chain scission is occurring in the neighbourhood of the anhydride unit.

The most plausible mechanism would be:

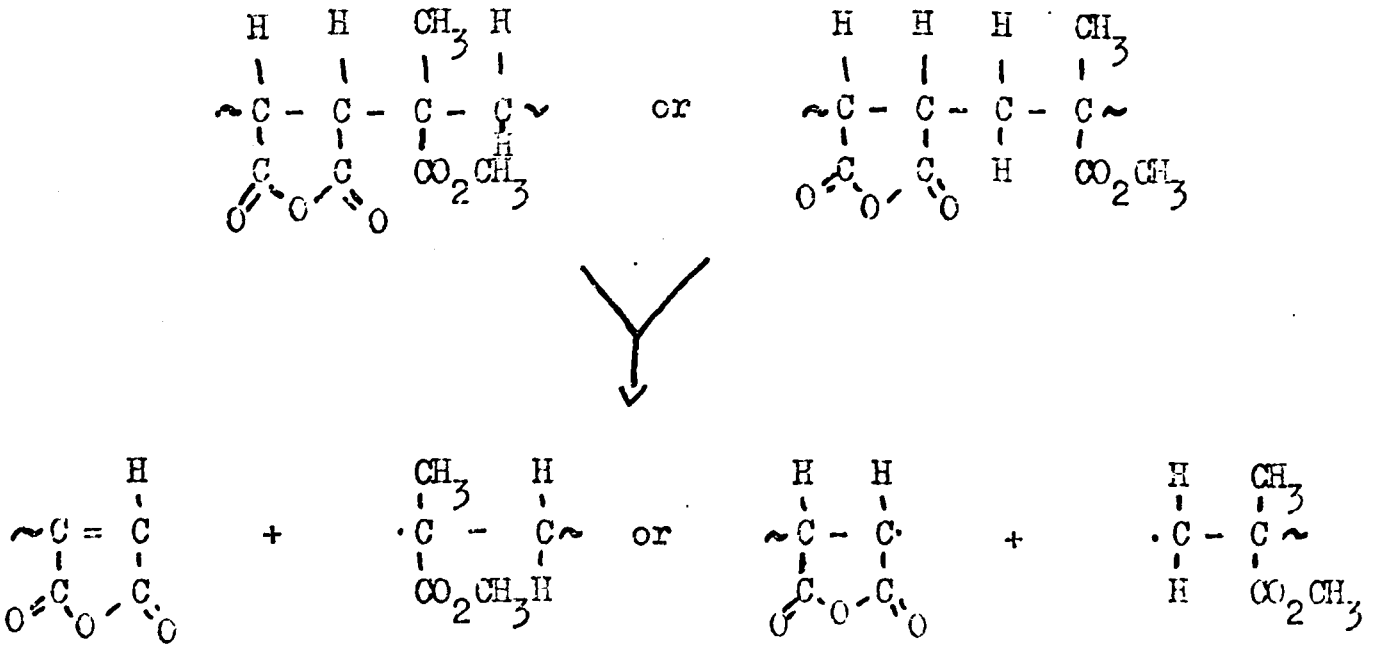

This mechanism would apply both to thermal and photodegradation in general terms although the initial bond cleavage may be different eg. in photodegradation, abstraction of one of the anhydride protons, but in thermaldegradation, scission of the bond between anhydride and MMA units.

In the degradation of the anhydride copolymers, unzipping does not continue through the anhydride groups. Therefore equation (3) now reads

$$x = \frac{y}{z + 0.5}$$

FIGURE 4.22 shows how the zip length varies with % weight loss for the copolymers. The zip length, in fact, is shown to be less in general, than the average number of MMA units between anhydride units. A possible explanation may be found by re-examining the mechanism:

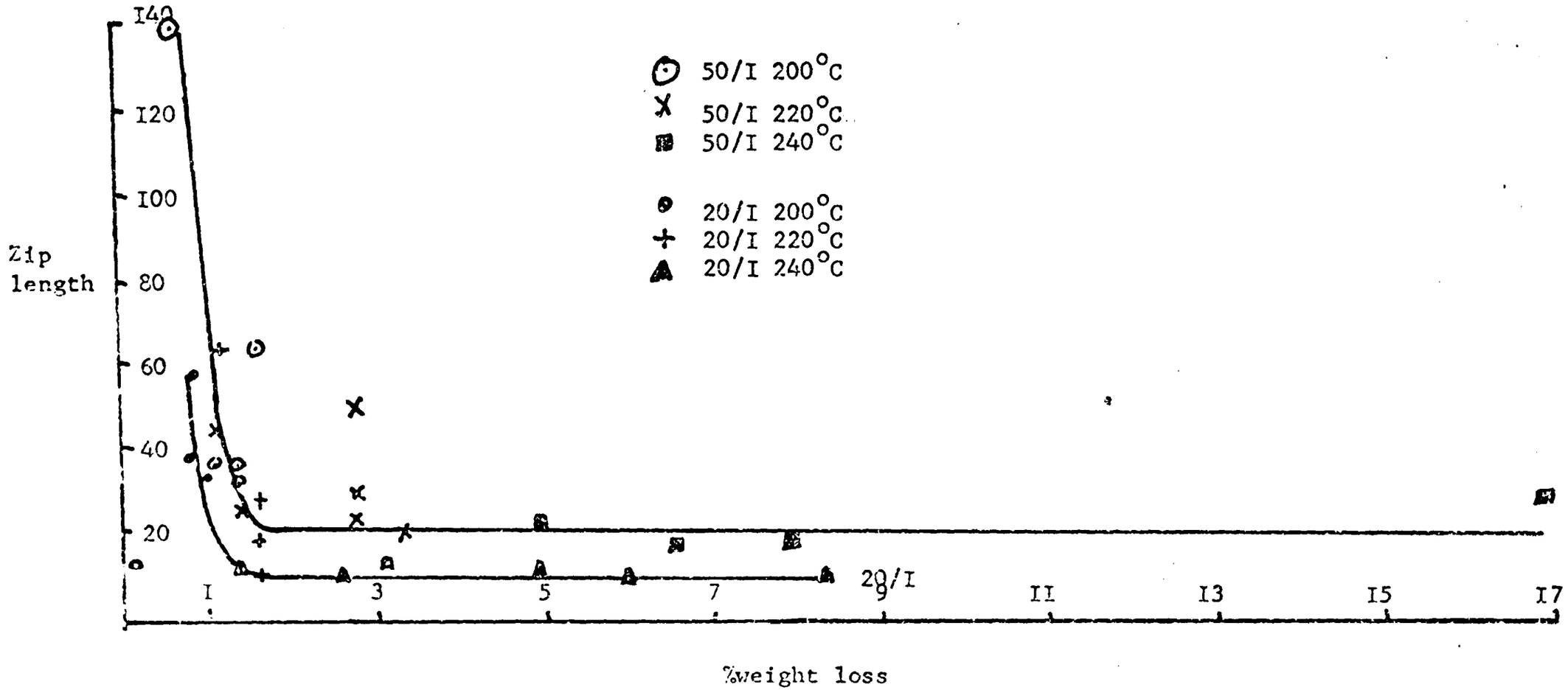

FIGURE 4.22 Zip length versus %weight loss for 50/I and 20/I copolymers

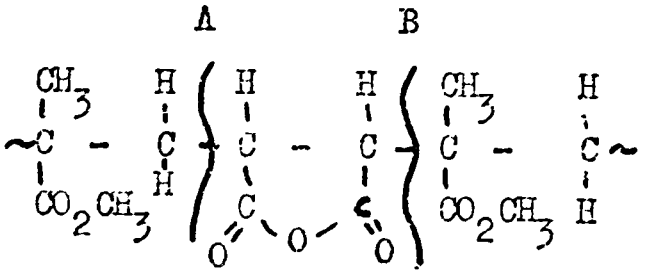

Scission at B can result in:-

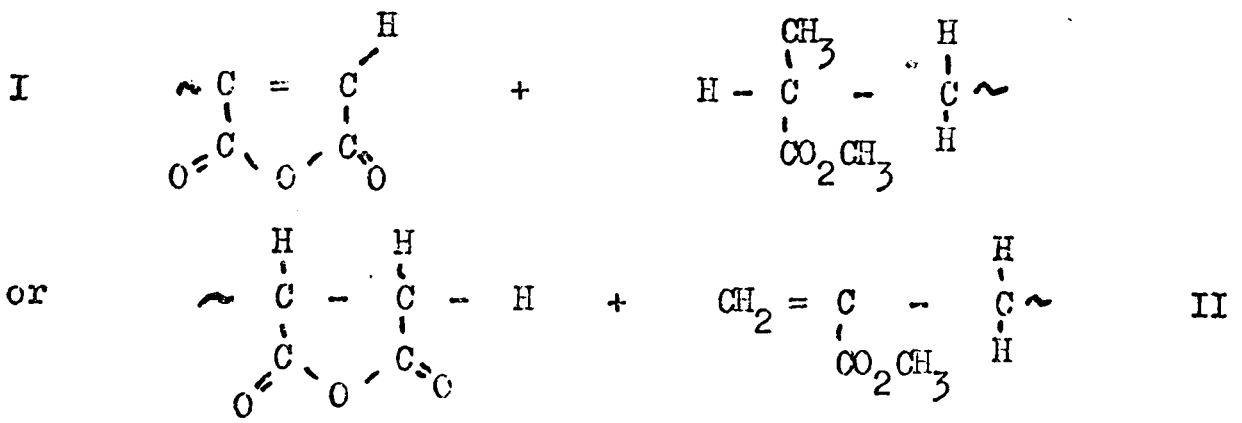

It it is assumed that structure I cannot unzip because it is anhydride terminated, it is only structure II, the unsaturated chain end, which is capable of unzipping.

Scission at A can result in:-

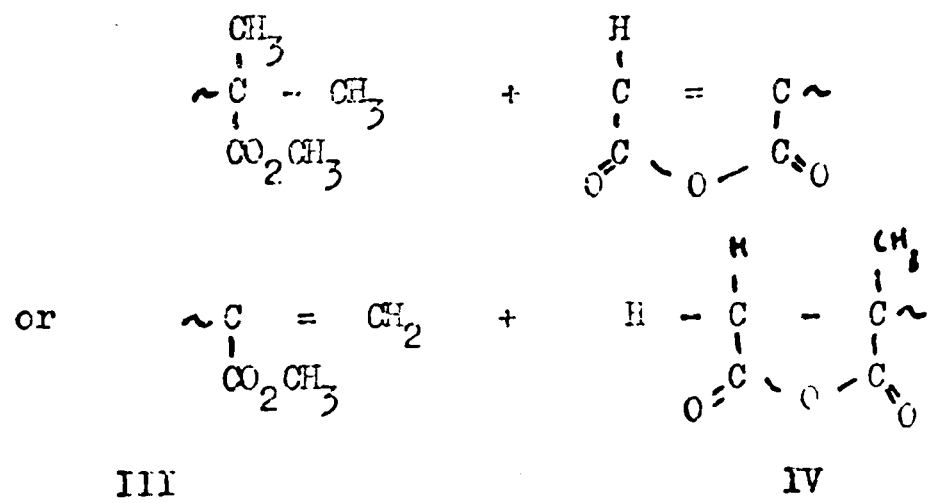

The first alternative seems possible but unzipping would not occur, but the formation of structures III and IV would involve a CH_3 shift or, at best, loss of CH_4. It would appear, therefore, that several possibilities exist in which scission next to an anhydride group may occur involving no loss of MMA. These reactions would reduce the average zip length and may explain the rather low values for zip length found in the anhydride copolymers. Only an extremely accurate analysis of the products of chain scission would help confirm the above tentative mechanism.

Further insight into the mechanism of degradation can be obtained as follows:

Taking a model of PMMA ten units in length and assuming that one chain scission occurs with no unzipping, a polymer of average length 5 units is left.

Applying equation (2):-

$$S = \frac{1-x}{P_t} - \frac{1}{P_o} \qquad \text{but} \quad x = o,\ P_t = S \text{ and } P_o = 10$$

$$\therefore \quad S = \frac{1}{5} - \frac{1}{10}$$

$$= 0.1$$

So there are 0.1 scissions per monomer unit.

For the case where chain scission is negligible and unzipping from chain ends is the predominant mode of degradation, we can

describes this on the model where a polymer of ten units unzips one by one until five, say, are left.

$$S = \frac{1-x}{P_t} - \frac{1}{P_o} \qquad x = 0.5,\ P_t = 5 \text{ and } P_o = 10$$

$$\therefore\ S = \frac{.5}{5} - \frac{1}{10} = 0$$

Obviously since no chain scission is involved, S = 0.

The analogy for the thermal degradation of anhydride polymer and PMMA would be when after, say, one chain scission, one of the fragments unzips partially, eg. $P_{10} \rightarrow P_5 + P_5$

$\rightarrow P_3$ + 2 unzipped units

$$S = \frac{1-x}{P_t} - \frac{1}{P_o} \quad \text{where } x = 0.2,\ P_t = 4\ P_o = 10$$

$$= \frac{1-0.2}{4} - \frac{1}{10}$$

$$= 0.1$$

There is again 0.1 scissions per monomer unit.

However in the instances where complete unzipping of a fragment occurs eg.

$$P_{10} \rightarrow P_5 + P_5$$

$\rightarrow$ 5 unzipped units

$$S = \frac{1-x}{P_t} - \frac{1}{P_o}$$

$$= \frac{1-0.5}{5} - \frac{1}{10}$$

$$= 0$$

Here, S = 0 although a chain scission has taken place.

Thus, where it has been shown for PMMA that the zip length

is about 700, molecular fragments of molecular weight 70,000 or less are in danger of completely unzipping and being lost as monomer. In purely thermal degradation, where molecular weights are all above 250,000 this effect is not likely to be serious. But in photothermal degradations of PMMA, molecular weights below 70,000 occur within one hour of starting degradation. This, then, explains why PMMA apparently undergoes chain scission faster at 150°C than at 170°C, because at 170°C, although it is probable that many more chain scissions are taking place, these scissions are not being recorded because of the complete unzipping of the smaller fragmented molecules.

This does not explain, however, why in FIGURE 4.19 the 100/1 copolymer apparently degrades faster than the 18/1 copolymer at 150°C nor again why both appear to degrade faster at 150°C than at 170°C. The reason for this is probably because of the size of the molecule which can diffuse across the membrane of the osmometer. Although the molecular weight able to diffuse across the membrane depends on the polymer, the temperature, the membrane etc., molecules of PMMA of molecular weight 10,000 are able to pass through. Presumably, copolymers of maleic anhydride will also be able to do so. This means that smaller molecules may not be measured as fragments, with the same result as in the case of unzipping fragments ie. an apparently lower rate of chain scission than is actually occurring.

If a polymer of length N_o units undergoes one chain scission, two chains of average length N_1 units will remain. If both fragments remain in the system then N_1 will be measured as $\frac{N_o}{2}$. But if polymer molecules of length 100 units or less are lost to the system by

diffusion through the membrane and therefore not measured, then we must take account of scissions one hundred units or less from either end of the original polymer chain. The chances of scission occurring in this region is 200 in M_o.

Thus M_1 will have two contributions:-

a) Where chain scission occurs near the end of the molecule and a small fragment is lost. The molecular weight of the smaller fragment will be, on average, 50 units. The contribution will be

$$\frac{200}{M_o} \left(M_o - 50 \right)$$

b) Where chain scission occurs such that both fragments remain in the system. The chances of this are $1 - \frac{200}{M_o}$ in M_o and so the contribution will be $\frac{M_o}{2} \left(1 - \frac{200}{M_o} \right)$

$$\therefore M_1 = \frac{200}{M_o} \left(M_o - 50 \right) + \frac{M_o}{2} \left(1 - \frac{200}{M_o} \right)$$

$$= 100 - \frac{10,000}{M_o} + \frac{M_o}{2}$$

Similarly for the next chain scission M_2 will be related to M_1 in the same way.

$$\therefore M_n = 100 - \frac{10,000}{M_n - 1} + \frac{M_{n-1}}{2}$$ where n is the number of times each molecule suffers one chain scission.

If this treatment is applied to the 20/1 copolymer (M_o = 11,500 units) and impose the condition that each molecule will undergo chain scission simultaneously, we will have the following degradation sequence:-

unit length	chain scissions
11,500	0
5,750	1
2,875	3
1,437	7

etc. assuming no diffusion takes place.

However, if diffusion occurs, then the above equation will apply. TABLE 4.10 compares the rate of scission calculated by each method. FIGURE 4.23 shows how the rate of chain scission as calculated from equation (3) quickly diverges from the ideal state when allowance allowance has been made for diffusion.

8. Conclusions

It has been shown that the measured molecular weights of polymers less than 100,000 may be inaccurate because of the tendency of small molecules to unzip completely and because of the error in calculation of molecular weights due to diffusion of small fragments through the osmometer membrane. Although the mode of degradation is apparent and mechanisms consistent with the degradation have been proposed, it is difficult to be precise about rates even in the early stages of reaction. Molecular weight analysis by osmometry is not sufficiently accurate to investigate the initial stages of degradation where diffusion and complete depolymerisation are relatively unimportant.

TABLE 4.10

Number of scissions	Molecular weight assuming no loss by diffusion (monomer units)	Molecular weight assuming diffusion (monomer units	Number of scissions/ monomer unit with diffusion $\times 10^{4}$
0	II,500	II,500	0
I	5,750	5,850	0.87
3	2,875	3,027	2.43
7	I,438	I,606	5.35
I5	7I9	898	I0.3
3I	360	575	I6.5
63	I80	37I	26.I

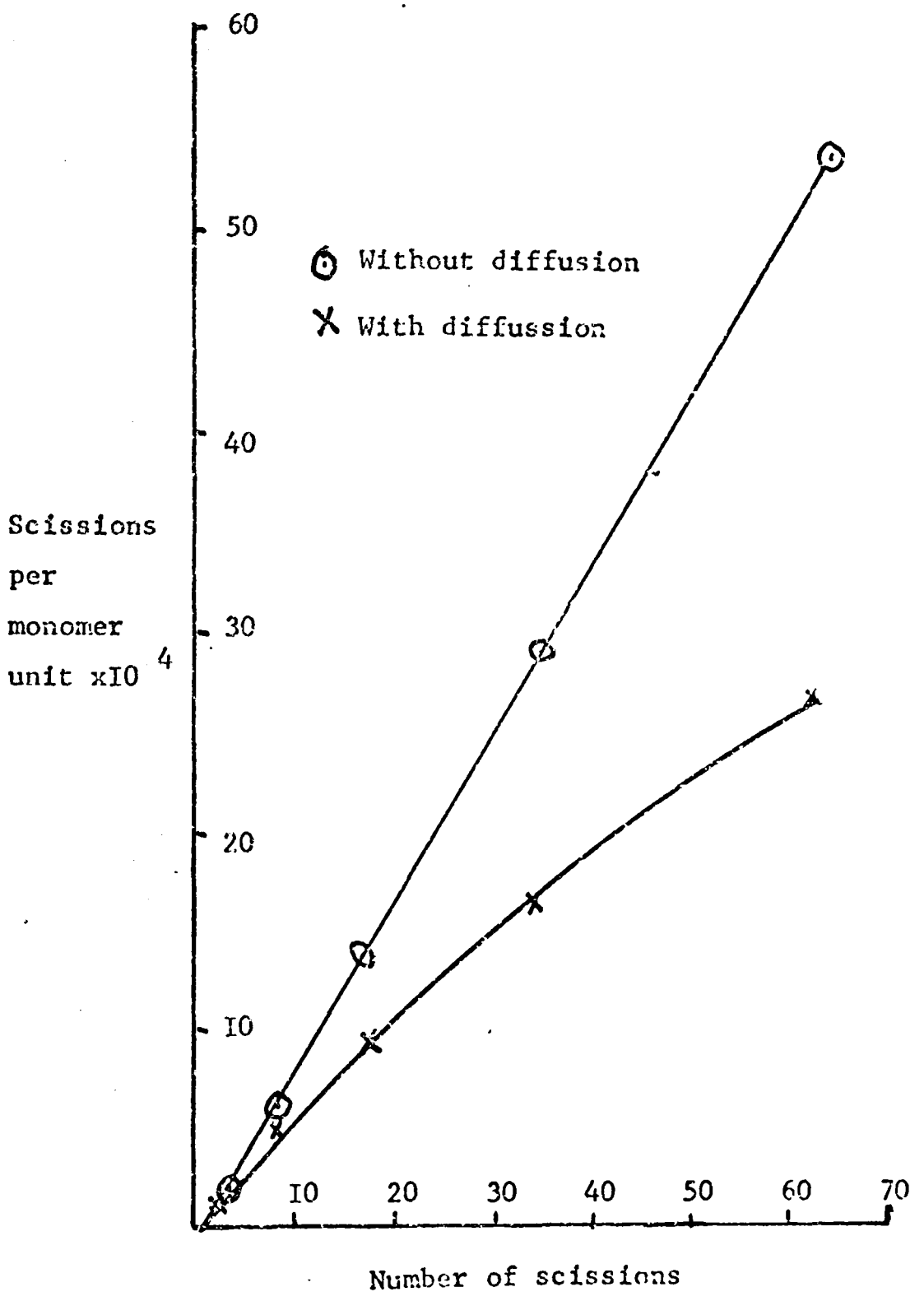

FIGURE 4.23 Scissions per monomer unit versus number of scissions

CHAPTER FIVE

EFFECTS OF SOLVENTS ON THE DEGRADATION OF PMMA AND COPOLYMERS WITH MALEIC ANHYDRIDE

1. Introduction

The presence of small amounts of small molecules in polymers is almost unavoidable particularly in those prepared by bulk polymerisation in which monomer may get trapped in a polymer matrix. Purification by reprecipitation seldom achieves a 100% pure polymer since most solvents are difficult to remove quantitatively. The presence of solvent may be particularly troublesome when samples are being prepared in the form of transparent films for the study of photodegradative processes. In many cases, such as the present study, films cannot be prepared simply by melting the sample and allowing it to cool in such a manner as to form a transparent film. The sample must be cast from a solution and the removal of the solvent may be difficult because of the nature of the solvent - polymer interaction and even the fragile physical nature of the sample.

Several workers have taken the view that simple evaporation of acetone/PMMA solutions is sufficient[44,19] while it has been shown that 24 hour evaporation, vacuum pumping at 70°C for 16 hours followed by 2 hours at room temperature prior to ultra-violet degradation of PMMA films cast from $MeCl_2$ still shows "small residual solvent".[59]

Grassie[115] has shown that, in general, it is necessary to

raise the sample above the softening point of the polymer to remove most of the solvent. Other techniques, such as freeze drying,[40] have also been employed.

The purpose of this chapter is to examine briefly the removal from and the effects of solvents on the photodegradation of the PMMA/ Maleic Anhydride copolymer system.

2. Results

Residual solvent can effect the analysis of degradation reactions in two ways. One is to upset mass calculations, for example, the apparent weight loss in thermal degradation may be due to residual solvent being lost and not to loss of volatiles due to chemical reaction within the sample. The other is the chemical interaction of the solvent directly or indirectly with the degrading sample.

The effect on the weight of the sample can be seen in TABLE 5.1 in which samples cast from the solution on to discs as described in previous chapters are evaporated and then allowed to undergo various treatments.

These results show how difficult it is to remove chloroform without simultaneously degrading the polymer film. In general, it can be said that prolonged heating and high temperatures are necessary. To examine these conditions separately, two experiments were performed. In the first, the sample was treated for a long period at a temperature below the degradation temperature but above Tg while in the second,

TABLE 5.I

Mass of film	37.8mg.
Mass of film after 4 hrs. in vacuum oven at I40°C	36.9mg.
Mass of film after I7 hrs. in vacuum oven at I40°C	36.0mg.
Mass of film	4I.7mg.
Mass of film after 4hrs. in vacuum oven at I40°C	40.7mg.
Mass of film after I7hrs. in vacuum oven at I40°C	39.8mg.
+ additional 4hrs. in vacuum oven at I40°C	39.6mg.
Mass of film	76.5mg.
Mass of film after 5hrs. in vacuum oven at I59°C	75.4mg.
+ 2 days at room temperature	75.4mg.
Mass of film	89.7mg.
Mass of film after I7hrs. in vacuum oven at 64°C	62.4mg.
+ additional I7hrs. in vacuum oven at I00°C	56.8mg.
Mass of film	I2I.5mg.
Mass of film after I7hrs. in vacuum oven at 64°C	83.5mg.
+ additional I7hrs. in vacuum oven at I00°C	76.8mg.
Mass of film + supporting disc	2298.0mg.
+ I7hrs. in vacuum oven at I50°C	2283.0mg.
+ additional I7hrs. in vacuum oven at I50°C	228I.4mg.
+ additional 34hrs. in vacuum oven at I50°C	2280.5mg.
Mass of film after 2 hrs. in vacuum at I60°C	43.0mg.
+ additional 2hrs. in vacuum oven at I60°C	42.3mg.
+ additional 2hrs. in vacuum oven at 240°C	30.7mg.
Infra-red analysis showed chloroform in the volatiles after the final heat treatment	
Mass of film	I20.4mg.
Mass of film after 2hrs. in vacuum oven at I60°C	92.7mg.
+ additional 2hrs. in vacuum oven at I60°C	90.3mg.
+ additional 2hrs. in vacuum oven at I60°C	88.9mg.
+ additional I2hrs. in vacuum oven at I60°C	88.2mg.

TABLE 5.I (continued)

Mass of film	94.1mg.
Mass of film after Ihr. in vacuum oven at I20°C	86.0mg.
+ additional I½hrs. in vacuum oven at I20°C	83.2mg.
+ additional Ihr. in vacuum oven at I20°C	82.2mg.
Mass of film	92.4mg.
Mass of film after Ihr. in vacuum oven at I20°C	87.4mg.
+ additional Ihr. in vacuum oven at I20°C	85.0mg.
+ " " " " " " "	84.6mg.
+ " " " " " " "	83.8mg.
+ " " " " " " "	83.0mg.
+ " " " " " " I60°C	72.9mg.
Mass of film	93.4mg.
Mass of film after Ihr. in vacuum oven at I60°C	80.8mg.
+ additional Ihr. in vacuum oven at I60°C	78.6mg.
+ " " " " " " "	77.3mg.
+ " " " " " " "	76.3mg.
+ " " " " " " "	75.6mg.
+ " " " " " " "	75.1mg.
+ " " " " " " "	74.6mg.
+ " " " " " " "	74.4mg.
+ " 2½hrs." " " " "	73.4mg.
+ " 2hrs. " " " " "	72.6mg.
+ " I2hrs. " " " " "	69.6mg.
Mass of film	93.1mg.
Mass of film after Ihr. in vacuum oven at I50°C	81.2mg.
+ additional Ihr. in vacuum oven at I50°C	79.2mg.
+ " 2½hrs." " " " "	77.0mg.
+ " I½hrs. " " " " "	76.4mg.
+ " " " " " " "	76.3mg.
+ " Ihr. " " " " "	75.7mg.
+ " I½hrs." " " " "	75.4mg.
+ " 2hrs." " " " "	75.1mg.
+ " " " " " " "	74.5mg.
+ " " " " " " "	74.3mg.

TABLE 5.I (continued)

Mass of film	45.6mg.
Mass of film after I7hrs. in vacuum oven at I20°C	38.9mg.
+ additional Ihr. in vacuum oven at I20°C	38.9mg.
Infra-red analysis showed chloroform in the volatiles	
+ additional 2hrs. at 200°C under vacuum	33.8mg.
Infra-red analysis showed MMA and chloroform in the volatiles	

With acetone as solvent:	
Mass of film	93.9mg.
Mass of film after Ihr. in vacuum oven at I20°C	88.9mg.
+ additional 2hrs. in vacuum oven at I20°C	87.7mg.
+ " Ihr. " " " " "	87.3mg.
+ " Ihr. " " " " "	87.Img.
+ " " " " " " "	86.9mg.

TABLE 5.2

a) Mass of film	I67.3mg.
Mass of film after ½hr. at 200°C in vacuum	I28.6mg.
Infra-red analysis showed MMA and chloroform in the volatiles	
b) Mass of film	I64.4mg.
Mass of film after I7hrs. in vacuum oven at I20°C	I40.7mg.
A sample was removed for analysis	
Mass of remaining sample	I2I.Img.
Mass of film after ½hr. at 200°C in vacuum	II0.2mg.
A further sample was removed	
Mass of remaining sample	90.0mg.
Mass of film after ½hr. at 200°C in vacuum	88.8mg.
Infr-red analysis showed MMA and chloroform in the volatiles	

the sample was maintained at a temperature above the melting point of PMMA but also above the degradation threshold for a short period of time. The results are shown in TABLE 5.2

Samples heated directly, after evaporation, to 200°C tended to blister and so became unsuitable for degradation studies. However, samples heated to 120°C still had substantial amounts of $CHCl_3$ left and, indeed, also even after treatment at 200°C.

TG also shows solvent retention rather more graphically. FIGURE 5.1 compares PMMA powder with the samples removed in the last experiment.

Because MMA is also evolved at 200°C it is not easy to calculate how much of the evolved gases comprise $CHCl_3$. Therefore, a 19/1 copolymer of MMA/maleic anhydride was used since it has been shown that evolution of MMA is inhibited by the anhydride units. Thuse the volatiles will be richer in $CHCl_3$.

Each film, after evaporation, was heated to 120°C under vacuum for 17 hours to remove most of the solvent and prevent blistering. Although the 19/1 copolymer is rather more sensitive to chain scission than PMMA it is still stable at 120°C for this length of time.

Films were then subjected to a period of one hour at various temperatures under the degradation conditions described in the previous chapters. Afterwards the films were analysed for % C by microanalysis. The molecular weight was measured and infra-red analysis of the gases

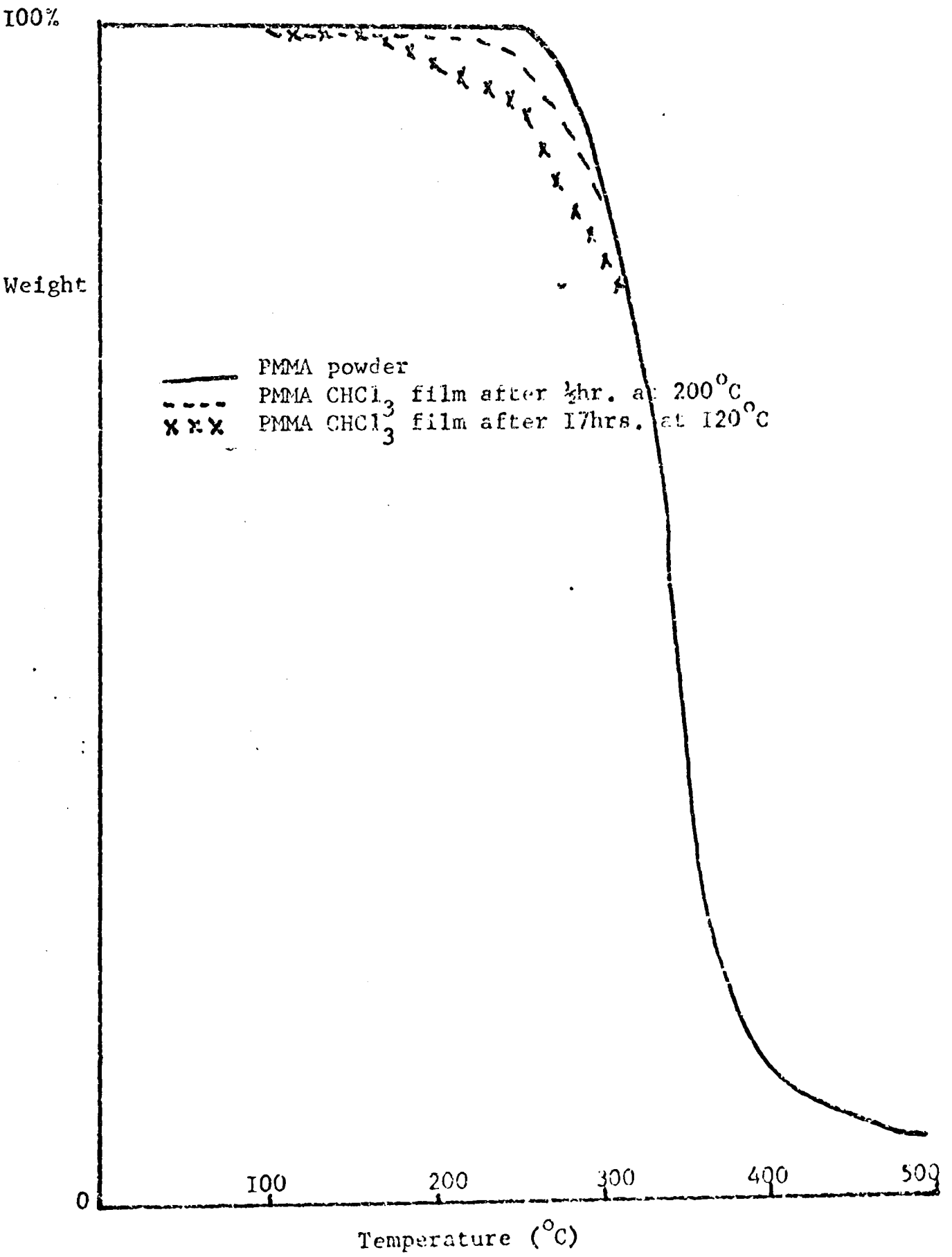

FIGURE 5.1 Thermogravimetric traces of PMMA

recorded. The results are shown in TABLE 5.3. $CHCl_3$ was seen in all infra-red traces of the volatiles.

Since elemental chlorine analysis was not available at this time, chlorine determination was calculated by observing the depression of the %C in the sample by the existence of $CHCl_3$ since $CHCl_3$ contains considerably less carbon by weight than the polymer. FIGURE 5.2 shows the calibration chart employed.

For comparison, PMMA was similarly treated at 120°C and 200°C and analysis for chlorine by the above method employed. These points are included in FIGURE 5.3 which shows how $CHCl_3$ is removed with increasing temperature.

The experiment was repeated using methyl acetate as solvent. However, although % weight losses were less than for $CHCl_3$, this does not necessarily mean that there is less solvent there to be removed. It may suggest that it is more difficult to remove. Unfortunately, it was impossible to measure the amount of solvent remaining by chemical analysis because of the chemical similarity, of methyl acetate to the degradation products of PMMA. Molecular weights were not measured because of the difficulty of removing the film from the silica discs.

Since most of the photodegradation work was carried out in transparent films, several solvents were examined in degradations under the following conditions:-

TABLE 5.3

Temperature of final Ihr. heating	Molecular weight	%weight loss (mg.)	$\%CHCl_3$ left	Total $\%CHCl_3$
I20°C	526,000	0	7.0	7.0
I50°C	469,000	2.3	7.2	9.5
I60°C	452,000	2.7	3.0	5.7
I70°C	575,000	3.7	2.9	6.6
I80°C	538,000	5.0	I.I	6.I
I90°C	460,000	6.0	0.6	6.6

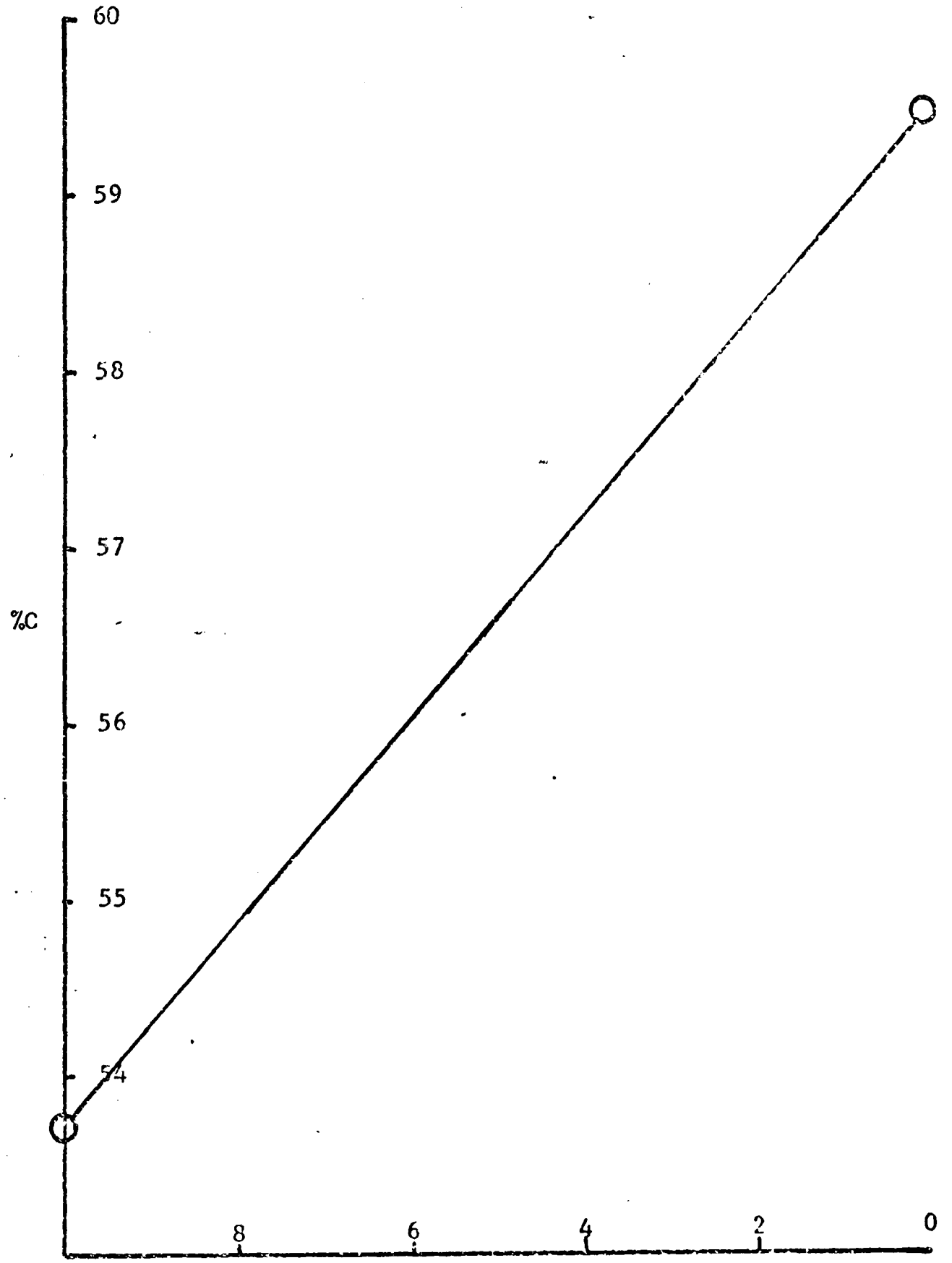

FIGURE 5.2 Calibration graph for %carbon versus %chloroform

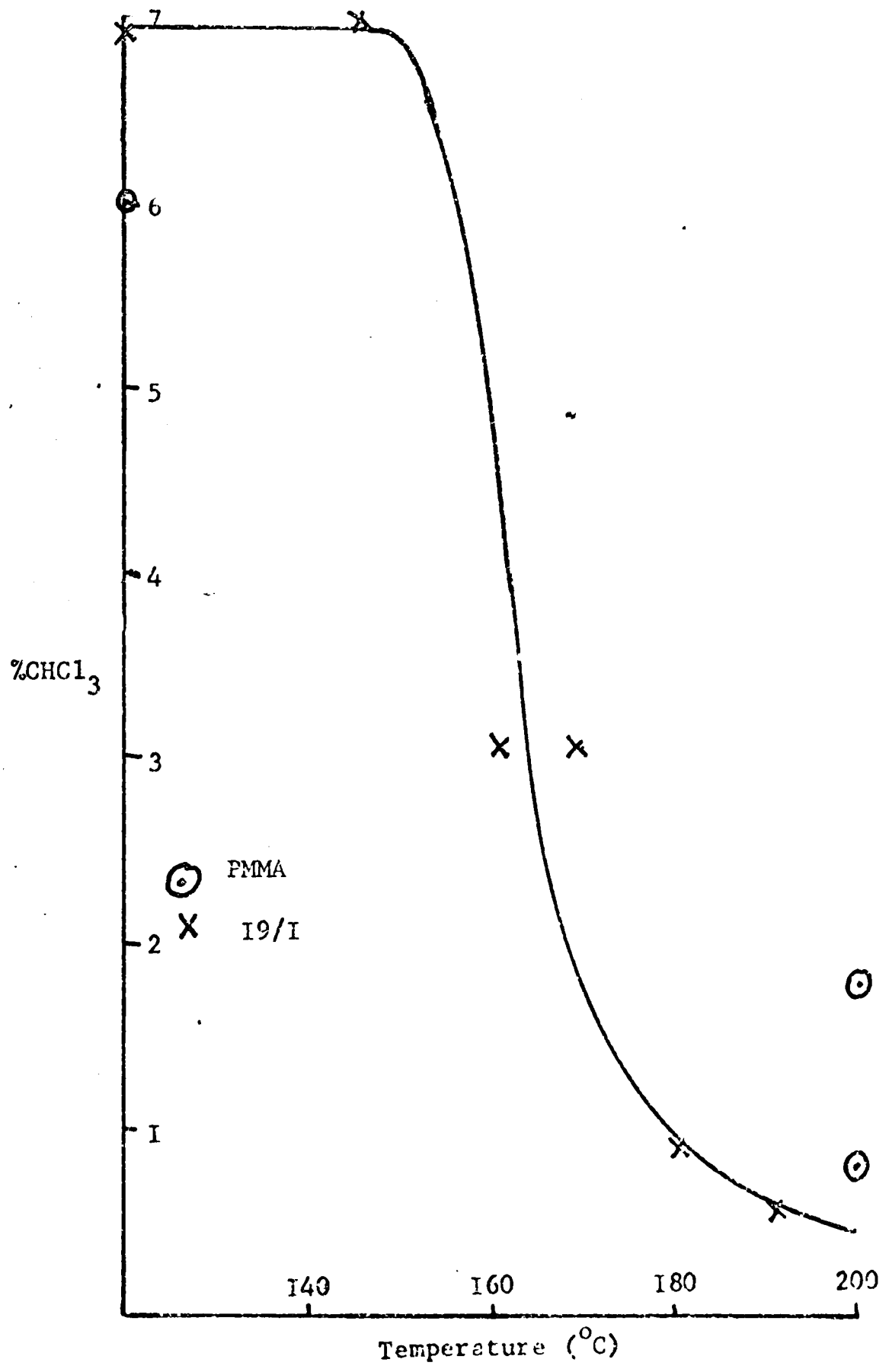

FIGURE 5.3 Chloroform content of PMMA and I9/I polymers at various temperatures

The solvent from four films cast from each solvent (50mg/ml) was allowed to evaporate overnight. They were heated under vacuum at 120° for 17 hours and then at 200°C for ½ hour. One sample was used for TG analysis and one for molecular weight analysis. The final two were degraded for 6 hours and 12 hours respectively under ultra-violet light at room temperature. The molecular weights are shown in in TABLE 5.4.

It can be seen that:-

a) In the TG traces, all samples showed the presence of residual solvent seen as a gradual falling of the trace from the 100% line. The amount by which each trace has dropped was taken as a rough measure of the amount of solvent left. The reading at 250°C was taken since it is at this point that PMMA starts to lose weight noticeably in TG. The results are shown in TABLE 5.5

b) The rate of degradation shown in FIGURE 5.4 and 5.5 suggest:-

i) the copolymer degrades faster than PMMA as shown in the previous chapter.

ii) that the thermal degradation is unaffected by solvent within the limits of experimental error.

iii) the rate of photodegradation is not appreciably different for each solvent within the limits of experimental error.

The effects of these solvents can be summerised:-

Chloroform - In the degradation of PMMA and the 18/1 copolymer the rate of chain scission was marginally greater with this solvent. Although it is thought that chloroform is capable of increasing the rate of degradation, it is not significant in this case especially considering

TABLE 5.4

PMMA

Time of irradiation (hrs.)	Solvent	Molecular weight	Number of chain scissions per monomer unit $xI0^{-4}$
0	____	2,8I0,000	0
0	methylene chloride	I,265,000	0.434
6	"	42I,000	2.02
I2	"	236,000	3.88
0	Chloroform	I,2I0,000	0.474
6	"	305,000	2.92
I2	"	2II,000	4.38
0	Acetone	903,000	0.752
6	"	562,000	I.42
I2	"	28I,000	3.20
0	Methyl acetate	8I5,000	0.874
6	"	342,000	2.57
I2	"	2I4,000	4.32
0	Toluene	790,000	0.902
6	"	389,000	2.2I
I2	"	3I2,000	2.85
		I8/I.	
0	_____	2,530,000	0
0	Chloroform	607,000	I.25
6	"	I60,000	5.85
I2	"	I3I,000	7.25
0	Methylene chloride	396,000	2.13
6	"	I44,000	6.53
I2	"	II4,000	8.36
0	Acetone	377,000	2.26
6	"	183,000	5.06
I2	"	II5,000	8.30
0	Toluene	516,000	I.54
6	"	226,000	4.02
I2	"	I42,000	6.63

TABLE 5.5

PMMA	%solvent remaining	I8/I	%solvent remaining
Chloroform	4	Chloroform	3
Methylene chloride	2	Methylene chloride	3
Toluene	2	Toluene	2
Methyl acetate	I	Methyl acetate	2
Acetone	0	Acetone films peeled off discs	

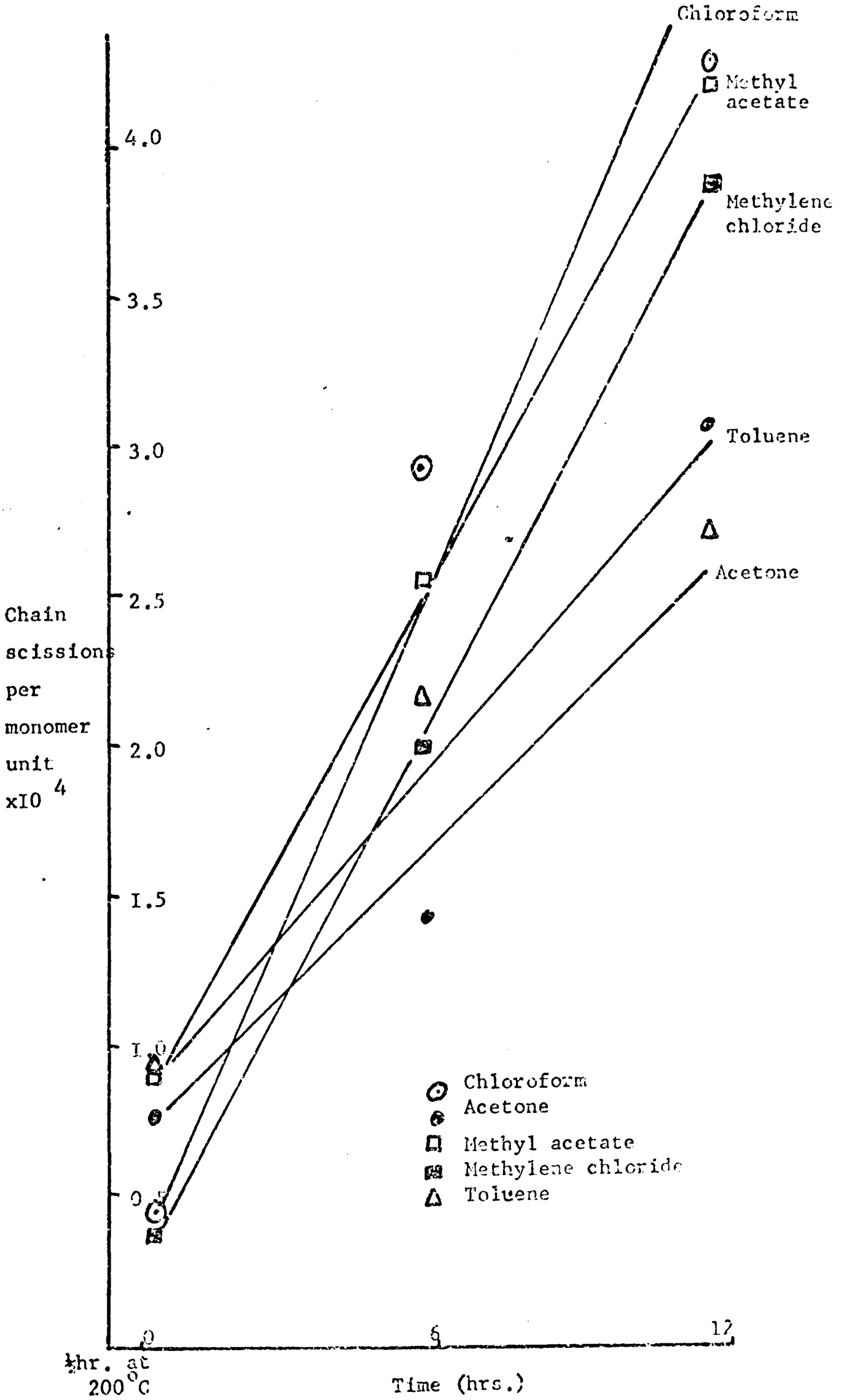

FIGURE 5.4 Rate of photodegradation of PMMA films cast from different solvents

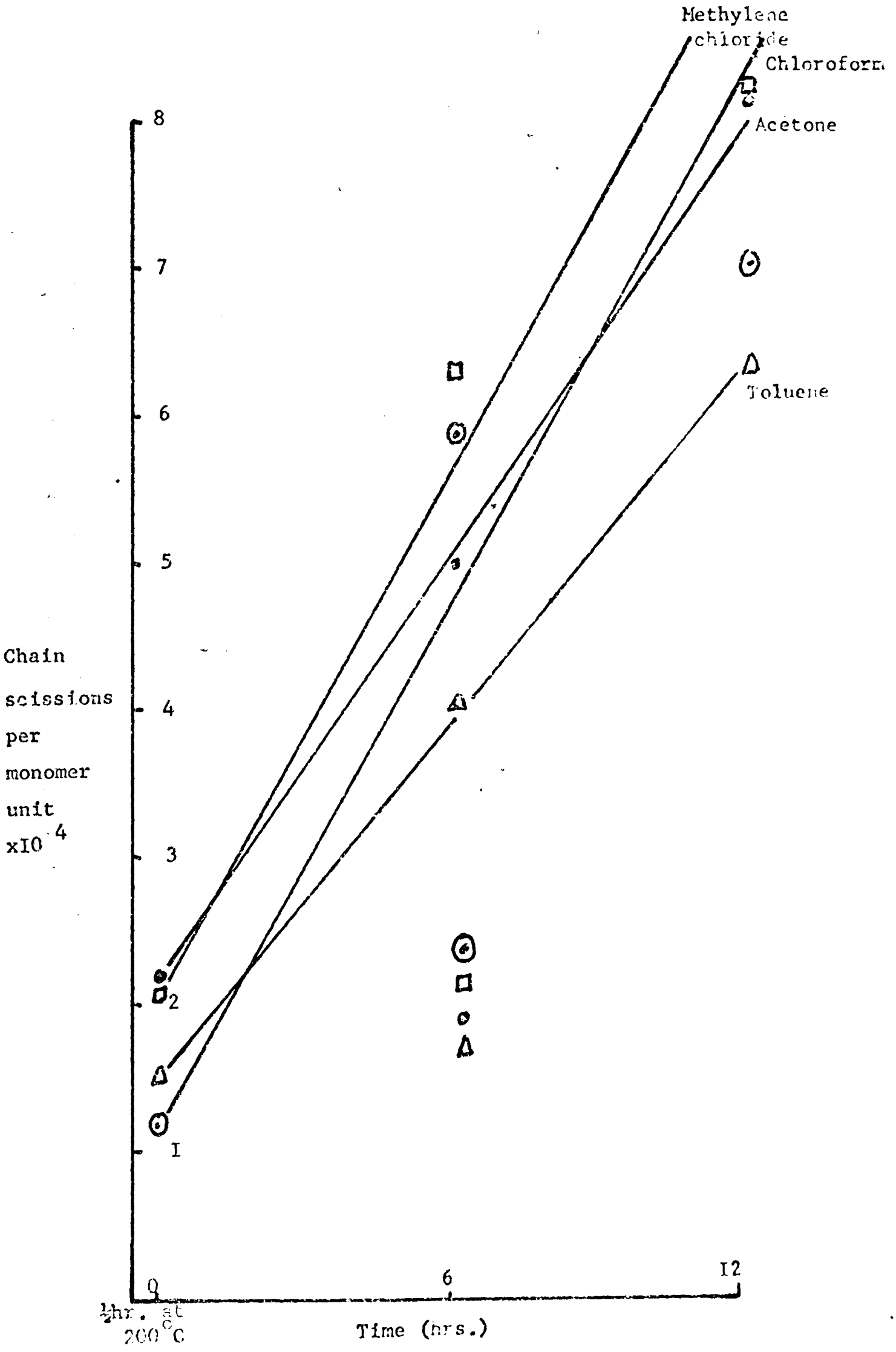

FIGURE 5.5 Rate of photodegradation of 18/I films cast from different solvents

that more chloroform was retained in the sample than other solvents.

Methylene chloride - Less in its effect than chloroform, however, it is unsuitable in the preparation of thin films because of its tendancy to form bubbles in the film as the solvent evaporates.

Methyl acetate - Difficulty was found in redissolving films cast from this solvent in toluene for molecular weight analysis.

Toluene - This solvent tends to absorb ultra-violet light and is not generally suitable for use in photodegradation.

Acetone - Films cast from this solvent tended to peel off the silica support disc.

3. Conclusions

In this chapter the problem of solvents in the degradation of thin films has been only briefly studied. While considerably more work could be done in this field, it is thought that the results do not prejudice the studies described in Chapter 4. The small amounts of solvent remaining were not considered high enough to affect the weight loss measurements seriously and the affect on photodegradation appears minimal.

However, work on solution photodegradation,[49,45,50] in which the problem is much more extreme, has shown that degradation of PMMA is sensitive to some solvents.

Ideally, a solvent should be able to dissolve a polymer sample to give an acceptably high concentration but also should be readily removed under gentle vacuum or heating conditions. The solvent should

also be photolytically inert, but this problem, according to Fox,[5] is unlikely to be completely solved.

CHAPTER SIX

THE DEGRADATION OF COPOLYMERS OF METHYL METHACRYLATE WITH METHYL VINYL KETONE AND METHYL ISOPROPENYL KETONE

1. Introduction

In this chapter, the effect of heat and ultra-violet radiation on MIK/MMA and MMA/MVK copolymer systems is examined. Each system is treated separately with the discussion incorporating all the results.

2. MMA/MVK

a) Thermal Degradation

i) TVA. McNeill[57] has already studied this polymer using the TVA technique. He showed that monomer is not evolved and that cyclisation occurs (see Chapter 1)

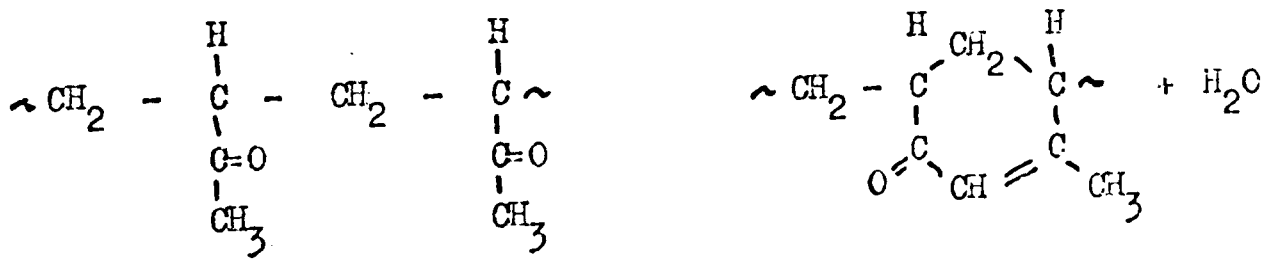

PMVK

In common with Hay,[63] he found water to be the only product evolved at 250°C. A typical TVA thermogram of PMVK is shown in FIGURE 6.1. For comparison, that for PMMA is shown in FIGURE 6.2. The main peak in the PMMA thermogram is at 374°C but, in PMVK, at 313°C. FIGURES 6.3, 6.4, 6.5 and 6.6 show the TVA traces of several copolymers. In general, the trend is for the main peak to move to lower temperatures as the content of MVK increases, allowing for the effects of molecular weight. In addition, the intensity of the -75°C trace decreases indicating that less MMA is being produced. As the MVK content of the polymer is increased, gains are seen in the -100°C and even -196°C traces but these decrease again as the composition moves towards pure PMVK. The main features of these traces, and of traces of the other copolymers are shown in TABLE 6.1. Exceptionally high molecular weights tend to increase the stability of the polymer, particularly the high MMA containing copolymers in which few unsaturated chain ends available to initiate depolymerisation. Thus a higher peak temperature is recorded.

Cold ring fractions, which were not analysed, were observed for samples containing large proportions of MVK. These fractions probably contained cyclised chain fragmented as described by McNeill[57] in his analysis of PMVK degradation.

ii) TG. The traces for PMMA, PMVK and several copolymers are shown in FIGURE 6.7

The trend here is for a dramatic increase in the rate of weight loss in the range 200°C - 350°C for copolymers containing small

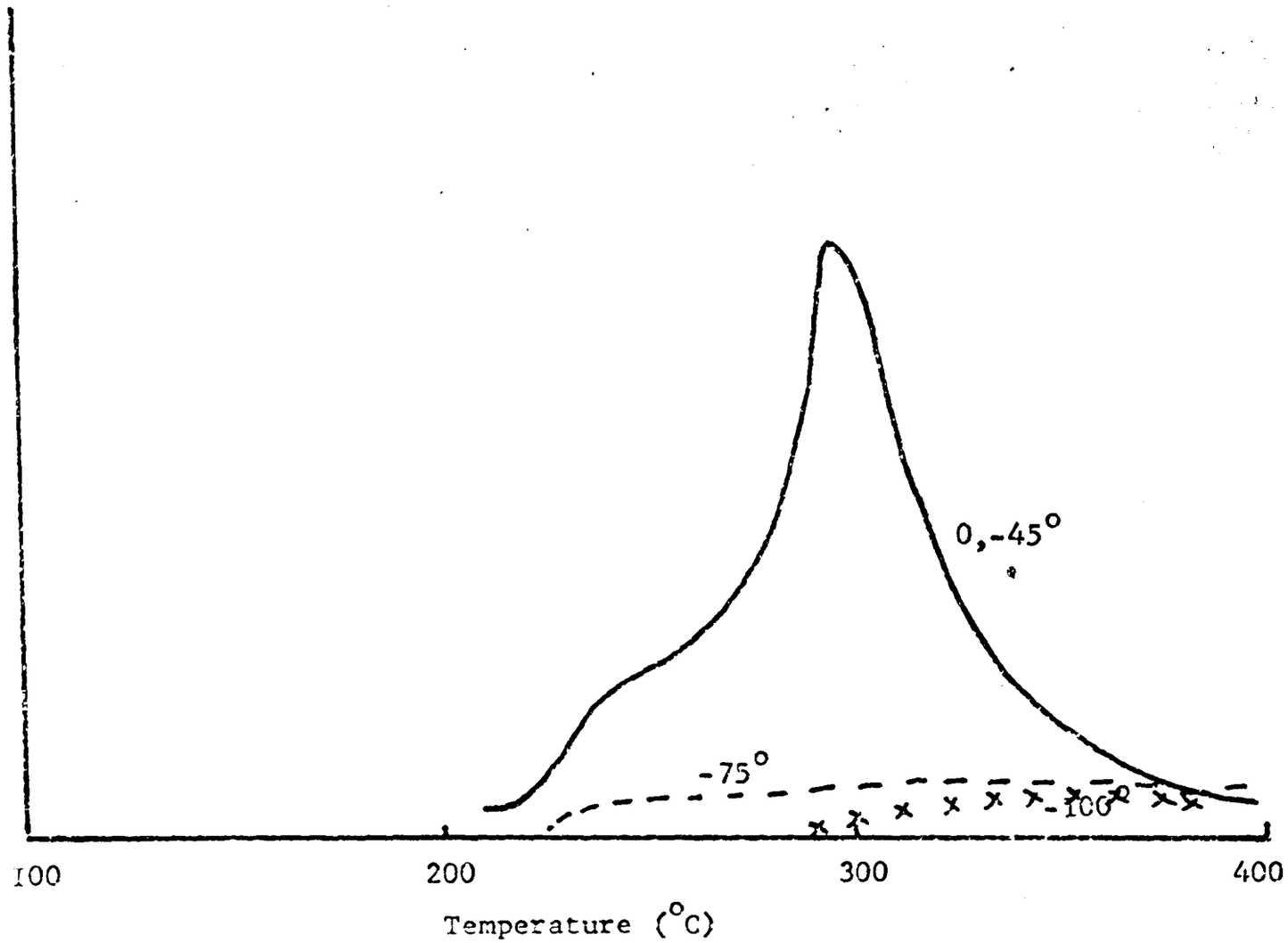

FIGURE 6.I T.V.A. thermogram of PMVK

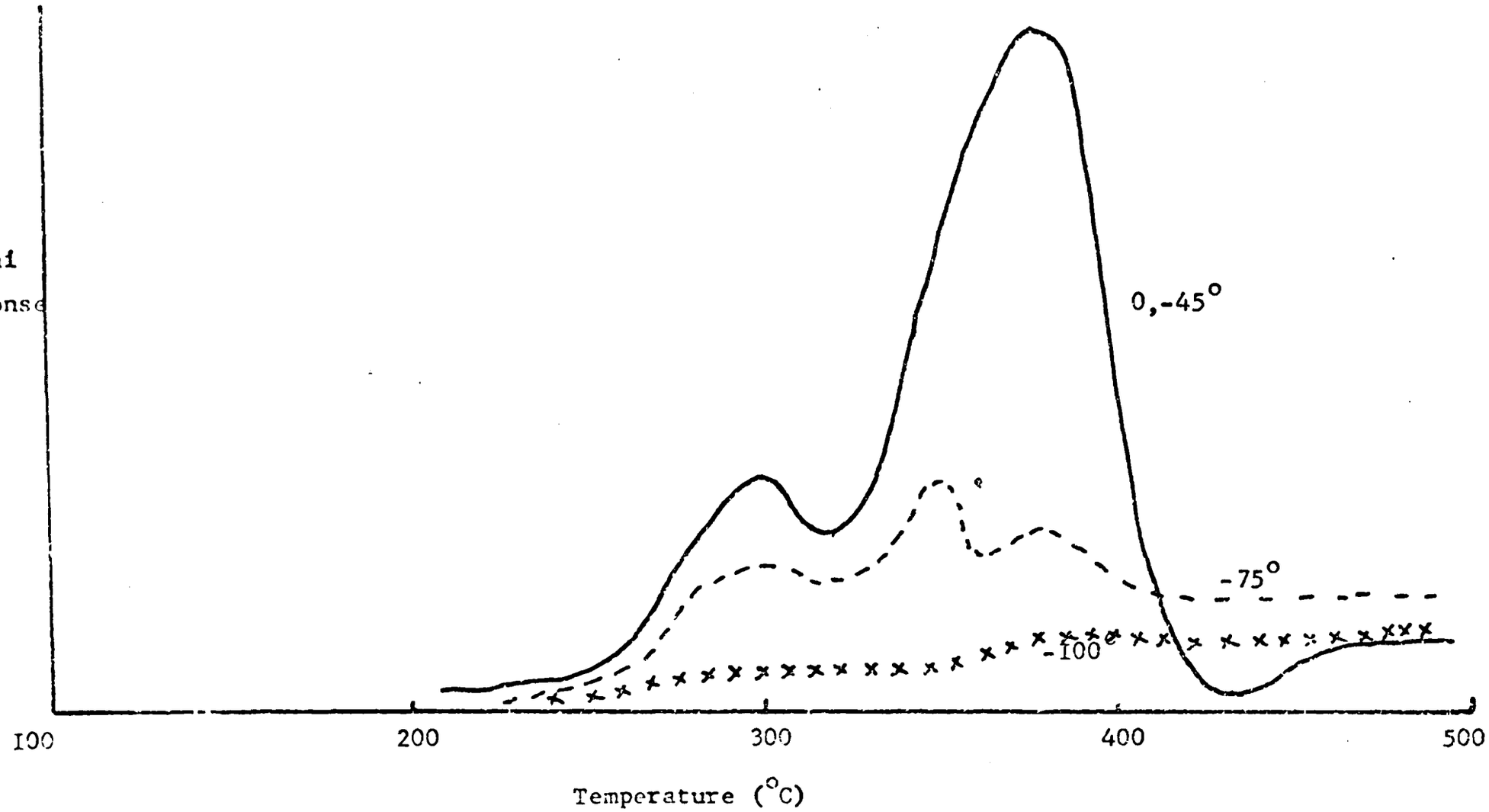

FIGURE 6.2 T.V.A. thermogram of PMMA

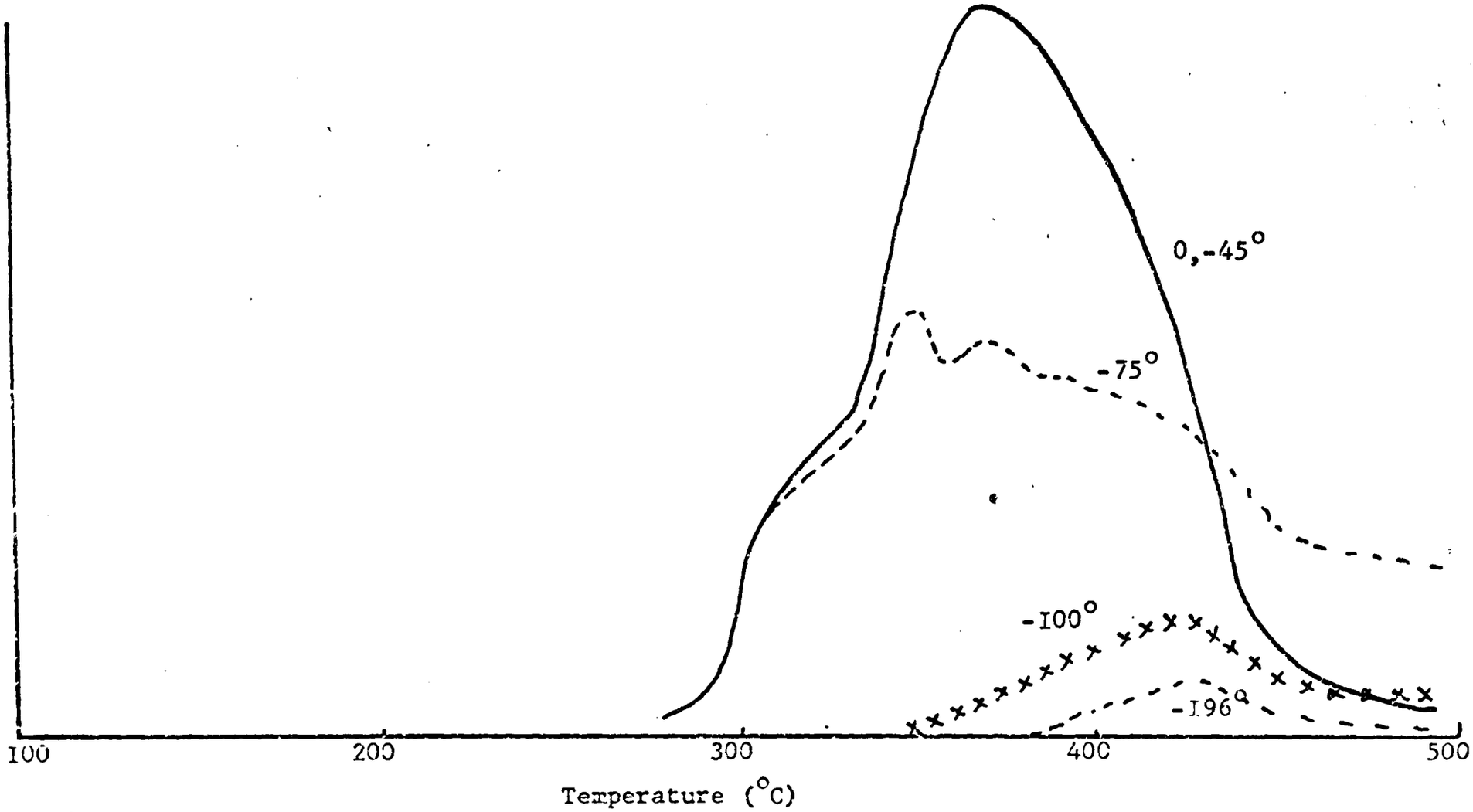

FIGURE 6.3 T.V.A. thermogram of 2%MVK

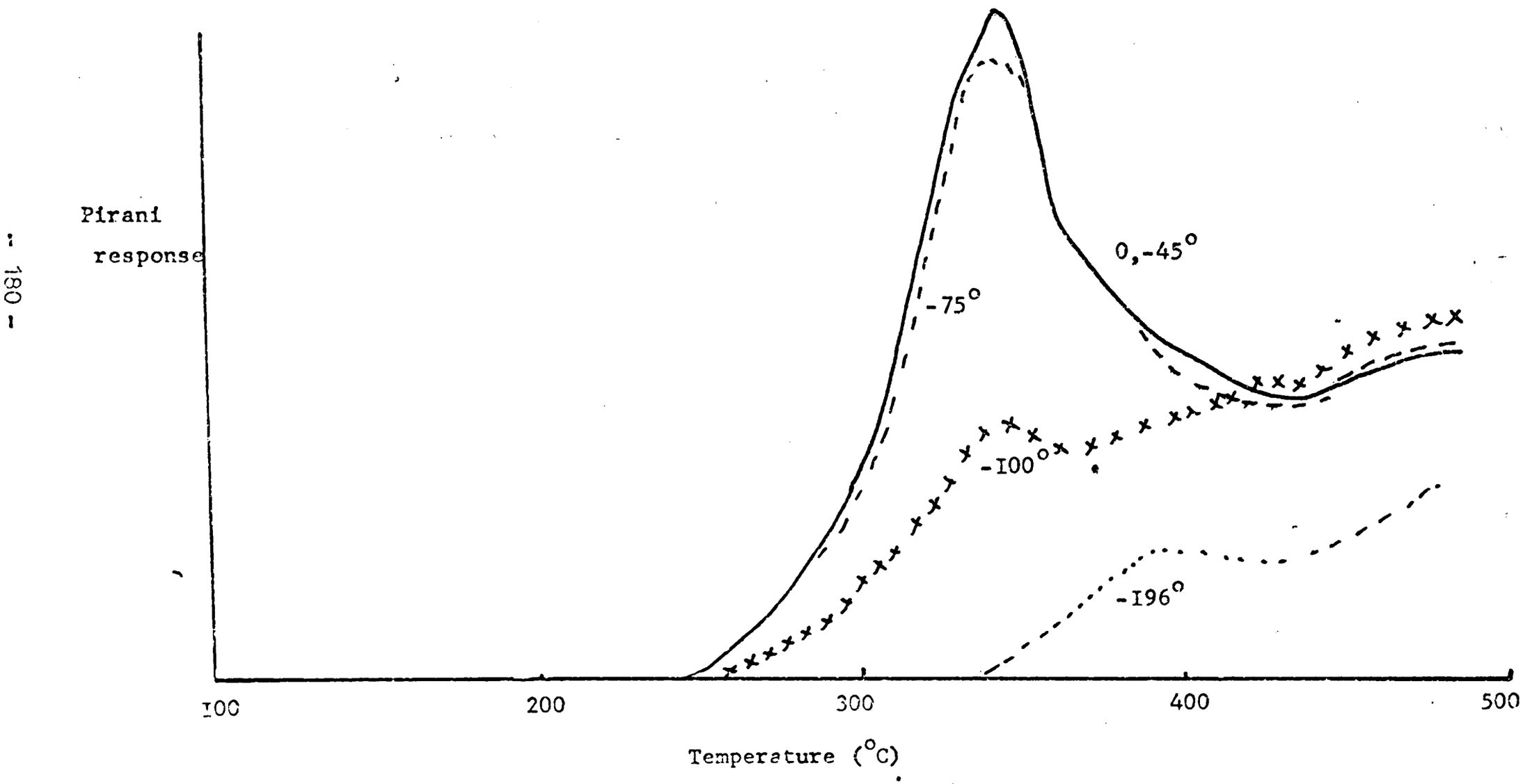

FIGURE 6.4 T.V.A. thermogram of 70/30 copolymer

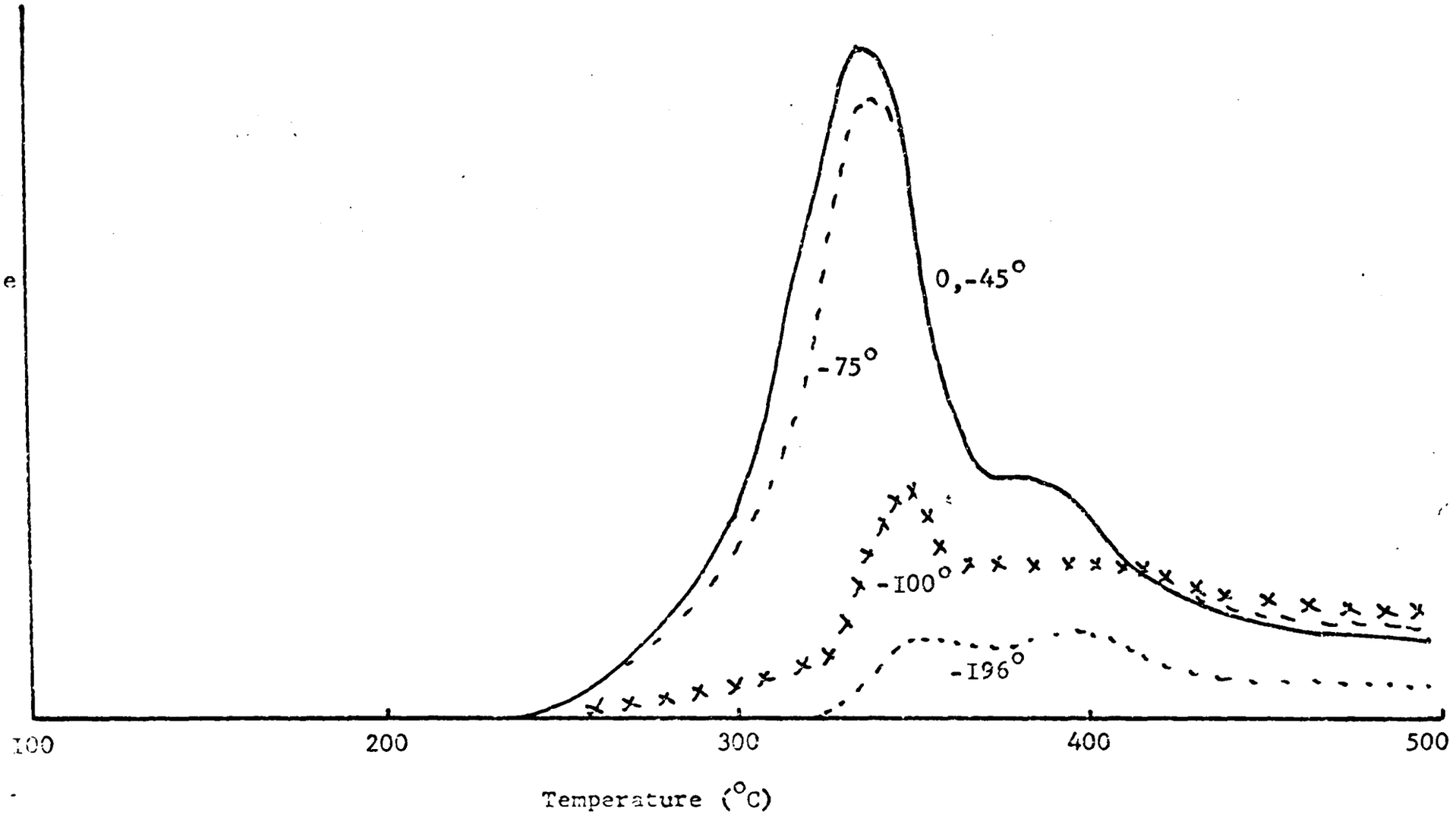

FIGURE 6.5 T.V.A. thermogram of 30/70 copolymer

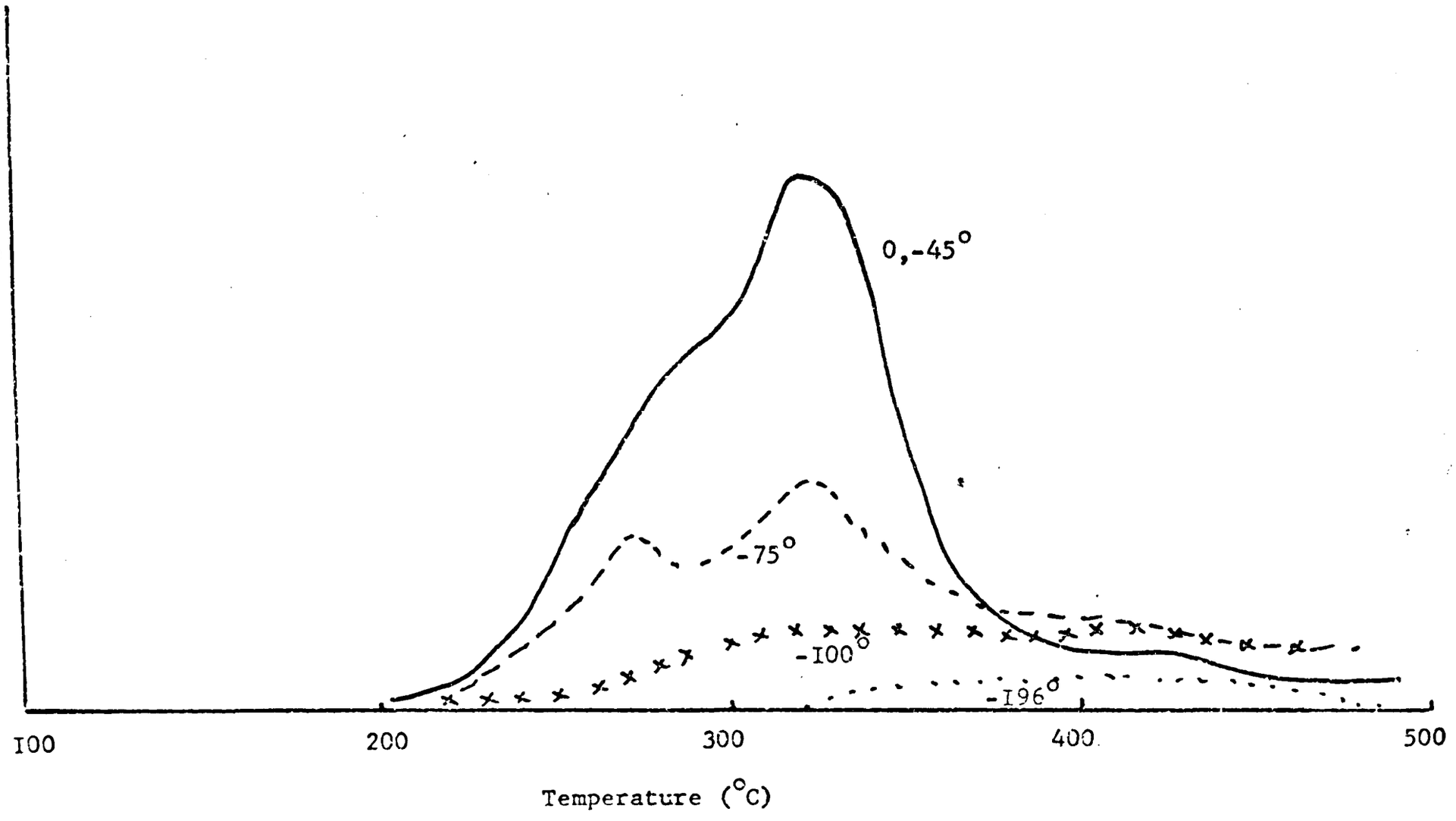

FIGURE 6.6 T.V.A. thermogram of 10/90 copolymer

TABLE 6.I

Polymer	Main peak temperature (^{o}C)	Molecular weight $xI0^{-3}$
PMMA	374	800
2%MVK	397	—
7%MVK	385	492
I5%MVK	39I	I,480
70/30 (AD)	352	697
50/50 (AD)	36I	6,300
30/70	352	545
I0/90	325	585
PMVK	3I3	II9

TABLE 6.2

Polymer	Temperature of degradation (^{o}C)	Time of degradation (hrs.)	%weight loss
PMMA	220	I	I.64
PMMA	220	2	2.59
PMMA	220	6.5	5.02
90/I0	220	I	I.37
90/I0	220	I	I.38
90/I0	220	2.5	I.90
90/I0	220	3.25	2.06
PMMA	240	I	2.46
PMMA	240	4.3	6.78
PMMA	240	6	7.85
90/I0	240	I	I.00
90/I0	240	3	I.2I
90/I0	240	6	3.I6

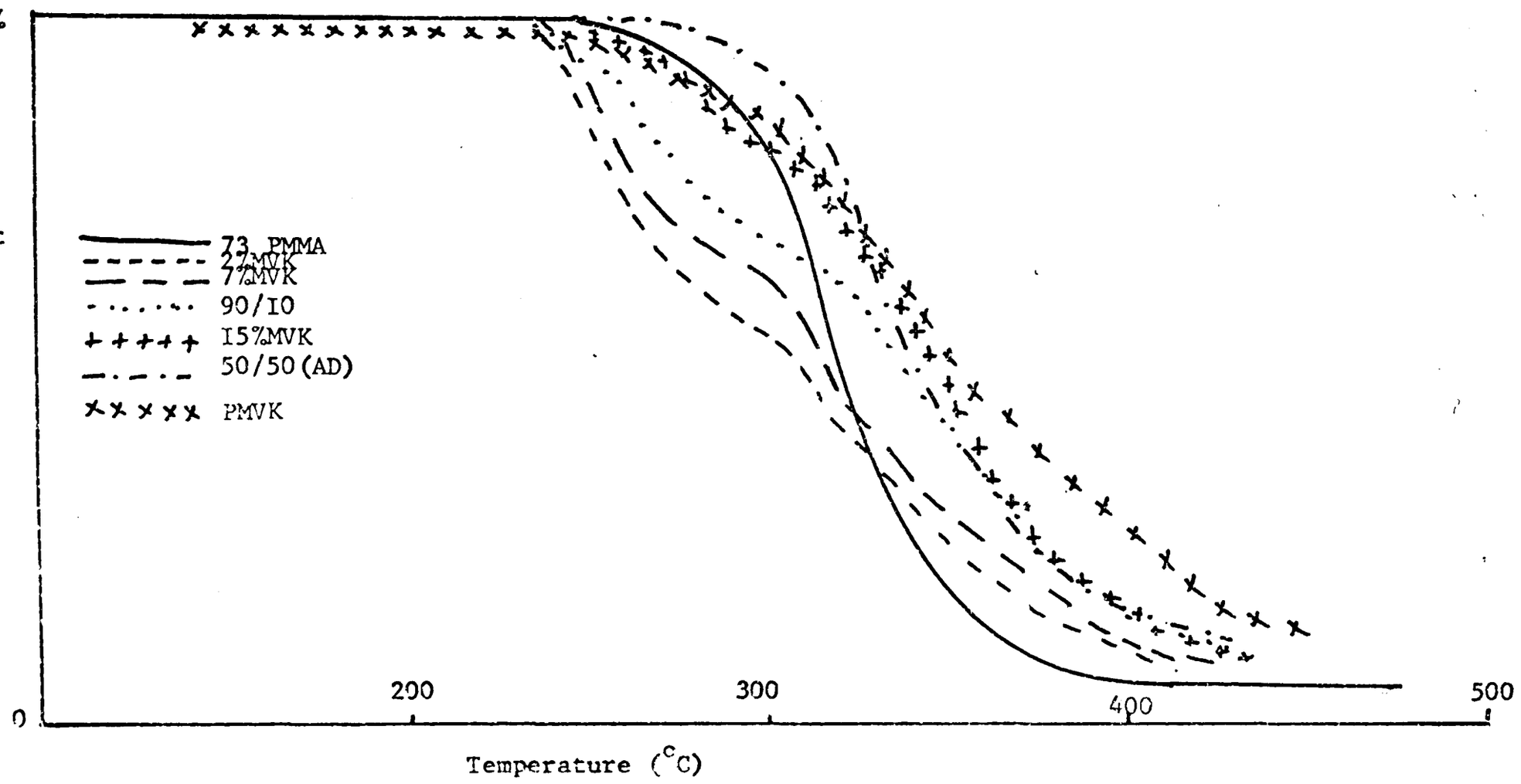

FIGURE 6.7 Thermogravimetric traces

amounts of MVK. As the MVK content increases, the rate of weight loss decreases. The 2% MVK and 7% MVK copolymers also show a two stage weight loss profile. All samples are more stable than PMMA at higher temperatures probably due to ring formation and less combustible residues.

iii) Thermal degradation in thin films. PMMA and the 90/10 copolymer were compared. The samples were cast from chloroform and degraded as described in Chapter 2. The results are tabulated in TABLE 6.2.

The results plotted in FIGURE 6.7a show that PMMA loses more weight than the copolymer. The only product detected was MMA in each case. Unfortunately, the residual copolymer would not dissolve in toluene for molecular weight examination.

b) Photodegradation of thin films

Again, only one copolymer was compared with PMMA, namely the 70/30 copolymer. Conditions for degradation were those described in Chapter 2. The degradation temperature was 150°C and the samples were cast from chloroform. The results, shown in TABLE 6.3 include molecular weight determinations on the degraded copolymer which, surprisingly, dissolved in toluene. Results from the degradation of PMMA were taken from TABLE 4.9.

These results which are illustrated in FIGURES 6.8 and 6.9 show that PMMA degrades slightly faster than the copolymer.

c) Photodegradation in solution

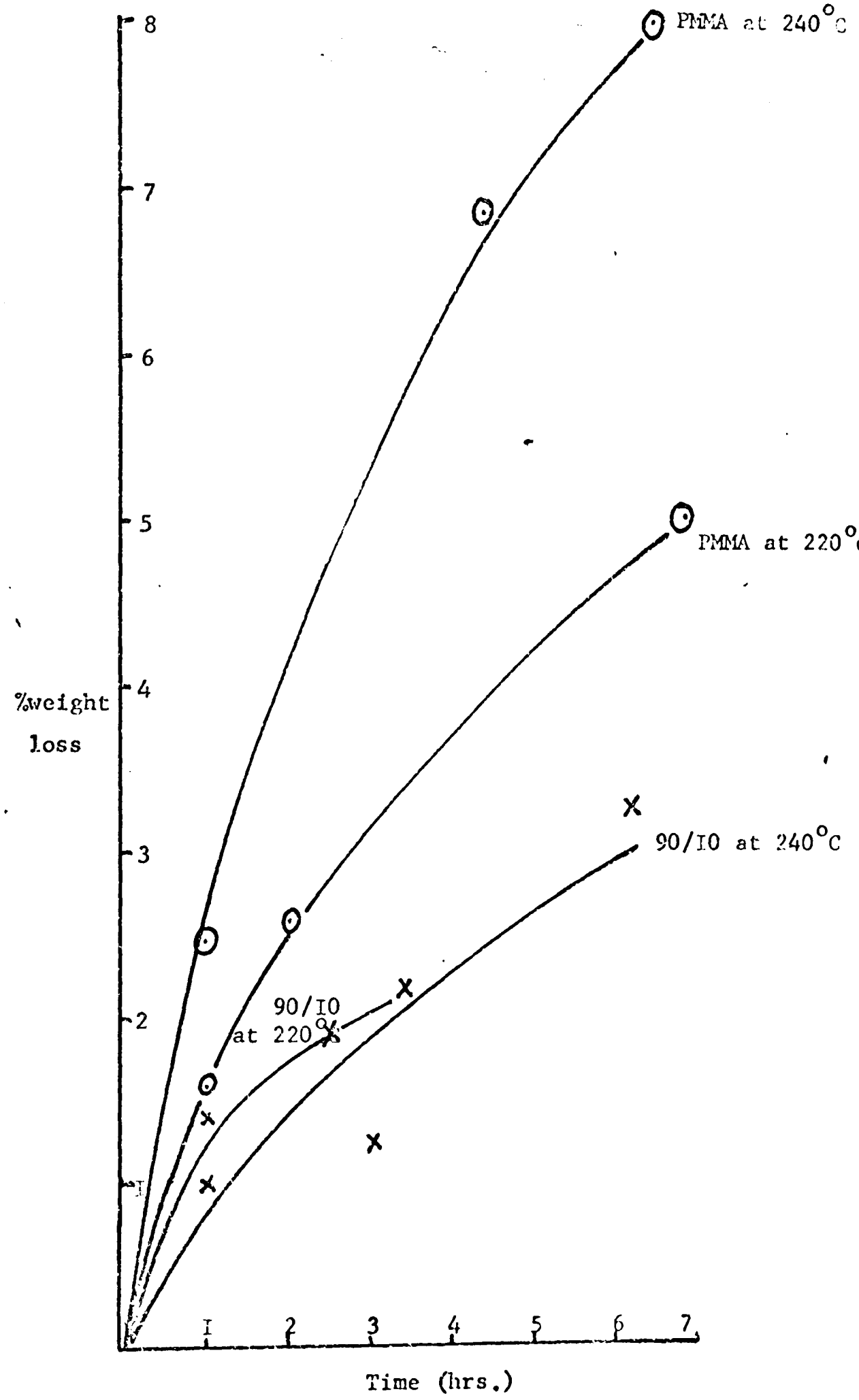

FIGURE 6.7a %weight loss versus time for thin film thermal degradation

TABLE 6.3

Polymer	Time of degradation (hrs.)	%weight loss	Molecular weight	Number of chain scissions per monomer unit $xI0^{-5}$
PMMA	I	6.6	42,200	2I2
PMMA	2.5	I4.0	20,900	402
70/30	0	0	520,000	0
70/30	0.5	2.3	70,500	I07
70/30	I	4.4	4I,500	I9I
70/30	I.5	7.I	33,800	230
70/30	2	8.7	29,200	265

TABLE 6.4

Polymer	Time of irradiation (hrs.)	Molecular weight $xI0^{-3}$	Number of chain scissions per monomer unit $xI0^{5}$
PMMA	0	685	0
PMMA	0.5	I2I	68
PMMA	I	67.6	I34
PMMA	I.5	59.3	I54
PMMA	2	39.2	242
90/I0	0	520	0
90/I0	0.5	32.9	254
90/I0	I	I8.I	493
90/I0	I.5	I4.4	627
90/I0	2	II.8	769
70/30	0	500	0
70/30	0.5	4I.0	I99
70/30	I	20.0	428
70/30	I.5	I6.5	522
70/30	2	I4.7	588

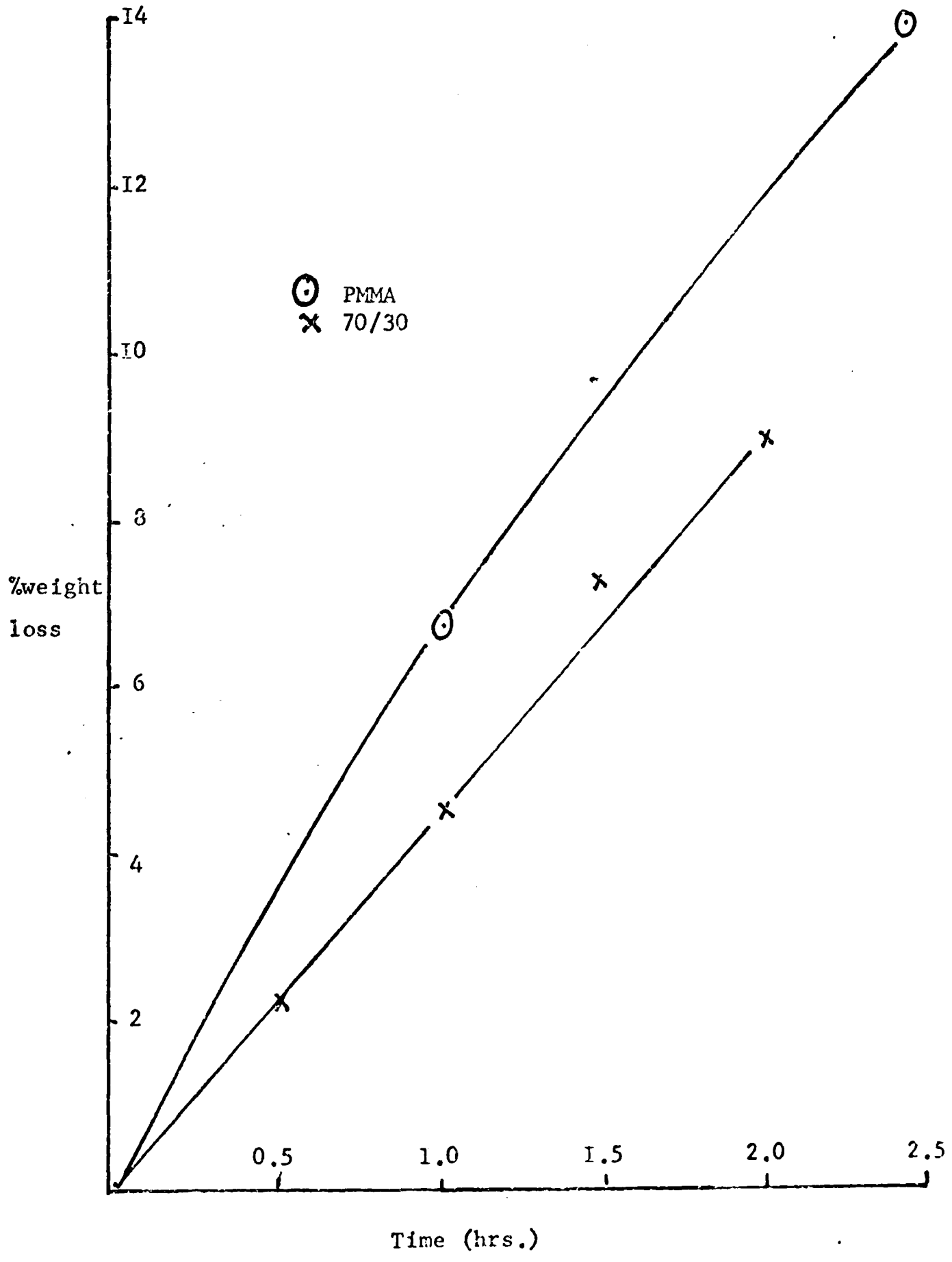

FIGURE 6.8 Photothermal degradation of thin films of PMMA and 70/30 copolymer at 150°C

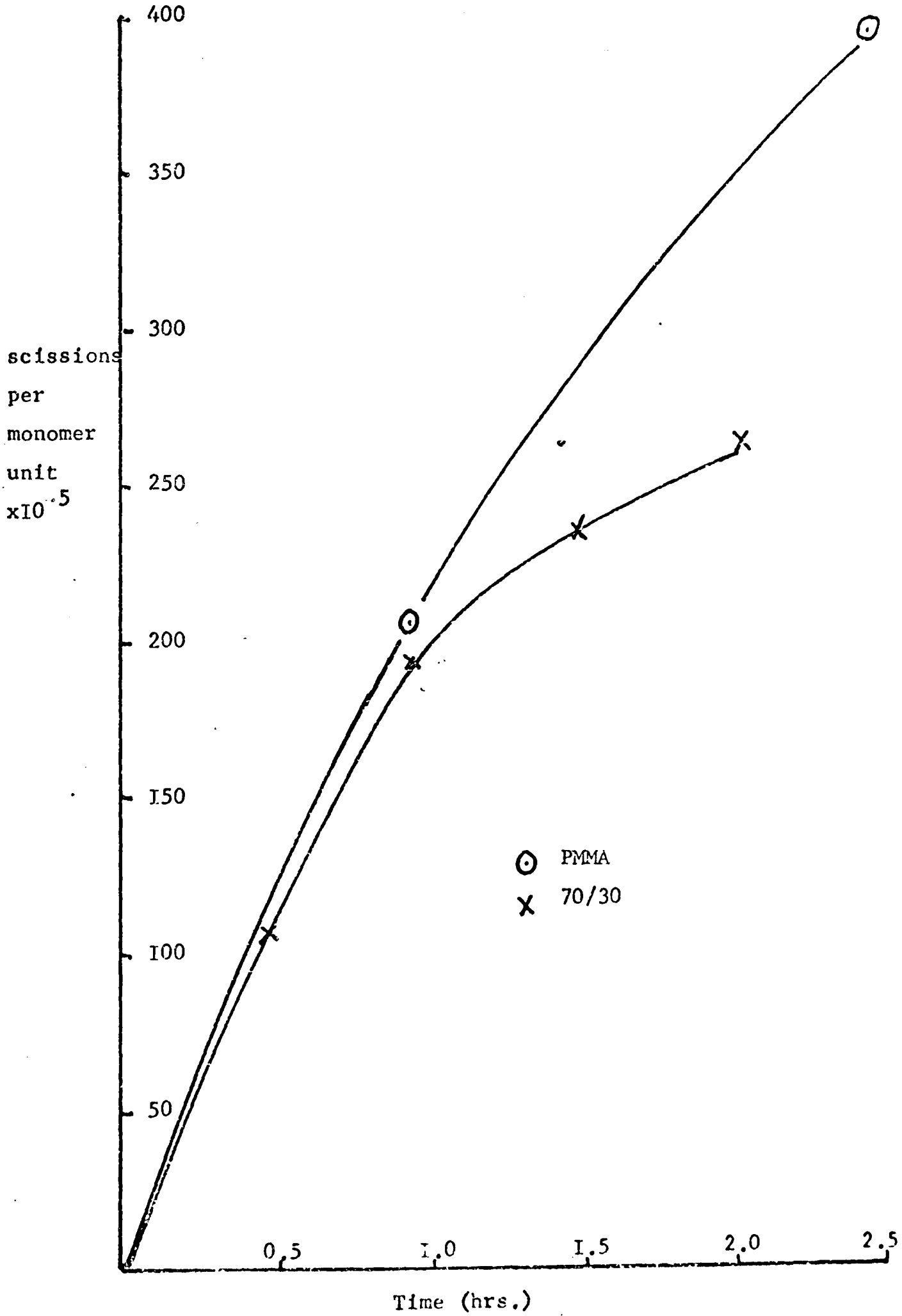

FIGURE 6.9 Photothermal degradation of thin films of PMMA and 70/30 copolymer at I50°C

PMMA and two copolymers were degraded in methyl acetate solution and molecular weights measured in toluene solution. The results are shown in TABLE 6.4. However, since high MVK containing copolymers do not dissolve readily in toluene, the experiments were repeated using butanone as solvent in molecular weight analysis. These results are shown in TABLE 6.5.

In these two experiments, two different lamps were employed. Results cannot, therefore, be compared except relative to the degradation of PMMA. Two samples had molecular weights too high to be recorded while, on the other hand, most degradations taken beyond one hour gave molecular weights too low to be measured in butanone.

The data in TABLES 6.4 and 6.5 are illustrated in FIGURES 6.10 and 6.11 respectively. The slopes of these lines represent the rates of degradation (TABLES 6.6 and 6.7) and the rate dependence on MVK content is shown in FIGURES 6.12 and 6.13.

3. MIK/MMA

a) Thermal Degradation

McNeill[57] has shown that cyclisation similar to that which occurs in PMVK, also occurs in PMIK although to a lesser extent. In contrast with PMVK, however, monomer is also produced. T. V. A. thermograms for PMIK and three copolymers are shown in FIGURES 6.14, 6.15, 6.16 and 6.17. The peak temperatures are detailed in TABLE 6.8

The T. V. A. thermograms are similar in shape because each

TABLE 6.5

Polymer	Time of irradiation (hrs.)	Molecular weight $xI0^{-3}$	Number of chain scissions per monomer unit $xI0^{5}$
PMMA	0	800	0
PMMA	0.5	483	8.2
PMMA	I.0	I58	50.7
PMMA	I.5	93	95
PMMA	2.0	78	II6
2%MVK	0	—	—
2%MVK	0.5	89	—
2%MVK	I.0	65	—
7%MVK	0	492	0
7%MVK	0.5	48	I85
7%MVK	I.0	27.3	333
90/I0	0	—	—
90/I0	0.5	76.3	—
90/I0	I.0	45.5	—
I5%MVK	0	I,480	0
I5%MVK	0.5	46	I9I
70/30 (AD)	0	697	0
70/30 (AD)	0.67	62.5	II3
70/30 (AD)	I	39.2	I87
50/50 (AD)	0	6,300	0
50/50 (AD)	0.5	52.5	I52
50/50 (AD)	I	33.I	243
30/70	0	545	0
30/70	0.5	67	I05
30/70	I	38	I97
I0/90	0	585	0
I0/90	0.5	96	65
I0/90	I	55.5	I22
PMVK	0	II9.5	0
PMVK	0.5	48	87.2
PMVK	I	54.5	69.9

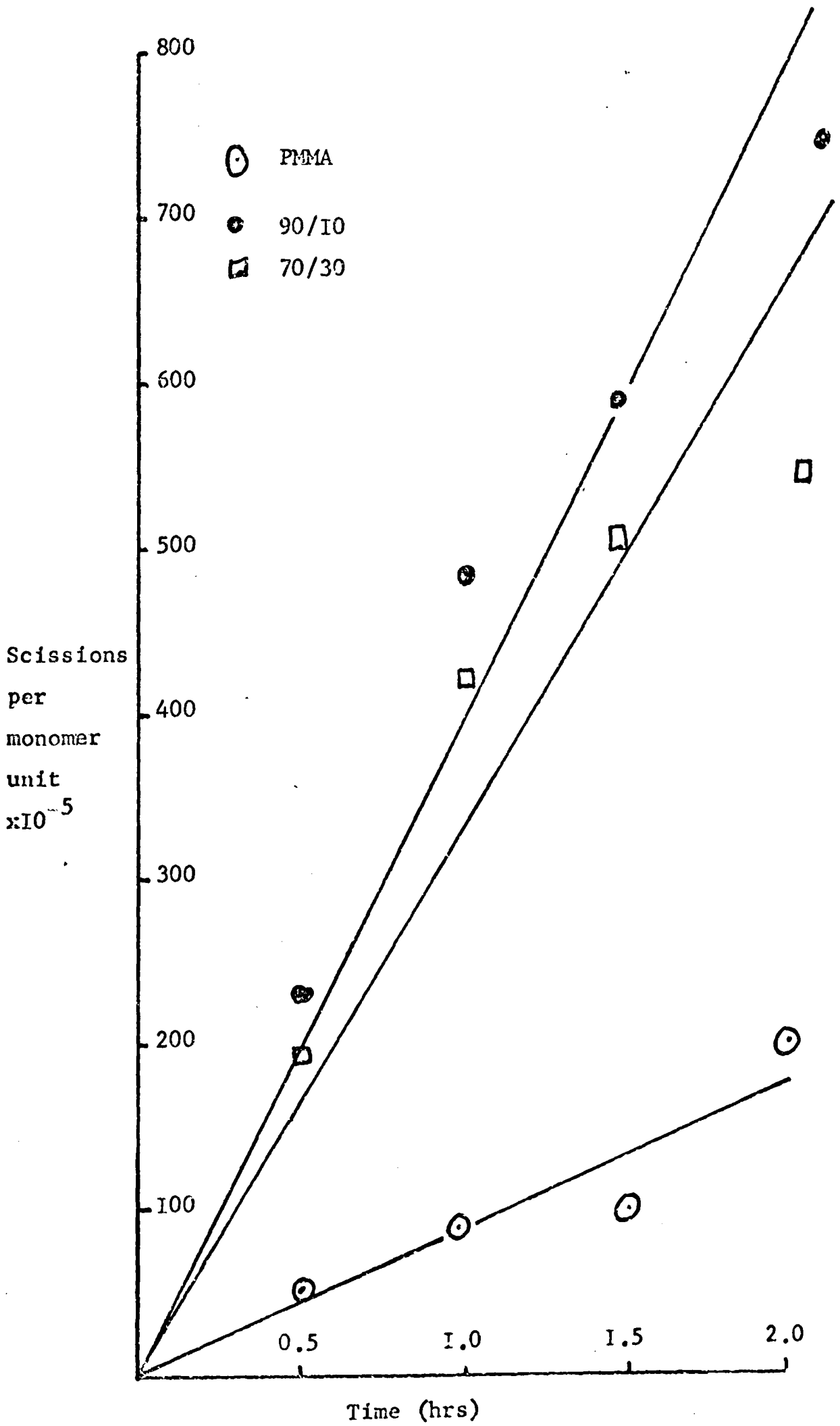

FIGURE 6.10 Photodegradation in solution of MMA/MVK copolymers

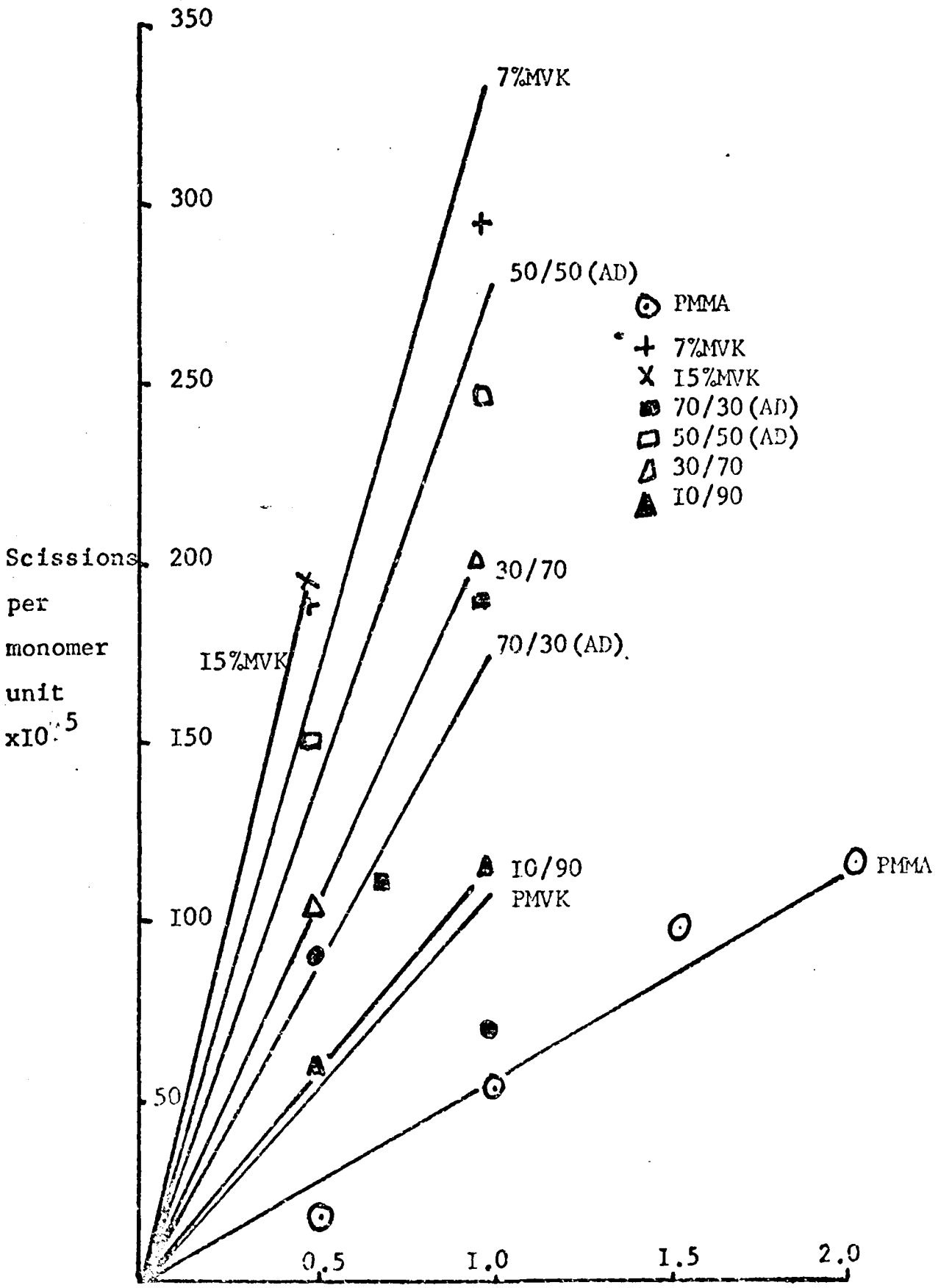

FIGURE 6.II Photodegradation in solution of MMA/MVK copolymers

TABLE 6.6

Polymer	Rate of degradation (scissions/monomer unit/hour xI0 ^{5})
PMMA	I2I
90/I0	438
70/30	365

TABLE 6.7

Polymer	Rate of degradation (scissions/monomer unit/hour xI0 ^{5})
PMMA	54
7%MVK	346
I5%MVK	382
70/30 (AD)	I76
50/50 (AD)	264
30/70	204
I0/90	II6
PMVK	I02

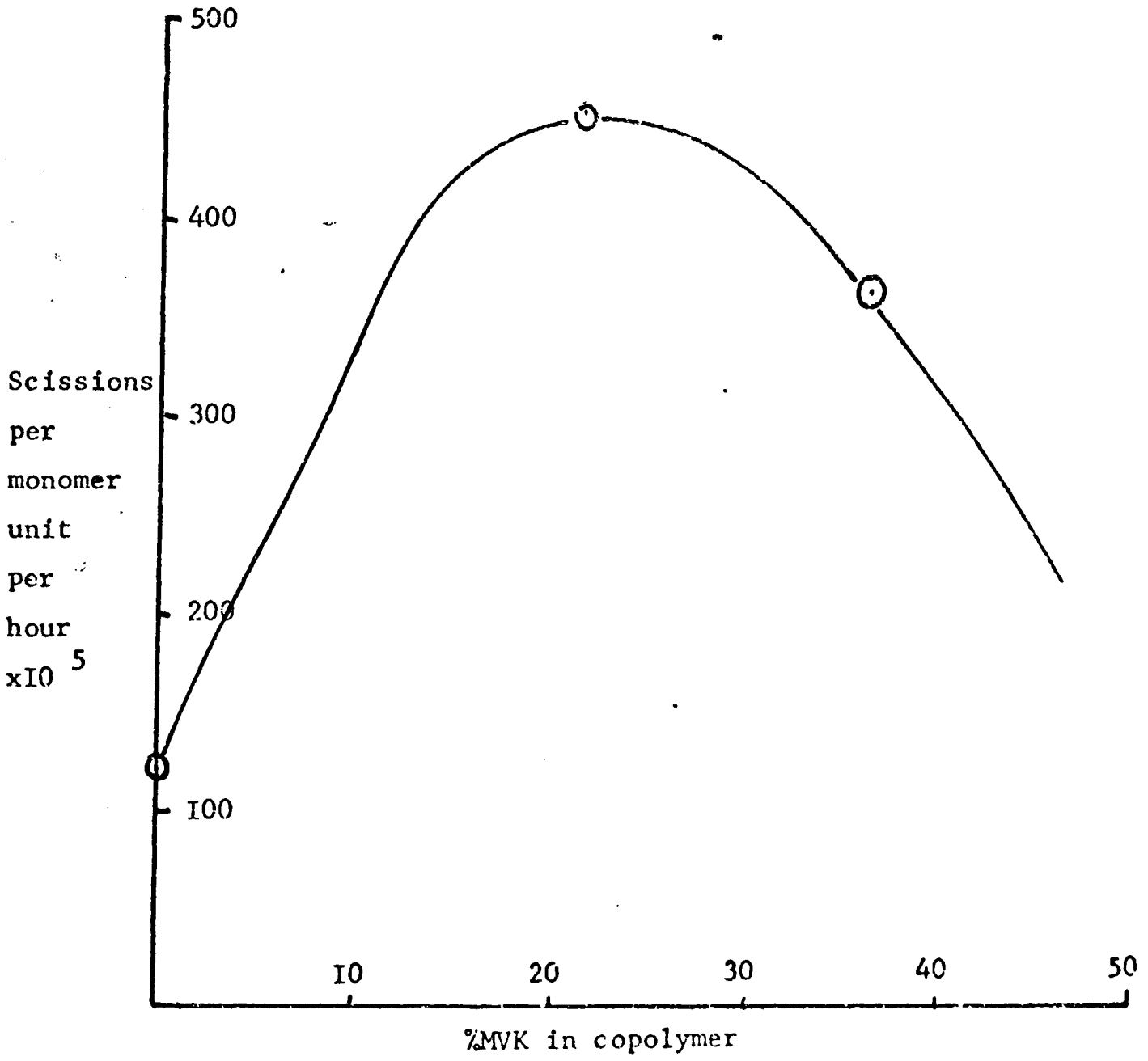

FIGURE 6.I2 Rate of photodegradation versus %MVK

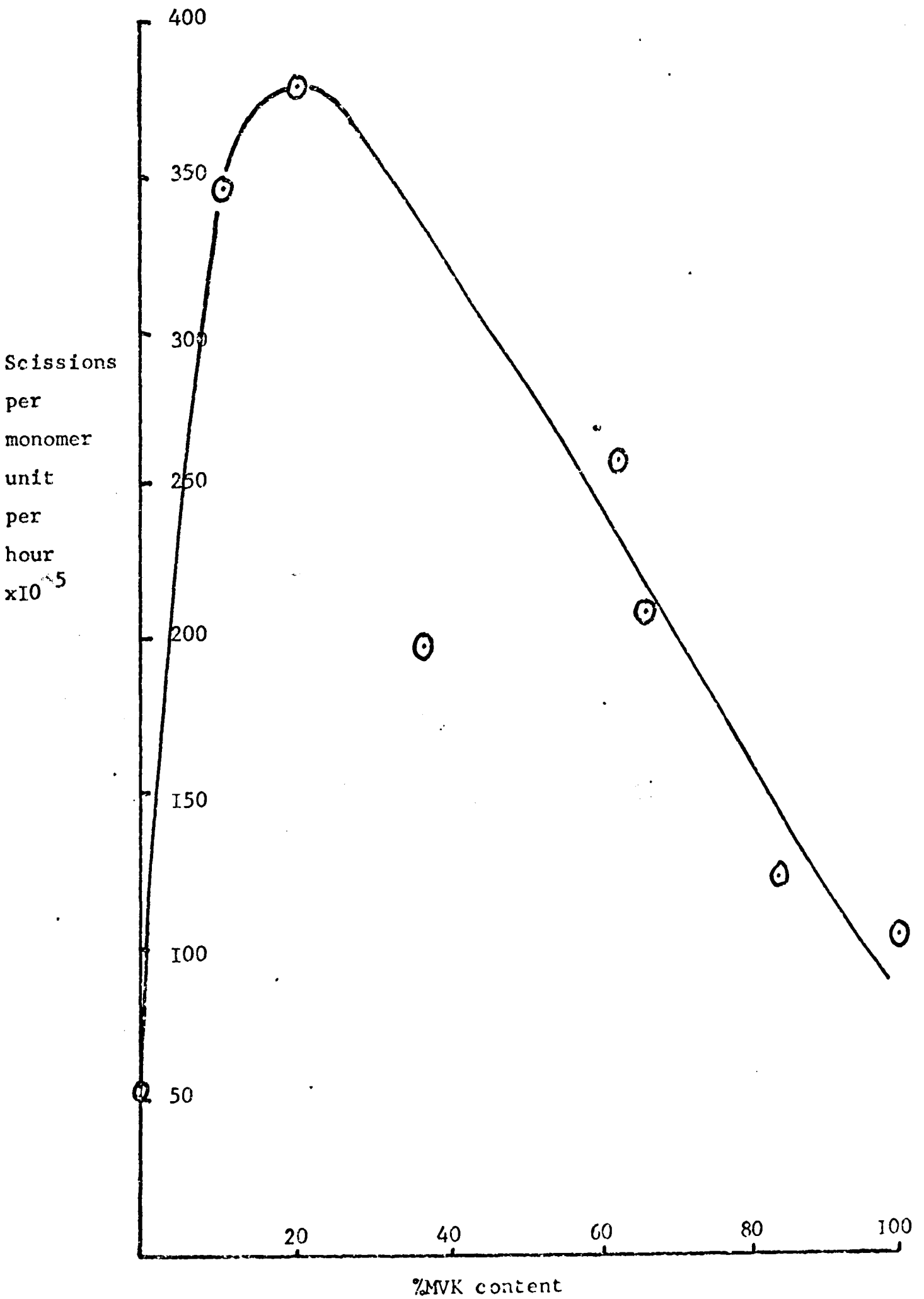

FIGURE 6.I3 Rate of photodegradation versus %MVK

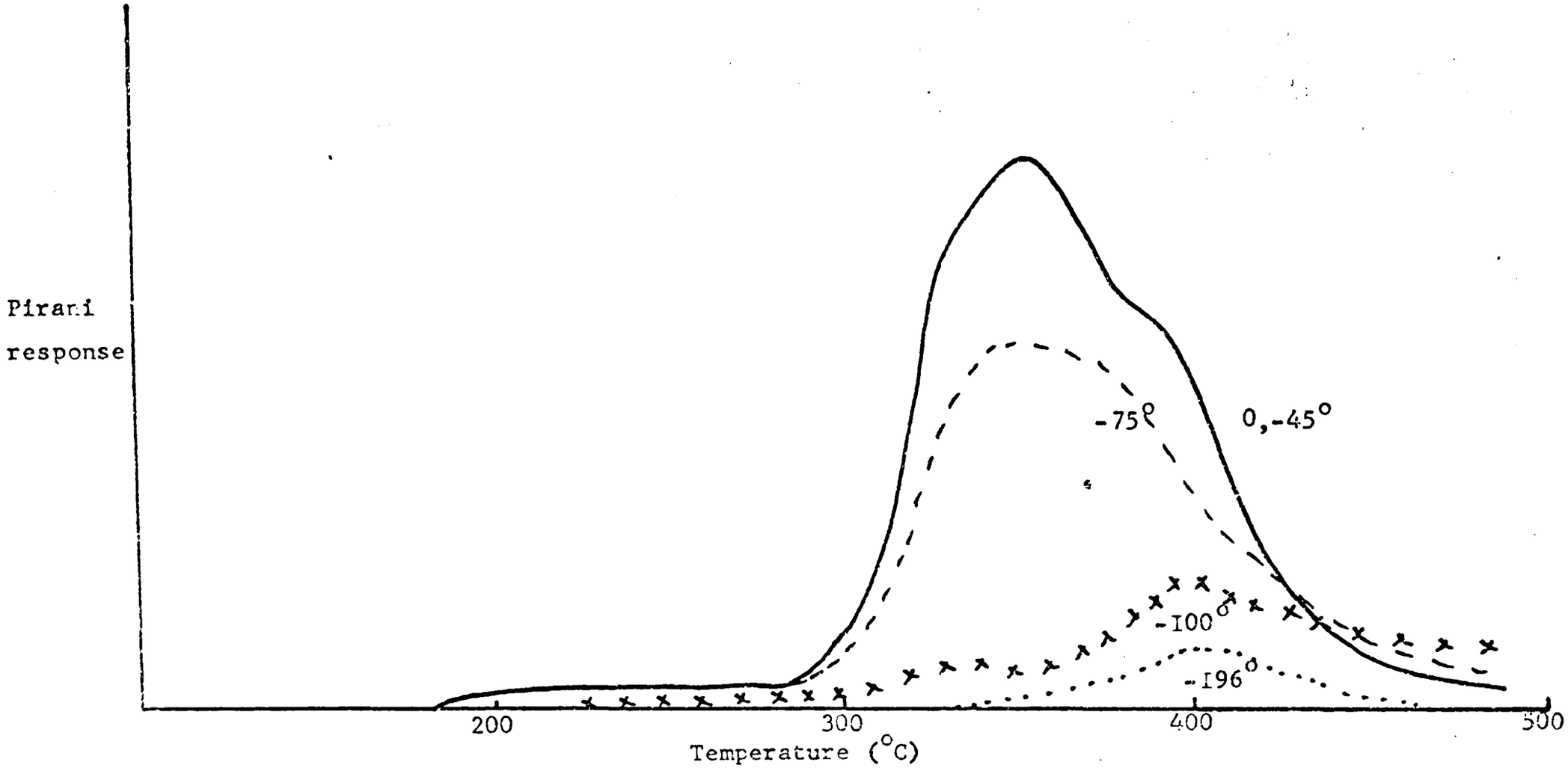

FIGURE 6.14 T.V.A. thermogram for PMIK

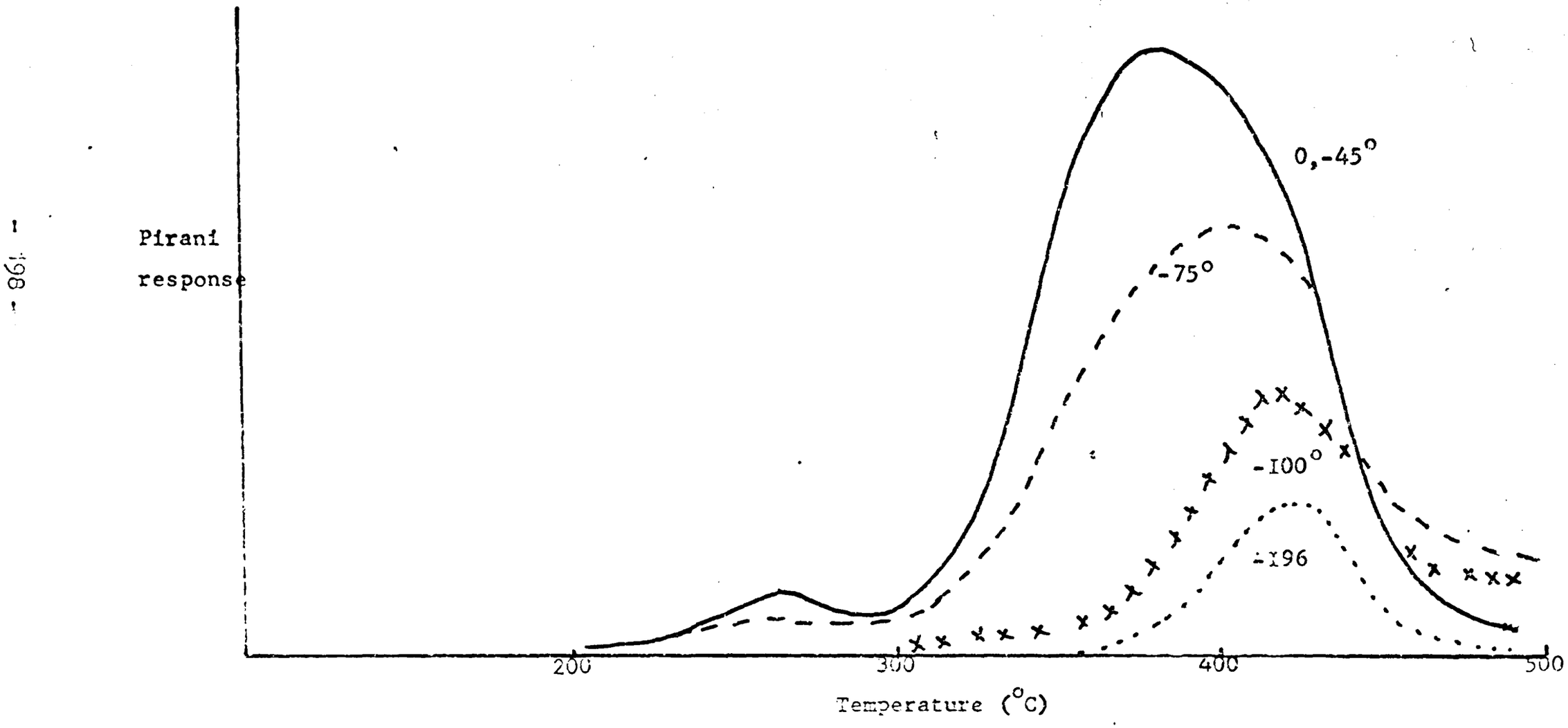

FIGURE 6.15 T.V.A. thermogram of I/2 copolymer

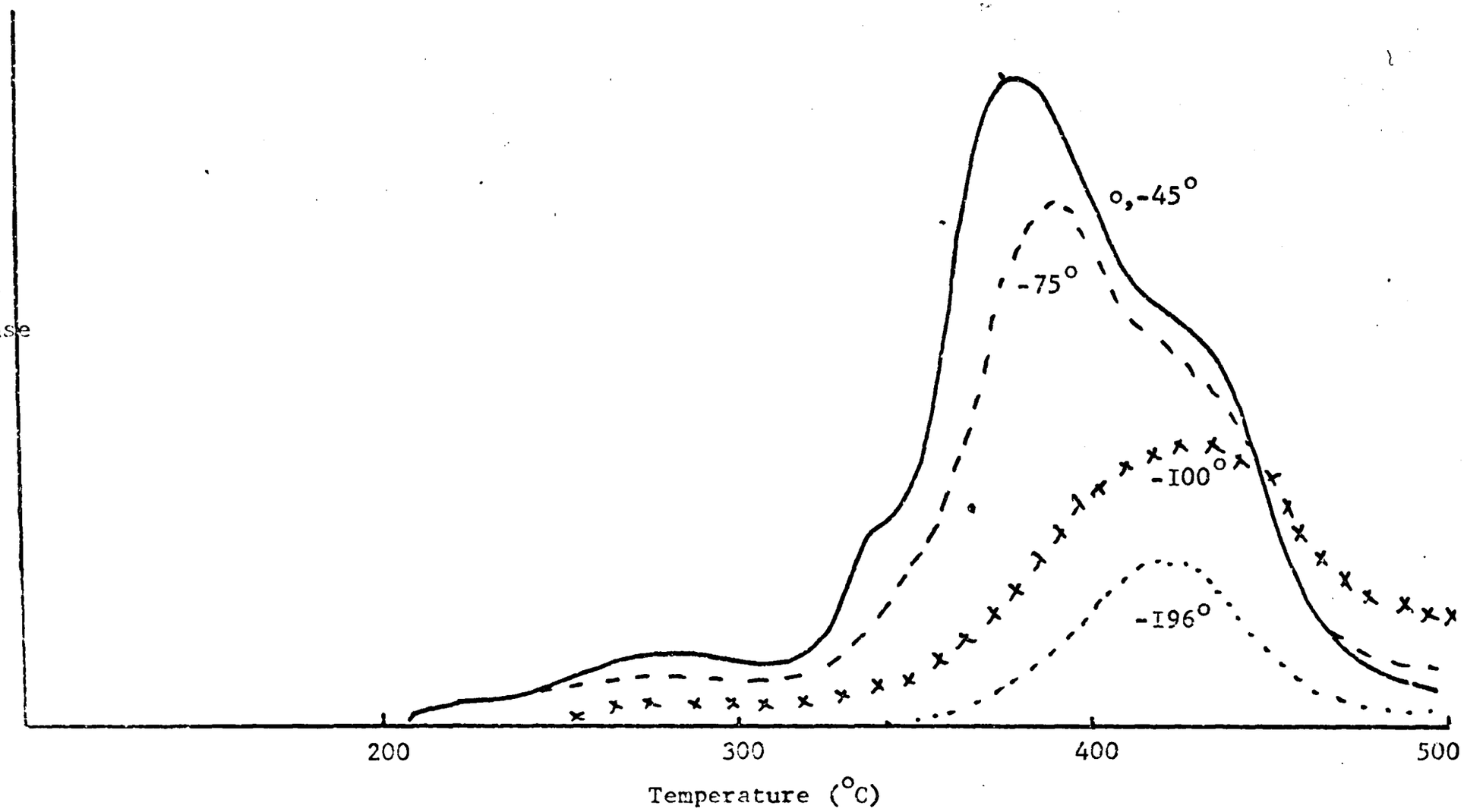

FIGURE 6.16 T.V.A. thermogram of I/I copolymer

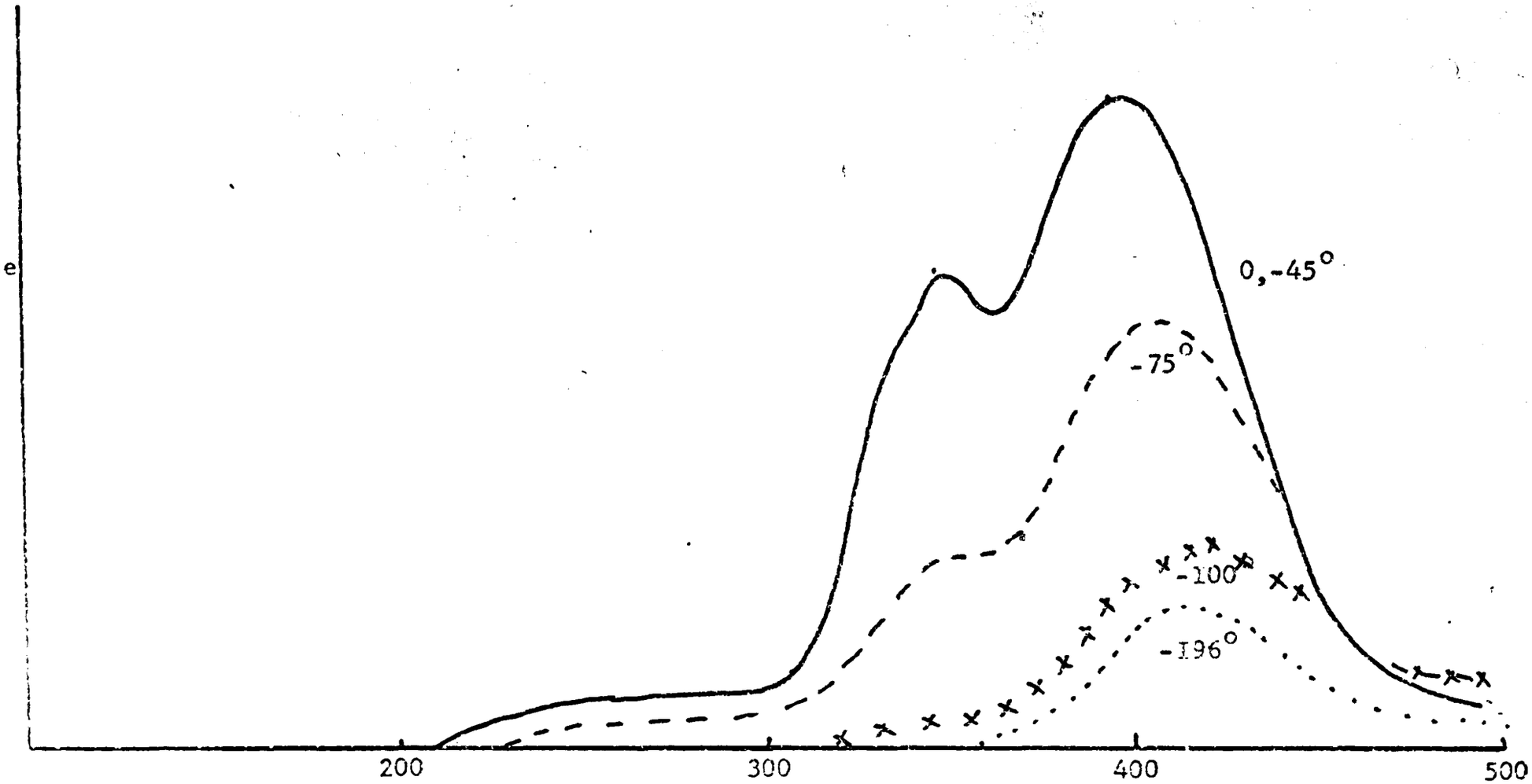

FIGURE 6.17 T.V.A. thermogram of 2/I copolymer

TABLE 6.8

Polymer	Main peak temperature (^{o}C)	Molecular weight $xI\tilde{0}^{3}$
PMMA	374	800
I/2	4I4	I78
I/I	395	8I.2
2/I	395	94.7
PMIK	360	40.3

TABLE 6.9

Polymer	Time of irradiation (hrs.)	Molecular weight $xI\tilde{0}^{3}$	Scissions per monomer unit $xI0^{5}$
PMMA	0	8I5	0
PMMA	0.5	2I6	34.4
PMMA	I	I32	63.4
PMMA	I.5	90	99.0
I/2	0	I78	0
I/2	0.5	60.3	I04
I/2	I	49.0	I40
I/I	0	8I.2	0
I/I	0.5	46.5	85.5
I/I	I	48.0	79.4
2/I	0	94.7	0
2/I	0.5	40.8	I25
2/I	I	49.0	88.0
PMIK	0	53.0	0
PMIK	0.5	40.3	50.0
PMIK	I	43.0	36.8

copolymer evolves two different monomers, MMA and MIK which behave similarly in the -75^{o} trace. Water is also evolved in ring cyclisation and this further confuses analysis. The copolymers do, however, appear to be more stable than the homopolymers. This is further borne out by the TG thermograms in FIGURE 6.18.

b) Thin film thermal degradation and photodegradation

The preparation of satisfactory thin films of MIK/MMA copolymers proved impossible. Acetone was found to be the only suitable solvent which would give films which did not turn opaque and, even then, only occasionally. On heating, the films peeled off the discs. Accordingly, degradation experiments could not be performed.

c) Photodegradation in solution

The polymers were degraded in three solvents:- Methyl acetate, butanone and chloroform. All molecular weights were performed in butanone solution.

i) Methyl acetate. The results are shown in TABLE 6.9 and plotted in FIGURE 6.19. From this graph, the rates of degradation can be found and are shown in TABLE 6.10 with the rate of degradation versus % MVK content shown in FIGURE 6.20.

ii) Butanone. The results are shown in TABLE 6.11 and treated in a similar manner as above in FIGURE 6.21, TABLE 6.12 and FIGURE 6.22.

iii) Chloroform. While the solution of MIK in chloroform

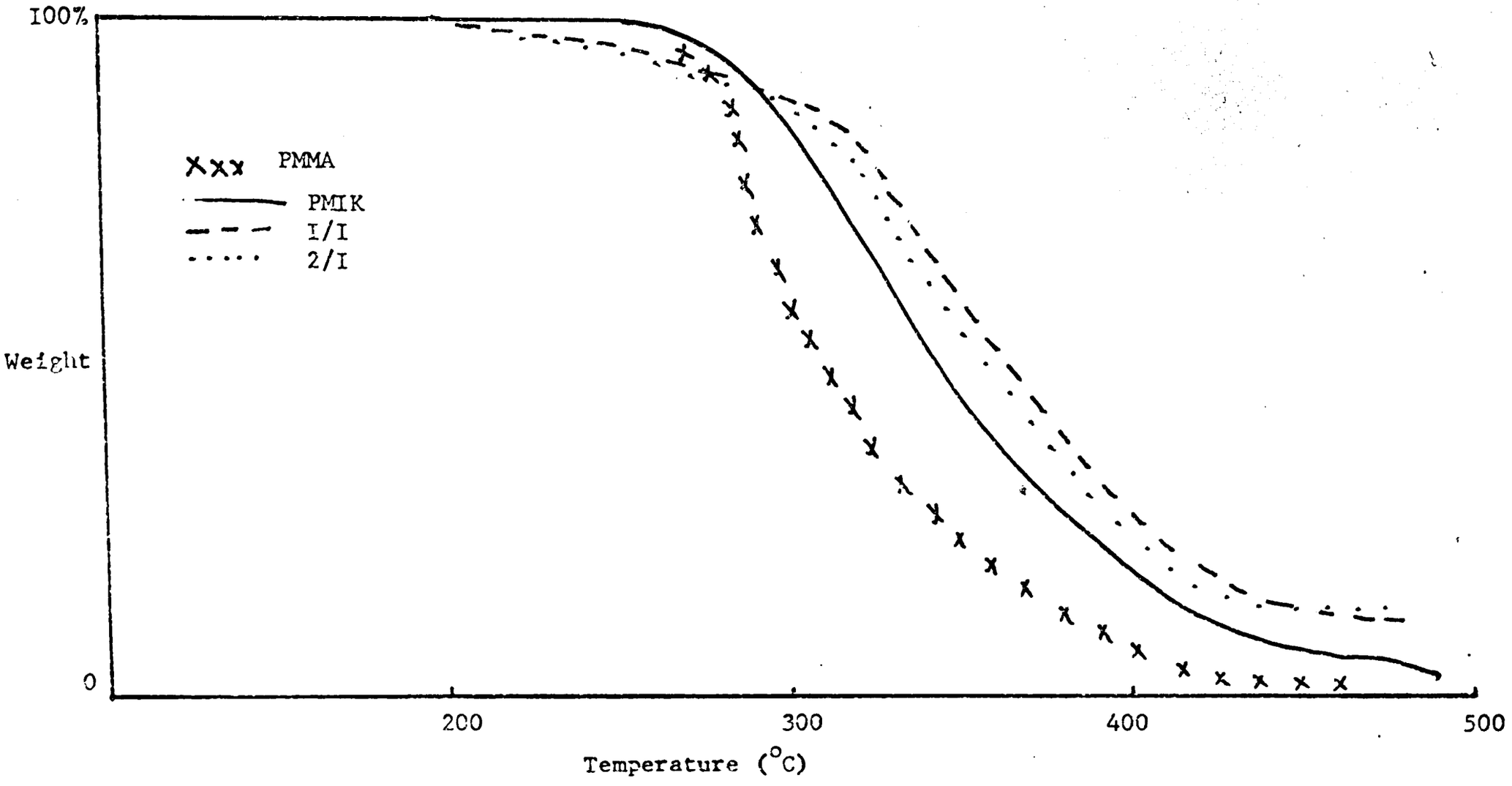

FIGURE 6.I8 Thermogravimetric traces

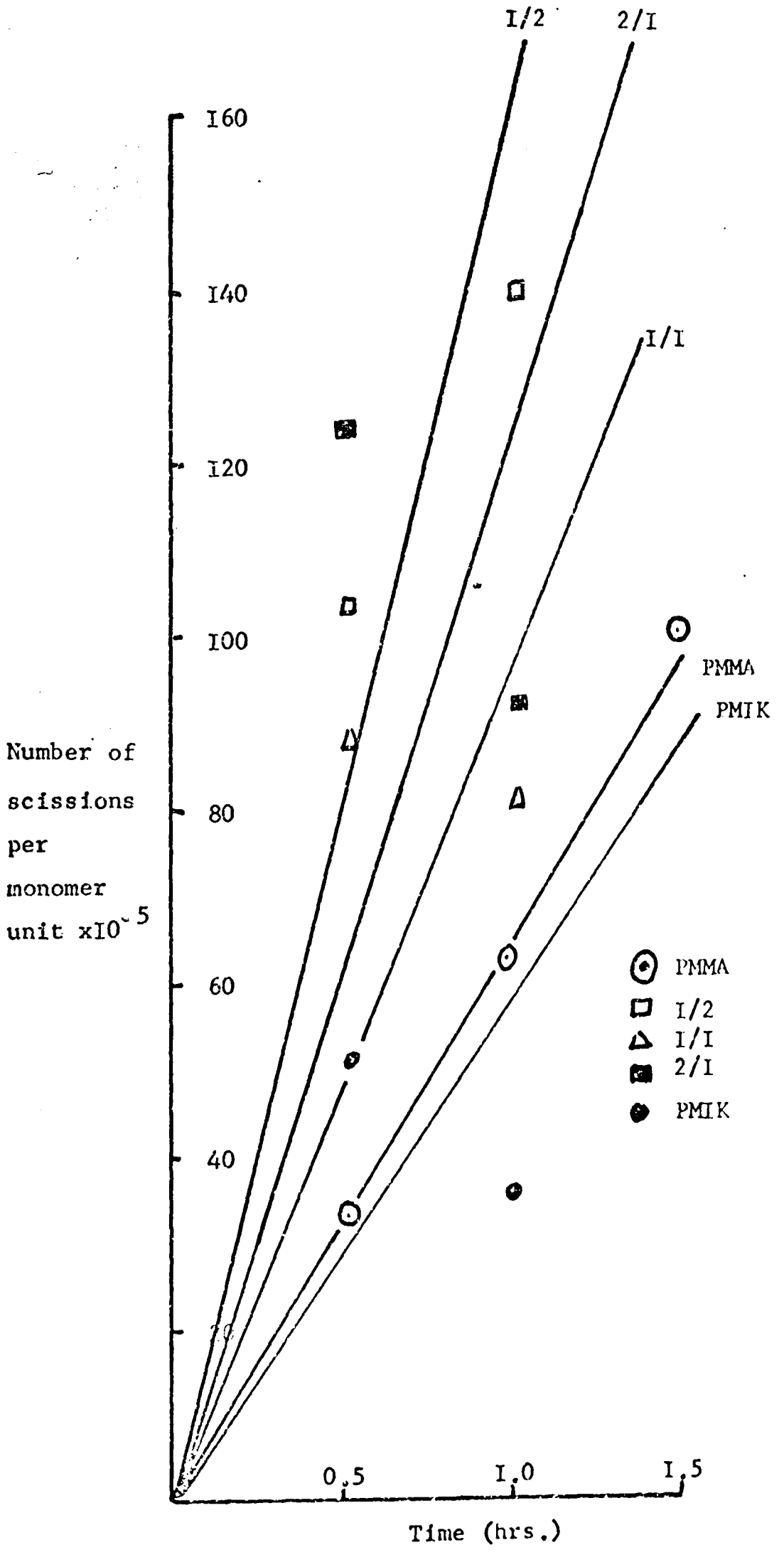

FIGURE 6.19 Photodegradation in solution of MIK/MMA copolymers

TABLE 6.I0

Polymer	Scissions/monomer unit/hour $xI0^{-5}$
PMMA	64
I/2	I64
I/I	I08
2/I	I36
PMIK	54

TABLE 6.II

Polymer	Time of irradiation (hrs.)	Molecular weight $xI0^{-3}$	Scissions per monomer unit $xI0^{-5}$
I/2	0	I78	0
I/2	0.5	I25	22.6
I/2	I	65	92.5
I/I	0	8I.2	0
I/I	0.5	I03	0
I/I	I	65	28.5
2/I	0	94.7	0
2/I	0.5	66.0	4I.I
2/I	I	63.0	47.4
PMIK	0	53.0	0
PMIK	0.5	46.7	2I.4
PMIK	I	43.8	33.3

TABLE 6.I2

Polymer	Scissions/monomer unit/nour $xI0^{5}$
I/2	74
I/I	28.5
2/I	58
PMIK	38

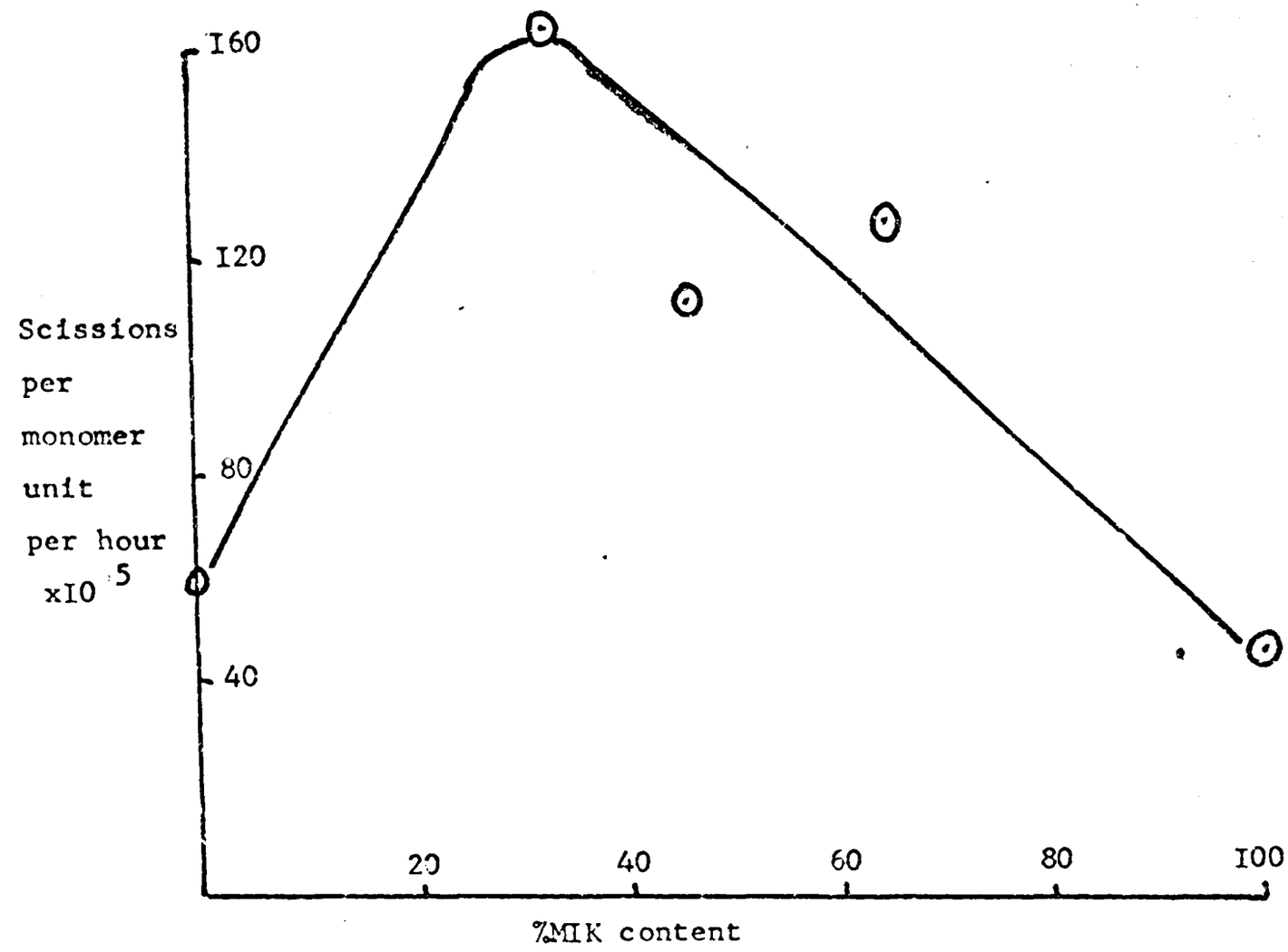

FIGURE 6.20 Rate of photodegradation versus %MIK content

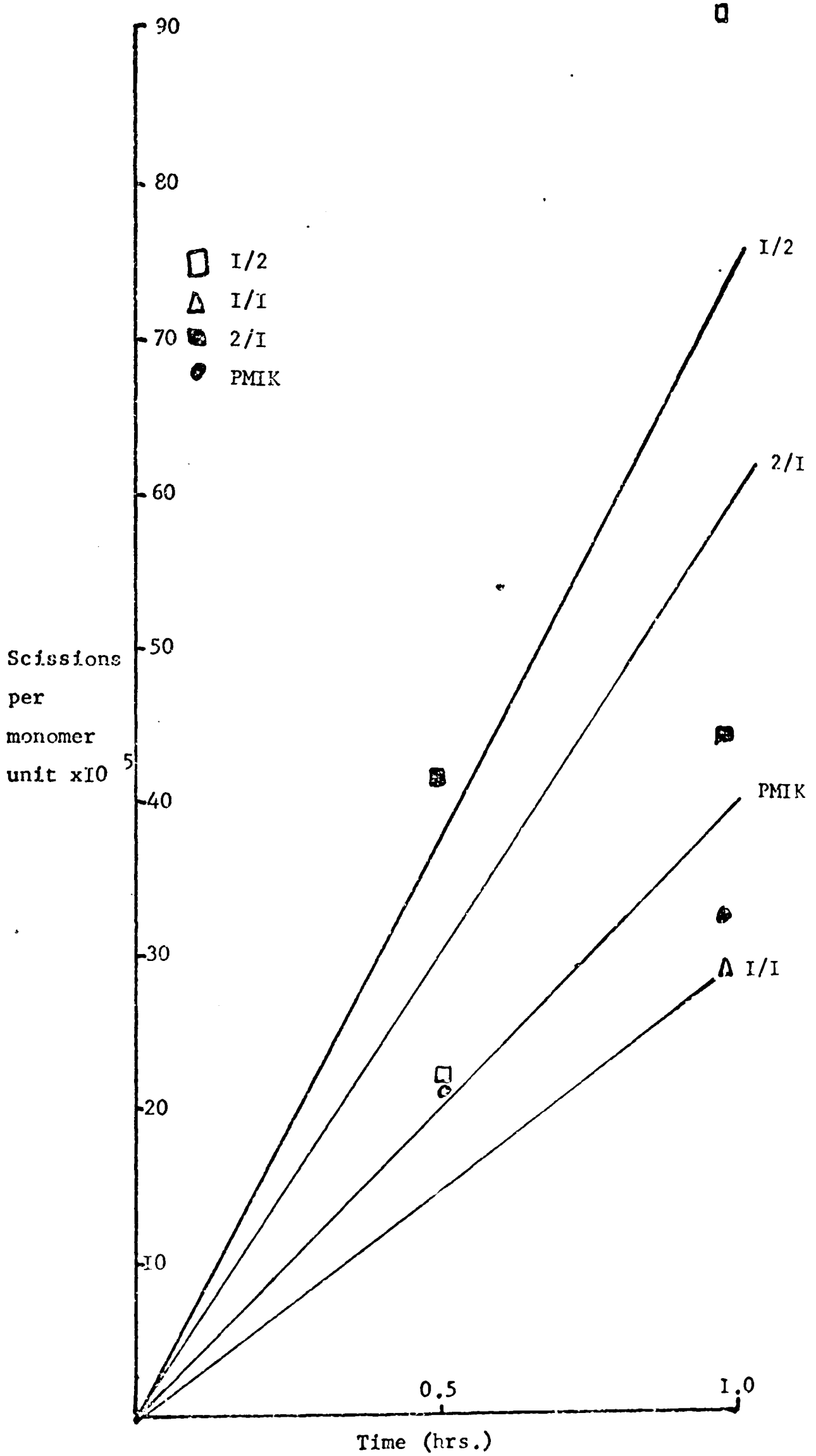

FIGURE 6.21 Photodegradation in butanone solution of MIK/MMA copolymers.

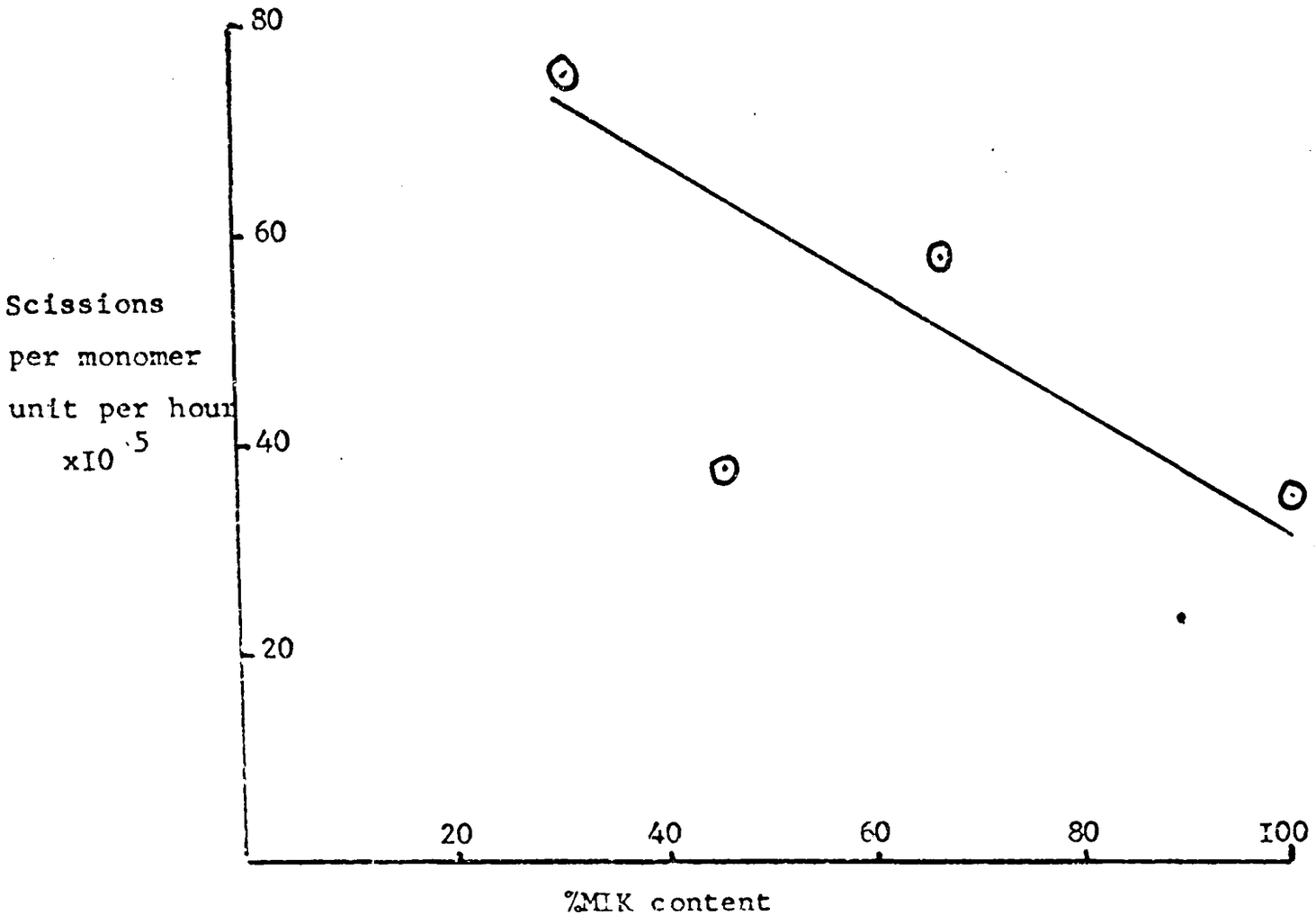

FIGURE 6.22 Rate of photodegradation versus %MIK content

was being degassed in silica cells prior to irradiation, it was noticed that the solution in one cell had become green in colour and in the other, blue. After irradiation, both solutions were very dark red in colour. The polymer remained red after the solvent had been removed.

After irradiation in chloroform solution, the 2/1 MIK/MMA copolymer was green in colour. The other copolymers and even PMMA appeared slightly yellow after irradiation in chloroform.

To follow these colour changes, samples were removed from the cell at certain times during irradiation and diluted with chloroform to 10% of its original concentration. The ultra-violet and visible spectra were then recorded on a Unicam SP800 spectrophotometer. The spectra are reproduced in FIGURE 6.23, 6.24 and 6.25.

In the two polymers examined, PMIK and 2/1 MIK/MMA the intensity of ketone absorption at about 290nm. increases, and also shifts slightly to higher wavelengths. In the 2/1 copolymer, this peak broadens and the tail moves into the visible region towards wavelengths of 450nm. In PMIK as the time of irradiation increases a second absorption peak appears and progressively shifts to higher wavelengths. (TABLE 6.13).

The 290nm. absorption arises from the forbidden $n \rightarrow \pi^*$ transition of the carbonyl chromophore, thus it has a small extinction coefficient. As the length of irradiation time increases, the extinction coefficient increases due to increased conjugation in the

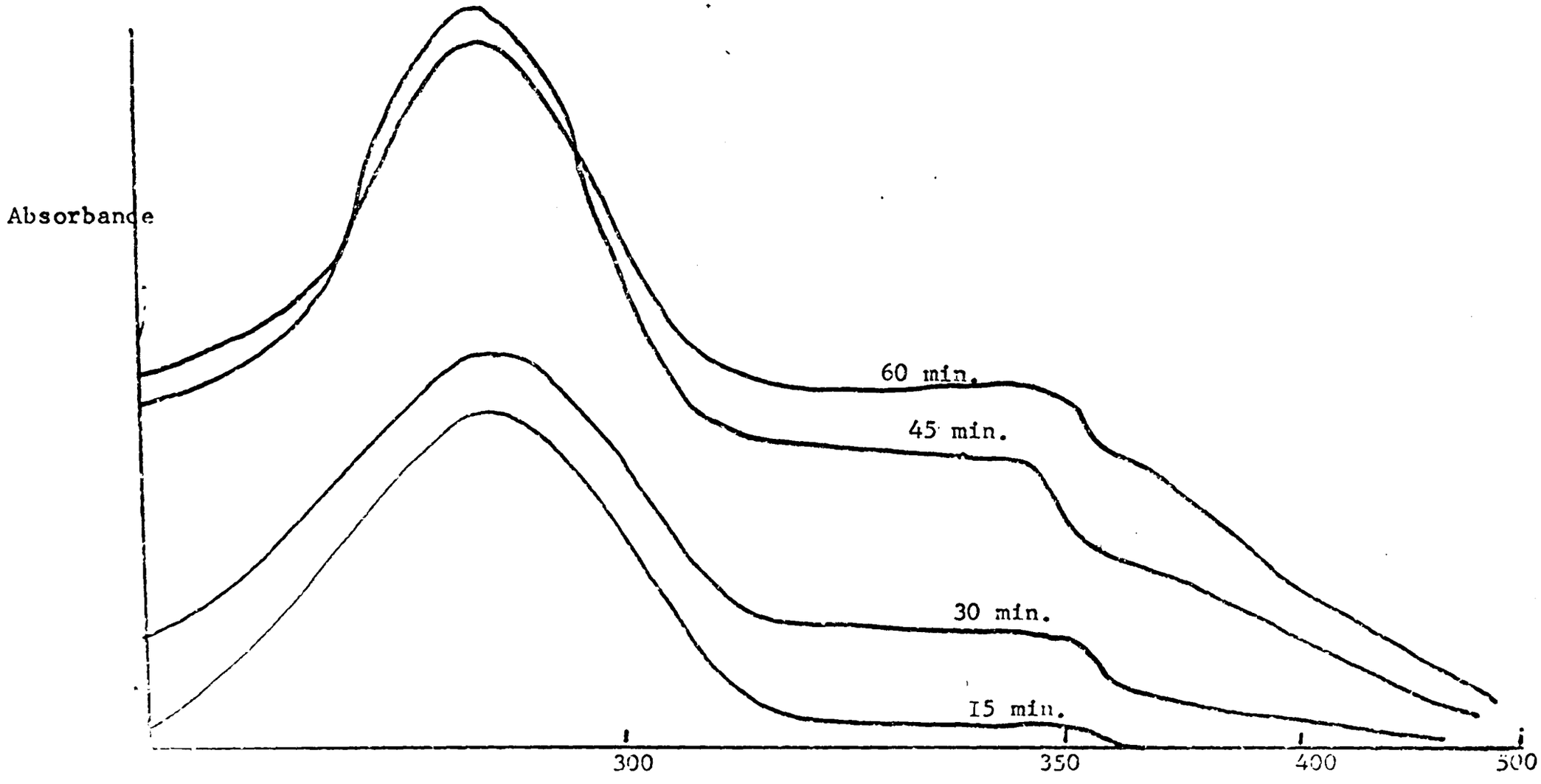

FIGURE 6.23 Ultra-violet spectra of PMIK

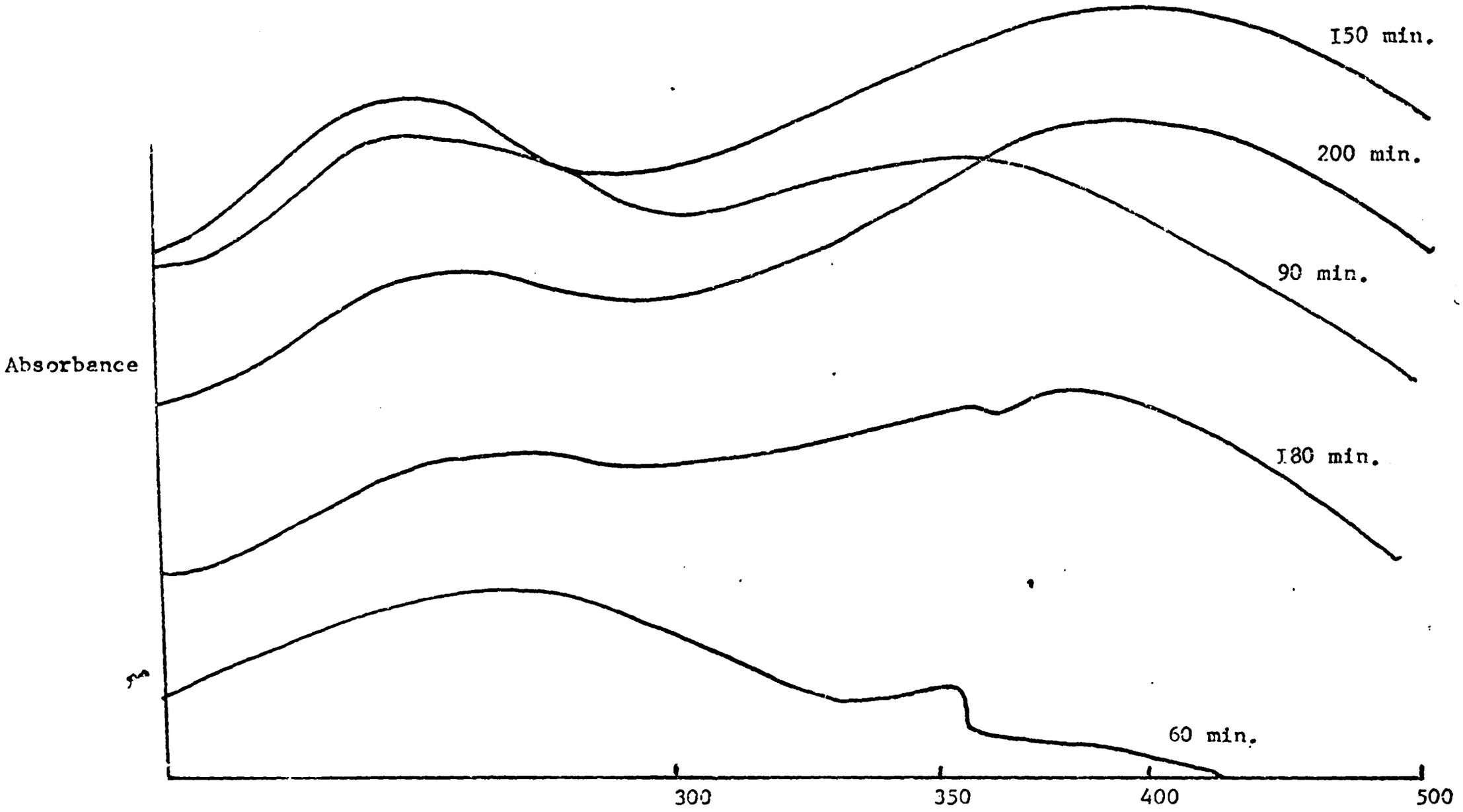

FIGURE 6.24 Ultra-violet spectra of PMIK

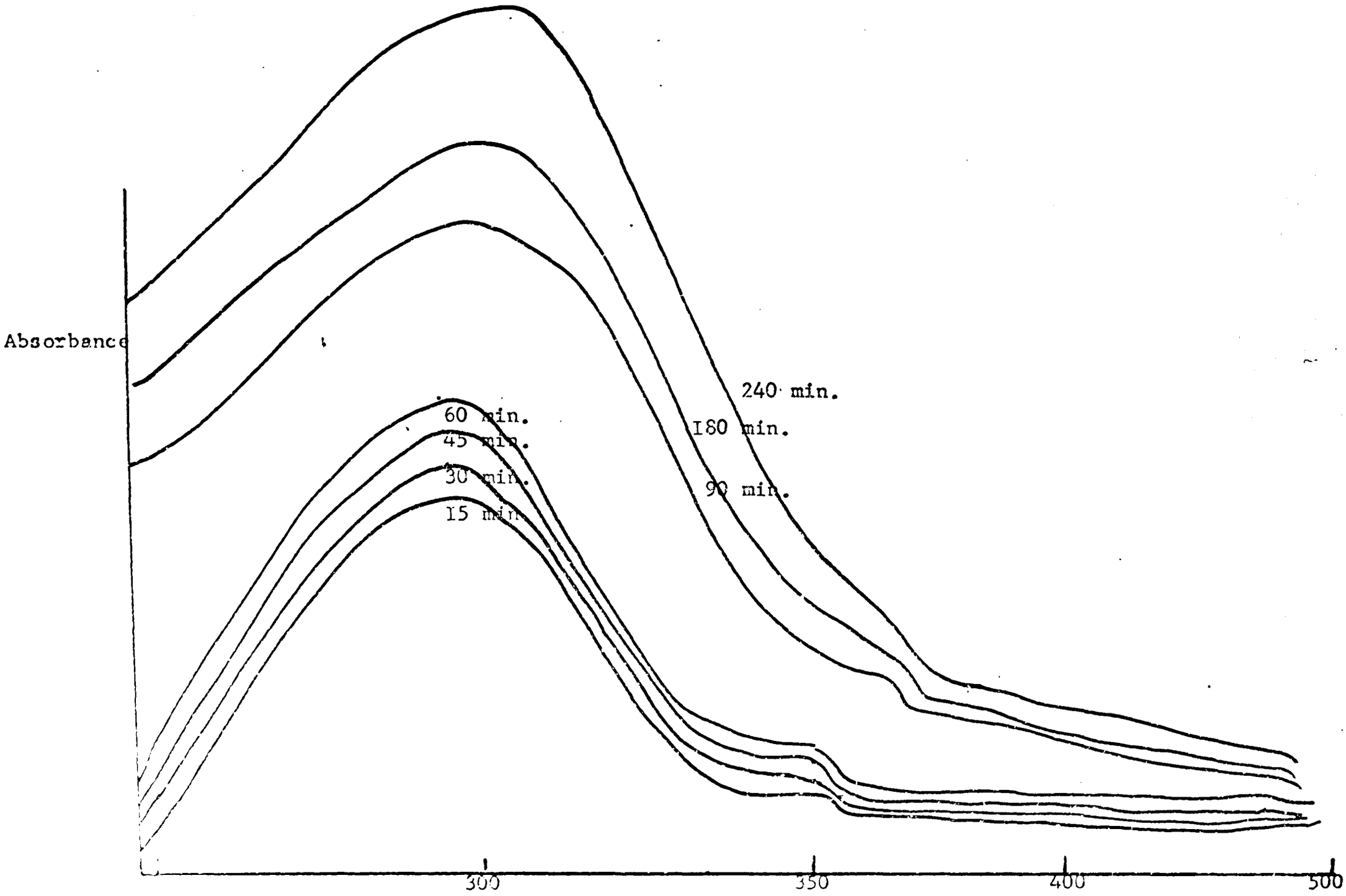

FIGURE 6.25 Ultra-violet spectra of 2/I MIK/MMA copolymer

TABLE 6.I3

Polymer	Time of irradiation (Minutes)	Wavelength (nm.)	Absorbance of a solution of concentration 25 mg./Io ml.	Wavelength (nm.)	Absorbance of a solution of concentration 25 mg./I0 ml.
2/I	0	288	0.96	—	—
2/I	I5	290	0.98	—	—
2/I	30	29I	I.03	—	—
2/I	45	29I	I.09	—	—
2/I	60	29I	I.I6	—	—
2/I	90	292	I.66	—	—
2/I	I80	293	I.84	—	—
2/I	240	295	> 2	—	—
PMIK	0	290	I.26	—	—
PMIK	I5	290.5	I.02	~ 350	0.04
PMIK	30	29I.5	I.06	~ 350	0.20
PMIK	45	293	I.56	~ 350	0.64
PMIK	60	292	I.62	~ 350	0.74
PMIK	90	295	5.6	390	5.6
PMIK	I20	296	—	399	I.85
PMIK	I50	297	5.35	4I4	6.88
PMIK	I80	297	2.56	400	3.48
PMIK	200	298	4.02	4I6	5.84
PMIK	~ I,000	298	—	450	—

molecule. If water is eliminated from MMK, a cyclohexene system is formed:-

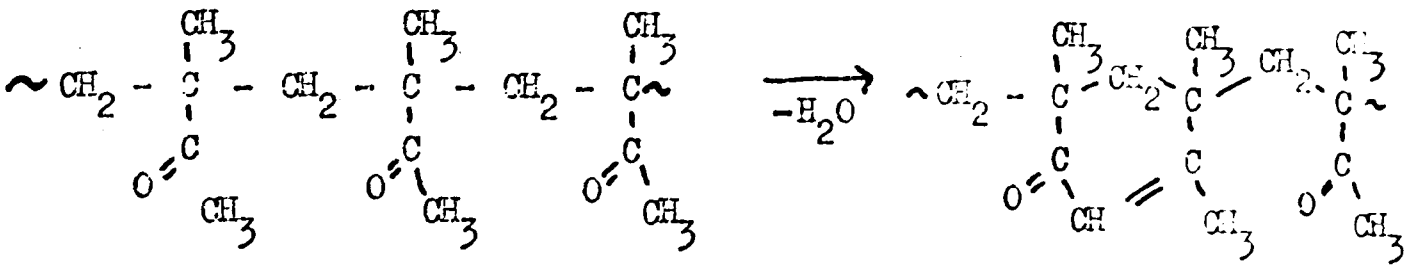

By repeating this reaction along a chain, as previously discussed, the following structure can be formed:-

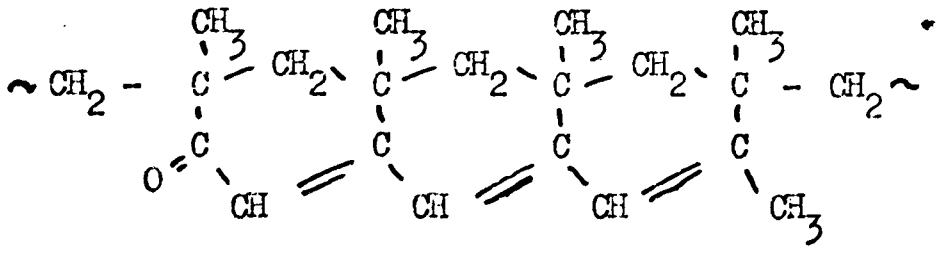

which has an absorption maximum at 340nm. Further extension of conjugation could take the absorption maximum to 450nm after several hours of irradiation (FIGURE 6.24).

This reaction can only take place to a more limited extent in the 2/1 copolymer, because the MIK units will be separated by MMA units, which will prevent the formation of a long conjugated system. Accordingly, peaks at higher wavelengths are not observed in methyl acetate.

Since no coloration was observed in methyl acetate and butanone solution, this phenomenon must be associated with the presence of chloroform, presumably by an energy transfer process.

Regrettably, the samples degraded in chloroform were unsuitable for molecular weight determination.

d) Discussion

As may be expected, the MIK/MMA and MMA/MVK systems share several degradation characteristics in common, particularly when treated by ultra-violet light. In thermal degradations, however, there is a slight difference since MIK units can unzip from chains while MVK cannot. Both MIK and MVK units appear to be potential weak sites for thermal degradation, for example, in PMVK:

a) the main peak temperature drops as the MVK content increases in TVA, and

b) small MVK content leads to rapid unzipping of MMA from the copolymers as can be seen in TG and TVA.

However, where there are several adjacent ketone groups, they may cyclise and block unzipping and this can be seen in the TG's and TVA's of both the MIK and MVK copolymers. The increase in the -100°C and - 196°C traces are probably due to small fragments associated with cyclisation, for example,

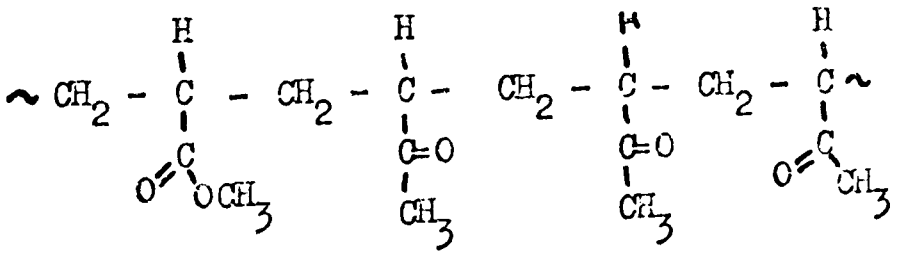

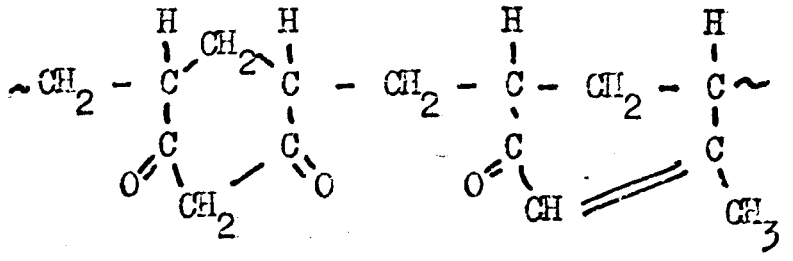

+ CH_3OH + CH_2O + H_2O

Because of increased cyclisation, there will be greater weight stability as unzipping is hindered and this is borne out in the TG's of both systems as the ketone content increases, even in the MIK/MMA copolymers where some unzipping of ketone can take place. The point at which the amount of ketone present in the system becomes sufficient to halt weight loss by unzipping is difficult to estimate in the MIK/MMA copolymers since the position will be confused by the unzipping of MIK in addition to MMA. However, the MMA/MVK system will probably behave in a similar way to the methyl acrylate/MMA system in which Grassie showed that the unzipping of MMA can proceed through single methyl acrylate units but not two adjacent methyl acrylate units. This would be further complicated by the ring formation of the MVK units. It could be predicted that when the mole fraction of MVK exceeds 0.5, there are bound to be many adjacent MVK units through which unzipping MMA units cannot pass and we will have a copolymer in which the unzipping MMA is stabilized by ketone but the presence of MMA units which are more resistant to chain scission than the MVK units, strengthen the polymer chain to chain scission. Since cyclisation of the ketone groups does not appear to occur until later in the degradation and at higher temperatures in TG, the mode of degradation appears similar to the methyl acrylate/MMA system.

In the MIK/MMA TG, we see that the 1/1 and 2/1 copolymers both stabilise at later stages, but not initially, due to MIK assisting MMA to unzip. Regrettably the 1/2 copolymer was not recorded on TG but the trace may fall below the PMIK line since the amount of MIK, may not have been enough to form rings to oppose the unzipping of MMA at higher temperatures.

The experiment on thin film isothermal degradation of 90/10 MMA/MVK copolymer appears to contradict the evidence presented by TG. The following argument, however, may explain it.

The copolymer would not dissolve in toluene after degradation and since the undegraded polymer readily dissolved, it may be assumed that cyclisation had taken place and this therefore, would inhibit MMA unzipping. The reason why this does not happen in TG where heating rates are fast, is probably one of relative rates of reaction. If cyclisation is a slow reaction, which it probably is, since there will be few adjacent MVK units, and even then, they will require specific preorientation before reaction, then in TG, unzipping will take place more quickly than cyclisation and so a dramatic weight loss is observed. But, in thin film, cast from a solvent which may help cyclisation by inducing preorientation, isothermal degradation at low temperatures over long periods of time may give the MVK units time to cyclise and block unzipping.

Increasing the temperature to 240°C may only help the rate of cyclisation over unzipping and produce even lower weight losses. More work in this area is certainly indicated by this unusual result.

In photothermal degradation of MMA/MVK, the copolymer has a similar rate of weight loss to PMMA even though the MVK content is 54%. This must be due to a greater rate of chain scission in photothermal than thermal degradation, although compared to PMMA the rate of chain scission is similar when it would be expected to be higher, as in solution photodegradation. This is probably because cyclisation is taking place to such an extent as to reduce the rate of chain scission, the cyclised regions being resistant to chain scission, which is to be expected.

Further work is also needed in this area and it may be necessary to invoke a mechanism by which a single MVK unit can react with an adjacent MMA unit to form a ring system, for example:-

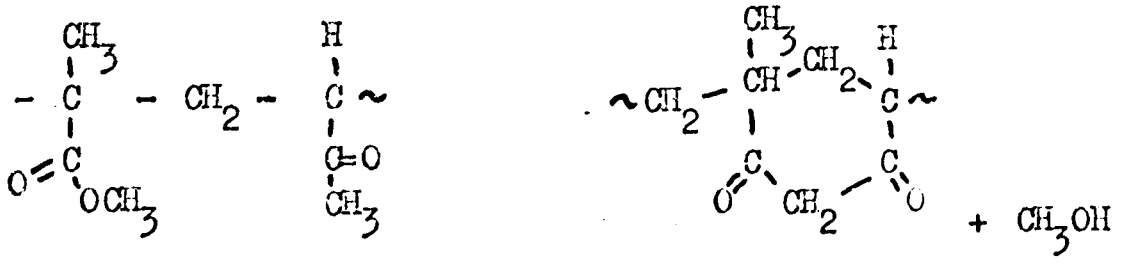

In solution, both the MMA/MVK and the MIK/MMA systems show a common feature in photodegradation, the maximum rate of degradation is achieved at around 20-30% ketone content. Initially, the presence of ketone units reduces the resistance of the copolymers to ultra-violet degradation, the ketone group absorbing the ultra-violet light more readily than the ester group. But as the ketone content increases, the excited ketone group will tend to cyclise with neighbouring groups and not give rise to chain scission. Therefore, the rate of chain scission will decrease with increasing ketone content.

Although Guillet[71] also observed an increase in the rate of photodegradation of a copolymer containing 3% MMA over the rate of

PMVK as discussed in Chapter 1, neither his nor Kato's[78] mechanism could account for the maximum observed in this work.

The limitations of time prevented a more detailed analysis of these copolymer systems. However, further work may resolve the likely mechanism of degradation.

REFERENCES

1. F. Wilkinson, Advances in Photochemistry, 3 241 (1964).
2. H. H. G. Jellinek, Degradation of Vinyl Polymers, Academic Press, New York. (1955)
3. H. H. G. Jellinek, Pure and Applied Chem., 4, 419 (1962).
4. N. Grassie, "Chemistry of High Polymer Degradation Processes", Interscience, New York (1956).
5. R. B. Fox, "Photodegradation of High Polymers "in" Progress in Polymer Science", Vol 1, A. D. Jenkins, ed., Pergamon Press, London (1967).
6. M. C. de Wilde and G. Smets, J. Poly. Sci., 5, 253 (1950).
7. D. C. Blackley and H. W. Melville, Mak. Chem., 18, 19 (1956).
8. R. L. Guile and J. C. Drougas, Dissertation Abstracts, 21, 3265 (1961).
9. R. L. Guile and J. C. Drougas, J. Poly. Sci., 55, 297 (1961).
10. J. L. Lang, W. A. Pavelich and H. D. Clarey, J. Poly. Sci., A1 1123 (1963).
11. D. Braun, I. A. El Sayed and J. Pomakis, Mak. Chem., 124, 249 (1969).
12. J. Tino and J. Placek, Europ. Poly. J., 7, 1615 (1971).
13. J. Tino, J. Placek and J. Pavlinek, Europ. Poly. J., 10, 291 (1974).
14. D. Braun and J. Pomakis, Mak. Chem., 175, 1411 (1974).
15. H. L. Hallensleben and H. Wurm, Europ. Poly. J., 9, 919 (1973).
16. I. Nagahiro, K. Nishihara and N. Sakota, J. Poly. Sci., 12, 785 (1974).
17. A. Barlow, R. S. Lehrle, J. C. Robb and D. Sutherland, Polymer, 8 533, 537 (1967).
18. I. C. McNeill, Europp. Poly. J., 4, 21 (1968).
19. H. H. G. Jellinek and M. D. Luh, Mak. Chem., 115, 89 (1968).
20. H. H. G. Jellinek and H. Kachi, J. Poly. Sci., C23, 87 (1968).
21. G. Bagby, R. S. Lehrle and J. C. Robb, Polymer, 10, 683 (1969).

22. G. S. Anufriev, O. F. Pozdnyakov and V. R. Regel, Vysok. soyed., 8, 834 (1966) (Polymer Science USSR, 8.2 916 (1966)).

23. S. L. Madorsky, J. Poly. Sci., 11, 491 (1953).

24. S. Bywater, J. Phys. Chem., 57, 879 (1953).

25. J. MacCallum, Europ. Poly. J., 2, 413 (1966).

26. I. C. McNeill, Europ. Poly. J., 6, 373 (1970).

27. W. S. Reid, J. Soc. Ind. Chem., 68, 244 (1949).

28. N. Grassie and H. W. Melville, Disc. Farad. Soc., 2, 378 (1947).

29. N. Grassie and H. W. Melville, Proc. Roy. Soc. (London), A199, 1, 14,24,39 (1949).

30. N. Grassie and E. Vance, Trans. Farad. Soc., 49, 184 (1953).

31. D. H. Grant and S. Bywater, Trans. Farad. Soc., 59, 2105 (1963).

32. J. R. MacCallum, Mak. Chem., 83, 137 (1965).

33. A. Brockhaus and E. Jenckel, Mak. Chem., 18, 262 (1956).

34. D. H. Grant and N. Grassie, Polymer, 1, 125 (1960).

35. N. Grassie and I. McLaren, unpublished.

36. N. Grassie, Monograph 26, Advances in Polymer Science and Technology.

37. J. R. MacCallum, Mak. Chem., 83, 129 (1965).

38. M. L. Frolova and A. V. Riabov, Polymer Science, USSR, 2, 1, (1961).

39. R. B. Fox, L. G. Isaacs and S. Stokes, J. Poly. Sci., A1, 1079 (1963).

40. J. P. Allison, J. Poly. Sci., (A1), 4, 1209 (1966).

41. M. I. Frolova, I. V. Neriskii and A. V. Riabov, Polymer Science, USSR, 3, 703 (1962).

42. R. B. Fox and T. R. Price, J. App. Poly. Sci., 11, 2373 (1967)

43. A. R. Schultz, J. Phys. Chem., 65, 967 (1961).

44. D. G. Gardner and L. M. Epstein, J. Chem. Phys., 34, 1653 (1961).

45. A. Charlesby and D. K. Thomas, Proc. Roy. Soc. A269, 104 (1962).

46. T. R. Price and R. R. Fox, Org. Coatings and Plastics Chem. Div., Am. Chem. Soc., Preprints, 26(2), 242 (1966).

47. M. I. Frolova, L. I. Efimov and L. V. Chekmodeeva, Plast. Massy., 1964(3), 38; C. A. 60, 16051e (1964).

48. H. Honig, Naturwiss, 45, 12 (1968).

49. R. R. Fox and T. R. Price, Polymer Preprints, 5, 390 (1964).

50. H. H. G. Jellinek and I. C. Wang, Kolloid-Z. und Z., Polymere, 202, 1 (1965).

51. N. S. Kardush and V. A. Krongauz, Vysok. Soyed. Ser B, 10, 271 (1968) C. A., 69, 10912n, (1968).

52. A. J. Davidson, B. Sc. thesis, Glasgow University (1971).

53. P. R. E. Cowley and H. W. Melville, Proc. Roy. Soc., A210, 461 (1952), A211, 320 (1952).

54. A. Charlesby and N. Moore, Int. J. App. Radiation and Isotopes, 15, 703 (1964).

55. J. R. MacCallum and C. K. Schoff, Trans. Farad. Soc., 67, 2372 (1971)

56. J. R. MacCallum and C. K. Schoff. Trans Farad. Soc., 67 2383 (1971).

57. I. C. McNeill and D. Neil, Europ. Poly. J., 7, 115 (1971).

58. C. S. Marrel and C. L. Levesque, J. Am. Chem. Soc., 60, 280 (1938)

59. C. S. Marrel, E. H. Riddle and J. O. Corner, J. Am. Chem. Soc., 64, 92 (1942).

60. K. Matsuzaki and T. C. Lay, Mak. Chem., 110, 185 (1967).

61. A. K. Chaudhari, Mak. Chem., 33, 249 (1959).

62. S. Iwatsuki, Y. Yamashita and Y. Ishii, Kogyo Kagaku Zusshi 66, 1162 (1963).

63. J. N. Hay, Mak. Chem., 67, 31 (1963).

64. N. Grassie and J. N. Hay, Mak. Chem., 64, 82 (1963)

65. F. T. Wall, J. Am. Chem. Soc., 64, 269 (1942).

66. J. E. Guillet and R. G. W. Norrish, Proc. Roy. Soc., (London), A233, 153, 172 (1955).

67. K. F. Wissbrun, J. Am. Chem. Soc., 81, 58 (1959).

68. A. R. Schultz, J. Poly. Sci., 47, 267 (1960).

69. G. H. Hartley and J. E. Guillet, Macromoles, 1, 165, 413 (1968).

70. M. Heskins and J. E. Guillet, Macromoles, 3, 224, (1970).

71. Y. Amerik and J. E. Guillet, Macromoles, 4, 375, (1971).

72. F. J. Golemba and J. E. Guillet, Macromoles, 5, 63, 212 (1972).

73. P. I. Plo and J. E. Guillet, Macromoles, 5, 405 (1972).

74. A. C. Sumersall and J. E. Guillet, Macromoles, 5, 411 (1972), 6, 218, 223 (1973).

75. E. Dan, A. C. Sumersall and J. E. Guillet, Macromoles, 6, 228 (1973).

76. E. Dan and J. E. Guillet, Macromoles, 6, 230 (1973).

77. A. C. Sumersall, E. Dan and J. E. Guillet, Macromoles, 7, 233 (1974).

78. M. Kato and Y. Yoneshige, Mak. Chem., 164, 159 (1973).

79. C. David, W. Demarteau and G. Geuskens, Polymer, 8, 497 (1967), 10, 21 (1969), 11, 61 (1970).

80. Aldrich Library of Infra-Red Spectra (1970).

81. S. Castellano and J. S. Waugh, J. Chem. Phys., 37, 1951 (1962).

82. Infra-Red Spectra of Selected Chemical Compounds, Meike and Langenbucher (1965).

83. Ditchburn, Proc. Roy. Soc., 236, 217 (1956).

84. Massey and Potter, Atmospheric Photochemistry, I. U. G. Monograph, 1,2 (1961).

85. W. A. Noyes and P. A. Leighton, The Photochemistry of Gases, Reinhold, pp 82-134 (1941).

86. Engelhard Hanovia Lamps, Slough, Bucks, England.

87. C. G. Hatchard and C. A. Parker, Proc. Roy. Soc., A235, 518 (1956).

88. J. G. Calvert and J. N. Pitts, Jnr., "Photochemistry", Wiley and Sons, New York (1967).

89. I. C. McNeill, J. Poly. Sci., A4, 2479 (1966).

90. I. C. McNeill, Europ. Poly. J., 6, 373 (1970).

91. H. Dostal, Monatsh., 69, 424 (1936).

92. T. Alfrey, Jr., and G. Goldfinger, J. Chem. Phys., 12. 205 (1944).

93. F. R. Mayo and F. M. Lewis, J. Am. Chem. Soc., 66, 1594 (1944).

94. R. Simha and H. Branson, J. Chem. Phys., 12, 253 (1944).

95. F. T. Wall, J. Am. Chem. Soc., 66, 2050 (1944).

96. D. C. Blackley and H. W. Melville, Mak. Chemie., 18, 19 (1956).

97. M. C. de Wilde and G. Smets, J. Poly. Sci., 5, 253 (1950).

98. M. H. Loucheux and A. Banderet, Bull. Soc. Chem. France 6, 1216, 1220 (1964).

99. M. H. Loucheux and A. Banderet, J. Poly. Sci., 48, 405 (1960).

100. Polymer Handbook, Editors - J. Brandrup and E. H. Immergut, Interscience (1966).

101. Enc. of Polymer Science and Technology, Interscience (1964).

102. M. Fineman and S. D. Ross, J. Poly. Sci., 5, 259 (1950).

103. A. J. Davidson, B. Sci., thesis, Glasgow University (1971).

104. N. Grassie, B. J. D. Torrance, J. D. Fortune and J. D. Gemmell, Polymer, 6, 653 (1965).

105. N. Grassie, I. C. McNeill and I. F. McLaren, Polymer Letters, 3, 897 (1965).

106. Y. Kato and A. Nishioka, Bull. Chem. Soc., Japan, 37, 1630 (1964).

107. I. Y. Slonim and A. N. Lyobimov, "The NMR of Polymers" New York (1970).

108. F. A. Bovey and G. V. D. Tiers, J. Poly. Sci., 44, 173 (1960).

109. C. E. Ham, "Copolymerisation", Chapter 1, Interscience (1964).

110. C. E. Ham, "Copolymerisation", Enc. of Polymer Sci. and Tech., Vol IV, 165-244, Interscience (1966).

111. C. E. Ham, J. Poly. Sci., 45, 169 (1960).

112. C. E. Ham, J. Poly. Sci., 54, 1 (1961).

113. N. Grassie, J. Poly. Sci., Vol VI No. 5, 643 (1951).

114. R. N. Haward, J. Poly. Sci., 3, 10 (1948).

115. C. E. Schildknecht, Vinyl and Related Polymers, Wiley, New York (1952) pp. 682ff.

116. F. W. Billmeyer Jnr. Textbook of Polymer Science, Wiley, (1971).